

University of Alberta

**Functional Characterization of Class I Arfs and their
Guanine Nucleotide Exchange Factors at the Golgi
Complex**

by

Florin Iulian Manolea

A thesis submitted to the Faculty of Graduate Studies and Research
in partial fulfillment of the requirements for the degree of

Doctor of Philosophy

Department of Cell Biology

© Florin Iulian Manolea

Fall 2009

Edmonton, Alberta

Permission is hereby granted to the University of Alberta Libraries to reproduce single copies of this thesis and to lend or sell such copies for private, scholarly or scientific research purposes only. Where the thesis is converted to, or otherwise made available in digital form, the University of Alberta will advise potential users of the thesis of these terms.

The author reserves all other publication and other rights in association with the copyright in the thesis and, except as herein before provided, neither the thesis nor any substantial portion thereof may be printed or otherwise reproduced in any material form whatsoever without the author's prior written permission.

EXAMINING COMMITTEE

Dr. Paul Melançon, Department of Cell Biology, University of Alberta

Dr. Johnny K. Ngsee, Department of Medicine, University of Ottawa

Dr. Richard Lehner, Department of Cell Biology, University of Alberta

Dr. Tom Hobman, Department of Cell Biology, University of Alberta

Dr. Zhixiang Wang, Department of Cell Biology, University of Alberta

ABSTRACT

We examined the function of ADP-ribosylation factors (Arfs) and their guanine nucleotide exchange factors (GEFs) that regulate recruitment of coat proteins on the Golgi complex. The large ArfGEF GBF1 localizes at the *cis*-Golgi complex while BIG1 and BIG2 localize at the *trans*-Golgi network (TGN). Complementary overexpression and RNA-based knockdown approaches established that GBF1 but not BIGs, is required for COPI recruitment, Golgi stack maintenance and sub-compartmentalization while BIGs appear specialized for clathrin adaptor recruitment and for assembly and maintenance of the TGN. Our observations disprove two widely accepted mechanisms for cargo export by establishing that COPII is the only coat required for sorting and export from the ER exit sites and that BIGs are not required for traffic of the cargo protein VSVG to the cell surface. Furthermore, we provide evidence that may ultimately explain how these ArfGEFs regulate different coats in spite of their well-characterized promiscuity towards class I and II Arfs. We prove for the first time that Arf3 is activated uniquely by BIGs at the TGN. Also, contrary to expectations, we demonstrate that Arf3 differs from Arf1 in regard to localization pattern as well as temperature sensitivity of membrane recruitment. Shifting temperature to 20°C for 2 hours, a method known to block cargo in *trans*-Golgi compartments, caused a dramatic redistribution Arf3 but not Arf1. Redistribution of Arf3 from Golgi membranes upon shift to 20°C was not immediate but occurred gradually over 20 minutes. Arf1 and Arf3 differ in sequence only in two short regions at the N- and C-termini. Analysis of swap constructs established that two amino acids in the N-

terminal region of Arf3 and Arf1 are responsible for directing the temperature sensitivity while two amino acids in the C-terminus directs Arf3's specific localization. Arf3 knockdown had no impact on any of the markers tested or on VSVG trafficking to the cell surface. My work provides solid evidence to support that ArfGEFs function at different compartments to regulate membrane recruitment of specific coat proteins, and may also regulate distinct sets of Arfs that localize preferentially to these particular compartments.

ACKNOWLEDGMENTS

Firstly, I would like to thank my professor Dr. Paul Melançon for patience and guidance both in the laboratory and with this thesis. I really appreciate the support he gave me while I became a good scientist, as well as throughout the process of becoming a physician in Canada.

I would like to thank past and present lab members that I had the opportunity to work with, starting with my good friend Dr. Justin Chun and continuing with Dr. Alejandro Claude, Dr. David Shields, Xinhua Zhao, Troy Lasell, Mary Schneider, Zoya Shapovalova, Ileana Strelkov, Lisa Channon and Anita Gilchrist.

I would like to give a huge thanks to my wife Luminita Manolea, whose support throughout these years has allowed me to reach all my goals. I would also like to thank my parents Elena and Pavel Manolea for supporting my curiosity and thirst of knowledge, regardless of the subject.

TABLE OF CONTENTS

CHAPTER ONE: INTRODUCTION	1
1.1. Introduction to the secretory pathway.....	2
1.1.1 Main components and main functions of the secretory pathway.....	2
1.1.2 Defects of the secretory pathway leading to diseases.....	2
1.1.3 Introducing the components of the secretory pathway and their molecular mechanisms for organelle maintenance and regulation of protein traffic.....	5
1.2. Transport between ER, ERGIC and Golgi complex.....	6
1.2.1. Description of the primary (intrinsic) mechanism for cargo sorting at ERES, driven and regulated by Sar1 and COPII.....	6
1.2.2. Regulatory mechanisms for COPII recruitment and subsequent cargo sorting at ERES.....	8
1.2.3. ERGIC, a stable sorting station between the ER and the Golgi complex?.....	9
1.2.4. Role of COPI in retrograde and anterograde protein traffic between ER and Golgi complex.....	10
1.3. The Golgi stack.....	11
1.3.1. The organization of the Golgi complex.....	12
1.3.2. COPI as the main protein coat acting at the Golgi stack.....	13
1.3.3 ADP ribosylation factors (Arfs) at the Golgi complex.....	14
1.3.4. GBF1 as the main ArfGEF present at the Golgi stack.....	18

1.3.5 ArfGAPs at the Golgi complex.....	22
1.3.6. Models for protein transport through the Golgi complex.....	23
1.4. <i>Trans</i> -Golgi network.....	25
1.4.1. Structure of the TGN.....	25
1.4.2. Arfs and ArfGEFs present at TGN.....	26
1.4.3. Sorting mechanisms at TGN - clathrin dependent sorting.....	28
1.4.4. Sorting mechanisms at TGN - clathrin independent sorting.....	29
1.5 Brefeldin A.....	30
1.6. Arf1 and Arf3 - specific vs. redundant functions.....	31
1.7. Rationale and objectives for each project.....	32
CHAPTER TWO: MATERIALS AND METHODS.....	34
2.1 Reagents.....	35
2.2 Cell culture.....	39
2.3 Antibodies.....	40
2.4 siRNA methods.....	43
2.5 Construction of plasmids.....	43
2.5.1 Construction of the Anti-GBF1, -BIG1, and -BIG2 short hairpin RNA-expressing pSUPER-tet Plasmids.....	44
2.5.2 Arfs tagged with GFP and mCherry.....	44
2.5.3 Arf3 untagged or tagged with HA.....	44
2.5.4 Swap chimeras and mutants between Arf3 and Arf1.....	45

2.6 Overexpression of VSVG-tsO45 and other cDNAs, temperature shift experiments.....	48
2.7 Immunofluorescence staining.....	50
2.8 Fluorescence microscopy.....	50
2.8.1 Epifluorescence microscopy.....	50
2.8.2 Confocal microscopy.....	50
2.9 Image quantification and analysis.....	51
2.9.1 Quantification of fluorescence signal overlap for VSVG-positive peripheral structures and ERGIC53 or Sec31 staining.....	51
2.9.2 Quantification of Golgi complex polarization by line profile analysis..	51
2.9.3 Quantification of VSVG trafficking.....	51
2.9.4 Quantification of the protective effect of BIG1/GBF1 overexpression on Arf3-GFP membrane recruitment after short BFA treatment.....	52
2.9.5 Quantification of Arf3/Arf1 redistribution after BIGs knockdown.....	52
2.9.6 Quantification of fluorescence signal overlap.....	53
2.9.7 Quantification of Arf3-GFP fluorescence signal intensities at the Golgi complex.....	53
2.10 Preparation of cell extracts and analysis by RT-PCR and immunoblots....	54
2.10.1 Analysis by RT-PCR.....	54
2.10.2 SDS-polyacrylamide gel electrophoresis.....	54
2.10.3 Immunoblotting.....	55
2.11 Analysis of Arf sequences.....	55

CHAPTER THREE: GBF1 AND BIGs ARE REQUIRED FOR ASSEMBLY AND	
MAINTENANCE OF THE GOLGI STACK AND <i>TRANS</i>-GOLGI NETWORK,	
RESPECTIVELY.....	57
3.1 Overview.....	58
3.2 Results.....	59
3.2.1 GBF1 and BIG1 regulate the recruitment of different coat proteins on the Golgi complex.....	59
3.2.2 Knockdown of GBF1 confirms its role in regulating assembly of the COPI coat.....	59
3.2.3 GBF1 knockdown does not prevent export from the ER but blocks cargo in post-ERES peripheral VTC structures.....	68
3.2.4 BIGs knockdown blocks recruitment of clathrin adaptors but does not prevent COPI recruitment or maintenance of the Golgi stack.....	72
3.2.5 BIGs knockdown disrupts assembly of the TGN.....	75
3.2.6 BIGs knockdown does not prevent cargo traffic to the cell surface or assembly of a polarized Golgi stack.....	79
3.3 Discussion.....	87
3.3.1 Effectiveness and selectivity of Golgi ArfGEFs knockdown.....	87
3.3.2 GBF1 is essential for COPI recruitment and assembly of the Golgi complex, but is not required for cargo concentration and export from ERES.....	88
3.3.3 BIGs are required for recruitment of clathrin adaptor and maintenance of the TGN.....	90

3.3.4 GBF1, but not BIGs, is required for assembly of a polarized Golgi stack.....	91
--	----

CHAPTER FOUR: ARF3 IS ACTIVATED SPECIFICALLY BY THE LARGE GUANINE

NUCLEOTIDE EXCHANGE FACTORS BIGs AT THE TRANS-GOLGI NETWORK... 95

4.1 Overview..... 96

4.2 Results..... 98

4.2.1 Arf3 localizes specifically to the *trans*-compartments of the Golgi complex..... 98

4.2.2 BIGs are critical for Arf3 recruitment to the *trans*-side of the Golgi complex..... 98

4.2.3 Arf3 distribution remains sensitive to BFA in CHO mutant cells with BFA resistant GBF1/COPI system..... 103

4.2.4 Temperature shift to and from 20°C slowly redistributes Arf3 between Golgi membranes and cytosol..... 106

4.2.5 Temperature sensitivity for membrane recruitment of Arf3 and Arf1 is encrypted within their N-terminal helices..... 110

4.2.6 The C-terminal helix dictates localization of Arf3 to *trans*-Golgi compartments..... 115

4.2.7 Arf3 knockdown does not disperse the TGN and does not block VSVG traffic at the Golgi complex..... 118

4.3 Discussion..... 126

4.3.1 Arf3 is uniquely recruited to the TGN..... 126

4.3.2 Arf3 is most likely activated by BIGs at the TGN.....	128
4.3.3 The unexpected localization of Arf3 to the <i>trans</i> -compartments of the Golgi complex is mediated by the C-terminus.....	129
4.3.4 The unusual temperature sensitivity of Arf3 is dictated by two specific amino acids present in the N-terminal helix.....	130
4.3.5 Redistribution of Arf3 following temperature shift is a relatively slow process.....	133
4.3.6 Arf3 function still remains a mystery.....	134
CHAPTER FIVE: GENERAL DISCUSSION AND FUTURE PERSPECTIVES.....	137
5.1 Synopsis.....	138
5.2 Mechanism of sorting from the Golgi complex to PM.....	141
5.3 Identifying Arf3 receptors localized to the TGN.....	141
5.4 Examining the function of Arf3 at the <i>trans</i> -side of the Golgi complex...	144
5.5 The mechanism of temperature (in)sensitivity of Arf3 and Arf1, respectively.....	146
5.6 Concluding remarks.....	149
CHAPTER SIX: REFERENCES.....	151

LIST OF TABLES

Table 2.1 List and source of chemicals and reagents.....	35
Table 2.2 Commercial Kits.....	37
Table 2.3 Commonly used buffers and solutions.....	38
Table 2.4 Polyclonal antibodies used for IF.....	40
Table 2.5 Monoclonal antibodies used for IF.....	41
Table 2.6 Antibodies used for immunoblotting	42
Table 2.7 Primers used for molecular cloning.....	46
Table 3.1 BIGs knockdown does not affect separation of <i>cis</i> - and <i>trans</i> -Golgi markers.....	86

LIST OF FIGURES

Figure 1.1 Diagram representing coats and compartments of the secretory pathway.....	3
Figure 1.2 Coat assembly on the membrane and regulating factors.....	16
Figure 1.3. Human members of the ArfGEF family.....	19
Figure 3.1. Overexpression of GBF1 and BIG1 protect different coat proteins and Golgi sub-compartments from BFA-induced redistribution.....	60
Figure 3.2. Synthetic siRNA oligos yield specific and effective knockdown of GBF1, BIG1, and BIG2 by RT-PCR analysis.....	61
Figure 3.3. Western blot analysis confirms effective and specific knockdowns of GBF1 and BIGs.....	63
Figure 3.4. Effective knockdown of GBF1 and BIG1 using synthetic siRNA oligos.....	64
Figure 3.5. Specific and effective knockdown of GBF1, BIG1, and BIG2 using siRNA sequences expressed from pSUPER vector.....	65
Figure 3.6. Knockdown of GBF1 prevents assembly of the Golgi complex...	66
Figure 3.7. Partial GBF1 knockdown produces Golgi complex fragmentation as marked by dispersed COPI staining.....	67
Figure 3.8. GBF1 and/or COPI knockdown block VSVG traffic and cause cargo accumulation in peripheral puncta and not ER.....	69
Figure 3.9. BFA treatment prevents accumulation of VSVG in VTCs even in cells lacking GBF1.....	73

Figure 3.10. GBF1 knockdown traps cargo in ERGIC53-positive VTCs that are separate from Sec31-positive ERES.....	74
Figure 3.11. BIGs knockdown blocks recruitment of TGN-specific coats, redistributes TGN markers, but does not prevent assembly the Golgi stack.....	76
Figure 3.12. BIGs knockdown prevents monensin-induced redistribution of GalT-GFP.....	78
Figure 3.13. BIGs knockdown does not block traffic of VSVG to the cell surface.....	80
Figure 3.14. BIGs knockdown does not block traffic of VSVG to the cell surface.....	82
Figure 3.15. BIGs knockdown does not prevent transport of VSVG to the cell surface.....	83
Figure 3.16. BIGs knockdown does not prevent assembly of a polarized Golgi stack.....	85
Figure 4.1. Arf3 localizes in a tag independent manner to a compartment distinct from the <i>cis</i> -Golgi.....	99
Figure 4.2. Arf3 localizes in a tag independent manner to the <i>trans</i> -side of the Golgi complex.....	100
Figure 4.3. Arf3 also localizes to a compartment clearly distinct from the <i>cis</i> - Golgi in HeLa cells.....	101

Figure 4.4. Arf3 also localizes to the <i>trans</i> -side of the Golgi complex in HeLa cells, regardless of the tag.....	102
Figure 4.5. Overexpression of BIG1, but not GBF1, protects Arf3 from BFA-induced redistribution.....	104
Figure 4.6. BIGs knockdown redistributes Arf3 but not Arf1 from Golgi membranes.....	105
Figure 4.7. Membrane recruitment of Arf3 remains BFA sensitive in BFY1 cells.....	107
Figure 4.8. Arf1 remains membrane associated after short BFA treatment while AP-1 fully redistributes in BFY1 cells.....	108
Figure 4.9. Arf3 fully redistributes in BFY1 cells after short BFA treatment while Arf1 remains membrane associated.....	109
Figure 4.10. Arf3 redistributes slowly between Golgi membranes and cytosol upon temperature shift to either 20°C or 37°C.....	111
Figure 4.11. Temperature shift to 20°C has no impact on Golgi membrane recruitment of Arf1-GFP, TGN46, BIG1, AP-1 or FAPP-PH-YFP.....	112
Figure 4.12. Arf3 and Arf1 differ only at their N- and C-termini.....	114
Figure 4.13. The N-terminal helix determines the temperature sensitivity of Arf3.....	116
Figure 4.14. Two residues in the N-terminal helix dictate the temperature sensitivity for membrane recruitment of Arf3 and Arf1.....	117
Figure 4.15. The C-terminal helix of Arf3 is required for concentration	

on the TGN.....	119
Figure 4.16. Two residues in the C-terminal helix are critical for the specific localization pattern of Arf3.....	120
Figure 4.17. Arf3-targeted siRNAs, either individually or a pool, efficiently prevent Arf3-GFP expression.....	122
Figure 4.18. Two commercial antibodies against Arf3 do not yield any immunoblot signal for either endogenous or overexpressed Arf3.....	123
Figure 4.19. Shift to 20°C, but not Arf3 knockdown, blocks VSVG traffic at the Golgi complex.....	124
Figure 4.20. Arf3 knockdown has no effect on either TGN structure or membrane recruitment of clathrin adaptors AP1 and GGA3.....	125
Figure 4.21. Sequence alignment of human, bovine and other non-mammalian Arfs.....	131
Figure 5.1. Diagram representing major findings and conclusions depicted on to the secretory pathway.....	140
Figure 5.2. Arf3-HA overexpression at high levels displaces endogenous GBF1 from the Golgi membranes.....	147
Figure 5.3. Arf3 could function in up-regulating BIGs and down-regulating GBF1 membrane recruitment.....	148

LIST OF SYMBOLS AND ABBREVIATIONS

AP	adaptor protein
Arf	ADP-ribosylation factor
ARNO	ARF nucleotide-binding site opener
ATCC	American type culture collection
BFA	brefeldin A
BIG	BFA-inhibited GEF
CHO	Chinese hamster ovary
COP	coatomer protein
COS	CV-1 (simian) in Origin, and carrying the SV40 genetic material
ddH ₂ O	double distilled water
DMSO	dimethyl sulfoxide
ECL	enhanced chemiluminescence
EM	electron microscopy
ER	endoplasmic reticulum
ERES	ER exit sites
ERGIC	ER-Golgi intermediate compartment
FAPPs	Four-phosphate-adaptor proteins
GalT	galactosyltransferase
GAP	GTPase activating protein
GBF1	Golgi-specific BFA resistance factor1
GDP	guanosine diphosphate
GEF	guanine nucleotide exchange factor
GFP	green fluorescent protein
GAP	GTPase activating protein
GGA	gamma-ear-containing, Arf-Binding Protein
HA	hemagglutinin
HRP	horseradish peroxidase
IF	immunofluorescence
IP	immunoprecipitation
Man II	mannosidase II
mCherry	monomeric Cherry (red fluorescent protein)
NRK	normal rat kidney
PtdInsP	Phosphatidyl-inositol phosphate(s)
PBS	phosphate buffered saline
PCR	polymerase chain reaction
PFA	paraformaldehyde
PH	pleckstrin homology
SDS-PAGE	sodium dodecyl sulphate-polyacrylamide gel electrophoresis
Sec7d	Sec7 domain
SNARE	soluble N-ethylmaleimide sensitive factor attachment receptor
TGN	<i>trans</i> -Golgi network
VSV	vesicular stomatitis virus
VSV-G	VSV-glycoprotein
VTC	vesicular tubular cluster

WT
w/v

wild type
weight per volume

CHAPTER ONE:

INTRODUCTION

1.1 Introduction to the secretory pathway

1.1.1 Main components and main functions of the secretory pathway

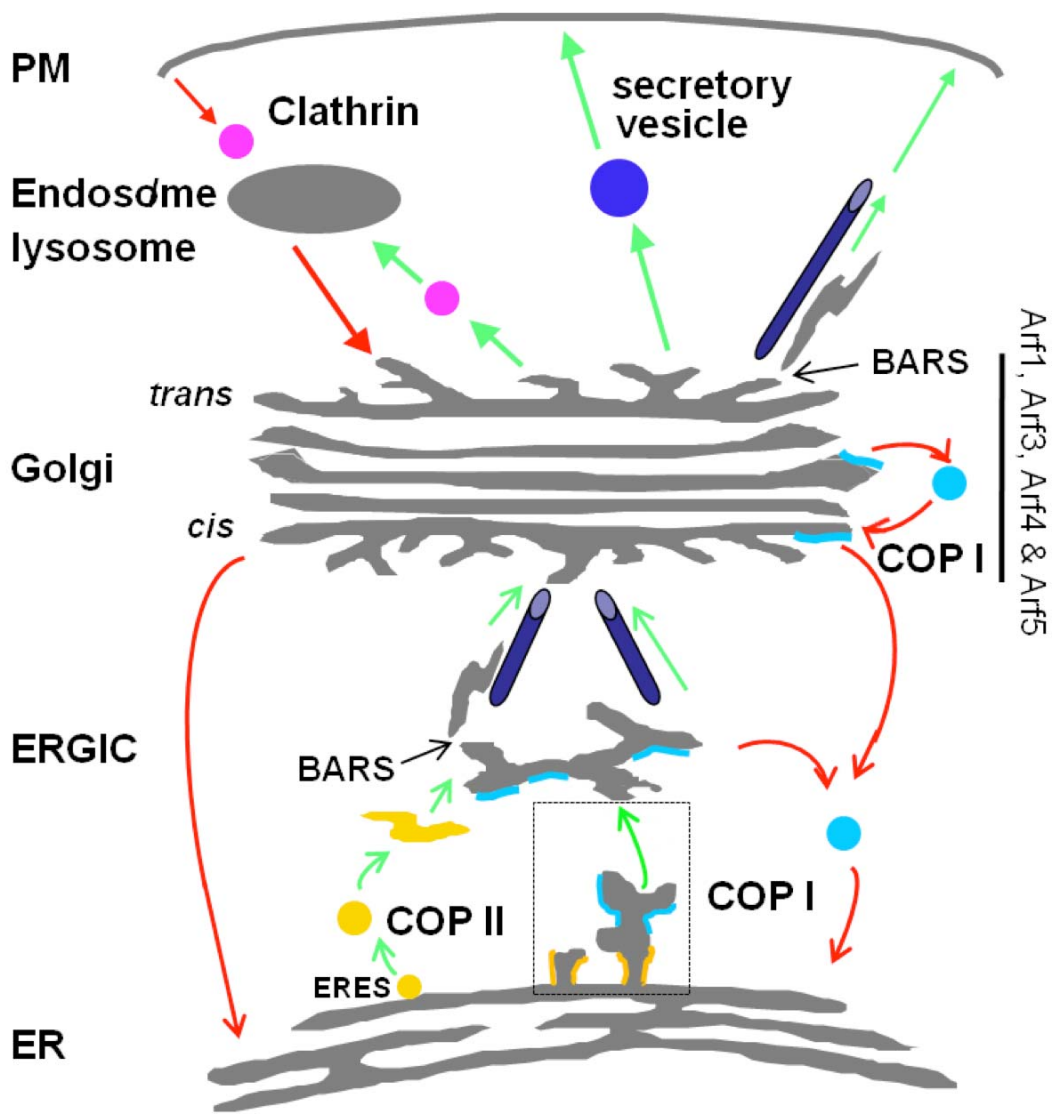
All eukaryotic cells are comprised of a complex endomembrane system. In this system, the secretory pathway delivers newly synthesized or recycled proteins, carbohydrates and lipids to their proper destinations. The secretory pathway is formed of several independent organelles such as the endoplasmic reticulum (ER), the ER-Golgi intermediate compartment (ERGIC) (only in mammalian cells), the Golgi complex comprised of the Golgi stack and the *trans*-Golgi network (TGN), the lysosomal/endosomal system and, finally, the plasma membrane (PM) (Bonifacino and Glick, 2004; Glick and Nakano, 2009). Each of these organelles functions in a specific sequence to sort and modify cargo that passes by to and from the PM (Figure 1.1). Newly formed cargo initially translocates into the ER where it is properly folded and then selected for transport from specialized ER exit sites (ERES) towards ERGIC, also called vesiculo tubular clusters (VTCs) (Fromme and Schekman, 2005; Luini et al., 2005). From ERGIC structures cargo carriers move towards the Golgi complex in a microtubule dependent manner (Presley et al., 1997a; Scales et al., 1997) where they fuse with the *cis*-cisterna of the Golgi complex. Then cargo proteins, while they move through the Golgi complex, are processed in a sequential order (Glick and Nakano, 2009). Subsequently, cargo molecules are sorted in the TGN to their final destinations that include the endosomes, lysosomes, PM or secretory granules (De Matteis and Luini, 2008; Rodriguez-Boulán and Musch, 2005). This anterograde transport towards the PM is balanced by retrograde traffic responsible for endocytosis and the retrieval of transport factors and receptors or resident enzymes to earlier compartments.

1.1.2 Defects of the secretory pathway leading to diseases

Despite significant advances in molecular cell biology, only recently the importance in proper sorting within the secretory pathway was underlined by the connection between mis-regulation at different levels within the secretory pathway and some diseases, including neurodegenerative diseases. Earlier morphological studies examining human brain tissue and animal models linked

Figure 1.1. Diagram representing coats and compartments of the secretory pathway.

Schematic of compartments illustrates bi-directional traffic and locates the approximate site of action of many of the coat proteins mentioned in chapter 1. Green and red arrows represent anterograde and retrograde transport pathways, respectively. COPII and COPI coats facilitate transport between the ER and *cis*-Golgi compartments, while clathrin coated vesicles carry cargo between the TGN and endosome/lysosomes. Transport from ERES in yeast requires only COPII (depicted on left), while in mammalian cells it seems to involve both COPII and COPII (boxed region). Retrograde transport from the Golgi complex to the ER occurs through both COPI-dependent (right) and COPI-independent (left) pathways. Microtubules that drive movement of pleiomorphic carriers from ERGIC to the Golgi complex and from the TGN to the plasma membrane are drawn as blue cylinders. The BARS-mediated fission that releases those carriers is indicated by black arrows. Arf1, 3, 4 and 5 are present throughout the Golgi complex.



Golgi complex fragmentation with Alzheimer disease (Baloyannis et al., 2004), amyotrophic lateral sclerosis (Stieber et al., 1998), Creutzfeldt-Jacob disease (Sakurai et al., 2000), multiple system atrophy (Sakurai et al., 2002; Takamine et al., 2000), Parkinson's disease (Fujita et al., 2006), spino-cerebellar ataxia type 2 (Huynh et al., 2003) and Niemann-Pick type C (Lin et al., 2007). Moreover, some experiments showed Golgi complex fragmentation in an early, preclinical stage of neurodegeneration (Karecla and Kreis, 1992; Mourelatos et al., 1996). Maybe, neuronal Golgi complex is a reliable index for the degree of degeneration (Stieber et al., 1996). Additionally, periventricular heterotopia, a malformation of the cortical development, can be caused by mutations in the vesicle transport ADP-ribosylation factor guanine exchange factor 2 (Arf-GEF2, also called BIG2) gene coding for an important regulator present at TGN and endosomes (Jie et al., 2006; Sheen et al., 2004). Furthermore, a mutation in Sec23A gene causes an autosomal recessive syndrome called Cranio-lenticulo-sutural dysplasia resulting from abnormal ER to Golgi complex traffic (Boyadjiev et al., 2006). Additional research, using a genetic screen identified Sec23, Sar1 and Rab1 as being important in proper development of dendrites, but not axons, in both *D. melanogaster* and rodent neurons (Ye et al., 2007).

1.1.3 Introducing the components of the secretory pathway and their molecular mechanisms for organelle maintenance and regulation of protein traffic.

Formation of the cargo carriers mentioned above depends on the spatially and temporarily regulated recruitment of specific coat proteins from the cytoplasm onto the membranes of individual components of the secretory pathway (Bonifacino and Lippincott-Schwartz, 2003). The specific recruitment of coat proteins for cargo sorting and membrane deformation provides the mechanism to explain how organelles acquire and maintain their unique lipid and protein composition in the face of such extensive exchange. Small GTPases together with their regulatory guanine exchange factors (GEFs) and GTPase activating proteins (GAPs) play critical roles in controlling recruitment of these coat proteins every

step of the way. In the following subchapters I will provide a brief description of the structures and molecular mechanisms that control transport from the ER to ERGIC and then to the Golgi complex, as well as a description of the formation and maintenance of ERGIC followed by the molecular machineries that function at the Golgi stack and at the TGN, and finish with an analysis of the literature regarding the redundant vs. non-redundant functions of the small GTPases Arf1 and Arf3 at the Golgi complex.

1.2 Transport between ER, ERGIC and Golgi complex

Transport between the ER, ERGIC and the Golgi complex is the earliest event in the secretory pathway and therefore these compartments are referred to as “the early secretory pathway” (Barlowe, 2000; Nickel and Wieland, 1998). This section describes the bi-directional transport between the ER, ERGIC and the *cis*-side of the Golgi complex. It begins with an introduction about maintenance of ERES and the molecular machinery that regulates transport out of ERES, followed by a description of ERGIC’s identity and function. Next I will describe the role of COPI in anterograde and retrograde ER to Golgi traffic while finishing with a focused picture of the actual understanding of the mechanism for transport from the ERGIC to the *cis*-Golgi complex.

1.2.1 Description of the primary (intrinsic) mechanism for cargo sorting at ERES, driven and regulated by Sar1 and COPII

COPs select cargo and serve as a scaffold for membrane deformation and vesicle budding (Bonifacino and Glick, 2004; Rabouille and Klumperman, 2005). Transport between the ER and the Golgi complex involves two types of COPs. The COPI coat has been implicated in both anterograde and retrograde traffic between the Golgi and VTCs (Duden, 2003). COPII-coated structures on the other hand mediate export of cargo from the ER (Barlowe, 2003; Tang *et al.*, 2005), which takes place only from specialized regions of the ER called ERES or transitional ER (tER). The ERES are long-lived, ribosome-free elements of the ER that are dedicated to the production of anterograde transport vesicles with the

help of COPII coat proteins (Bannykh and Balch, 1997; Bannykh et al., 1996; Mancias and Goldberg, 2005).

The COPII coat selects, concentrates and promotes export of cargo from ERES to the ERGIC. The COPII coat consists of two heterodimeric protein complexes Sec23/Sec24 and Sec13/Sec31 together with the small GTPase Sar1. The assembly of the COPII coat at ERES starts when the nucleotide exchange factor Sec12 activates Sar1 by promoting the release of GDP and subsequent GTP binding (Futai et al., 2004). Following activation, Sar1-GTP binds tightly to the ER membrane via a GTP-triggered membrane anchor and recruits the Sec23/Sec24 complex. Next, the newly formed heterotrimer Sec23/Sec24-Sar1 participates in selection of cargo molecules (Aridor et al., 1998; Kuehn et al., 1998; Miller et al., 2003), cargo receptors like ERGIC-53 (Appenzeller et al., 1999) and p24 (Muniz et al., 2000) and soluble N-ethylmaleimide-sensitive factor attachment protein receptors (SNAREs), to form the prebudding complex (Sato and Nakano, 2004). The Sec24 subunit of the prebudding complex has been shown to bind directly to a number of cargo molecules (Miller et al., 2003). The polymerization of the COPII coat starts with the recruitment of the Sec13/Sec31 complex onto the prebudding complex, driving further the membrane deformation. When Sec13/Sec31 binds, it will also increase the intrinsic GAP activity of Sec23 towards Sar1 (Antonny et al., 2001). Sar1 hydrolysis of its GTP to GDP will initiate coat disassembly. Current evidence suggests that repetitive rounds of COPII polymerizations and depolymerization promote concentration of cargo at ERES and control for a high efficiency of cargo transport. The discovery of several isoforms of Sec23, Sec24 and Sec31 brings up the possibility of a diverse population of COPII coats with different affinities for cargo molecules (Fromme et al., 2008; Wendeler et al., 2007).

In vitro reconstitution experiments elegantly proved that the minimal COPII machinery necessary for vesicle budding is comprised of Sec23/Sec24, Sec13/Sec31 and Sar1 (Barlowe, 1995). On the other hand, additional factors are necessary to properly regulate spatially and temporally the assembly of the COPII coat. Previous studies have shown that Sec16 interacts with all of the COPII

components, except Sec13 (Espenshade et al., 1995; Gimeno et al., 1996; Shaywitz et al., 1997; Supek et al., 2002). This surprising observation suggests that Sec16 has a pivotal role in COPII assembly and function (Shaywitz et al., 1997; Supek et al., 2002) and is in agreement with the observation that Sec16 might act as a main player in ERES formation and maintenance by organizing COPII into clusters at this location (Connerly et al., 2005).

1.2.2 Regulatory mechanisms for COPII recruitment and subsequent cargo sorting at ERES

Even though the mechanism for regulating cargo sorting at ERES seems to be clear in the yeast *S. cerevisiae*, this is not the case for mammalian cells. Cell-free assays using *S. cerevisiae* extracts unambiguously established that Sar1-dependent recruitment of COPII drives cargo sorting, as well as budding and release of carriers targeted to the Golgi complex (Barlowe, 2003; Fromme and Schekman, 2005). However, no such general agreement over the mechanism for regulation of cargo export from the ER exists for animal cells. In these cells, treatment with brefeldin A (BFA) or expression of a GDP-arrested Arf mutant blocks export of anterograde cargo from the ER, and interferes with its concentration at ERES (Barzilay et al., 2005; Ward et al., 2001). Such observations suggest that formation and release of carriers from ERES in animal cells is more complex and likely involves a two-step process that depends on sequential action of both Sar1 and Arfs (Altan-Bonnet et al., 2004; Garcia-Mata et al., 2003). In this two-step model, Sar1 initially recruits COPII, concentrates cargo and organizes ER export domains by recruiting additional peripheral proteins such as SNAREs, rab1 and its effector p115 (Moyer et al., 2001; Weide et al., 2001). Subsequently, recruitment of golgi-specific brefeldin A resistant guanine nucleotide exchange factor 1 (GBF1), possibly through its interaction with p115 (Garcia-Mata and Sztul, 2003) leads to Arf activation and the recruitment of numerous effectors that will mature the ER export domains into ERGIC membranes prior to their release as separate carriers bound for the Golgi complex (Altan-Bonnet et al., 2004). This model is consistent with the observation that expression of a dominant negative mutant of rab1b causes dispersal of the Golgi as observed with BFA, possibly by preventing

sequential recruitment of p115 and GBF1 (Alvarez *et al.*, 2003). The two-step model is further supported by the fact that several enteroviral 3A proteins that target GBF1 and block Arf activation, also prevent export from the ER and trap cargo in ERES rather than peripheral VTCs (Wessels *et al.*, 2006a; Wessels *et al.*, 2006b).

1.2.3 ERGIC, a stable sorting station between the ER and the Golgi complex?

In mammalian cells, the immediate destination of cargo proteins sorted into ERES is the ERGIC. The ERGIC, also known as pre-Golgi intermediate (Saraste and Kuismanen, 1992) or VTCs (Bannykh *et al.*, 1996) was originally identified as a complex membrane system consisting of vesicles and tubules (Hauri and Schweizer, 1992).

There is still an ongoing debate about the formation of ERGIC. For a very long time in the literature the dogma was that the ERGIC arises *de novo* by fusion of uncoated COPII vesicles. Further experimental evidence supports this idea by confirming that COPII vesicles possess the machinery for homotypic fusion (Xu and Hay, 2004). However, this *de novo* COPII dependent mechanism has been seriously challenged by a new idea, stating that ERGIC is a pre-formed structure that accepts the incoming COPII vesicles by heterotypic fusion (Béthune *et al.*, 2006).

Recent work strongly supports the idea of ERGIC being stationary entities from which anterograde transport towards the Golgi complex and retrograde transport towards the ER takes place (Ben-Tekaya *et al.*, 2005). Taking advantage of dual label live cell imaging, Hauri and colleagues showed that ERGIC, labeled by GFP-ERGIC-53, is a long lived stationary compartment from which multiple rounds of anterograde carriers, marked by the signal-sequence-DsRed, leave towards the Golgi complex (Ben-Tekaya *et al.*, 2005). These data support the notion previously proposed in the literature that ERGIC represents the first sorting compartment to produce anterograde and retrograde cargo (Martinez-Menarguez *et al.*, 1999). To summarize, COPII drives cargo selection and vesicle budding at ERES, then these vesicles lose their COPII coat molecules and fuse with the

ERGIC, a stationary, stable compartment. From ERGIC retrograde cargo returns to ER while anterograde cargo moves on microtubules towards the Golgi complex, both processes being COPI dependent.

1.2.4 Role of COPI in retrograde and anterograde protein traffic between ER and Golgi complex

COPI promotes at ERGIC both retrograde sorting of proteins that have to be retrieved back to ER as well as anterograde sorting for carriers destined for the *cis*-side of the Golgi complex. The 700 kDa heptameric COPI coat was originally identified as the protein responsible for coating vesicles present at the periphery of the Golgi complex and within the Golgi stack, (Lee et al., 2004; Orci et al., 1986). *In vitro* treatment with the nonhydrolyzable analog of GTP, GTP γ S enhanced the presence of coated vesicles next to the Golgi stacks and facilitated the purification and identification of COPI (Melancon et al., 1987). The COPI coat is composed of seven independent subunits: α , β , β' , γ , δ , ϵ and ζ . Four of the subunits, β , γ , δ and ζ , show sequence homology with the clathrin-binding adaptor protein (AP) complexes while the α , β' and ϵ subunits could function in a similar fashion as clathrin, providing a structural scaffold (Lee et al., 2004). All seven subunits pre-assemble into a stable cytosolic protein complex called coatomer, and then they are recruited *en bloc* to the membranes of the ERGIC and Golgi complex (Elsner et al., 2003; Hara-Kuge et al., 1994; Waters et al., 1991).

COPI plays a crucial role in retrograde transport from the Golgi complex and ERGIC towards ER (Letourneur et al., 1994; Orci et al., 1987). The retrieval of resident ER proteins or transport cofactors starts as early as in the ERGIC. COPI, with the help of the KDEL receptor binds KDEL-bearing luminal ER proteins from ERGIC or the Golgi complex (Majoul et al., 1998; Majoul et al., 2001). The KDEL receptor, as well as the other membrane proteins that are transported back to the ER by COPI, contain on their cytoplasmic side a carboxy-terminal dilysine signal KKXX which seems to be both necessary and sufficient to direct retrograde transport of membrane proteins back to ER (Cosson and Letourneur, 1994; Velloso et al., 2002). Interestingly, while the KKXX sequence binds to COPI on the α and β' subunits the transmembrane proteins of the p24

family require dimerization and bind to the γ subunit (Bethune et al., 2006) suggesting that different COPI subunits might provide unique specificities for different types of cargo. In addition to the COPI-dependent retrograde pathway there is evidence for a poorly understood COPI-independent pathway that is employed by cargo that lacks the KDEL or KDEL-like motif (Sandvig and van Deurs, 2002; Storrie et al., 2000).

Paradoxically, COPI plays an important role not only in retrograde traffic, but also in anterograde traffic from ERGIC to the Golgi complex and in ERGIC maintenance. Several observations support the role of COPI in anterograde transport. First, neutralizing antibodies against β -COP blocked the transport of a temperature restricted mutant form of the Vesicular Stomatitis Virus (VSV) Glycoprotein (VSV-G ts045) and caused its accumulation into ERGIC structures both *in vivo* (Pepperkok et al., 1993) and *in vitro* (Peter et al., 1993). Second, the same VSV-G ts045 protein is blocked between the ER and Golgi complex in a Chinese Hamster Ovary (CHO) cell line expressing a mutant form of ϵ -COP (Guo et al., 1994). Even though there are some clues about the molecular role of COPI in anterograde transport, more research is needed to uncover the complete picture. Previous research suggested that soluble anterograde cargo can be concentrated by exclusion from COPI-decorated domains at ERGIC (Martinez-Menarguez et al., 1999). Further research proposed the existence of an early COPI-dependent step in anterograde cargo sorting at ERGIC (Stephens and Pepperkok, 2002). Also, the consistent detection of COPI within ERGIC structures comes in agreement with all the COPI functions proposed above (Griffiths et al., 1995; Oprins et al., 1993).

1.3 The Golgi stack

Even though the Golgi complex was considered to be a single organelle comprised of multiple densely packed interdependent units, it actually appears to be composed of two functionally distinct compartments: the Golgi stack and the TGN. This subchapter will describe first the Golgi stack organization and then the main molecular players: COPI, Arfs, ArfGEFs and ArfGAPs that regulate its

maintenance and its function. The TGN will be discussed in the following subchapter.

1.3.1 The organization of the Golgi complex

The Golgi complex, central sorting station of the secretory pathway, exhibits a very intricate structural organization that likely reflects the complexity of trafficking and sorting events that take place within this organelle (Mogelsvang et al., 2004; Rambourg and Clermont, 1990). It comprises three main structural elements: two extensive tubular-reticular networks on the *cis*- and *trans*-sides flanking a central stack of flat disc-shaped cisternae. The flat cisternae that form the core of the Golgi complex (compact zones) appear interconnected by lateral tubular networks (non-compact zones) to form a continuous membrane ribbon (Mogelsvang et al., 2004; Rambourg and Clermont, 1990). Sub-cellular fractionation and immuno-cytochemical analysis further established that *cis*-, medial-and *trans*-Golgi elements contain different sets of resident enzymes and that the Golgi complex is therefore functionally compartmentalized (Farquhar and Palade, 1998; Polishchuk and Mironov, 2004). For example, the early acting enzyme mannosidase I localizes to *cis*-Golgi membranes, while later acting ones such mannosidase II (ManII) and sialyltransferase concentrate in medial-and *trans*-compartments, respectively.

As mentioned above, accumulating evidence points towards the Golgi complex being comprised of two separate compartments that are structurally, molecularly and functionally different from one another: the Golgi stack and the TGN. First and foremost, the two major components of the Golgi complex have distinct sets of Arf-GEFs and coats that do not intermix: GBF1/COP1 for the Golgi stack and BIGs/clathrin for the TGN (Zhao et al., 2002). Second, when mammalian cells are treated with BFA, the Golgi stack fuses with ER while TGN markers relocate to endosomes (Chege and Pfeffer, 1990; Lippincott et al., 1991; Wood et al., 1991). Third, many TGN localized proteins contain in their cytosolic tails signal sequences for adaptor mediated retrieval from endosomes (Bonifacino and Rojas, 2006) while the glycosylation enzymes located in the Golgi stack use a different type of localization signal (Opat et al., 2001). Lastly,

the distinction between the Golgi stack and the TGN is particularly evident in plant cells or in *S. cerevisiae* where the TGN and the Golgi stack are most of the times physically separate (Glick and Nakano, 2009; Ombretta and Jürgen, 2008; Uemura et al., 2004). Despite intensive work on the molecular regulatory components of the Golgi complex, the mechanism that keeps these two compartments well segregated in the context of such a dynamic organelle still remains a mystery.

1.3.2 COPI as the main protein coat acting at the Golgi stack

COPI is the only coat complex that is recruited onto the membranes of the Golgi stack. The mechanism of COPI assembly and Arf-dependent membrane recruitment seems to be fairly well understood. As described for the recruitment of COPII at ERES by activated Sar1-GTP, COPI assembly begins through initial membrane recruitment by Arf1-GTP. The mechanism of Arf membrane recruitment and activation by ArfGEFs will be discussed in detail later. Once at the membrane, the active Arf1-GTP directly binds the COPI coatomer through its β and γ subunits (Zhao et al., 1997). The newly formed COPI-Arf1-GTP complex acts as a “priming complex” for further coat assembly (Springer et al., 1999). Although the membrane recruitment of COPI from cytosol by Arf1-GTP is a critical initial step (Ostermann et al., 1993), subsequent interactions between the COPI and additional membrane proteins, like the p24 cargo receptors proteins may be necessary to stabilize COPI membrane association (Dominguez et al., 1998).

In vitro studies, with the help of GTP γ S, established that the minimal machinery required for the formation of COPI vesicles is composed of Arf1 and the coatomer (Ostermann et al., 1993; Spang et al., 1998). However, the efficient incorporation of cargo proteins into COPI vesicles requires multiple rounds of GTP hydrolysis on Arf1 (Lanoix et al., 1999; Nickel et al., 1998; Pepperkok et al., 2000). Additional studies established that ArfGAP1 not only promotes COPI membrane recruitment but can even be detected on COPI vesicles (Poon et al., 1999; Rein et al., 2002; Yang et al., 2002). All these findings come as a surprise in light of previous data showing that GAP activity and GTP hydrolysis are

necessary for COPI vesicle uncoating (Bremser et al., 1999). Then, in order to prevent premature uncoating but still allow the ArfGAP to promote efficient cargo sorting and transport, GTP hydrolysis on Arf proteins must be tightly regulated. One appealing possibility might be to allow the ArfGAP to be active only after the budding process. This regulation might be achieved only if the ArfGAP would have a way to sense the membrane curvature, possibility supported by the observation that ArfGAP1 activity is stimulated by an increase in membrane curvature (Bigay et al., 2003).

Since COPI function is so closely related with the mechanism of protein traffic at the Golgi complex I will present the proposed functions for the COPI coat in the context of the models that had been put forward to explain how protein traffic progresses through the Golgi complex, at the end of this subchapter.

1.3.3 ADP ribosylation factors (Arfs) at the Golgi complex

ADP ribosylation factors (Arfs) control the recruitment of COPI at the ERGIC and Golgi stack (D'Souza-Schorey and Chavrier, 2006; Nie and Randazzo, 2006) as well as the recruitment of clathrin and its adaptors at the TGN (Boehm et al., 2001; Boman et al., 2002; Ooi et al., 1998; Puertollano et al., 2001b; Robinson and Kreis, 1992). Arfs are small ~21 kDa GTPases that belong to the Ras superfamily. Arfs were identified as a protein cofactor necessary for the cholera toxin to catalyze the ADP-ribosylation of G_s heterotrimeric G protein (Kahn and Gilman, 1984). Subsequently, Arfs were discovered to be key regulators of vesicular traffic, lipid metabolism and cytoskeleton organization (D'Souza-Schorey and Chavrier, 2006; Donaldson, 2003; Myers and Casanova, 2008; Nie et al., 2003).

Arfs are present in all eukaryotic organisms examined to date and seem to be highly conserved (Li et al., 2004). Sequence comparison of the six mammalian Arfs delineates three classes (Chavrier and Goud, 1999): class I (Arf1, 2, and 3), class II (Arf4 and 5), and class III (Arf6) (Boman and Kahn, 1995; Pasqualato et al., 2002). With the exception of Arf6 that functions at the plasma membrane and endosomes (D'Souza-Schorey et al., 1995; Donaldson and Honda, 2005; Peters et al., 1995), Arfs localize to the Golgi complex (Hosaka et al., 1996; Stearns et al.,

1990; Tsai et al., 1992). Class I Arfs share 96% sequence identity and its members are the most abundantly expressed in cells and tissues examined (Cavenagh et al., 1996). Class II Arfs are 90% identical to each other and are expressed at a much lower level than class I Arfs (Cavenagh et al., 1996) while Arf6, the only member of class III Arfs shows the least degree of sequence identity to the other Arfs. This is consistent with data suggesting class I and II Arfs localize and function at different locations within the cell than class III Arfs.

Arfs act as molecular switches, cycling between an inactive GDP-bound form and the active GTP-bound form. The activation of Arfs is promoted by their regulatory ArfGEFs while the inactivation is produced by ArfGAPs that stimulates the hydrolysis of GTP to GDP (D'Souza-Schorey and Chavrier, 2006; Donaldson and Jackson, 2000; Nie and Randazzo, 2006) (Figure 1.2).

The mechanism of Arf activation, promoted by the interaction with the Sec7 domain of the ArfGEF, seems to be reasonably well understood. Most of the inactive Arf-GDP is cytosolic with its amphipathic N-terminal helix retracted in a hydrophobic groove on the protein. There is evidence showing that a small fraction of the inactive Arf-GDP could undergo a conformational change, moving the myristoylated N-terminus out of the groove and making it available for a weak interaction with the phospholipid bilayer (Antonny et al., 1997). This initial interaction as well as further maintenance of the membrane recruitment for the active Arf was thought to be dependent on the myristoylation, since the membrane interaction is completely abolished if myristoylation is prevented (Franco et al., 1995; Franco et al., 1996; Goldberg, 1998). Most probably following the Arf weak membrane binding, the Sec7 domain of the ArfGEF will engage two important regions of the Arf, switch 1 and switch 2. This interaction between the ArfGEF and the Arf will promote a series of conformational changes in the Arf structure, resulting in opening of the switch 1 and 2 regions and movement of the interswitch region (Renault et al., 2003). The sliding of the interswitch into the hydrophobic groove blocks the movement back of the N-terminus and provides a

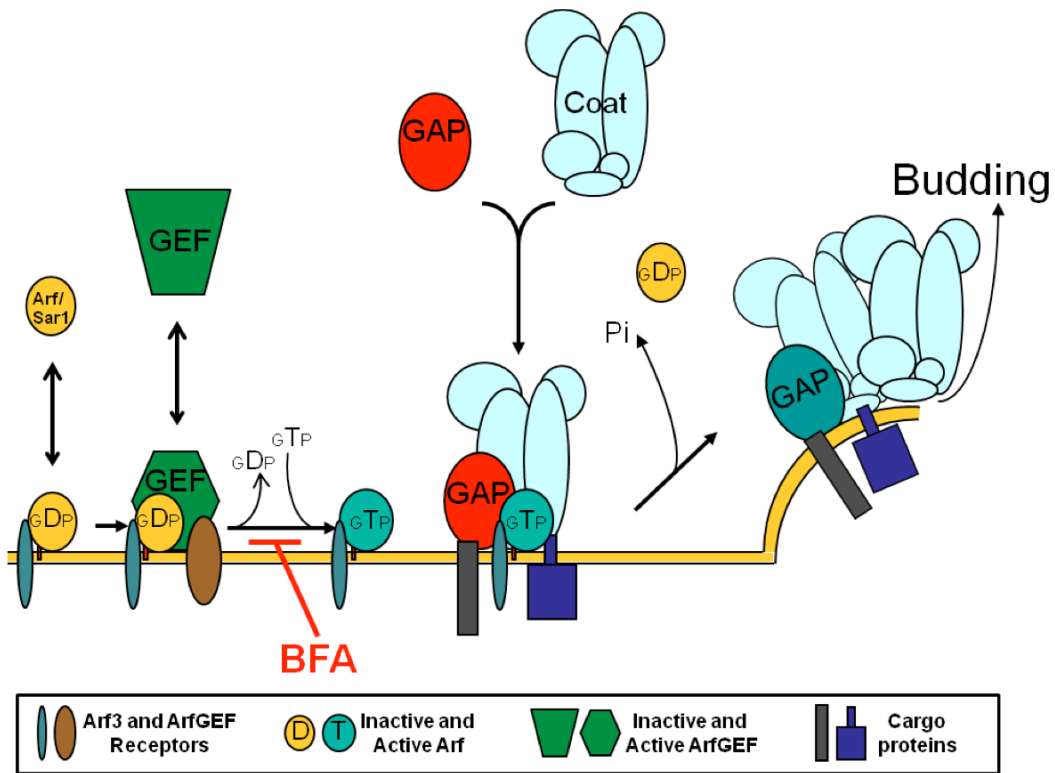


Figure 1.2. Coat assembly on the membrane and regulating factors

Diagram illustrating Arf-dependent coat assembly at the membrane. Soluble Arf-GDP and GEF are recruited to the membrane through association with organelle-specific receptors. Binding of Arf-GDP to the membrane is accompanied by extrusion of the myristoylated N-terminal amphipathic helix. At the membrane, the GEF promotes release of GDP and binding of GTP, a reaction blocked by the drug BFA. Arf-GTP locked on the membrane recruits both GAP and coat proteins that together promote cargo selection and membrane deformation.

good mechanism for “locking” the Arf at the membrane in the active GTP-bound form (Antonny et al., 1997; Goldberg, 1998). During this conformational change, the rearrangement of the Arf promotes the action of the Sec7 domain through a key amino acid called “the glutamic finger” together with the Mg²⁺ ion to induce the expulsion of the GDP (Beraud-Dufour et al., 1998; Renault et al., 2002).

In its active conformation Arfs function by recruiting and/or activating a variety of effector proteins. The diversity of Arf effectors goes in agreement with the variety of Arf cellular functions, which include formation of vesicles on Golgi membranes (Taylor et al., 1994) by facilitating the recruitment of COPI (Donaldson et al., 1992a; Fischer et al., 2000; Liang and Kornfeld, 1997), recruitment of AP-1, 3 and 4 (Boehm et al., 2001; Ooi et al., 1998; Robinson and Kreis, 1992) and Golgi localized, gamma-ear-containing, Arf binding proteins (GGAs) at the TGN and endosomes (Lippincott-Schwartz et al., 1998; Puertollano et al., 2001b; Takatsu et al., 2002), activation of either phospholipase D (Liang et al., 1997) or phosphatidylinositol 4-phosphate 5-kinase (Honda et al., 1999). Among all the mammalian Arfs, Arf1 and Arf6 have been the most studied. Arf1 has been shown to regulate ER-to-Golgi transport (Balch et al., 1992), intra-Golgi transport (Taylor et al., 1992), nuclear vesicle dynamics (Boman et al., 1992) endosome fusion (Lenhard et al., 1992) and last but not least COPI, AP1, AP3 and GGAs membrane recruitment (Liang and Kornfeld, 1997; Lippincott-Schwartz et al., 1998; Puertollano et al., 2001b; Takatsu et al., 2002). On the other hand, Arf6 regulate multiple aspects of endosomal trafficking as well as structural organization and rearrangement at the PM (D'Souza-Schorey and Chavrier, 2006; Donaldson, 2003).

Little is known about the function of class II Arfs. Arf4 has been shown to regulate the sorting of rhodopsin into post-Golgi carriers (Deretic et al., 2005). Recently, our lab showed that Arf4 and Arf5 might serve as “regulator” Arfs to control GBF1 membrane recruitment at ERGIC (Chun et al., 2008), maybe in a similar fashion as activated Arf6 acts as a “regulator” Arf to promote recruitment of the Arf nucleotide-binding site opener (ARNO) protein for subsequent activation of Arf1 on endosomes (Cohen et al., 2007). Arfs 1 to 5 may perform

partially redundant functions since depletion of any single one of the Arfs does not disrupt the Golgi complex or block secretion, while knockdown of two Arfs in combination appears necessary to observe an effect (Volpicelli-Daley et al., 2005). A more detailed discussion of the redundant and non-redundant functions of class I Arfs (Arf1 and Arf3) can be found at the end of this chapter.

The idea of membrane receptors for Arfs came into discussion since the weak interaction between the myristoylated N-terminus of the Arf and the lipid bilayer could not provide either the stability of the association or the spatial specificity for a particular location within the secretory pathway. The first suggestion for a proteinaceous Arf receptor came from a study showing that from the two populations of Arfs found on the Golgi membranes only one was saturable (Helms et al., 1993). Furthermore, biochemical studies provided evidence for Arf1-GDP association with membranes, prior to nucleotide exchange (Beraud-Dufour et al., 1999). Subsequent studies identified potential Arf receptors. The p23 protein, member of the p24 family, was the first to be proposed to function as Arf1 receptor since p23, through its cytosolic region, has been shown to directly bind Arf1 (Gommel et al., 2001; Majoul et al., 2001). SNARE proteins have also been proposed to function as Arf receptors (Honda et al., 2005; Rein et al., 2002). More recently, Donaldson and colleagues provided evidence for the recruitment of Arf1 by the early-Golgi SNARE protein membrin, that involves a central motif in Arf1, ¹¹⁰MXXE¹¹³ (Honda et al., 2005). Finally, work in our laboratory by Justin Chun provided evidence for specific receptors for Arf4-GDP and Arf5-GDP at ERGIC (Chun et al., 2008).

1.3.4 GBF1 as the main ArfGEF present at the Golgi stack

Several Arf-GEFs have been characterized to date, all of which contain a conserved Sec7 domain responsible for Arf activation (Cox *et al.*, 2004; Mouratou *et al.*, 2005) (Figure 1.3). It is interesting how the presence of GEF activity on Golgi membranes was demonstrated in 1992 (Donaldson et al., 1992b; Helms and Rothman, 1992), four years before the identification of the first ArfGEF proteins

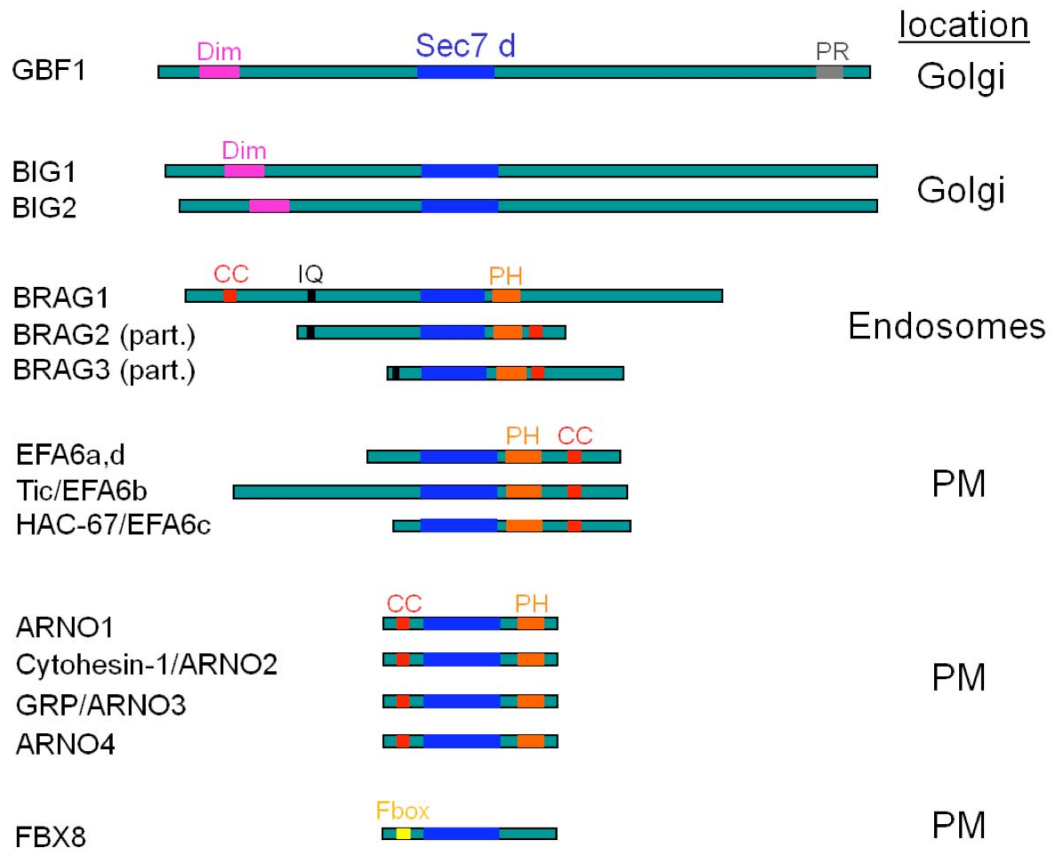


Figure 1.3. Human members of the ArfGEF family.

Representative members of six different subfamilies of *Homo sapiens* Arf-GEFs are shown, with colored bars representing various domains shared by some or all members. These domains include: **Sec7**: Sec7 domain common to all ArfGEFs; **Dim**: Dimerization domain; **PR**: Proline Rich domain; **PH**: pleckstrin homology domain; **CC**: coiled-coiled domain; **IQ**: IQ domain; **Fbox**: Fbox motif. The location where the majority of the proteins localize labeled on the right hand side, for each family.

ARNO (Chardin et al., 1996) and Gea1p (Peyroche et al., 1996). Since then, a large number of surprisingly diverse members have been added to the family of ArfGEFs (Cox et al., 2004). In eukaryotic cells, ArfGEFs are classified into six sub-families that range in size from small (~40 to 80 kDa, including CYH/ARNO and EFA6) to intermediate (~100 to 150 kDa, including BRAG and SYT1) to large (~160 to 230 kDa, including GBF/GEA and BIG/Sec7) (Cox *et al.*, 2004; Mouratou *et al.*, 2005). Several domains have been recognized in the sequence of the intermediate and small ArfGEFs. The ARNO/Cytohesin and EFA6 sub-families possess both pleckstrin homology (PH) and coiled-coiled domains, the BRAGs have only PH domains while the large ArfGEFs do not have either PH or coiled-coiled domains (Figure 1.3).

Unlike the PH or coiled-coiled domains, the central Sec7 domain is present in all the ArfGEF proteins and is responsible for catalyzing the nucleotide exchange reaction. The Sec7 domain contains approximately 200 amino acids, a strong homology to the yeast protein Sec7p (Jackson and Casanova, 2000) and can promote the nucleotide exchange reaction by itself (Chardin et al., 1996; Mansour et al., 1999; Sata et al., 1998). The crystal structure of the Sec7 domain of different ArfGEFs reveals that it consists of ten α -helices arranged in the shape of an elongated cylinder (Cherfils et al., 1998; Mossessova et al., 1998; Renault et al., 2002). Two regions containing the most conserved sequences are situated in a hydrophobic groove (Cherfils and Chardin, 1999; Goldberg, 1998). The first region, called motif 1, contains an invariant glutamate residue, also called “glutamic finger” which promotes the GDP release (Beraud-Dufour et al., 1998; Goldberg, 1998) while the second region, called motif 2, contains a number of hydrophobic residues important in substrate binding (Cherfils and Chardin, 1999; Goldberg, 1998). The importance of the “glutamic finger”, which inserts near the nucleotide phosphates to destabilize the crucial Mg^{2+} ion and subsequently push out the GDP molecule from its socket (Beraud-Dufour et al., 1998; Goldberg, 1998), was confirmed by a series of mutagenesis studies. The charge reversal E/K mutation in either ARNO (Beraud-Dufour et al., 1998) or GBF1 (Garcia-Mata et al., 2003) prevents Arf activation with dominant-negative effects over the

endogenously expressed ArfGEFs. The E/K mutation is thought to promote the formation of a stable complex between the Sec7 domain and Arf-GDP (Renault et al., 2003; Shin and Nakayama, 2004).

Two sub-families of large-sized Arf-GEF called GBF1/GEA and BIG/SEC7 are present in all eukaryotes and appear to regulate Arf activation for coat recruitment on the Golgi complex (Bui et al., 2009; Cox et al., 2004). We are going to focus on the GBF1/GEA sub-family over the next paragraph while the BIG/SEC7 sub-family will be presented in the next sub-chapter.

The GBF/GEA sub-family includes the yeast Gea1p and Gea2p, Arabidopsis GNOM/Emb30p and mammalian Golgi-specific BFA resistance factor (GBF) 1 (Cox et al., 2004). Gea1p and Gea2p (Peyroche et al., 1996) localize at the Golgi complex where they appear to play redundant roles in structure maintenance and function of the Golgi complex in yeast (Peyroche et al., 2001). Unlike its homologues, GNOM/Emb30p does not localize to the Golgi complex but was found to associate with endosomes where it plays an important role in recycling auxin transport components (Bonifacino and Jackson, 2003; Geldner et al., 2003). GBF1, the only member of this sub-family in mammals, was identified in our laboratory during an attempt to clone the factor responsible for the BFA resistance of a mutant CHO cell line, BFY1 (Yan et al., 1994). Surprisingly, further analysis of wild type CHO cells and BFY1 cells suggested that GBF1 could not be responsible for BFA resistance of mutant cells since both the abundance and sequence of the transcripts were identical between the two cell lines (Claude et al., 1999). Nevertheless, overexpression of GBF1 allows growth in the presence of BFA and the term **Golgi-specific BFA resistance Factor** remained. GBF1 colocalizes with COP1 on the Golgi complex (Claude et al., 1999) and remains the only known ArfGEF to localize to the ERGIC and *cis*-side of the Golgi complex (Garcia-Mata et al., 2003; Kawamoto et al., 2002; Zhao et al., 2006; Zhao et al., 2002). GBF1 has been proposed to have specificity for both class I and class II Arfs *in vitro* and *in vivo* (Claude et al., 1999; Kawamoto et al., 2002). A number of studies suggested the link between GBF1 and COPI membrane recruitment either at ERGIC or at the Golgi complex (Garcia-Mata et

al., 2003; Kawamoto et al., 2002; Monetta et al., 2007; Zhao et al., 2006; Zhao et al., 2002).

Besides BFA, several other tools have been used to study the function of GBF1. Taking advantage of the inhibitory effect of the viral protein 3A on GBF1, the regulatory role of GBF1 on Arf1-mediated COPI membrane recruitment was reasserted (Belov et al., 2007; Wessels et al., 2006a; Wessels et al., 2006b). Furthermore, Haslam and coworkers showed that treatment of cells with golgicide A, a new drug that inhibits GBF1 function resulted in rapid dissociation of COPI vesicle coat from Golgi membranes and subsequent disassembly of the Golgi and *trans*-Golgi network (Saenz et al., 2009). Taken together, all these observations support an important role for GBF1 at the ERGIC and the Golgi stack.

1.3.5 ArfGAPs at the Golgi complex

While ArfGEFs promote Arf activation, the ArfGAPs catalyze the reaction which will inactivate the Arfs by inducing hydrolysis of GTP to GDP. Active Arf proteins possess a very low intrinsic rate of hydrolysis and ArfGAPs are necessary to efficiently regulate Arf inactivation. All ArfGAPs share an essential zinc finger domain and a conserved arginine residue critical for their activity (Nie and Randazzo, 2006). Among the sixteen members of the mammalian ArfGAP family identified to date, some function at the Golgi complex (Donaldson, 2000; Nie and Randazzo, 2006; Randazzo and Hirsch, 2004). ArfGAP1 (Cukierman et al., 1995) remains the most studied member of the ArfGAP family. Initial characterization confirmed it promoted GTPase activity on Arf1 with subsequent COPI coat dissociation (Bremser et al., 1999; Tanigawa et al., 1993). However, further work revealed that ArfGAP1 also binds cargo molecules like KDEL receptor and COPI coat, simultaneously facilitating vesicle formation as well as cargo selection and sorting (Aoe et al., 1997; Aoe et al., 1999; Lee et al., 2005). The mechanism of ArfGAP1 regulation on COPI coat assembly/disassembly was presented above (section 1.3.2). In addition, ArfGAP2 and ArfGAP3 seems to function also in COPI assembly, in a non-redundant fashion with ArfGAP1 (Frigerio et al., 2007). While ArfGAP1 activity seems to be regulated by membrane curvature (Bigay et al., 2005; Drin et al., 2007; Mesmin et al., 2007)

ArfGAP2 and ArfGAP3 function might be regulated by the COPI coat (Kliouchnikov et al., 2009; Weimer et al., 2008). ARAP1 is another ArfGAP that functions at the Golgi complex since overexpression of ARAP1 affected greatly the Golgi morphology (Miura et al., 2002). Several additional Arf-GAPs function in late Golgi compartments and endosomes (Inoue and Randazzo, 2007). These ArfGAPs likely also perform a structural function since ACAP-1 was recently shown to act as a coat to mediate endocytic recycling of specific cargo molecules (Li et al., 2007).

1.3.6 Models for protein transport through the Golgi complex

Imaging of live cells revealed that the Golgi complex is not static as initially assumed from its intricate structure, but rather surprisingly dynamic and linked to several other organelles by active bi-directional transport routes (Bonifacino and Glick, 2004). As described also in subchapter 1.2, in animal cells cargo initially translocated into the ER is selected for transport from specialized ERES to ERGIC (Fromme and Schekman, 2005; Tang *et al.*, 2005). Shortly after their formation, pleiomorphic carriers are transported on microtubules towards the Golgi complex (Presley et al., 1997b; Scales et al., 1997) where they collect, fuse into a network and subsequently become a flattened *cis*-Golgi cisterna (Bonifacino and Glick, 2004). The following paragraphs describe the contradictory models that attempt to describe the mechanism that facilitates cargo progression through the Golgi complex.

Current evidence suggests that cargo molecules progress through the Golgi stack following the cisternal maturation model, whereby newly formed *cis*-cisternae containing cargo progressively move towards the *trans* side as they lose early-acting Golgi enzymes and acquire late-acting ones (Losev et al., 2006; Matsuura-Tokita et al., 2006; Pelham, 2001; Puthenveedu and Linstedt, 2005). The evidence supporting this model comes from the demonstration that COPI vesicles lack cargo proteins, like VSVG, and instead contain Golgi enzymes that need to be transported backwards, like Mannosidase II (Gilchrist et al., 2006; Martinez-Menarguez et al., 2001). Further evidence to support this model comes from the observation that both small cargo, like VSVG, (Mironov et al., 2001) as

well as large protein structures, like procollagen (Bonfanti et al., 1998) or algal scales (Becker et al., 1995; Mironov et al., 2001), while no megavesicles have been seen in algae (Donohoe et al., 2007), does not leave the lumen of the Golgi cisternae.

A major competing model, the vesicular transport model, proposes that each Golgi cisterna represents a static compartment with a stable composition of processing enzymes while cargo is ferried in COPI vesicles that bud from one cisterna and fuse with the next one in a *cis-* to *trans-* direction (Farquhar and Palade, 1981; Rothman, 1994). The model was initially proposed after noticing the multitude of vesicles around the Golgi rims at the EM level (Palade, 1975) and further supported by the data obtained from *in vitro* vesicular transport experiments (Rothman, 1994; Rothman and Orci, 1992; Rothman and Wieland, 1996) and by data showing the presence of anterograde cargo proteins in COPI vesicles (Nickel et al., 1998; Pepperkok et al., 2000).

Because neither of the two extreme models presented above explain or fit all available data, new models have emerged. First, the percolating vesicle model combines features of the cisternal maturation model and the vesicular transport model (Orci et al., 2000; Pelham and Rothman, 2000). In this model, a subset of COPI coat vesicles promotes the forward movement of the cargo proteins while a different subset of COPI vesicles directs the retrograde traffic of escaped resident Golgi enzymes (Rothman and Wieland, 1996). An alternate continuity-based model was developed when tubular inter-cisternal connections were observed by electron tomography (Trucco et al., 2004). These connections induced by the VSVG cargo wave appear to function as transport routes for both cargo and Golgi enzymes while the COPI vesicles lack both cargo and enzymes (Trucco et al., 2004). Lastly, a rapid partitioning model was proposed to explain the observation that cargo molecules exit the Golgi complex with exponential kinetics and without the lag resulting from the transit time postulated by the other models (Patterson et al., 2008). In this model, intra-Golgi transport of cargo proteins and enzymes would occur by rapid partitioning between two lipid phases and rapid exchange

between connected cisternae (Patterson et al., 2008). The role of COPI vesicles in this model still has to be addressed.

As is usually the case when proposed models both contradict themselves and share common ground, the truth likely lies in between. In this case, features that vary between models could arise from necessary adaptation to a certain physiologic or non-physiologic condition. Future work will be necessary to reveal which mechanisms for cargo progression through the Golgi complex are necessary for a baseline secretion and which are compensatory.

1.4 *Trans*-Golgi network

The TGN was always considered to be the compartment where cargo sorting and exit would occur at the end of its passage through the Golgi complex. The cargo would be sorted for delivery to various destinations that include the endosome, PM, lysosomes or secretory granules (Rodriguez-Boulán and Musch, 2005). This section initially describes the structure of the TGN, followed by the characterization of the molecular machinery that act at this compartment, including Arfs and ArfGEFs, ending with a description of clathrin dependent and clathrin independent sorting mechanisms.

1.4.1 Structure of the TGN

TGN architecture has fascinated scientists over the years to the same degree as the Golgi morphology has. The name of *trans*-Golgi network was first proposed by Griffiths and Simonds for the compartment previously called Golgi endoplasmic reticulum lysosomes (GERL) (Griffiths and Simons, 1986). The intense research in the area was always fueled by the idea that function can be suggested by morphology (Mogelsvang et al., 2004). Initially the TGN was thought to be the single *trans*-most cisternae of the Golgi complex and the network that connects to it (Orci et al., 1987). However, EM tomographic studies looking at the sites of sorting and exit from the Golgi complex revealed that they are comprised not only from one, but two to three distinct *trans*-cisternae (Ladinsky et al., 1994; Ladinsky et al., 2002; Mogelsvang et al., 2004). The high resolution 3D images obtained by EM tomography identified clathrin-coated buds only on the *trans*-

most cisterna of the Golgi complex (Mogelsvang et al., 2004), (Ladinsky et al., 1999), suggestive for a unique site for sorting cargo destined for the endosomal/lysosomal pathway. At the same time, these data suggested that cargo destined for the PM should exit from the two antepenultimate and penultimate *trans*-cisternae.

1.4.2 Arfs and ArfGEFs present at TGN

The complexity of the molecular machinery that acts at the TGN parallels the multitude of sorting mechanisms that must operate simultaneously to distribute cargo to multiple destinations like endosomes, lysosomes or the PM. The main regulators of the TGN sorting machinery are the ArfGEFs BIG1 and BIG2 and the clathrin coat, all of them restricted to the TGN. However, no such evidence currently exists to indicate a specific compartmentalization of Arfs between the Golgi stack and the TGN. Indeed, the literature predicts that Golgi-localized Arfs, previously described in section 1.3.3, should also be present at TGN. Potential non-redundant function of Arfs at the TGN, with focus on Arf1 and Arf3, will be presented in detail throughout the last sub-chapter of the introduction.

The yeast Sec7p is a large ArfGEF belonging to the Sec7/BIG subfamily, which includes also the mammalian BIG1 and BIG2. Sec7p was first identified using a series of secretion-defective mutants in *S. cerevisiae* (Novick et al., 1980) and its function is essential for yeast secretion and growth (Achstetter et al., 1988). Sec7p localizes to late Golgi compartments (Franzusoff et al., 1991; Mogelsvang et al., 2003) where it activates Arf1p to regulate the recruitment of both the clathrin coat and the newly discovered exomer coat at the TGN (Wang et al., 2006).

BIG1, previously called p200-GEP, and BIG2 were first identified from bovine brain cytosol as a ~670 kDa macromolecular complex based on their BFA-inhibited GEF activity (Morinaga et al., 1996). Peptides obtained from the purified proteins showed the highest sequence similarity with each other and with Sec7p (Morinaga et al., 1996) and facilitated subsequent cloning of their cDNAs (Togawa et al., 1999). The proteins show a high degree of sequence similarity and domain organization (Mouratou et al., 2005). Initial analysis by

immunofluorescence and sub-cellular fractionation localized BIGs to the Golgi complex (Yamaji et al., 2000) but subsequent studies localized the proteins more specifically to the TGN (Mansour et al., 1999; Shinotsuka et al., 2002a; Shinotsuka et al., 2002b; Zhao et al., 2002). Co-immunoprecipitation (co-IP) established that ~70 to 75% of these two ArfGEFs actually form hetero-dimers and exist in the cytosol in a macromolecular complex of >670kDa (Yamaji et al., 2000). These results suggest that ~25 to 30% of these proteins that do not form hetero-dimers could also have independent functions in unrelated processes within the cell. *In vitro* work suggests that both BIG1 and BIG2 catalyze nucleotide exchange preferentially on Arf1 and Arf3, with some activity towards Arf5 and contradictory results for Arf6 (Islam et al., 2007; Jackson and Casanova, 2000; Morinaga et al., 1999; Shin et al., 2004; Togawa et al., 1999). Over the following years the functions of BIG1 and BIG2 were studied extensively. BIG1 has been suggested to bind myosin IXb and regulate its GAP activity towards RhoA (Saeki et al., 2005), to accumulate into the nuclei of serum-starved HepG2 cells in a microtubule and protein kinase A (PKA) dependent manner (Citterio et al., 2006) and to be necessary for correct glycosylation and function of integrin β 1 (Shen et al., 2007). On the other hand, BIG2 has been suggested to function as an A kinase-anchoring protein (AKAP) (Li et al., 2003), to be important in the structural integrity of the recycling endosomes (Shin et al., 2004), to regulate transferrin (Tfn) uptake and Tfn receptor recycling (Shen et al., 2006), most probably through its interaction with Exo70 and the exocyst complex (Xu et al., 2005). BIG2 might also regulate the extracellular release of tumor necrosis factor receptor (TNFR) 1 exosome-like vesicles in human vascular endothelial cells (Islam et al., 2007). Recent data provide further evidence for regulation of BIG1 and BIG2 activity by PKA and protein phosphatase 1 γ (Kuroda et al., 2007). Lastly, experiments employing knockdown of BIG2 confirmed its role in endosome recycling maintenance while knockdown of BIG1 does not have an obvious impact on the TGN or morphology of recycling endosomes (Ishizaki et al., 2008). The same study suggest that BIG1 and BIG2 might play redundant

roles in regulating the AP-1 dependent traffic from TGN to endosomes (Ishizaki et al., 2008).

1.4.3 Sorting mechanisms at TGN- clathrin dependent sorting

Packaging of endosome-targeted cargo at the TGN involves clathrin and several adaptor proteins, including the multimeric AP-1, AP-3, AP-4 and the adaptor-like molecules GGAs (Bonifacino, 2004; Robinson, 2004). Both AP-1 and GGAs might help in regulating the selective transport of mannose 6 phosphate receptors (M6PR) and their cargo from the TGN to endosomes (Doray et al., 2002; Puertollano et al., 2001a; Zhu et al., 2001). Current evidence suggests a multi-step process in which all three GGAs act in concert at the TGN to concentrate their ligands in coated regions where a series of dephosphorylation and re-phosphorylation reactions of GGAs, M6PR and AP-1 subunits eventually leads to transfer of the ligand from GGAs to AP-1 (Ghosh and Kornfeld, 2004). This would explain why AP-1 was found to be highly enriched in purified in clathrin coated vesicles while the GGAs were not detected in these vesicles (Robinson, 2004). One possibility to enhance the recruitment of AP-1 and GGAs at the TGN is through phosphatidylinositol 4-phosphate (PI4P), which is produced when Arf1 recruits and activates the PI 4-kinase III β (De Matteis and Godi, 2004a; Wang et al., 2007; Wang et al., 2003).

The only signal sequence for TGN to endosome sorting identified to date is DXXLL, which is recognized by the VHS domain of the GGAs (Bonifacino and Traub, 2003). This signal was found to be present in several transmembrane receptors and other proteins that cycle between the TGN and endosomes, such as cation-independent- and cation-dependent-M6PRs (CD- and CI-M6PR), sortilin, low-density-lipoprotein-receptor-related protein 3 and 10 (LRP3 and LRP10), sorting-protein-related receptor containing low-density-lipoprotein-receptor class A repeats (SorLA), β -secretase, GGA1 and GGA3 (Bonifacino, 2004; Bonifacino and Traub, 2003). The D residue, generally found in the context of a cluster of acidic residues, and the LL residues are critical since mutation of any of them to A leads to appearance of the proteins at the cell surface (Bonifacino and Traub, 2003). Another complementary piece of evidence underlining the importance of

proper sorting for delivery of acidic hydrolases to lysosomes comes from the use of a dominant-negative GGA construct which causes the retention of the CI- and CD-M6PRs at TGN and its depletion from the periphery (Puertollano et al., 2001a; Puertollano et al., 2001b).

An alternate way to direct cargo sorting at the TGN might be by post-translational modifications. *O*- and *N*-Glycosylation can be sensed as luminal signals for PM targeting (Scheiffele et al., 1998; Yeaman et al., 1997) while ubiquitination, sensed by the GAT (GGA and Tom1) domain of the GGAs can target the protein to endosomes (Piper and Luzio, 2007; Scott et al., 2004). Phosphorylation of membrane proteins can either generate new sorting motifs or modulate the activity of pre-existing sorting motifs (Bonifacino and Traub, 2003; Hinners and Tooze, 2003).

1.4.4 Sorting mechanisms at TGN- clathrin independent sorting

Additional mechanisms for sorting at the TGN, independent of the clathrin coat, have been identified. One major mechanism involved in sorting cargo proteins to the PM involves the affinity of the cargo proteins for membrane micro-domains enriched in sphingolipids and cholesterol. Arf1-PI4P enriched membranes will further promote the recruitment of lipid-transfer proteins, like OSBP1, CERT and FAPP2 (De Matteis et al., 2007) promoting the formation and enlargement of these lipid micro-domains. The cholesterol and sphingolipids, main components of these “lipid rafts”, coalesce to form a liquid-ordered membrane bilayer for which some proteins, like the glycosyl phosphatidylinositol (GPI)-anchored proteins, present a specific high affinity (De Matteis and Luini, 2008).

One other mechanism important in formation and maintenance of additional distinct TNG sub-domains that contain specific cargo proteins might be regulated by the GRIP-golgins (Derby et al., 2004; Gleeson et al., 2004; John et al., 2005; Kakinuma et al., 2004). A different mechanism that might also work to segregate cargo proteins at TGN is based on the intrinsic properties of the cargo proteins of cargo receptors to oligomerize and produce clusters (Borgonovo et al., 2006; Delphine et al., 2007; Hannan et al., 1993). Finally, the newly identified

yeast coat exomer may function for sorting and budding specialized endosomal cargo from TGN (Wang et al., 2006).

1.5 Brefeldin A

Brefeldin A (BFA), a fungal metabolite, has a profound effect on the secretory pathway in eukaryotic cells. Initial experiments established that BFA reversibly blocks traffic of proteins like VSVG to the cell surface in mammalian cells (Misumi et al., 1986). Subsequent studies uncovered that treatment with BFA produced rapid and complete disassembly of the Golgi complex and redistribution of Golgi enzymes to the ER (Lippincott et al., 1990; Lippincott et al., 1989). It was observed that within one minute of BFA treatment Arf1 and COPI dissociate from Golgi membranes (Donaldson et al., 1991; Donaldson et al., 1990; Orci et al., 1991; Robinson and Kreis, 1992). Clathrin adaptor proteins AP-1, 3, 4 and GGAs dissociate from the Golgi complex and endosomal membranes in about the same time frame after BFA treatment (Robinson, 2004). Interestingly, BFA treatment causes the Golgi complex to part into the Golgi stack that redistributes to the ER, and the TGN that fuses with early endosomes (Klausner et al., 1992).

Further analysis revealed that BFA specifically inhibits nucleotide exchange on Arf1 (Donaldson et al., 1992b; Helms and Rothman, 1992). The GEF activity of a large number of ArfGEFs, including Gea1p, Gea2p, Sec7p, GNOM/Emb30, BIG1 and BIG2, has now been shown to be inhibited by BFA (Cox et al., 2004; Jackson and Casanova, 2000). While kinetic analysis established that BFA acts as an uncompetitive inhibitor (Mansour et al., 1999), crystallographic studies revealed that BFA inserts at the interface between the Arf and the Sec7 domain preventing GDP displacement and locking the Arf-GDP-BFA-Sec7d into an abortive complex (Mossessova et al., 2003; Renault et al., 2002; Renault et al., 2003; Zeghouf et al., 2005). These data suggest that *in vivo* treatment of cells with BFA should be followed by formation and accumulation of a stable complex between the ArfGEF and the effector Arf. However, recent experiments from our lab could not detect an accumulation of these complexes (Chun et al., 2008). While BFA does not discriminate between the GBF1 and the

BIGs, a specific inhibitor of GBF1 function, golgicide A, was recently described (Saenz et al., 2009).

1.6 Arf1 and Arf3 - specific vs. redundant functions

With the exception of Arf6 that acts exclusively at the PM and endosomes, little is known of the specific function of Arf1-5 (D'Souza-Schorey and Chavrier, 2006). The multiple Arfs present on the Golgi complex could contribute to specificity if they localized to distinct compartments or interacted with unique effectors. Taylor *et al.*, provided the initial evidence for distinct biochemical properties between Arf1 (GGBF) and Arf3 (GGBF*), indicating that Arfs may play non-redundant roles at the Golgi complex (Taylor *et al.*, 1992). It is striking how the authors had the insight to write at the end of the discussion: “we speculate that GGBF and GGBF* may direct assembly of coats from different organelles such as the Golgi and the trans Golgi network”. Unfortunately, several follow-up studies failed to support this hypothesis and suggested instead that Arf3 and Arf1 play redundant roles at the Golgi complex, redundancy supported by the 96% sequence identity and similar localization (Hosaka et al., 1996; Kawamoto et al., 2002). For example, multiple Arf3 effectors were identified, including Arfaptin 1, Arfaptin 2 (Kano et al., 1997), mitotic kinesin-like protein 1 (MKLP1) (Boman et al., 1999) and phospholipase D (PLD) (Cockcroft et al., 1994), but none of these discriminated between Arf1 and Arf3. Furthermore, *in vitro* and *in vivo* studies established that the Golgi-localized GEFs GBF1 or BIGs could activate equally Arf1 and Arf3 (Islam et al., 2007; Kawamoto et al., 2002; Morinaga et al., 1999; Shin et al., 2004; Togawa et al., 1999). Lastly, Donaldson and colleagues identified a centrally located MXXE motif, present in all Class I Arfs, that targets Arf1 to its receptor membrin on *cis*-Golgi membranes and should target Arf3 similarly (Honda et al., 2005).

Even though the majority of data to date suggest that Arf1 and Arf3 perform redundant roles and localize to similar membranes, more recent observations suggest different functions. In an attempt to identify specific function for each of the Arfs using an shRNA-based approach, Volpicelli-Daley *et*

al., discovered that double knockdown of Arf(1+4) and Arf(3+4) resulted in dramatically different effects (Volpicelli-Daley *et al.*, 2005). More recently, Chun *et al.*, reported that Arf3, unlike Arf1 or class II Arfs, did not localize to ERGIC structures or Golgi compartments containing GBF1 (Chun *et al.*, 2008);(Chun unpublished observations).

1.7 Rationale and objectives for each project

Since the identification of Arfs (Kahn and Gilman, 1984) and their GEFs (Chardin *et al.*, 1996), much progress has been made in understanding their functions in regulating lipid metabolism as well as the recruitment of coat proteins and adaptors (D'Souza-Schorey and Chavrier, 2006; Donaldson, 2003; Myers and Casanova, 2008; Nie *et al.*, 2003). Previous data from our laboratory and other laboratories indicate that GBF1 localizes to the *cis*-Golgi and performs a crucial role in membrane recruitment of COPI by activated Arf1 (Claude *et al.*, 1999; Garcia-Mata *et al.*, 2003; Kawamoto *et al.*, 2002; Monetta *et al.*, 2007; Zhao *et al.*, 2006; Zhao *et al.*, 2002). For the work described in chapter 3, we hypothesized that GBF1 and BIGs must have different functions since they have distinct sub-cellular localizations and co-localize with different coat proteins. Using a combination of overexpression and knockdown experiments, we examined GBF1 and BIGs function in Golgi stack and TGN organization, membrane recruitment of specific coat proteins, as well in cargo progression through the secretory pathway.

The large majority of available data regarding Arf1 and Arf3 suggest that the two almost identical proteins should function in a redundant fashion (D'Souza-Schorey and Chavrier, 2006). However, a serendipitous observation in our lab that Arf3 may localize to a different compartment than GBF1, as well as a few observations in the literature suggesting that Arf3 might be different than Arf1 (Chun *et al.*, 2008; Taylor *et al.*, 1992; Volpicelli-Daley *et al.*, 2005) encouraged us to hypothesize that Arf3 localizes to the TGN where its activity should be regulated specifically by BIGs. The restricted Arf3 localization and the known effect of temperature shift to 20°C that blocks cargo proteins at TGN led us to

examine the impact of lowering the temperature on Arf3 membrane recruitment. Using a combination of overexpression of different tagged forms, swap chimera and swap mutants of Arf3 and Arf1 we investigated which region and which amino acids are critical for the particular localization pattern and for the temperature (in)sensitivity. We also probed the function of Arf3 and the potential connection between Arf3 and the 20°C temperature block using Arf3 targeted RNAi.

CHAPTER TWO:

MATERIALS AND METHODS

2.1 Reagents

During the course of this work, the chemicals, reagents, enzymes, and commercial kits were used according to the instructions provided by the respective manufacturer unless otherwise stated. All use of reagents was in accordance with procedures set out by the Environmental Health and Safety of the University of Alberta and Workplace Hazardous Materials Information System (WHMIS).

Table 2.1 List and source of chemicals and reagents

Reagent	Supplier
acetic acid, glacial	Fisher Scientific
acrylamide/bis (30%; 29:1)	Biorad
agarose (UltraPure™)	Invitrogen
agarose (UltraPure™; low melting point)	Gibco (Invitrogen)
ammonium chloride	Caledon
ammonium persulfate	Bio-rad
Ampicillin	Novopharm
Bactotryptone	BD
bacto-yeast	BD
Blasticidin	Invitrogen
bovine serum albumin	Sigma
brefeldin A	Sigma
bromophenol blue	Sigma
calcium chloride	BDH
calf intestinal alkaline phosphatase (CIAP)	Invitrogen
CO ₂ -independent medium (- L-glutamine)	Gibco (Invitrogen)
Complete, EDTA-free protease inhibitor cocktail tablets	Roche
deoxycholic acid sodium salt	Sigma
DTT (dithiothreitol)	Fisher Scientific
DMEM (Dulbecco's Modified Eagle Medium)	Gibco (Invitrogen)

DMSO (dimethyl sulfoxide)	Sigma
dNTP (deoxyribonucleotide triphosphate)	Invitrogen
Doxycycline	Sigma
EDTA (ethylenediamine-tetraacetic acid)	Sigma
Fermentas PageRuler™ Prestained Protein Ladder Plus	Fermentas
Fetal bovine serum (FBS)	Gemini Bio-Products
Fibronectin	Sigma
FuGENE 6 transfection reagent	Roche
Gelatine	Fisher Scientific
GeneRuler 1 kb DNA Ladder	Fermentas
Glycerol	Fisher Scientific
Glycine	Roche
hydrochloric acid	Fisher Scientific
Hygromycin	Invitrogen
Igepal CA-630 (NP-4)	Sigma
Isopropanol	Fisher Scientific
Kanamycin	Sigma
L-glutamine	Gibco
magnesium chloride	BDH
magnesium sulphate	Fisher Scientific
Methanol	Fisher Scientific
O-phenathroline	Sigma
Opti-MEM	Gibco (Invitrogen)
Paraformaldehyde	Sigma
penicillin/streptomycin	Gibco (Invitrogen)
PBS (phosphate buffered saline; Dulbecco's)	Gibco (Invitrogen)
phosphate-free DMEM	Invitrogen
Platinum® Pfx DNA polymerase	Invitrogen
Ponceau S	Sigma
potassium chloride	BDH

Precision Plus protein standard	Bio-rad
Prolong® Gold with DAPI antifade reagent	Molecular Probes (Invitrogen)
protein A sepharose CL-4B	GE Healthcare
restriction endonuclease	Invitrogen or NEB
sodium bicarbonate	Caledon
sodium chloride	Fisher Scientific
SDS (sodium dodecyl sulfate)	Bio-rad
sodium fluoride	Sigma
sodium hydroxide	Fisher Scientific
sucrose	Sigma
SYBR Safe DNA gel stain	Molecular probes (Invitrogen)
T4 DNA ligase	Invitrogen
TEMED (tetramethylethylenediamine)	OmniPur
thymidine	Sigma
TransIT-LTI transfection reagent	Mirus
Tris	Roche
Triton X-100	VWR
Trypsin-EDTA	Gibco (Invitrogen)
Tween	Fisher Scientific

Table 2.2 Commercial Kits

Kit	Supplier
Bio-Rad DC Protein Assay	Bio-Rad Laboratories
ECL Plus Western Blotting Detection System	GE Healthcare
GeneJET Plasmid miniprep kit	Fermentas
QIAGEN Plasmid Maxi kit	QIAGEN

QIAGEN Plasmid Midi kit	QIAGEN
QIAprep spin miniprep kit	QIAGEN
QIAquick gel extraction kit	QIAGEN
QIAquick PCR purification kit	QIAGEN

Table 2.3 Commonly used buffers and solutions

Solution	Composition
Luria-Bertani (LB) Broth	1% bactotryptone, 0.5% bacto-yeast extract, 1% (w/v) NaCl, pH 7.0
Paraformaldehyde (3%)	3% paraformaldehyde, 0.1 mM CaCl ₂ , 0.1 mM MgCl ₂
Permeabilization buffer	0.1% (v/v) Triton X-100, 0.05% SDS in PBS
Phosphate buffered saline (PBS)	2.7 mM KCl, 1.5 mM KH ₂ PO ₄ , 137.9 mM NaCl, 8.1 mM Na ₂ HPO ₄
Quench buffer	50 mM NH ₄ Cl in PBS
Running buffer	25 mM Tris-HCl, 190 mM glycine, 0.1% SDS
SDS-PAGE sample buffer (6X)	30% (v/v) glycerol, 1% SDS, 0.6 M DTT, 0.012% bromophenol blue, 70% (v/v) 4X Tris-HCl/SDS buffer, pH 6.8)

Separating gel (4X Tris-HCl/SDS, pH 8.8)	0.4% SDS, 1.5 M Tris-HCl, pH 8.8
SOC medium	2% bactotryptone, 0.5% bacto-yeast extract, 10 mM NaCl, 2.5 mM KCl, 10 mM MgCl ₂ , 10 mM MgSO ₄ , 20 mM glucose
Stacking gel (4X Tris-HCl/SDS, pH 6.8)	0.4% SDS, 0.5 M Tris-HCl, pH 6.8
TAE (50X)	2 M Tris, 5.71% (v/v) glacial acetic acid, 50 mM EDTA, pH 8.0
Transfer buffer	25 mM Tris-HCl, 190 mM glycine, 20% (v/v) methanol, 2.5% (v/v) isopropanol
T-TBS	50 mM NaCl, 0.5% (v/v) Tween-20, 20 mM Tris-HCl, pH 7.5

2.2 Cell culture

The cell lines used for the work described in this thesis include HeLa (ECACC; Sigma-Aldrich, 93021013), NRK-52E cells (ATCC CRL-1571), CHO (Pro⁻⁵; ATCC CRL-1781). The process of obtaining the BFY-1 cell line from the parental CHO Pro⁻⁵ cell line was described by Yan et al., 1994 (Yan et al., 1994). BHK-21 and A549 cells were gifts from Dr. Tom Hobman (University of Alberta, Canada).

Cell monolayers were maintained in Dulbecco's modified Eagle's medium (DMEM) supplemented with 10% FBS, 100 µg penicillin/ml, 100 µg streptomycin/ml and 2 mM *L*-glutamine at 37°C inside a water jacketed incubator

kept at 5% CO₂. For the temperature shift experiments, the medium was changed with CO₂ independent DMEM supplemented with 10% FBS.

2.3 Antibodies

The source and dilution for primary antibodies used in the work for this thesis are listed below in Tables 2.4 and 2.5 for immunofluorescence (IF) and Table 2.6 for immunoblotting. For IF, secondary goat antibodies conjugated with either Alexa Fluor 488, Alexa Fluor 594, Alexa Fluor 555 or Alexa Fluor 660 were purchased from Molecular Probes (Eugene, OR) and used at 1:600 dilution. For immunoblots, proteins were detected using a horseradish peroxidase (HRP)-conjugated goat anti-rabbit IgG or anti-mouse IgG secondary antibody that was purchased from Bio-Rad Laboratories (Mississauga, ON) and used at 1:2500 dilution.

Table 2.4 Polyclonal antibodies used for IF

Antibody	Dilution	Source
anti-BIG1 (9D3)	1:300	(Zhao et al., 2006), (Claude et al., 1999), (Manolea et al., 2008)
anti-BIG2	1:100	Dr. Kazuhisa Nakayama, Kyoto University, Kyoto, Japan
anti-GBF1 (9D2 IgG)	1:400	(Zhao et al., 2006)
anti-GFP	1:2000	Dr. Gary Eitzen; University of Alberta, Edmonton, Canada
anti-mannosidase II	1:800	Dr. Kelley Moremen; University of Georgia, Athens, USA

anti-Sec31	1:500	Dr. Bor Luen Tang; Institute of Molecular and Cell Biology, Singapore, (Tang et al., 2000)
anti-sortilin (goat)	1/200	R&D System
anti-TGN46 (sheep)	1:1000	AbD Serotec, Kidlington, Oxford, UK

Table 2.5 Monoclonal antibodies used for IF

Antibody	Dilution	Source
anti- β -coatomer protein I (clone M3A5)	1:400	Dr. T. Kreis; University of Geneva, Switzerland; (Allan and Kreis, 1986)
anti-AP-1 (clone 88)	1:600	BD Biosciences Pharmigen
anti-Arf1, 3, 4 and 5 (clone 1D9)	1:400	Abcam Inc.
anti-GBF1 (clone 25)	1:400	BD Biosciences Pharmigen
anti-GGA3 (clone 8)	1/200	BD Biosciences Pharmigen
anti-ERGIC-53 (clone G1/95)	1:1000	Dr. Hans-Peter Hauri, Basel University, Switzerland
anti-hemagglutinin (HA) (clone 3F10) *	1:100	Roche Diagnostics (Laval, Canada)

anti-p115 (clone 7D1)	1:1000	Dr. Gerry Waters; Princeton University, Princeton, USA; (Waters et al., 1992)
Anti-VSVG (clone P5D4)	1:250	Dr. Tom Hobman (Kreis and Lodish, 1986)

* This is a rat monoclonal antibody; all others are mouse monoclonal antibodies

Table 2.6 Antibodies used for immunoblotting

Antibody	Dilution	Source
anti-ClassI Arf (clone ARFS 3F1)	1/250	Abcam Inc.
anti-Arf3 rabbit poly.	1/250	Protein Tech Group Inc.
anti- β -coatomer protein I (clone M3A5)	1:3000	Dr. T. Kreis; University of Geneva, Geneva, Switzerland; (Allan and Kreis, 1986)
anti-AP-1	1:5000	BD Biosciences Pharmigen
anti-BIG1 (9D3)	1:1000	(Zhao et al., 2002), (Claude et al., 1999),(Manolea et al., 2008)
anti-BIG2	1:1000	Dr. Kazuhisa Nakayama, Kyoto University, Kyoto, Japan
anti-calnexin	1:20000	Stressgen Biotechnologies

anti-GBF1 9D4 (final bleed)	1:2500	(Manolea et al., 2008)
anti-GGA3	1:5000	BD Biosciences Pharmigen
anti-TGN46	1:2000	AbD Serotec, Kidlington, Oxford, UK

2.4 siRNA methods

Pools and individual siRNAs targeting different regions of human (h) GBF1 (MU-019783), hBIG1 (MU-012207), hBIG2 (MQ-012208), h β -COP (MQ-017940) and hArf3 (LQ-011581) were purchased from Dharmacon. We followed the Oligofectamine (Invitrogen) transfection protocol for HeLa cells as described (Harborth et al., 2001). Different combinations of targeting duplexes, time points, and siRNA concentrations were assessed to optimize conditions for most effective knockdown.

For the experiments presented in this thesis, HeLa cells were incubated with a pool of siRNAs targeting sequences 2 and 3 for GBF1, each at a concentration of 100 nM. For BIGs knockdown, we used a pool of siRNAs targeting sequences 2 and 3 for BIG1 (75 nM each) and 1–4 for BIG2 (50 nM each). For β -COP knockdown we used sequence 2 at 200 nM. For Arf3 we used a pool of siRNAs targeting sequences 6 and 8, each at a concentration of 100 nM. Note that lower siRNA concentrations (50 nM instead of 75 nM for BIG1 and 25 nM instead of 50 nM for BIG2) were sufficient for effective BIGs knockdown (loss of BIG1 and redistribution of AP-1). As control, cells were exposed to matching concentrations (200–300 nM) of a nonspecific GL2 luciferase siRNA designed as described previously (Elbashir et al., 2002).

2.5 Construction of plasmids

2.5.1 Construction of the Anti-GBF1, -BIG1, and -BIG2 short hairpin RNA-expressing pSUPER-tet Plasmids

To create an inducible form of pSUPER (OligoEngine, Seattle, WA, USA) under the control of the *tet* repressor, Javier Rosas replaced the promoter sequence of this plasmid with the promoter of the pTER plasmid (Clontech, Mountain View, CA). Briefly, a 2498-base pair fragment between the HindIII and BamHI sites from pTER was first amplified by PCR and cloned into the pGEM-T Easy vector (Promega, Madison, WI) using overhanging 3' deoxyadenine residues. A 1537-base pair fragment containing the promoter with the *tet* repressor sequence was then liberated with HindIII and AflIII and used to replace the pSUPER promoter using the same restriction sites. The resulting pSUPER-tet plasmid was verified by sequencing.

To generate Arf-GEF-targeting plasmids, pSUPER-tet was linearized by double digestion with HindIII and BglII and synthetic 60-base pair oligomers encoding the desired short hairpin RNA (shRNA) sequences were ultimately inserted using these restriction sites. The double-stranded oligo sequences were designed with cohesive BglII and HindIII sites: (5') GATCCCCTTCAAGAGAYYYYYYYYYYYYYYYYYTTTTTA (3') where the 19-nucleotide X and Y residues corresponded to the target sense and antisense sequences identified by Dharmacon (Lafayette, CO) as likely candidates for siRNA-mediated silencing of GBF1, BIG1, and BIG2 expression. All constructions were verified by sequencing. Plasmids were transfected into HeLa cells using 1 µg of plasmid per well of a six-well dish, and cells were fixed after 96 h to allow an extra 24 h for expression and processing of shRNAs.

2.5.2 Arfs tagged with GFP and mCherry

The construction of the plasmids encoding Arf1 and Arf3 tagged with either GFP or mCherry has been previously described (Chun et al., 2008).

2.5.3 Arf3 untagged or tagged with HA

We constructed the vectors to allow inducible expression of untagged Arf3 or tagged with the HA epitope. To allow unidirectional cloning of the Arf3 cDNA from pEGFP-N1 into pcDNATM4/TO vector (Invitrogen), the MCS in

pcDNATM4/TO had to first be flipped in the opposite orientation. This was achieved by digesting with PmeI (which cuts bluntly at both ends of the MCS) and re-ligating the isolated MCS fragment. Plasmids with the reversed MCS within the new pcDNATM4/TO(-) vector were identified by screening for the release of a 502 base pair band using NdeI and XbaI.

For the construction of the plasmid encoding untagged Arf3, Zoya Shapovalova used appropriate forward and reverse primers to perform PCR and lift the Arf3 cDNA found in a pET21d vector (Berger, 1998). The reverse primer maintained the stop codon and KpnI site while the forward primer included a XhoI site. The PCR fragment was cleaved with KpnI and XhoI and ligated into similarly cut pcDNATM4/TO(-) vector. The construction of the HA tagged Arf3 was performed in two steps. First, Zoya Shapovalova modified pcDNATM4/TO(-) vector (Invitrogen) by inserting annealed oligos encoding the HA tag at the 3' end of the MCS between the KpnI and HindIII sites. A stop codon was introduced after the HA sequence. In the second step, a PCR fragment encoding Arf3 was ligated into the newly modified pcDNATM4/TO(-)-HA vector digested with XhoI and KpnI to generate a cDNA with Arf3 in frame with the HA tag at the C-terminus of the protein.

2.5.4 Swap chimeras and mutants between Arf3 and Arf1

Arf1_3 and Arf3_1 swap chimeras that contain the N and C-terminal part of each Arf were constructed using PCR. The primers were designed as follows. For the forward primer, an XhoI site was included at the 5' end for insertion in the plasmid and three additional bases included to facilitate cleavage after PCR reaction. A total of 20 nucleotides were included after the last mismatch. Reverse primers were constructed following the same rules as for forward primers except that a KpnI site was now included at the 3' end. PCR reactions were performed using a plasmid encoding Arf3 as template. The resulting PCR products were digested with XhoI and KpnI and ligated into either similarly cut pEGFP-N1 vector to yield Arf1_3-GFP and Arf3_1-GFP. In order to obtain Arf1_3 and Arf3_1 tagged with HA Ian Clarke digested the Arf1_3-GFP and Arf3_1-GFP plasmids using

XhoI and KpnI to release the Arf3/1 chimeras. These inserts were cloned into similarly cut pcDNATM4/TO(-)-HA vector to yield Arf1_3-HA and Arf3_1-HA.

For the construction of Arf3FF (L9F/I13F) and Arf1LI (F9L/F13I) double mutants we used also a PCR approach. As before, the forward primers included an XhoI site at the 5' end for insertion in the plasmid, 3 extra nucleotides at 5' end to facilitate cleavage after PCR reaction and an additional 20 nucleotides after the last mismatch. The reverse primers were the same reverse primers used for the construction of the Arf3/Arf1 chimera. The resulting PCR products were digested with XhoI and KpnI and ligated into similarly cut pEGFP-N1 vector to yield Arf3FF-GFP and Arf1LI-GFP.

For the construction of Arf3A174S or Arf3K180Q single mutants we used also a PCR approach. As before, Ian Clarke performed PCR reactions using Arf3 as template, a standard Arf3Nfor as a forward primer and either Arf3CSrev or Arf3CQrev reverse primers bearing the point mutations A174S and K180Q, respectively. The resulting PCR products were digested with XhoI and KpnI and ligated into similarly cut pEGFP-N1 vector to yield Arf3A174S-GFP and Arf3K180Q-GFP.

Table 2.7 Primers used for molecular cloning

Primer Name	Sequence	Construct
Arf3for	TAT ACC ATG GGC AAT ATC TTT GGA AAC CTT CTC AAG AGC CCA CTC GAG ACC ATG GGC AAT ATC TTT GGA AAC	Arf3 untagged in pcDNA 4/TO
Arf3rev	ACC GAC CGG TTA GTC GAG TTT TTG TTC TTC ACT CCA TGG ACAC	Arf3 untagged in pcDNA 4/TO
HAfor2	CTT ACC CAT ACG ATG TTC CAG	pcDNA 4/TO(-)-

	ATT ACG CTT A	HA
HArev2	AGC TTA AGC GTA ATC TGG AAC ATC GTA TGG GTA AGG TAC	pcDNA 4/TO(-)- HA
Arf3for	CCA CTC GAG ACC ATG GGC AAT ATC TTT GGA AAC CTT CTC AAG AGC CTG ATT	Arf3/1 chimera
Arf1for	CCA CTC GAG ACC ATG GGC AAT ATC TTT GCA AAC CTT TTC AAG GGC CTG TTT	Arf3/1 chimera
Arf3Crev	CAC AGG TAC CGC CTT CTT GTT TTT GAG CTG ATT GGC CAG CCA GTC CAG GCC TTC GTA CAG	Arf3/1 chimera
Arf1Crev	CAC AGG TAC CGC CTT CTG GTT TCT GAG CTA ATT GGA CAG CCA GTC CAG GGC TTC GTA CAG	Arf3/1 chimera
Arf3NFFfor	CCA CTC GAG ACC ATG GGC AAT ATC TTT GGA AAC CTT TTC AAG AGC CTG TTT GGG AAG AAG GAG ATG CGC ATC	Arf3FF
Arf1NLIfor	CCA CTC GAG ACC ATG GGC AAT ATC TTT GCA AAC CTT CTC AAG GGC CTG ATT GGG AAG AAG GAG ATG CGC ATC	Arf1LI

Arf3CSrev CAC AGG TAC CGC CTT CTT GTT **Arf3A174S-GFP**
TTT GAG CTG ATT GGA CAG CCA
GTC CAG GCC TTC GTA CAG

Arf3CQrev CAC AGG TAC CGC CTT CTG GTT **Arf3K180Q-**
TTT GAG CTG ATT GGC CAG CCA **GFP**
GTC CAG GCC TTC GTA CAG

2.6 Overexpression of VSVG-tsO45 and other cDNAs, temperature shift experiments

Most experiments were performed with cells grown on glass coverslips either in 6-well plates or 12-well plates purchased from Falcon Plastics (Oxnard, CA). For transient expression from plasmids, cell were grown on coverslips, transfected with the specified amount of each plasmid using either FuGENE 6 (Roche Diagnostics, Indianapolis, IN) or TransIT-LTI transfection reagent (Mirus, Madison, WI) according to manufacturer's instructions. Transfected cells were further cultured for the specified amount of time prior to fixation.

The vesicular stomatitis virus glycoprotein (VSVG)–GFP encoding plasmid was a kind gift from Dr. John F. Presley (McGill University, Montreal, QC, Canada). A VSVG-tsO45 virus stock was obtained from Dr. William Balch (Scripps Institute, La Jolla, CA) and grown into a working stock by infection of BHK cells at low multiplicity of infection. Measurement of VSVG traffic in siRNA-treated cells involved separate transfections steps and various combinations of temperature shifts, as illustrated in Figure 3.8. Briefly, HeLa cells plated at ~15% confluency were transfected with the appropriate siRNA duplexes 24 h later. For VSVG-tsO45-GFP expression, knockdown cells were washed 50 h after siRNA addition, transfected again with 1 µg of VSVG-encoding plasmid, and returned to a 37°C incubator for a further 18 h. These cells were then transferred to a 40°C water-jacketed CO₂ incubator for 4 h, followed by shift to the permissive temperature 32°C for various lengths of time. This shortened

incubation at 40°C minimized cellular stress and proved sufficient to accumulate newly synthesized VSVG-protein in the ER. The 32°C incubation was performed in a water bath and required the use of CO₂ independent media (Invitrogen). Cells were fixed at different time points after shift to 32°C, as specified (Figures 3.8A, 3.9, 3.13, 3.14 and 4.17). For experiments shown in Figure 3.8B, cells were transferred directly from 37 to 32°C to bypass the temperature shift to 40°C while for experiments for the Figure 4.17 the cells were shifted to either 20°C or 32°C. For experiments involving live virus, cells were infected with VSVtsO45 1 h before being shifted to 40°C as described previously (Zhao et al., 2006). VSVG was detected using a mouse monoclonal antibody (Kreis and Lodish, 1986). VSVG-GFP was detected either directly using intrinsic GFP fluorescence or by IF using a combination of antibody raised against GFP and ALEXA488-conjugated secondary antibody. The latter method yielded stronger and more stable signal that permitted analysis of cells with low to moderate levels of VSVG in order to avoid artefacts due to overloading the ER with unfolded proteins.

For the 20°C temperature block experiments, the cells were either fixed directly from the incubator for the 37°C condition or shifted to 20°C. For the latter condition cells were washed and incubated in room temperature CO₂ Independent Media (Invitrogen) and kept at 20°C in a water bath for the indicated time. Then the cells were fixed with 3% PFA at 20°C for the first 5 minutes and then for another 15 minutes at 37°C.

For the monensin treatment experiments, HeLa cells grown to ~60% density were transfected with 2 µg plasmid encoding GalT-GFP per 60-mm plate. After 24 h, cells were replated on glass coverslips at ~15% confluency and transfected with the appropriate siRNA duplexes 24 h later. 72 hours after siRNA transfection, cells were treated with either 4 µM monensin or equivalent volume of methanol for the periods of time specified and then fixed and processed for IF.

For Arf-GEF overexpression studies (Figures 3.1 and 4.5), BHK cells or HeLa cells grown on glass coverslips to ~50% density were transfected with 1 µg of purified pCEP4 vector plasmid encoding either GBF1 (Claude et al., 1999) or BIG1 (Mansour et al., 1999), using FuGENE 6 according to the manufacturer's

instructions. For exogenous expression of Golgi markers, HeLa cells were cotransfected with 1 μg of plasmid encoding HA-furin that was obtained Dr. J. Bonifacino (Cell Biology and Metabolism Branch, NIH, Bethesda, MD). 24 hours after transfection, cells were briefly treated with 10 μM or 5 $\mu\text{g}/\text{ml}$ BFA or an equivalent volume of DMSO, fixed, and processed for IF using the indicated antibodies.

2.7 Immunofluorescence staining

The IF procedure was carried out on cells grown on glass coverslips sterilized by ethanol and flaming. After drug treatment (if any drug treatment was necessary), cells were washed once with PBS and fixed with 3% paraformaldehyde (with 100 μM calcium chloride and 100 μM magnesium chloride in PBS) at either 37°C or 20°C for 20 min. Fixation was terminated by incubation with quench buffer (50 mM ammonium chloride in PBS) for 10 min and this was followed by incubation with a permeabilization buffer (0.1% Triton X-100 in PBS). When cells were stained using the M3A5 (COPI) antibody 0.05% SDS was added to the permeabilization buffer. Prior to incubation with antibodies, cells were blocked using three, 5 min incubations with 0.2% gelatin in PBS. Cells double labelled with mouse and rabbit antibodies were processed in a similar fashion as described before (Zhao *et al.*, 2002).

2.8 Fluorescence microscopy

2.8.1 Epifluorescence microscopy

Epifluorescence images were obtained using an Axioskop II microscope (Carl Zeiss, Thornwood, NY) equipped with a 63X objective (plan-Apocromat, NA=1.4) and a CoolSNAPHQ monochrome CCD Photometrics camera (Tucson, AZ). The images were exported as 12 bit images using Image Pro 5.1.

2.8.2 Confocal microscopy

Confocal images were obtained with a LSM 510 microscope (Carl Zeiss) equipped with a 63 \times objective (NA=1.4) using 488 nm laser excitation and a 500-

550 nm bandpass filter for Alexa488 and GFP, 543 nm laser excitation and a >560 nm longpass filter for Alexa594. When two markers were imaged in the same cells, each fluorophore was excited and detected sequentially (multitrack mode) to avoid channel bleed-through. Laser intensity and filters were adjusted to give maximum signal but avoid saturation (grayscale intensity of 255). Tests confirmed that under our detection conditions, images obtained in the red and green channels were in register to within 60 nm. Unless otherwise indicated, a single focal plane (0.8-1 μm) was analyzed.

2.9 Image quantification and analysis

2.9.1 Quantification of fluorescence signal overlap for VSVG-positive peripheral structures and ERGIC53 or Sec31 staining

Quantification of the extent of signal overlap between VSVG-GFP-positive peripheral puncta and either ERGIC53 or Sec31 (Figure 3.10) was performed essentially as previously described (Zhao *et al.*, 2002). Briefly, NIH Image J was used to generate separate masks for the green and red signal using a range of threshold values that retained all discernable peripheral structures. At least 5 cells were analyzed for each pair. Results are expressed as percentage of total spots chosen for analysis in the green mask that were concentric with spots in the red mask.

2.9.2 Quantification of Golgi complex polarization by line profile analysis

For Figure 3.16, to examine the relative signal distribution between a *cis*-Golgi marker (p115 or GBF1) and a *trans*-Golgi marker (GalT-GFP) within a single stack, we selected red and green structures of similar intensity that clearly appeared contiguous and in close proximity (less than 0.8 μm). The line profile analysis was performed using Image-ProPlus Software (Media Cybernetics, Silver Spring, MD). Efficient BIGs knockdown was confirmed by either redistribution of BIG1 or AP-1 juxtannuclear staining.

2.9.3 Quantification of VSVG trafficking

To quantitate the impact of BIGs knockdown on VSVG trafficking shown in Figure 3.14, we scored for the presence of VSVG at Golgi only (\circ , \bullet) or at Golgi

and PM (Δ, \blacktriangle) at each time point after release for both Mock (\bullet and \blacktriangle , solid line) and BIGs knockdown (\circ and Δ , dashed line) cells. Efficient BIGs knockdown was confirmed by redistribution of BIG1 juxtannuclear staining. A minimum of 25 cells were analysed for each condition. The fraction of cells with the indicated pattern was expressed as percentage and is shown as a function of time after shift down to 32°C.

To quantitate the impact of temperature shift to 20°C on VSVG trafficking shown in Figure 4.17, we scored for the presence of VSVG at ER only (white bars), Golgi only (hatched bars) or at Golgi and PM (black bars) at each time point after release from 40°C block for both 32°C (control) and 20°C shifted cells. A minimum of 25 cells were analysed for each condition. The fraction of cells with the indicated pattern was expressed as percentage and is shown as a function of time after shift down from 40°C.

To quantitate the impact of Arf3 knockdown on VSVG trafficking shown in Figure 4.17, we scored for the presence of VSVG at ER only (white bars), Golgi only (hatched bars) or at Golgi and PM (black bars) at each time point after release for both Mock knockdown and Arf3 knockdown cells. A minimum of 25 cells were analysed for each condition. The fraction of cells with the indicated pattern was expressed as percentage and is shown as a function of time after shift down to 32°C.

2.9.4 Quantification of the protective effect of BIG1/GBF1 overexpression on Arf3-GFP membrane recruitment after short BFA treatment

To examine the impact of BIG1 or GBF1 overexpression on Arf3-GFP membrane recruitment after short BFA treatment shown in Figure 4.5, we scored for the presence or absence of Arf3-GFP at the Golgi in cells overexpressing either BIG1 or GBF1 following 2 min treatment with 5µg/ml BFA. The bars represent the percentage of cells with Arf3 still localized to the Golgi complex in cells overexpressing either BIG1 or GBF1. A minimum of 30 cells were analysed for each condition from at least four separate experiments.

2.9.5 Quantification of Arf3/Arf1 redistribution after BIGs knockdown

To quantitate the impact of BIGs knockdown on Arf3 or Arf1 membrane recruitment reported in Fig 4.6, we scored for the presence or absence of Arf3 or Arf1 at the Golgi in cells with BIGs knockdown or cells treated with Mock siRNAs. Efficient BIGs knockdown was measured by redistribution of AP-1 juxtannuclear staining. The bars represent the percentage of cells with Arf3 (black bars) or Arf1 (hatched bars) localized to the Golgi complex, either in cells with BIGs knockdown or with Mock knockdown.

2.9.6 Quantification of fluorescence signal overlap

Quantification of the extent of signal overlap between p115 and GalT-GFP, GBF1 and GalT-GFP (Figure 3.16), Arf3-GFP with either BIG1, GBF1 or p115, Arf3-HA with either BIG1 or GBF1, Arf3 (-mCherry or -HA or untagged) with GalT-GFP (Figures 4.1 and 4.2), Arf1₃-GFP with either GBF1, p115 or BIG1, Arf3₁-GFP with either GBF1, p115 and BIG1 (Figure 4.15), Arf3(A174S)-GFP with either p115 and TGN46 and Arf3(K180Q)-GFP with either p115 and TGN46 (Figure 4.16) was performed in a very similar fashion for each pair using Metamorph software (version 6.1). For both markers the areas corresponding to the Golgi complex were identified by using an inclusive threshold set to contain total membrane signal. In order to eliminate background noise signal outside of the Golgi area, a median filter of 2 pixels was applied when necessary. Next, the integrated signal intensity for each marker was determined by the software. Finally, the degree of colocalization was reported as a percentage of overlap between the integrated intensity for the first marker overlapping with the second marker.

2.9.7 Quantification of Arf3-GFP fluorescence signal intensities at the Golgi complex

The distribution of Arf3-GFP (Figure 4.10) was quantified using Metamorph software (version 6.1). The GFP signal intensity at the Golgi complex was quantified by first manually tracing a region of interest around juxtannuclear GFP-positive structures excluding as much as possible the nonspecific signal between the ribbons and then measuring the integrated signal intensity within this area. Subsequently, the signal intensity for the whole cell

was quantified by manually drawing a region of interest around the whole cell and then measuring the integrated signal intensity. In order to determine the background intensity we first drew a round region with an area of approximately the same size as a nucleus in a region where no cells were present. Subsequently we calculated the mean background intensity per pixel by dividing the integrated signal intensity to the number of pixels present in this specific area. Next, to be able to calculate the background intensity for both the Golgi complex and the whole cell the mean background intensity per pixel was multiplied with the number of pixels in both of these areas. Each of these values for total background intensity were subtracted from the initial integrated signal intensity value to obtain the final estimate for background corrected integrated signal intensity at the Golgi and for the whole cell. At least 20 cells were analyzed for each time point for each experiment. The integrated intensities and respective areas were exported to Microsoft Excel in order to calculate the background corrected values that were then expressed as the ratios of Arf3 signal at the Golgi complex relative to total GFP signal. Ratios were plotted for each temperature shift experiment as a function of time.

2.10 Preparation of cell extracts and analysis by RT-PCR and immunoblots

2.10.1 Analysis by RT-PCR

For RT-PCR analysis (Figure 3.2), $1-2 \times 10^6$ cells grown in each well of a six-well plate were trypsinized, washed, and processed using the RNeasy kit according to manufacturer's instructions (Qiagen, Chatsworth, CA). Recovered RNA was analyzed using Qiagen one-step RT-PCR kit according to manufacturer's instructions using gene-specific primers. PCR conditions and cycle numbers were optimized for each primer pair to yield single products of expected size whose level varied in proportion to the amount of RNA added.

2.10.2 SDS-polyacrylamide gel electrophoresis

Proteins samples were analyzed by electrophoresis on tris-glycine SDS polyacrylamide gels (SDS-PAGE) calibrated with pre-stained molecular weight standards (Bio-Rad Laboratories or Fermentas). Prior to SDS-PAGE sample

buffer addition small aliquots of each sample were used to determine the protein concentration using the Bio-Rad DC Protein Assay kit. Frozen cell lysates, previously treated with SDS-PAGE sample buffer, were re-heated for 5 minutes at 95°C and subjected to centrifugation for 1 min at 13,000 rpm at room temperature. 75 µg of each sample was loaded per lane on either a 7.5% (Figure 3.3) or a 15% (Figures 4.18 and 4.19) slab SDS gel. Samples were separated on a 6.5 inch wide slab gel apparatus (CBS Scientific, Del Mar, CA), first at 70V for 30 min through the stacking gel, then at 120V through the resolving gel.

2.10.3 Immunoblotting

Following separation of samples by SDS-PAGE, protein analysis by immunoblotting was carried out essentially as previously described (Harlow and Lane, 1988). Proteins were transferred to nitrocellulose membranes at 100 V for 2 h or 26 V overnight in a transfer buffer (25 mM Tris-HCl, 190 mM glycine, 20% (v/v) methanol, 2.5% (v/v) isopropanol). Protein transfer was assessed by incubating membranes with Ponceau S (0.1% (w/v) Ponceau S, 5% (v/v) acetic acid) followed by two rinses with Milli-Q ddH₂O. Nitrocellulose membranes were blocked for 1 h in TTBS (50 mM NaCl, 0.5% (v/v) Tween, 20 mM Tris-HCl, pH 7.5) containing 5% skim milk. Membranes were then incubated for 1 h with primary antibodies (see Table 2.6) diluted in TTBS containing 2% milk. Following 3 x 10 min washes with TTBS, the membranes were incubated with HRP-conjugated secondary antibodies (Bio-Rad Laboratories, Hercules, CA) that were detected by enhanced chemiluminescence (ECL) using the ECL-plus system (GE Healthcare) following the manufacturer's instructions. The membranes were exposed to Super RX medical X-ray film (Fujifilm) in a FBXC 810 autoradiography cassette (Fisher Scientific) for different lengths of time to avoid signal saturation and then the films were developed using an X-OMAT 2000A processor (Kodak).

2.11 Analysis of Arf sequences.

Previous phylogenetic analysis identified six supergroups (Hampl et al., 2009; Li et al., 2004), and with the exception of **Rhizaria**, extensive genomic information

is available for each of those supergroups. Upon consultation with Dr. Joel Dacks (University of Alberta), Dr. Paul Melançon elected to search the genome of two representative species from each of those five groups. From **excavata**, were chosen *Giardia lamblia* and *Trypanosoma brucei*; from **chromalveolata**, *Tetrahymena thermophila* and *Toxoplasma gondii*; from **archaeplastida** *Physcomitrellap. (EDQ59057)*, *Chlamydomonas reinhardtii*; from **amoebzoa**, *Dictyostelium discoideum* and from the very diverse **opisthokonta** *Saccharomyces cerevisiae* (a fungus), *Drosophila melanogaster* and *Caenorabhditis elegans* (invertebrates) and finally *Homo sapiens* (a mammal). Proteomes (translated genomes) were queried with HsArf1 using a protein-protein Basic Local Alignment Search Tool (BLASTP) to identify the first Arf. The BLASTP query was then repeated using a syngenic sequence. Single Arf sequences were identified from the following genomes: *Giardia l.* (XM_001704927); *Trypanosoma b.* (XP_827586); *Tetrahymena t.* (XM_001011573); *Toxoplasma g.* (AAF35891); *Physcomitrellap.* (EDQ59057); *Dictyostelium d.* (EAL62820). Two related sequences were identified in *Chlamydomonas r.* that were tentatively identified as class I (CRU27120) and class III Arf (XM_001690841). Arfs sequences from Opisthokonta have been previously analyzed (Li et al., 2004).

CHAPTER THREE:

GBF1 AND BIGS ARE REQUIRED FOR ASSEMBLY AND MAINTENANCE OF THE GOLGI STACK AND *TRANS*-GOLGI NETWORK, RESPECTIVELY

A version of this chapter has previously been published as "*Distinct functions for Arf nucleotide exchange factors at the Golgi complex: GBF1 and BIGs are required for assembly and maintenance of the Golgi stack and TGN, respectively*" Manolea F., Claude A., Chun J., Rosas J. and Melançon P. (2008) *Molecular Biology of the Cell* 19: 523-535.

I generated all the data presented in this chapter with the exception of panels C and D in Figure 3.1 created by A. Claude and panel B in Figure 3.2 produced by L. Channon.

3.1 Overview

We examined the relative function of the two classes of GEFs for ADP-ribosylation factors that regulate recruitment of coat proteins on the Golgi complex. Complementary overexpression and RNA-based knockdown approaches established that GBF1 regulates COPI recruitment on *cis*-Golgi compartments, while BIGs appear specialized for adaptor proteins on the *trans*-Golgi. Knockdown of GBF1 and/or COPI did not prevent export of VSVGtsO45 from the ER, but caused its accumulation onto peripheral vesiculo-tubular clusters. In contrast, knockdown of BIG1 and BIG2 caused loss of clathrin adaptor proteins and redistribution of several TGN markers, but had no impact on COPI and several Golgi markers. Surprisingly, BIGs knockdown prevented neither traffic of VSVGtsO45 to the plasma membrane nor assembly of a polarized Golgi stack. Our observations indicate that COPII is the only coat required for sorting and export from the ER exit sites, while GBF1 but not BIGs, is required for COPI recruitment, Golgi sub-compartmentalization and cargo progression to the cell surface. BIGs appear specialized for clathrin adaptor recruitment and for assembly and maintenance of the TGN.

3.2 Results

3.2.1 GBF1 and BIG1 regulate the recruitment of different coat proteins on the Golgi complex

Several overexpression studies have largely supported functional and selective links between the *cis*-Golgi localized GBF1 and the COPI coat, and on the other hand the *trans*-Golgi localized BIGs and the clathrin adapter AP-1. For example, Nakayama and colleagues established that overexpression of GBF1 overcomes the effects of BFA on Arfs and COPI (Kawamoto *et al.*, 2002). This protective effect appears specific since gross overexpression of GBF1 did not prevent release of the clathrin adapter AP-1 (Figure 3.1B), while even moderate GBF1 overexpression was sufficient to abrogate the effects of BFA on COPI and the *medial*-Golgi marker Man II (Figure 3.1 A and C). As expected from this specificity, overexpression of GBF1, while it overcame the effects of BFA on the Golgi stack (Claude *et al.*, 1999; Kawamoto *et al.*, 2002; Niu *et al.*, 2005; Zhao *et al.*, 2006) (see also Figure 3.1C), did not prevent redistribution of the TGN detected with exogenous HA-furin (Figure 3.1D).

Overexpression of BIGs has effects opposite to GBF1 on stabilization of COPI and clathrin adaptors. Previous work demonstrated that BIG2 overexpression prevented release of the clathrin adaptor AP-1 but not that of COPI (Shinotsuka *et al.*, 2002b). Similarly, BIG1 overexpression did not overcome the effects of BFA on COPI (Figure 3.1A) and the Golgi stack (Figure 3.1C), but did prevent the effects of BFA on the membrane recruitment of the clathrin adaptor AP-1 (Figure 3.1B). Altogether, these results strongly suggest that the two Arf-GEF subfamilies regulate the recruitment of distinct coat proteins on the Golgi complex.

3.2.2 Knockdown of GBF1 confirms its role in regulating assembly of the COPI coat

To examine in more detail the relative function of GBF1 and BIGs in the Golgi complex, we turned to complementary siRNA-based methods to knockdown their expression. RT-PCR analysis established that pools of RNA duplex oligonucleotides targeted to GBF1, BIG1 or BIG2 (Figure 3.2A) effectively and

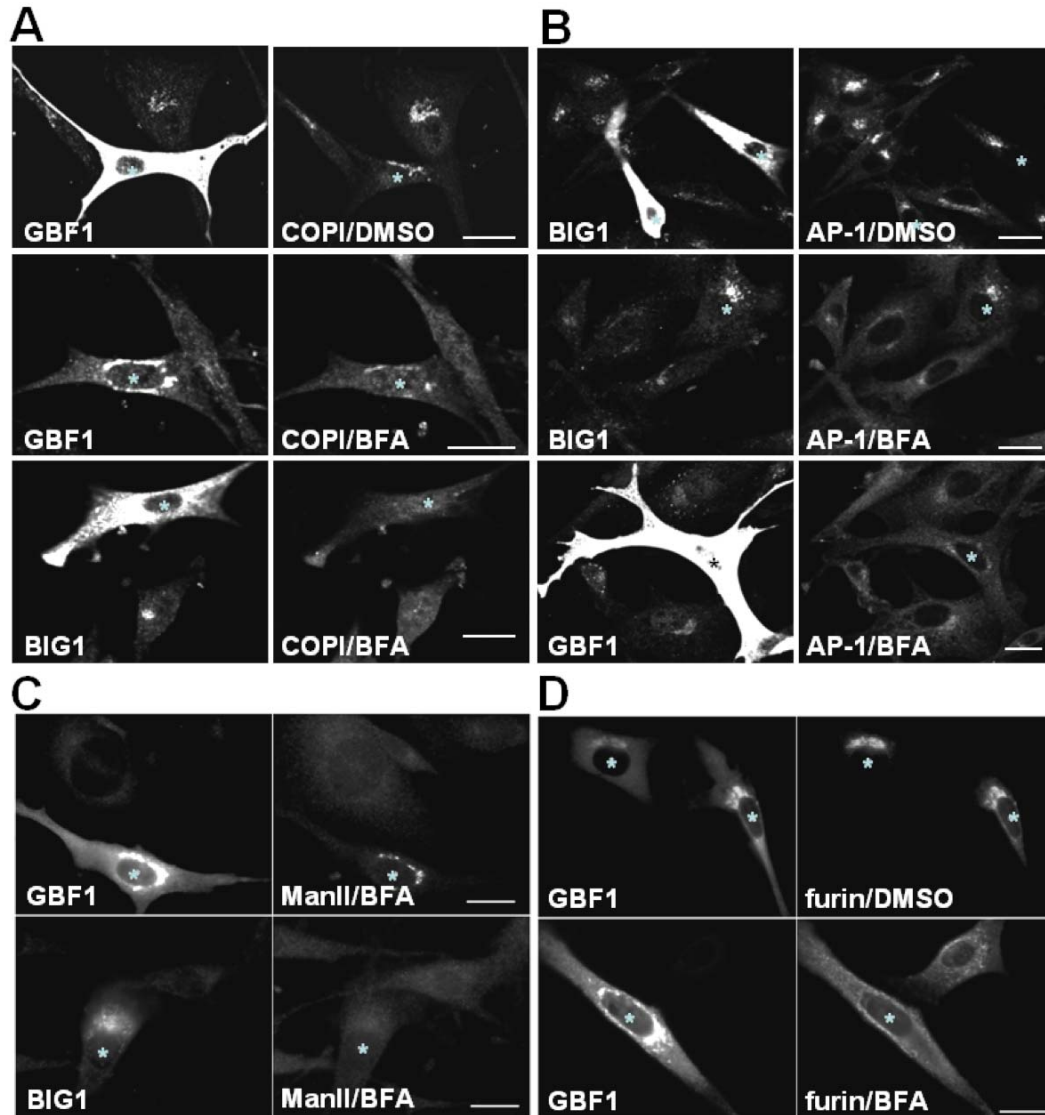


Figure 3.1. Overexpression of GBF1 and BIG1 protect different coat proteins and Golgi sub-compartments from BFA-induced redistribution.

BHK-21 cells were transfected with GBF1 or BIG1 encoding plasmids as indicated (**A**, **B**, **C**) or with an equimolar mixture of GBF1 and HA-tagged furin plasmids (**D**). After 24 h, cells were treated with 10 μ M BFA or an equivalent volume of DMSO for either 2 min (**A**, **B**) or 20 min (**C**, **D**). Following fixation, cells were double stained as indicated for either GBF1 or BIG1, in combination with either COPI (**A**), AP-1 (**B**), ManII (**C**) or HA-furin (**D**). Transfection and immuno-staining were performed as described in Chapter 2. Small asterisks indicate the position of the nucleus of transfected cells. Images shown are representative of more than 2 separate experiments. Bar, 20 μ m.

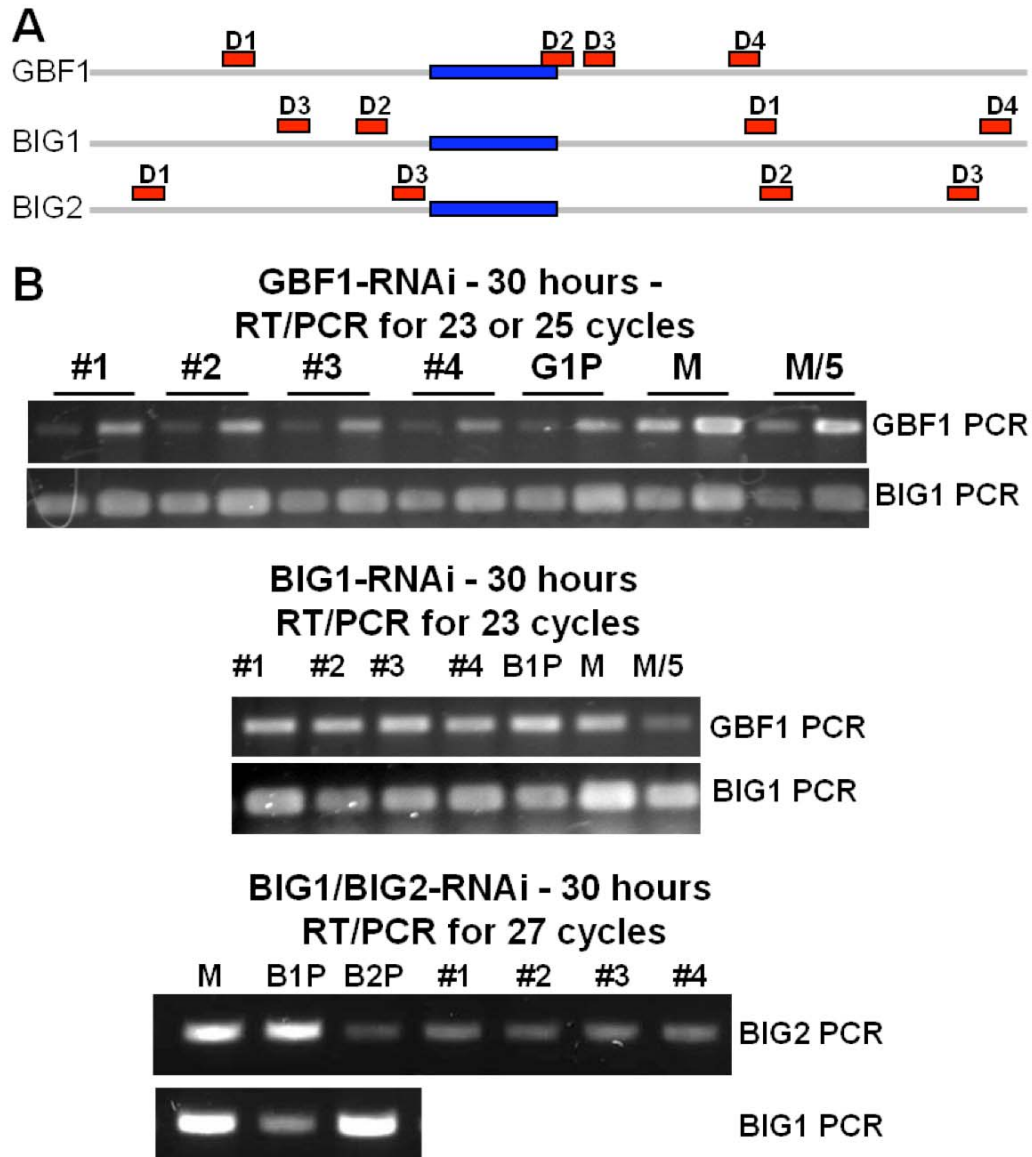


Figure 3.2. Synthetic siRNA oligos yield specific and effective knockdown of GBF1, BIG1, and BIG2 by RT-PCR analysis.

A. Diagram illustrating the relative positions of duplexes obtained from Dharmacon. Sec7 domain in blue. **B.** HeLa cells were mock-transfected (M) or transfected with 100 nM of either individual siRNAs or a pool of all four RNAs (P). polyA RNA was isolated 30 hour post-transfection and RT-PCR reactions were performed with GBF1 or BIG1 or BIG2 specific primers. Some PCR reactions were performed with 1/5 as much RNA obtained from mock -transfected cells or GBF1 siRNAs treated cells.

selectively knocked down mRNA levels by more than 90% within 30 h of transfection (Figure 3.2B). Analysis of cell extracts by immuno-blotting established that GBF1 knockdown efficiently reduced GBF1 levels with no detectable effect on either β -COP, calnexin, BIGs or other TGN markers examined (Figure 3.3). Similarly, BIGs knockdown reduced BIGs protein levels with no detectable effect on AP-1, GGA3, TGN46, β -COP, GBF1 or calnexin (Figure 3.3). To further establish specificity of the knockdown, we individually tested several RNA duplexes targeting different regions of the GEFs. With the exception of BIG1 #1, all individual duplexes yielded knockdown comparable to the pools; nevertheless, two each of the GBF1 (#2 and #3), BIG1 (#2 and #3) and BIG2 (#1 and #3) targeted RNA duplexes appeared most effective (Figure 3.4) and were selected for further analysis. Vectors encoding both GFP and short hairpin RNAs corresponding to those sequences were constructed. Analysis of transfectants readily identified in the GFP channel confirmed that each RNA sequence effectively suppressed expression of the targeted Arf-GEF (Figure 3.5).

The availability of duplexes that effectively and selectively knockdown Golgi-localized Arf-GEFs allowed us to examine their function in more detail. As shown in Figure 3.6, A and B, GBF1 knockdown abrogated juxta-nuclear localization of COPI in the vast majority of RNA-treated cells. Quantitative analysis confirmed that treatment of monolayers with GBF1-targeted RNA duplexes for 72 hours eliminated juxta-nuclear staining for COPI in greater than 90% of transfected cells (110 cells counted in 3 separate experiments). In some cases, particularly at shorter times post RNA-transfection, GBF1 knockdown was partial and resulted in appearance of several dispersed Golgi fragments showing no or weak GBF1 staining and some residual COPI (Figure 3.7). For this reason, complete loss of detectable membrane-associated COPI was used routinely as a more sensitive measure of effective GBF1 knockdown.

Previous observations with BFA or GDP-arrested mutant forms of Arf1 (Dascher and Balch, 1994) predict that lack of COPI recruitment should not impact the function of the COPII coat at ERES but eventually lead to loss of detectable Golgi structures. As expected, GBF1 knockdown (confirmed by loss

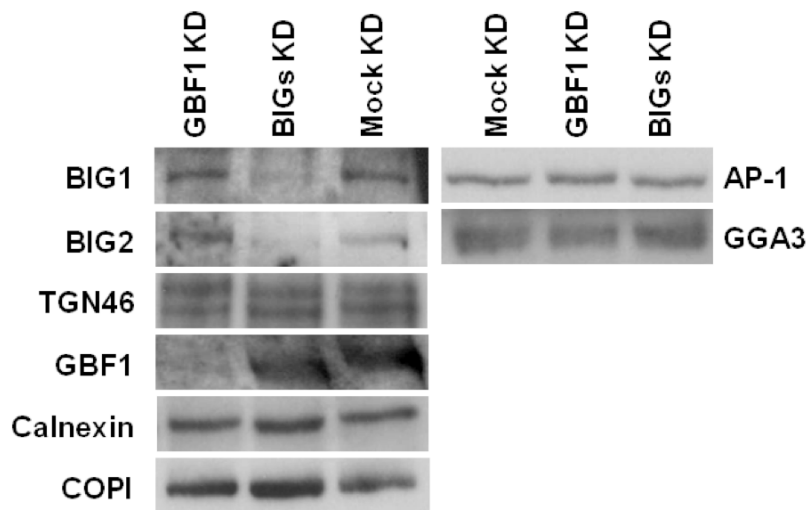


Figure 3.3. Western blot analysis confirms effective and specific knockdowns of GBF1 and BIGs

HeLa cells were transfected with siRNAs targeting either GBF1, or both BIG1 and BIG2 for 72 h as described in Chapter 2. Detergents lysates were prepared and equal amounts of total protein were separated on a 7.5% SDS-PAGE gel. Following transfer to a nitrocellulose membrane, blots were probed with the indicated antibodies. GBF1 KD efficiently reduced GBF1 levels with no detectable effect on either β -COP, calnexin, BIGs or the other TGN markers examined. Similarly, BIGs KD reduced BIG1 and BIG2 levels with no detectable effect on AP-1, GGA3, TGN46, β -COP, GBF1 or calnexin. Blots shown are representative of 3 separate KD experiments.

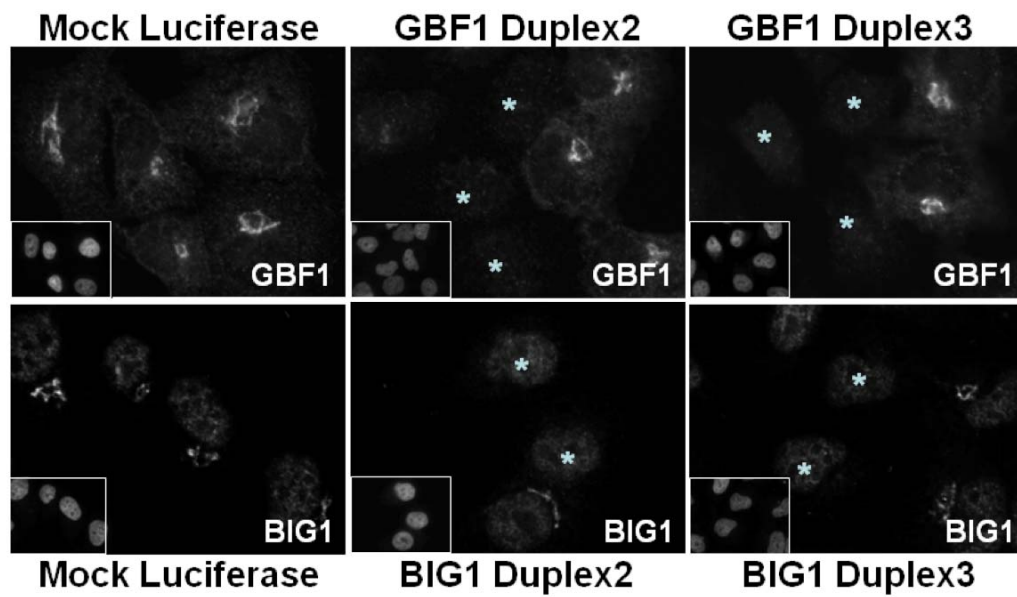


Figure 3.4. Effective knockdown of GBF1 and BIG1 using synthetic siRNA oligos.

HeLa cells were transfected with individual duplexes targeting either GBF1 or BIG1 as described in Chapter 2. Cells were fixed 72 hours post-transfection and stained for GBF1 or BIG1. Transfectants marked with asterisk. Insets show DAPI staining. Images are representative of at least 3 separate KD experiments.

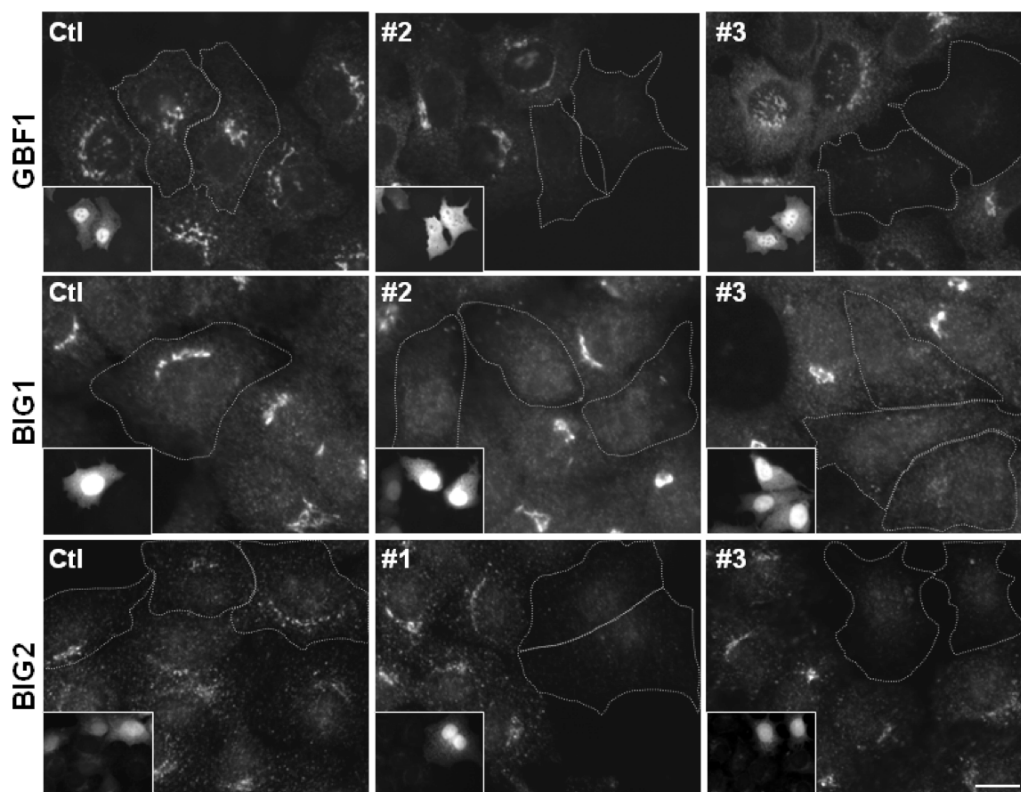


Figure 3.5. Specific and effective knockdown of GBF1, BIG1, and BIG2 using siRNA sequences expressed from pSUPER vector.

HeLa cells were transfected with 1 μ g of GFP-encoding pSUPER plasmids modified with a tet repressor regulated cassette driving expression of either nothing (Ctl) or various individual shRNAs targeting GBF1, BIG1, or BIG2 (see Chapter 2 for construction details). After 96 h, cells were fixed and stained for the markers indicated on the left. Outlines mark GFP-positive transformed cells that were identified in the green channel (shown in inset). Images shown are representative of at least 3 separate experiments. Bar, 20 μ m.

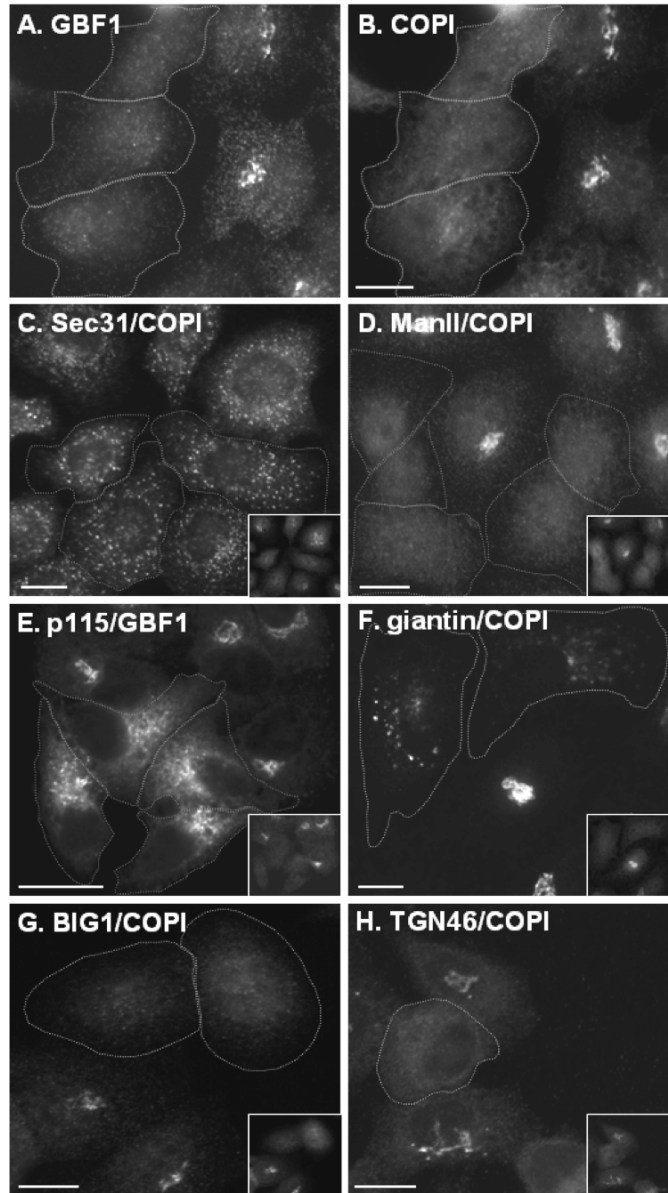


Figure 3.6. Knockdown of GBF1 prevents assembly of the Golgi complex.

HeLa cells were transfected with an equimolar mixture of GBF1-targeting siRNA duplexes #2 and #3 as described in Chapter 2. After 72 h, cells were fixed and double-stained for the markers indicated. Top panels (A, B) show the pattern observed with GBF1/COPI double-staining. The remaining panels (C-H) display the distribution of various ERES (Sec31), Golgi (ManII, p115, giantin), and TGN (BIG1, TGN46) markers, with the inset showing the pattern obtained with the second marker (GBF1 or COPI). Cells with effective KD (loss/redistribution of GBF1/COPI) were outlined. Images shown are representative of at least 3 separate experiments. Bar, 20 μ m.

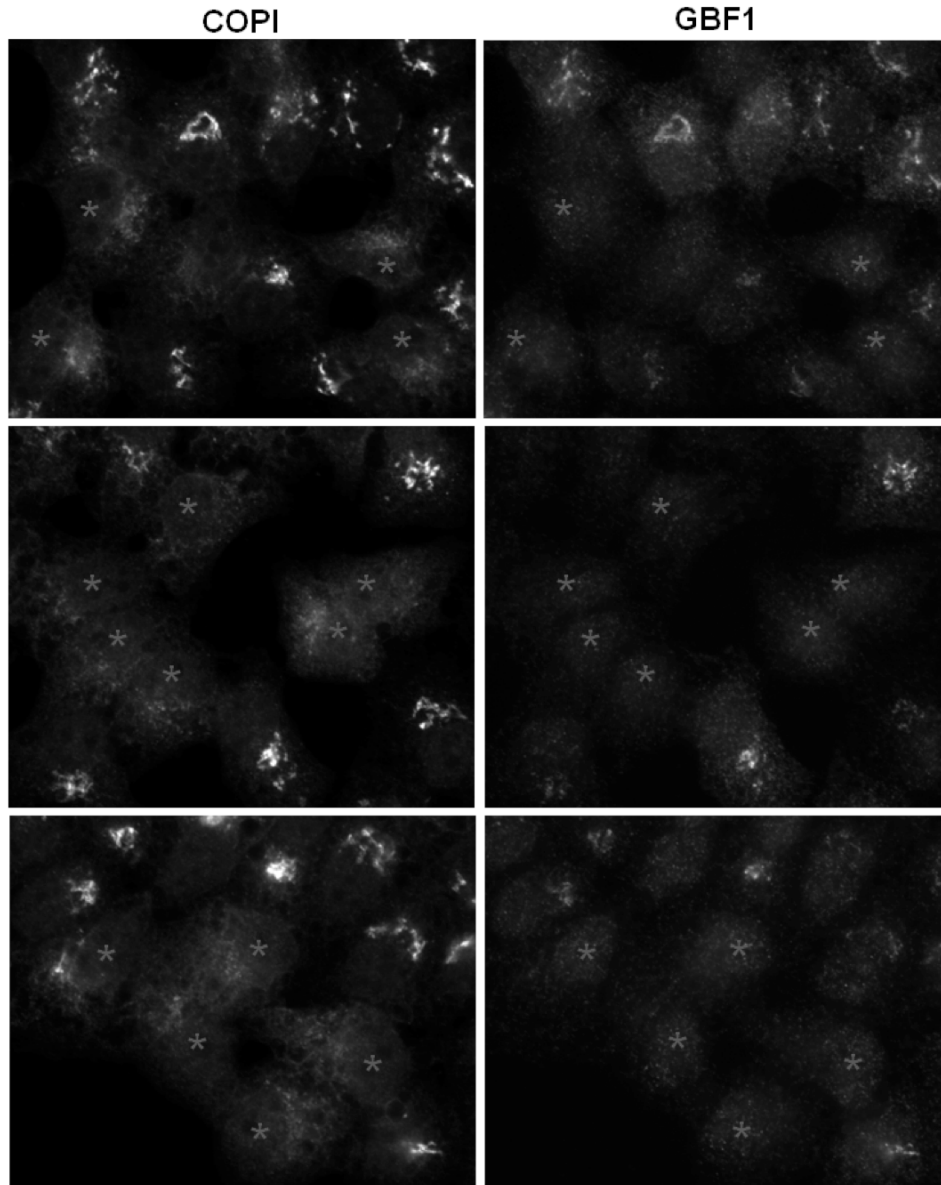


Figure 3.7. Partial GBF1 knockdown produces Golgi complex fragmentation as marked by dispersed COPI staining.

HeLa cells were transfected with an equimolar mixture of GBF1-targeting siRNA duplexes #2 and #3 as described in Chapter 2. After 72 h, cells were fixed and double-stained for GBF1 and COPI... Cells with partial GBF1 KD, identified by apparent loss of GBF1 staining but retention of fragmented COPI staining, were marked by an asterisk. Images shown are representative of at least 3 separate experiments.

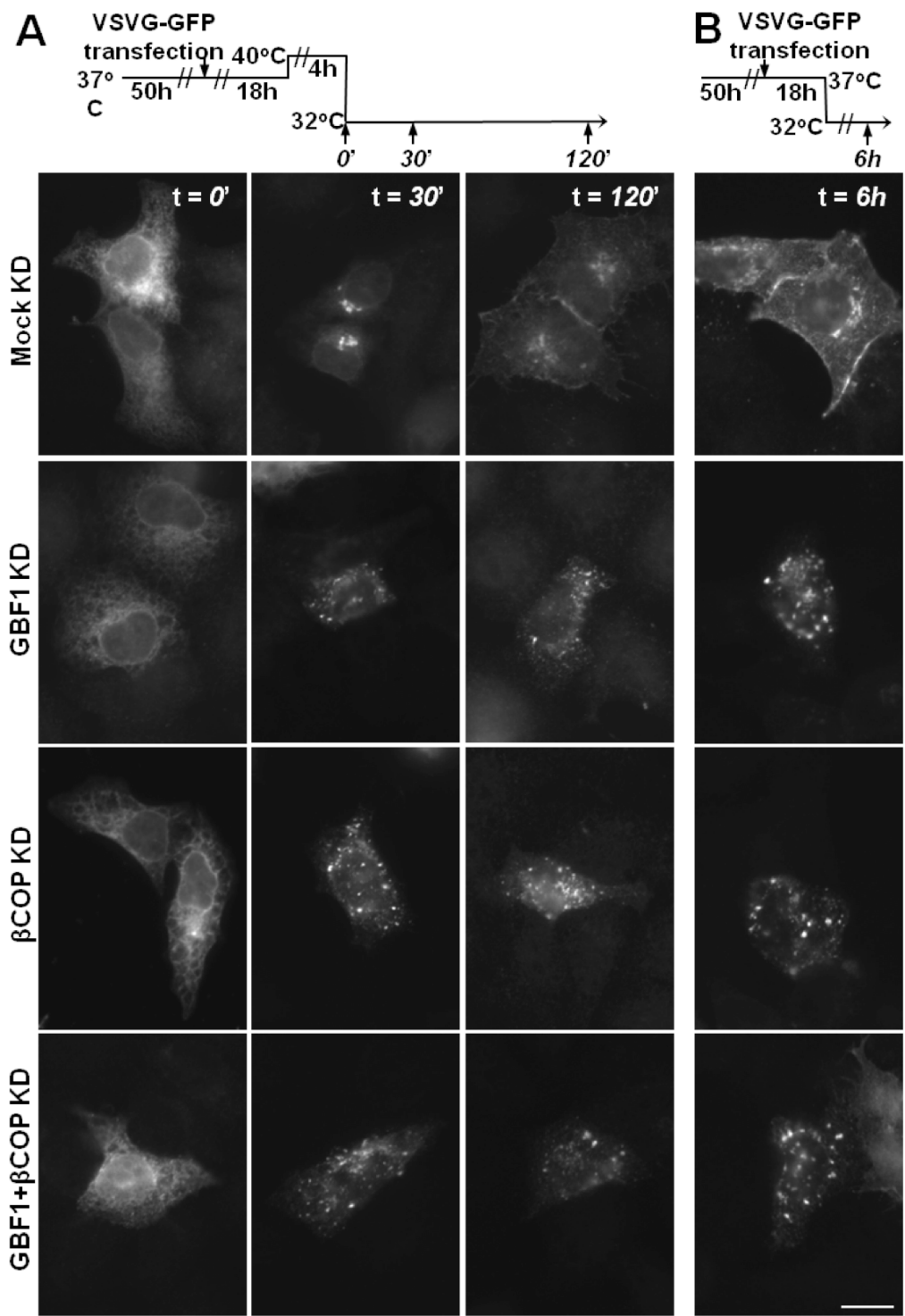
of GBF1/COPI staining, insets) caused no significant change in the overall number and distribution of the ERES marker Sec31 (Figure 3.6 C). In contrast, loss of GBF1 led to complete redistribution of juxta-nuclear signal for the well-characterized *medial*-Golgi marker ManII (Figure 3.6D). GBF1 knockdown also caused redistribution the *cis*-Golgi markers p115 and giantin (Figure 3.6, E and F). Interestingly, as previously observed following BFA treatment (Nelson et al., 1998; Seelig et al., 1994; Seemann et al., 2000), a significant fraction of these proteins accumulated in peripheral puncta, confirming that these proteins efficiently traffic and accumulate into post-ERES structures in absence of a functional COPI coat. We expected disruption of Golgi traffic to also affect the TGN since this organelle receives material from both endosomes and the Golgi stack. Indeed, as shown in Figure 3.6, G and H, loss of the Golgi complex led to redistribution of both BIG1 and the TGN marker TGN46. These results confirm that GBF1 is required for the membrane recruitment of COPI and assembly of the Golgi complex.

3.2.3 GBF1 knockdown does not prevent export from the ER but blocks cargo in post-ERES peripheral VTC structures

It has been argued that cargo export from the ER requires a functional COPI system (Altan-Bonnet *et al.*, 2004). This conclusion is based on the observation that BFA blocks export of anterograde cargo molecules such as VSVG and largely prevents their concentration at ERES or VTCs (Ward *et al.*, 2001). The identification of knockdown conditions that effectively reduce GBF1 levels allowed us to test if a functional COPI system and the activity of GBF1 was necessary for cargo traffic out of ERES. To measure cargo traffic out of the ER, we took advantage of a thermo-sensitive mutant of VSVG (VSVG-tsO45) (Bergmann, 1989) that can be accumulated in the ER at the non-permissive temperature (40°C) and released synchronously upon shift to a permissive temperature (32°C). Cells were transfected with a plasmid encoding a GFP-tagged form of VSVG-tsO45 50 hours after RNA-transfection with either luciferase (Mock), or GBF1-targeted RNA duplexes. As illustrated in Figure 3.8A, cells were shifted to the non-permissive temperature to accumulate VSVG

Figure 3.8. GBF1 and/or COPI knockdown block VSVG traffic and cause cargo accumulation in peripheral puncta and not ER.

A, B. HeLa cells were transfected with siRNA duplexes targeting luciferase (Mock), GBF1, and/or β COP, as indicated on the left. Fifty hours after transfection, cells were transfected again with a plasmid encoding VSVGtsO45-GFP and then temperature-shifted and fixed, as illustrated. For panel **A** cells were shifted to the nonpermissive temperature for 4 h before the shift to permissive temperature, whereas in **B** cells were shifted directly to from 37°C to permissive temperature. Cells were double-stained for COPI and GFP. Images reveal the VSVG-GFP pattern observed at the indicated times after shift to permissive temperature. Knockdown was confirmed by redistribution of COPI (not shown). Images shown are representative of at least 3 separate experiments. Bar, 20 μ m.



in the ER, and analyzed at various time points following a shift to the permissive temperature.

GBF1 knockdown blocked traffic of VSVG to the cell surface, but to our surprise did not prevent VSVG accumulation in peripheral punctate structures. The images shown in Figure 3.8A, confirmed that in cells treated with irrelevant RNA, a large fraction of VSVG present in the ER at the beginning of the temperature shift (t=0) trafficked to the cell surface within two hours. In sharp contrast, VSVG cleared the ER but never accumulated in a juxta-nuclear structure or reached the cell surface in cells transfected with GBF1-targeted siRNA (Figure 3.8A), even 120 min after temperature shift. Instead, VSVG accumulated in small bright puncta in the cell periphery. Importantly, accumulation of VSVG in peripheral structures was not caused by cellular stress or aggregation of misfolded proteins at the non-permissive temperature (40°C) since similar puncta accumulation was observed when cells were shifted directly to 32°C, bypassing incubation at 40°C (Figure 3.8B).

To obtain independent confirmation that the effect of GBF1 knockdown resulted from lack of COPI recruitment, we tested in parallel the impact of reducing levels of the β -subunit of COPI on Golgi assembly and function. This subunit plays a critical role in several COPI function such as Arf binding (Zhao *et al.*, 1997) and cargo recruitment (Eugster *et al.*, 2004), and its knockdown was expected to result in the effective loss of COPI activity. As described in Methods, four β -COP-targeted RNA duplexes were tested for their ability to disperse Golgi markers and the most effective one, duplex number 2, was selected for further analysis. Treatment with this RNA duplex led to similar accumulation of VSVG cargo into peripheral puncta (Figure 3.8, A and B). To ascertain that export from ERES was not due to residual COPI activity, we re-examined cargo transport in cells subjected to double knockdown. As shown in Figure 3.8, A and B (bottom panels), loss of both GBF1 and COPI did not prevent complete clearing of VSVG from the ER and its accumulation in peripheral puncta.

The accumulation of cargo in puncta observed in GBF1 and COPI knockdown initially appeared inconsistent with the results previously reported

with BFA. This apparent discrepancy prompted us to examine the impact of BFA treatment on cargo accumulation in GBF1 knockdown cells. Interestingly, treatment with BFA prior to the shift to permissive temperature prevented accumulation of VSV-G in puncta and yielded the previously reported (Ward *et al.*, 2001), largely reticular pattern in both mock and GBF1 knockdown cells (Figure 3.9). The observation that BFA treatment prevents accumulation of cargo into peripheral VTCs, even in GBF1 knockdown cells, suggests that the drug affects not only GBF1 activity but additional steps critical to cargo export from ERES or cargo maintenance at VTCs.

Further analysis of the VSVG positive peripheral puncta identified them as post-ERES structures. Images shown in Figure 3.10 (top panels) first confirmed that they lack COPI, as expected. Furthermore, the VSVG-positive peripheral structures stain for ERGIC53, but not for Sec31, and therefore likely correspond to VTCs (Figure 3.10, middle and bottom panels). Quantitative analysis of these and five similar images confirmed that greater than $87\pm 6\%$ of the VSVG positive puncta ($n=287$) also contain ERGIC53 while fewer than $15\pm 3\%$ overlapped with Sec31 ($n=161$). Altogether, these results demonstrate that cargo sorting from ERES and transport to peripheral VTCs can take place even in the absence of GBF1/COPI.

3.2.4 BIGs knockdown blocks recruitment of clathrin adaptors but does not prevent COPI recruitment or maintenance of the Golgi stack

Arf activation at the TGN has been implicated in the recruitment of several clathrin adaptor molecules such as AP-1 and GGAs (Bonifacino and Traub, 2003), a process likely controlled by the TGN-localized BIGs. Since BIG1 and BIG2 form heterodimers and likely perform redundant function at the TGN (Yamaji *et al.*, 2000), knockdown of both BIGs was necessary to examine their function. To eliminate BIGs, we selected a combination of BIG1- and BIG2-targeted RNA duplexes that as mentioned above proved effective in reducing levels of both BIG1 and BIG2 in several immuno-blot (Figure 3.3) and IF experiments (Figure 3.4 and 3.5). Overall, BIG1 and BIG2 appeared less stable

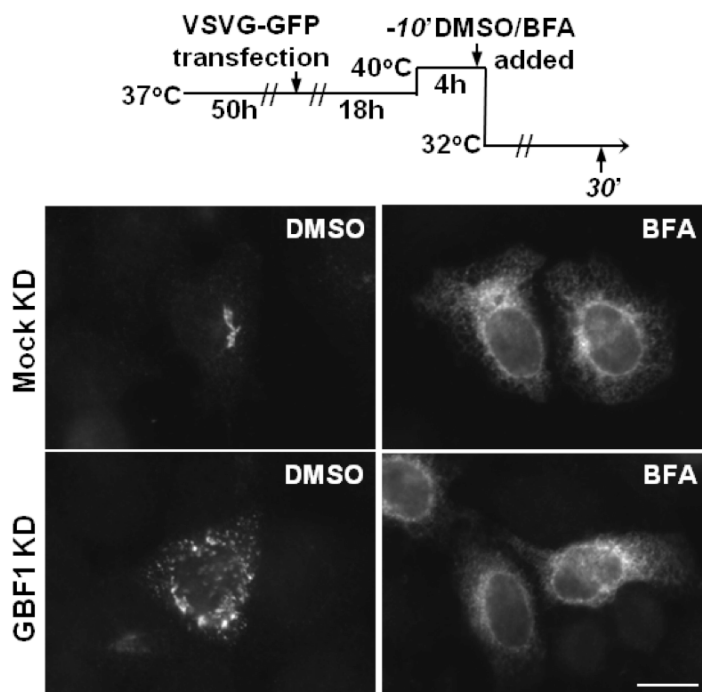


Figure 3.9. BFA treatment prevents accumulation of VSVG in VTCs even in cells lacking GBF1.

HeLa cells were transfected with siRNA duplexes targeting luciferase (Mock) or GBF1, as indicated on the left. Fifty hours after transfection, cells were transfected again with a plasmid encoding VSVGtsO45-GFP, then temperature shifted, treated with DMSO/10 μ g/ml BFA, and fixed, as illustrated in the top diagram. Cells were double-stained for COPI and GFP. Images in the bottom panels reveal the GFP-VSVG pattern. Knockdown was confirmed for DMSO treated samples by redistribution of COPI (not shown). Images shown are representative of at least 2 separate experiments. Bar, 20 μ m.

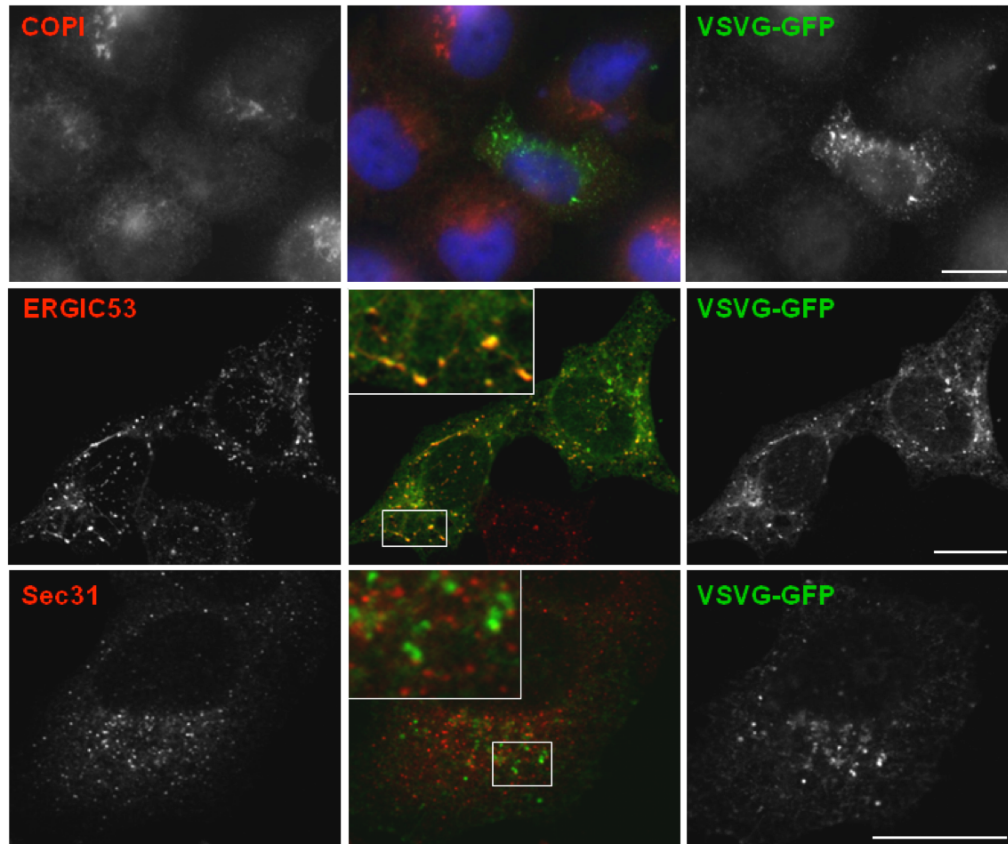


Figure 3.10. GBF1 knockdown traps cargo in ERGIC53-positive VTCs that are separate from Sec31-positive ERES.

HeLa cells were transfected first with siRNA duplexes targeting GBF1 and 50 h later with a plasmid encoding VSVGtsO45-GFP as described in Chapter 2. After 18 h, cells were shifted to 40°C for 4 h and then to 32°C for 120 min, as illustrated in Figure 3.7. Fixed cells were double-stained for the indicated markers. Single-slice confocal images are shown. Insets display threefold magnification of boxed areas of merged images shown in center panels. Images shown are representative of at least 2 separate experiments. Bar, 20 μ m.

than GBF1 and were undetectable by IF in greater than 70% of the cells as early as 48 h after transfection.

To confirm the involvement of BIGs in clathrin adaptor recruitment, we first examined the impact of BIGs knockdown on the distribution of endogenous AP-1 and GGA3. As shown in Figure 3.11, A and B, BIGs knockdown eliminated bright juxta-nuclear staining for AP-1, yielding a weaker and more dispersed punctate pattern. We observed identical AP-1 redistribution whether performing knockdown treatment for 2 or 3 days, which led us to conclude that residual membrane association of clathrin adaptors likely reflects Arf activation by endosome associated Arf-GEFs of the ARNOs and EFA6 sub-families (D'Souza-Schorey and Chavrier, 2006). Quantitative analysis of these and similar images from three separate experiments confirmed that BIGs knockdown caused AP-1 redistribution in greater than 85% of transfected cells (n=61). BIGs knockdown similarly caused redistribution of endogenous GGA3 from a compact juxtannuclear structure to a diffuse pattern (Figure 3.11C).

The effects of BIGs knockdown appear specific for clathrin adaptors since loss of BIGs had no measurable impact on the recruitment of the COPI coat (Figure 3.11D). As expected from the presence of COPI on juxtannuclear structures, loss of BIGs had no impact on the localization of *cis*- or *medial*- Golgi markers such as GBF1 (Figure 3.16), p115 or ManII (Figure 3.11, E and F). Retention of Golgi structures cannot reflect partial BIGs knockdown since a 2-day treatment with siRNA duplexes was sufficient to eliminate BIG1 staining and extending BIGs knockdown to 3 days did not cause detectable reduction or fragmentation of Golgi signal in any of the transfectants examined. BIGs knockdown for 3 days did not cause detectable reduction or fragmentation of Golgi signal (Man II, p115, and COPI) in any of the transfectants examined (n=30, 142, and 39, respectively).

3.2.5 BIGs knockdown disrupts assembly of the TGN

BIGs knockdown and/or consequent loss of adaptor recruitment in the Golgi region leads to loss of a detectable TGN. The first indication that BIGs may be essential for TGN assembly came from examination of the well-characterized

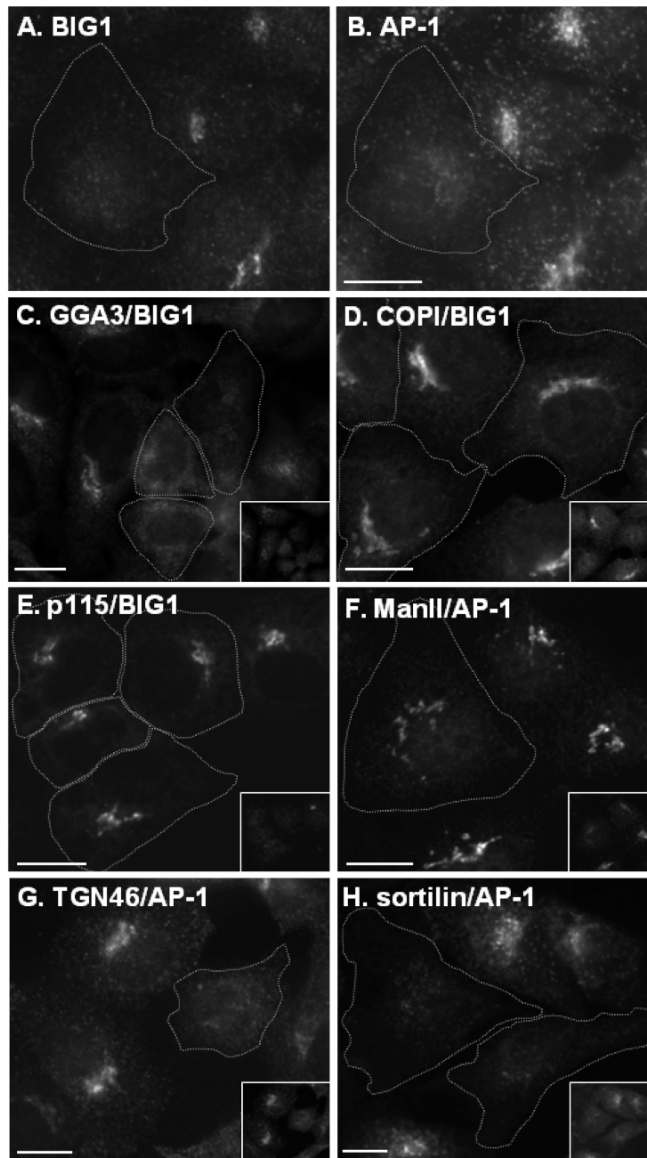


Figure 3.11. BIGs knockdown blocks recruitment of TGN-specific coats, redistributes TGN markers, but does not prevent assembly the Golgi stack.

HeLa cells were transfected with pools of siRNA duplexes targeting both BIG1 (#2 and #3) and BIG2 (#1–4) as described in Chapter 2. Fixed cells were double-stained for the indicated markers. **A, B** The pattern observed with BIG1/AP-1 double-staining. **C–H** The distribution of various Golgi (COPI, p115, ManII) and TGN (GGA3, TGN46, sortilin) markers with the inset showing pattern obtained with the second marker (BIG1 or AP-1). Cells with effective KD (loss/redistribution of BIG1/AP-1) were outlined. Images shown are representative of at least 3 separate experiments. Bar, 20 μm.

TGN membrane marker TGN46. Effective BIGs knockdown, as measured by AP-1 redistribution (inset), caused dispersal of TGN46 (Figure 3.11G). This marker did not accumulate at the cell surface but rather relocated to weak puncta scattered throughout the cytoplasm, as previously observed in GBF1 knockdown cells (Figure 3.6H). To further probe the impact of BIGs knockdown, we examined the distribution of cargo receptors that cycle between the TGN and endosomes to transport lysosomal hydrolases and whose function rely on GGAs (Bonifacino and Traub, 2003; Ni *et al.*, 2006). These sorting receptors include not only canonical mannose 6-phosphate receptors, but also the more recently described sortilin, a member of the Vps10p family. In sharp contrast to the control, BIGs knockdown reproducibly prevented normal localization of sortilin; this marker redistributed to a weak dispersed pattern and did not appear to accumulate at the cell surface (Figure 3.11H).

To examine whether the redistribution of TGN markers resulted from a defect in assembly and maintenance of a functional TGN, we took advantage of the fact that treatment with the proton ionophore monensin traps a sub-set of Golgi enzymes such as GalT into dispersed vacuoles derived from the TGN (Borsig *et al.*, 1999; Puri *et al.*, 2002; Schaub *et al.*, 2006). GalT resides primarily in *trans*-Golgi cisternae but does cycle to and from the TGN where it becomes trapped in monensin-treated cells (Schaub *et al.*, 2006). Any residual trafficking to the TGN in BIGs knockdown cells should therefore be detectable by accumulation of GalT in remaining TGN structures following treatment with monensin. We first verified that BIGs knockdown had no impact on the Golgi localization of GalT and its co-distribution with the *medial*-Golgi marker ManII (Figure 3.12, top panels). Secondly, we confirmed that in control cells a brief 15 min treatment with monensin was sufficient to cause accumulation of GalT in vacuoles clearly separate from the Golgi ribbon marked by ManII (Figure 3.12, middle panels). As shown in Figure 3.12 (bottom panels), monensin did not change the GalT juxta-nuclear distribution in BIGs knockdown cells, even when the treatment was lengthened from 15 to 30 min. Quantitative analysis revealed

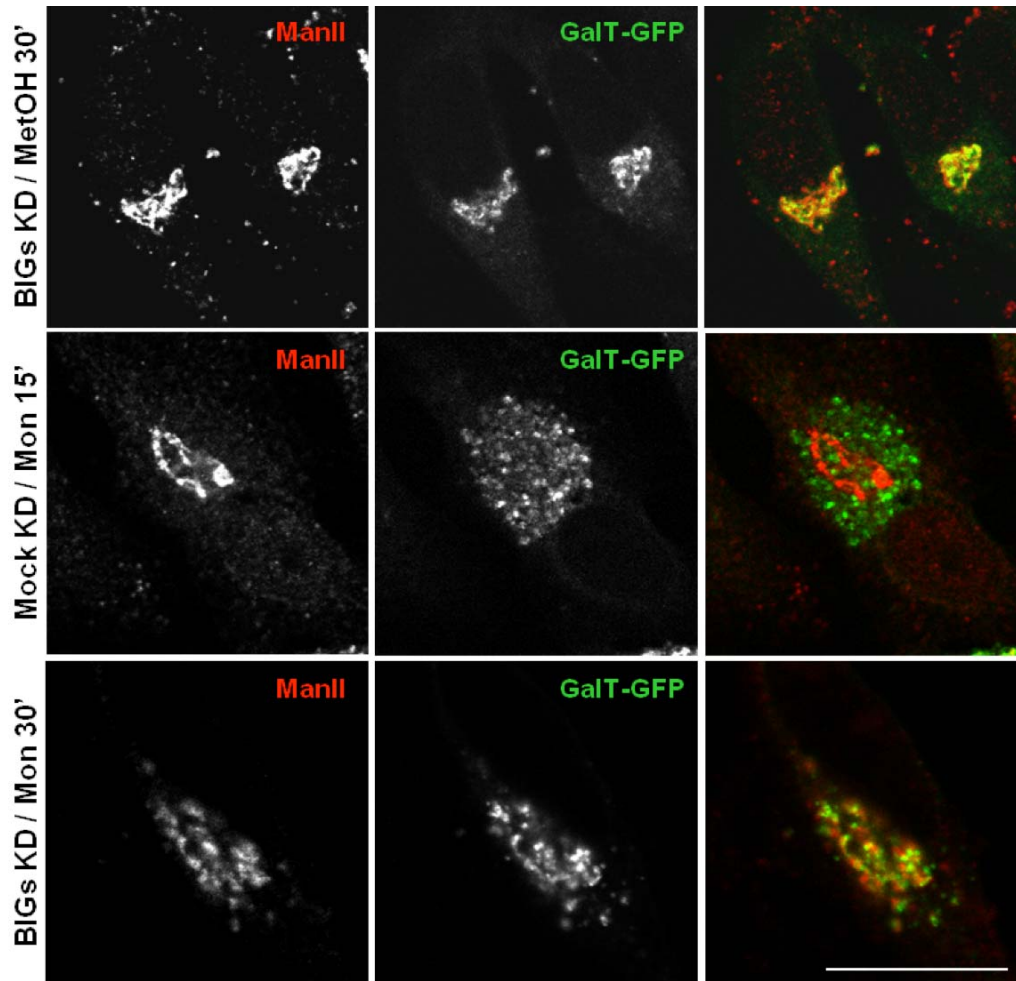


Figure 3.12. BIGs knockdown prevents monensin-induced redistribution of GalT-GFP.

HeLa cells were transfected with a plasmid encoding GalT-GFP and a pool of siRNA duplexes targeting either luciferase (Mock), or BIG1 and BIG2 (BIGs) as described in Chapter 2. Seventy-two hours after siRNA transfection, cells were treated with either methanol or 4 μ M monensin for the indicated periods of time. Cells were then fixed and stained for ManII and AP-1. Cells with effective BIGs KD were identified by loss of AP-1 juxtannuclear staining (not shown). Single-slice confocal images of the ManII (red) and GFP signal are shown. Merged images shown on the right. Images shown are representative of at least 3 separate experiments. Bar, 20 μ m

that GalT redistributed to dispersed vacuoles distinct from ManII positive Golgi ribbons in greater than 91 ± 4 % of control cells (n=117), while this occurred in fewer than $14\pm 10\%$ of knockdown cells (n=46). The lack of GalT redistribution in the majority of BIGs knockdown cells demonstrates that effective knockdown was achieved, and strongly suggests that BIGs play a critical role in assembly of the TGN.

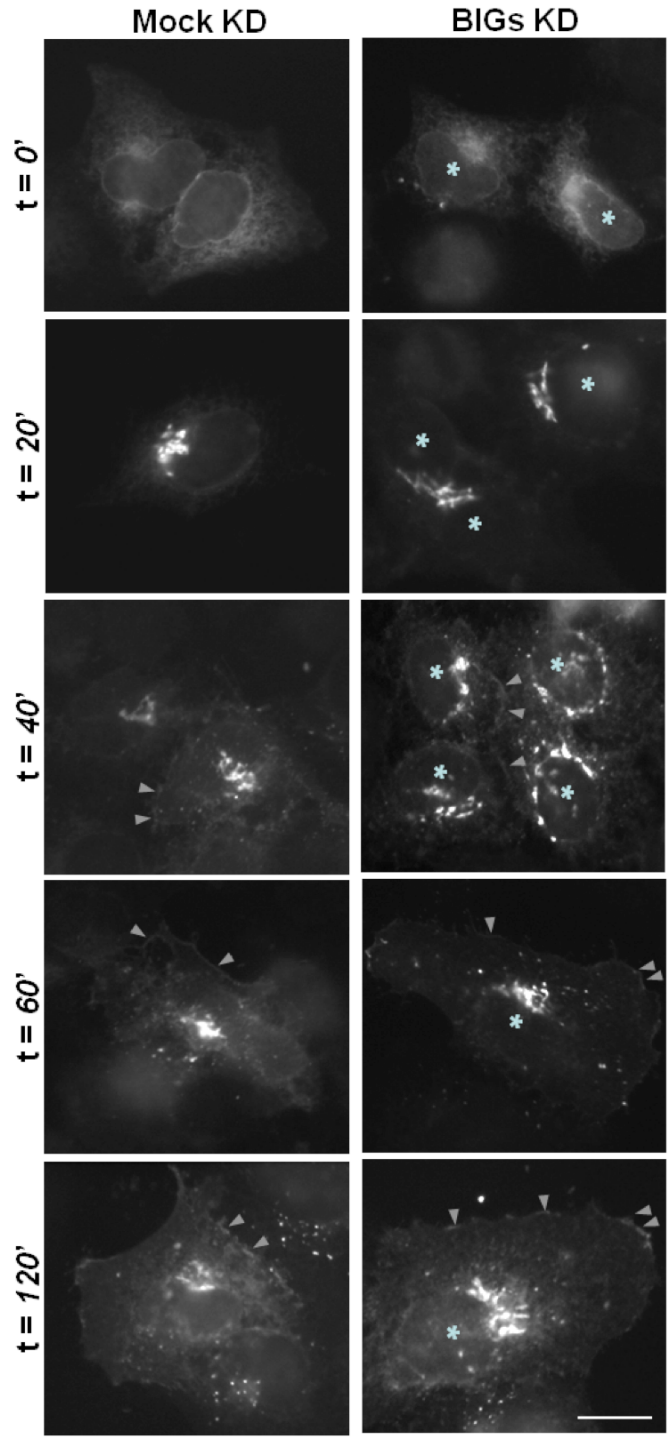
3.2.6 BIGs knockdown does not prevent cargo traffic to the cell surface or assembly of a polarized Golgi stack

To determine whether the structures detected with several Golgi markers in BIGs knockdown cells remained functional we first examined traffic of VSVG-tsO45-GFP. Expression of BIGs was knocked down in HeLa cells as before, and then these cells were subjected to a VSVG expression and temperature shift protocol similar to that described in Figure 3.8A. As shown in Figure 3.13 and 3.14, BIGs knockdown did not prevent VSVG transport to the juxta-nuclear region or its appearance at the cell surface. VSVG reached the juxta-nuclear region 20 min after shift to the permissive temperature and clearly accumulated at the PM within two hours. Similar results were obtained either by infecting cells with the mutant strain of VSV producing VSVGts045 or by transfecting cells with a plasmid encoding for VSVGts045-CFP (Figure 3.15). Furthermore, loss of BIGs appeared not to affect the kinetics of VSVG traffic since, at all time points examined, the fraction of cells with VSVGts045-GFP at the Golgi or the PM were nearly identical in mock and BIGs knockdown cells (Figure 3.14). These results clearly demonstrate that BIGs and a functional TGN are not required for efficient sorting of some cargo molecules to the PM of non-polarized cells.

The observation that BIGs knockdown does not prevent cargo traffic to the cell surface suggests that the GBF1/COPI coat machinery may be sufficient to drive assembly of a Golgi stack that can not only produce carriers for the PM but may have retained its characteristic polarized organization. We tested this possibility by examining the impact of BIGs knockdown on the relative distribution of several markers with limited distribution within the Golgi stack. HeLa cells were subjected to BIGs knockdown and examined by IF using a triple

Figure 3.13. BIGs knockdown does not block traffic of VSVG to the cell surface.

HeLa cells were transfected with siRNA duplexes targeting either luciferase (Mock) or BIG1 and BIG2 (BIGs), as indicated on the top. Fifty hours after transfection, cells were transfected again with a plasmid encoding VSVGtsO45-GFP, then temperature shifted, and fixed, as illustrated in Figure 3.7. Cells fixed at the indicated times after shift-down to 32°C were double-stained for BIG1 and GFP. Knockdown was confirmed by redistribution of BIG1 (not shown). Images reveal the GFP-VSVG pattern observed at the times shown on the left side of the panels. Arrowheads mark plasma membrane (PM) where VSVG accumulates. The nuclei of cells with effective KD (loss of BIG1) were marked by asterisks. Images shown are representative of at least 6 separate experiments. Bar, 20 μm .



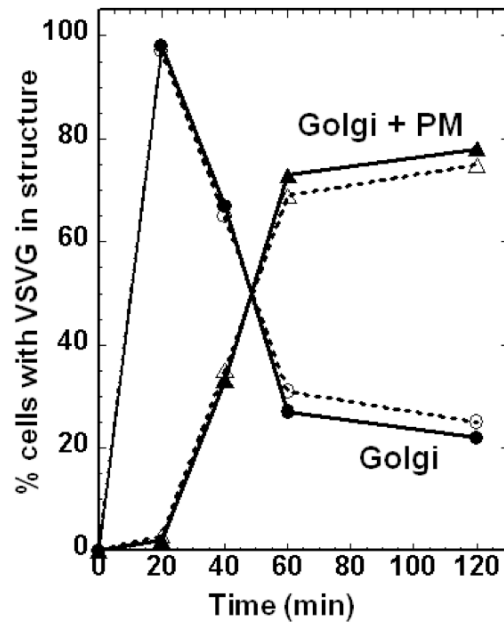


Figure 3.14. BIGs knockdown does not block traffic of VSVG to the cell surface.

HeLa cells were transfected with siRNA duplexes targeting either luciferase (Mock) or BIG1 and BIG2 (BIGs). Fifty hours after transfection, cells were transfected again with a plasmid encoding VSVGtsO45-GFP, then temperature shifted, and fixed, as illustrated in Figure 3.7. At each time point after release for both Mock (● and ▲, solid line) and BIGs KD (○ and Δ, dashed line) cells, a minimum of 25 cells were scored for presence of VSVG at Golgi only (○, ●), or at Golgi and PM (Δ, ▲). The fraction of cells with the indicated pattern was expressed as percentage and is shown as a function of time after shift-down to 32°C.

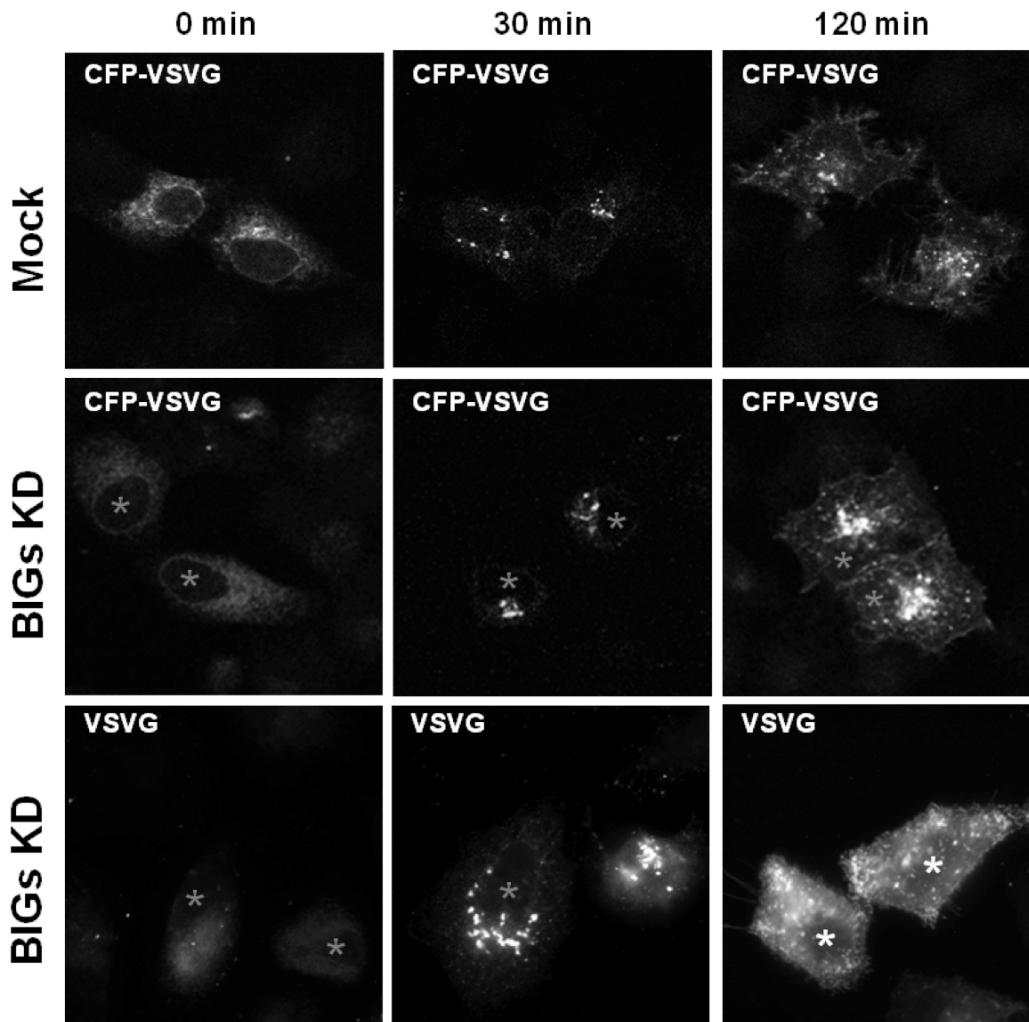


Figure 3.15. BIGs knockdown does not prevent transport of VSVG to the cell surface.

HeLa cells were transfected with either luciferase-targeted RNA (top row) or a pool of RNA duplexes comprised of BIG1 150nM (D2 and D3) & 200 nM BIG2 (D1, D2, D3 and D4) (middle and bottom rows). 44 hours later, they were transfected with 1 μ g plasmid encoding VSVGts045-CFP and shifted to 40 $^{\circ}$ C for 8 hours to accumulate cargo protein in the ER (top and middle rows). For the bottom row cells were infected with the live virus strain producing VSVGts045 and after 3 hours cells were shifted to 40 $^{\circ}$ C for another 2 hours. Cells were then either fixed (t=0) or shifted to 32 $^{\circ}$ C for either 30 or 120 min. Transfectants with effective KD are marked by asterisks. Images are representative of at least 2 separate KD experiments.

labelling protocol. As shown in Figure 3.16, BIGs knockdown did not prevent assembly of a polarized Golgi stack in which *cis*-Golgi markers such as p115 and GBF1 remain well resolved from a *trans*-cisterna marker such as GalT-GFP. Effective BIGs knockdown was confirmed using BIG1 and AP-1 as markers (blue channel). Bottom most panels show an image of an enlarged area in which the red (*cis*) and green (*trans*) signals have been merged. Normal separation of *cis*- and *trans*-markers was observed in all transfectants examined (68 cells from three separate experiments).

To better illustrate the spatial resolution of the Golgi markers, we measured signal intensity along the white line shown in the merged image and reported values for each marker in the graphs on the right. The graphs confirmed good overlap of BIG1 and AP-1 with GalT-GFP in mock-treated cells, and clear separation of *cis*- and *trans*-markers in both mock-treated and BIGs knockdown cells. Quantitative analysis of the average distance between *cis*- and *trans*-Golgi markers in several regions ($n > 6$) of cells from two separate experiments established that the average distance between p115/GalT or GBF1/GalT peaks were nearly identical in control and BIGs knockdown cells. Furthermore, quantitative analysis of fluorescence signal overlap in several images similar to those shown in Figure 3.16 confirmed that both pairs of *cis/trans* markers remained well-resolved in BIGs knockdown cells (Table 3.1). Altogether, these results strongly suggest that GBF1/COPI, but not BIGs/clathrin, is essential to drive assembly and maintenance of a polarized Golgi stack.

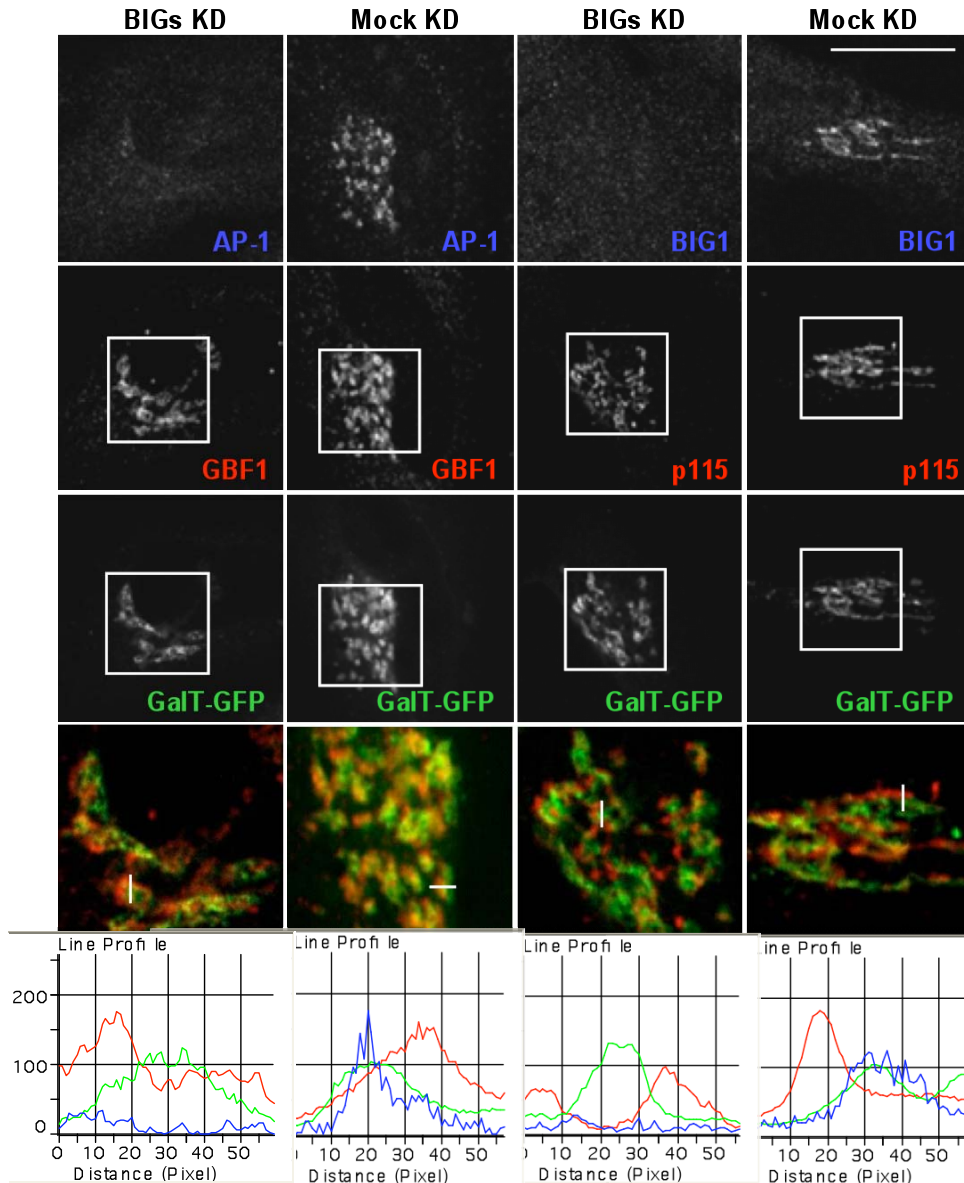


Figure 3.16. BIGs knockdown does not prevent assembly of a polarized Golgi stack.

HeLa cells were transfected with a pool of siRNA duplexes targeting either luciferase (Mock), or BIG1 and BIG2 (BIGs). After 48 h, cells were transfected again with a plasmid encoding GalT-GFP. Cells were fixed 24 h later and double-stained for either BIG1/p115 or AP-1/GBF1. Single-slice confocal images are shown. Merged images display the red and GFP signal from the enlarged boxed areas. Graphs in the right column report pixel intensity profiles in all three channels along the white bar shown in the merged panels. Images shown are representative of at least 3 separate experiments. Bar, 20 μ m.

Table 3.1 BIGs knockdown does not affect separation of *cis*- and *trans*-Golgi markers

	p115 vs GalT	GBF1 vs GalT
Mock	29±5% (n=6)	36±9% (n=8)
BIGs KD	27±9% (n=19)	30±10% (n=23)

The extent of signal overlap in percent between the two indicated markers was measured as described in methods. Shown is the average \pm SD obtained for the indicated conditions.

3.3 Discussion

We exploited complementary overexpression and knockdown approaches to examine the relative functions of GBF1 and BIGs at the Golgi complex. As expected from their distinct localizations, overexpression of GBF1 and BIG1 had opposite effects on the sensitivity of the COPI and AP-1 coats to BFA. GBF1 stabilized COPI and protected *cis*-compartments but not AP-1 or HA-furin positive *trans*-Golgi membranes; in contrast BIG1 protected AP-1 but not COPI. Knockdown with several specific RNA duplexes or shRNAs confirmed that GBF1 and BIGs perform distinct functions in the Golgi complex. GBF1 knockdown caused redistribution of COPI and most Golgi markers to a diffuse pattern while tethering factors such as p115 and giantin redistributed into puncta and reticular structures. Contrary to expectations, knockdown of GBF1 and COPI, singly or in combination, did not prevent export of VSVGtsO45 from the ER, but caused its accumulation into ERGIC53-positive puncta separate from Sec31-positive ERES. On the other hand, BIGs knockdown had no impact on the COPI machinery or several Golgi markers but caused loss of clathrin adaptor proteins as well as redistribution of TGN46 and the sorting receptor sortilin. Further tests with monensin confirmed loss of detectable sorting of GalT to the TGN. Despite these clear effects on the TGN, BIGs knockdown prevented neither traffic of VSVGtsO45 to the PM, nor assembly of a polarized Golgi stack. Our observations indicate that COPII is the only coat required for sorting and export from ERES. Furthermore, GBF1 but not BIGs appears necessary for COPI recruitment and cargo progression from VTCs to cell surface. The maintenance of a polarized Golgi stack in absence of BIGs suggests that the GBF1-COPI machinery is sufficient to drive the maturation process responsible for Golgi organization.

3.3.1 Effectiveness and selectivity of Golgi ArfGEFs knockdown

Several experiments established that the knockdown methods used in our study led to selective and effective loss of the targeted proteins. Multiple observations confirmed the selectivity of the knockdown effects. These include the fact that similar knockdown effects were observed using any one of several sequences

targeting different regions of the mRNA, and whether sequences were delivered by direct transfection of duplexes or by plasmid-driven synthesis of short hairpin RNA. The observation that targeting either β -COP or GBF1 had the same impact on ER export and the Golgi complex further supports our conclusion that knockdowns were selective.

The extent of knockdown varied within a given cell population, and depended on the nature of the target and length of treatment. These variations allowed us to identify with confidence cells displaying effective knockdown of targeted proteins. For example, we could readily recognize cells with partial knockdown for GBF1 (Figure 3.7); these cells lacked or showed little detectable GBF1 but still displayed a fragmented Golgi complex stained weakly with COPI (Figure 3.7). By selecting cells with no remaining COPI staining we could ensure that all cells analyzed had effective GBF1 knockdown. In the case of BIGs, short treatment (48 hrs) proved effective at eliminating BIG and dispersing AP-1 IF signal. The fact that lengthening treatment to 72 hours had no further impact on the distribution of TGN and Golgi markers established that effective knockdown had been achieved.

3.3.2 GBF1 is essential for COPI recruitment and assembly of the Golgi complex, but is not required for cargo concentration and export from ERES

Results obtained through our combined use of overexpression and RNA-dependent silencing established that GBF1, but not BIGs, is required to activate Arfs for recruitment of COPI. The localization of GBF1 to early compartments of the Golgi complex first suggested a functional link between GBF1 and COPI (Kawamoto *et al.*, 2002; Zhao *et al.*, 2002). Subsequent studies revealed that overexpression of the charge-reversal dominant negative mutant GBF1[E794K] (Garcia-Mata *et al.*, 2003), microinjection of neutralizing GBF1 antibodies (Zhao *et al.*, 2006) or use of the drug Golgicide A as a specific inhibitor of GBF1 function (Saenz *et al.*, 2009) caused loss of COPI recruitment and subsequent disassembly of the Golgi complex. The loss of COPI recruitment and Golgi structure following GBF1 knockdown (Figure 3.6), as well as the coat and compartment-specific protection conferred by GBF1 overexpression (Figure 3.1),

extend these observations and confirm this functional link. We have no explanation for the surprising observation by Lefrançois *et al.*, suggesting that GBF1 appears necessary for GGA activation at the TGN (Stéphane and Peter, 2007), since all other laboratories, including ours, support GBF1 function at the *cis*-Golgi for COPI recruitment.

The availability of tools for the effective knockdown of GBF1 and COPI allowed us to test the 2-step model which proposes that Arfs and COPI are required for traffic out of ERES. Contrary to predictions from this model, we observed that the GBF1/COPI machinery was not required for the concentration and export of VSVG cargo from ERES. These results are consistent with a wealth of information derived from yeast cell-free assays (Barlowe, 2003; Sato and Nakano, 2007) and the recent identification of COPII carriers in animal cells (Zeuschner *et al.*, 2006). These results are also consistent with our previous demonstration that GBF1 does not associate with ERES, but rather with VTCs that are close but physically separate from ERES (Zhao *et al.*, 2006). Finally, our result have been confirmed recently by the use of the specific GBF1 inhibitor golgicide A, which does not block VSVG trafficking at ERES, but the cargo accumulates at ERGIC (Saenz *et al.*, 2009).

To explain the apparent block in cargo export by BFA or Arf mutants (Ward *et al.*, 2001), we propose that these treatments do not block export of cargo from the ER, but rather prevent cargo retention in VTCs by promoting retrograde traffic from VTCs to the ER. This model is based on our recent demonstration that BFA causes VTCs to lose their cargo to the ER through a microtubule-dependent mechanism (Zhao *et al.*, 2006). This could occur if the inactive GBF1 trapped on membranes by BFA (Niu *et al.*, 2005; Szul *et al.*, 2005; Zhao *et al.*, 2006) somehow interfered with protein sorting at ERES and/or VTCs. Alternatively, BFA could affect additional targets such as BFA-induced ADP-ribosylated substrate (BARS) that has been implicated in membrane scission of COPI vesicles (Yang *et al.*, 2005) and whose activity is inhibited by BFA-induced ADP-ribosylation (Weigert *et al.*, 1999).

Surprisingly, a previous publication by Sztul and colleagues (Sztul et al., 2007) reported that GBF1 knockdown did not prevent assembly of the Golgi complex and transport of all cargo molecules to the cell surface. This report is in clear contradiction with the results presented in this chapter or the previous reports using the GBF1[E794K] mutant (Garcia-Mata *et al.*, 2003) or Golgicide A (Saenz et al., 2009) that GBF1 knockdown prevented the formation of motile transport competent carriers necessary for assembly and maintenance of the Golgi complex. We conclude that Sztul and colleagues actually achieved only partial GBF1 knockdown and analysed cells with fragmented Golgi complexes, as marked by the punctate COPI staining (Figure 3.6).

In GBF1 knockdown cells, VSVG cargo accumulated in VTCs that contained several tethering factors such as p115 and giantin, but failed to either mature into Golgi resident enzymes-containing structures or to associate with microtubules and migrate to the cell center. The fact that VSVG but not Golgi resident enzymes accumulated in VTCs likely reflects the presence in VSVG of a di-acidic sorting signal efficiently recognized by COPII (Nishimura *et al.*, 1999; Sato and Nakano, 2007). The reason for the lack of movement to the cell center remains unknown but, as proposed by Sztul and colleagues (Garcia-Mata *et al.*, 2003), it may be related to the absence of COPI-driven active protein sorting that normally drives formation of membrane domains critical for recruitment of other proteins such as rabs and motors/accessory proteins (Short *et al.*, 2005).

3.3.3 BIGs are required for recruitment of clathrin adaptor and maintenance of the TGN

Previous work established that BIGs localize at the TGN and overlap with clathrin, suggesting that BIGs regulate Arf activation for recruitment of GGAs and other adaptor proteins such as AP-1 (Yamaji *et al.*, 2000; Zhao *et al.*, 2002). We confirmed here the functional link between BIG1 and AP-1 by showing that BIG1 overexpression stabilizes AP-1 but not COPI against dispersal following short BFA treatment. Nakayama and colleagues confirmed a similar link between BIG2 and AP-1 using related approaches (Shinotsuka et al., 2002b). As predicted, BIGs knockdown caused loss of both AP-1 and GGA3 from the juxta-

nuclear region. This redistribution of AP-1 is similar to that reported following BFA treatment of several cell lines in which the Golgi complex is either naturally resistant to BFA or acquired resistance following mutagenesis. For example, the Golgi stack of MDCK and PtK1 cells (Robinson and Kreis, 1992) or mutagenized CHO-K1 cells (Torii *et al.*, 1995) remains unperturbed following BFA treatment while some AP-1 localizes to disperse puncta. In all cases, residual membrane association of clathrin adaptors likely results from Arf activation by endosome-associated BFA resistant Arf-GEFs of the ARNO and EFA6 sub-families (D'Souza-Schorey and Chavrier, 2006).

Previous attempts to test the model that GGAs and APs recognize sorting signals in endosomal-targeted cargo and drive maturation of the TGN, focused on blocking the function of either AP1, 3 and 4 or GGAs (Bonifacino and Traub, 2003; Gleeson *et al.*, 2004). However, expression of dominant negative mutants or silencing of either types of adaptors led to variable outcomes ranging from tubulation of the Golgi, accumulation of endosomal cargo in the TGN or its dispersal to peripheral endosome structures (Ghosh *et al.*, 2003; Puertollano *et al.*, 2001a; Puertollano *et al.*, 2001b). These apparent discrepancies should not be surprising, however, since current evidence suggests that adaptors function in both anterograde and retrograde traffic, and at the TGN participate in a multistep process involving both GGAs and APs (Ghosh and Kornfeld, 2004); loss of only a subset of the adaptors would imbalance this process, with complex consequences. Effective knockdown of BIGs circumvented this problem by preventing recruitment of both APs and GGAs to the Golgi complex. Under these conditions, we could readily detect loss of a recognizable juxta-nuclear TGN structure stained by TGN46 or sortilin. Disruption of sorting to the TGN was confirmed by clear loss of GalT accumulation in dispersed vacuoles following monensin treatment. We predict that simultaneous silencing of all GGAs and several APs will be required to observe effects similar to those we report for BIGs knockdown.

3.3.4 GBF1, but not BIGs, is required for assembly of a polarized Golgi stack

One of the more surprising results of our study was the observation that BIGs knockdown did not prevent assembly of a polarized Golgi stack in mammalian cells. The Golgi complex acts as a dynamic sorting station that exploits two separate coats to receive and package material for both anterograde and retrograde traffic. For this reason, we expected that loss of its clathrin-based sorting machinery would seriously disrupt complex homeostatic mechanisms that normally maintain Golgi structure and function. Furthermore, previous work in *S. cerevisiae* had already established that loss of Sec7p, the single orthologue of BIGs, completely alters Golgi morphology and blocks protein secretion: Sec7 temperature sensitive mutants accumulate large numbers of stacked Golgi membranes (Berkeley bodies) with concomitant block in traffic to the vacuole and cell surface (Deitz et al., 2000; Esmon et al., 1981; Franzusoff and Schekman, 1989; Novick et al., 1980; Rambourg et al., 1993). Contrary to expectation, we observed that in BIGs knockdown cells Golgi stacks not only retained a degree of polarization similar to that of control cells, but also efficiently trafficked VSVG to the cell surface (Figures 3.13, 3.14, 3.15 and 3.16).

The apparent discrepancy between the impact of Sec7 inactivation and BIGs knockdown may reflect differences in the organization of the secretory pathways of *S. cerevisiae* and animals. Yeast Golgi elements appear as fine or coarse nodular networks that are neither cisternal nor arranged in stacks (Kepes et al., 2005; Morin-Ganet et al., 2000; Rambourg et al., 2001). Several morphogenetic studies revealed a gradual transformation of Golgi elements following their initial assembly from ER-derived vesicles: from tubular clusters, they become a network of fine tubules linked by nodes that transform into a thicker nodular network which eventually releases secretory granules by rupture of tubular areas. Of particular significance, mixed forms containing two networks of different calibers have been observed (Morin-Ganet *et al.*, 2000) and it is therefore likely that the transformation from early to late elements involves concerted action of both the COPI and clathrin coats within a transiently

continuous network. This view is consistent with recent description of Golgi maturation in live yeast (Losev *et al.*, 2006; Matsuura-Tokita *et al.*, 2006), and may explain why early and late Golgi elements may not be able to function independently in *S. cerevisiae*. In other words, loss of Sec7 would prevent further maturation of the nodular network and cause accumulation of membranes unable to release any cargo carriers.

In contrast, the Golgi complex of animal cells occurs as a structured stack of flattened cisternae with varying extent of fenestration that is flanked by extensive tubular-reticular networks (Mogelsvang *et al.*, 2004; Rambourg and Clermont, 1990; Thorne-Tjomsland *et al.*, 1998). Previous work established that several tethering factors such as p115, GM130 and GRASP can associate independently from oligosaccharide modifying enzymes to form a ribbon-like reticulum that can act as a structural scaffold for the Golgi stack (Seemann *et al.*, 2000). Our results suggest that the GBF1-dependent recruitment of the COPI coat is sufficient to promote the formation of specialized membrane domains and cargo carriers that can move cargo from VTCs, assemble on this matrix and subsequently drive the maturation process to yield a polarized stack. Arfs regulate not only COPI but also lipid remodelling enzymes and we cannot exclude the possibility that GBF1 may also be critical for control of phosphoinositide levels and assembly of the β -III spectrin cytoskeleton (De Matteis and Godi, 2004b). The fact that one can eliminate BIGs and maintain much of this organization suggests that these mechanisms are robust and that stacking may permit the observed uncoupling of *cis* and *trans*-acting coats.

The observation that VSVG trafficked normally to the cell surface in BIGs knockdown cells remains consistent with the well-established role of the TGN in sorting of cargo to various destinations in both non-polarized and polarized cells (Bard and Malhotra, 2006; Bonifacino and Traub, 2003; Rodriguez-Boulan *et al.*, 2005; Rodriguez-Boulan and Musch, 2005). Maturation by the COPI coat in animal cells may allow the creation of membrane domains on the *trans*-side that become enriched in anterograde cargo proteins and eventually peel off the stack to carry some or all of its content to the cell surface. Under normal conditions such

intermediates would likely be absorbed in the TGN from which cargo would be then sorted to its various destinations. Our results establish that whatever mechanisms normally drive traffic of VSVG from the TGN remain operational in absence of TGN and BIGs/clathrin dependent sorting. The absence of a detectable TGN in BIGs knockdown cells further suggests that little if any of the membranes released from the Golgi stack remain in this area. Further work will clearly be required to establish when and how the BIGs machinery is recruited to late cisternae to facilitate membrane retention, formation of the TGN and sorting of endosomal cargo.

CHAPTER FOUR:

**ARF3 IS ACTIVATED SPECIFICALLY BY THE LARGE GUANINE NUCLEOTIDE
EXCHANGE FACTORS BIGS AT THE *TRANS*-GOLGI NETWORK**

4.1 Overview

As established in chapter 3, two classes of Arf-GEFs regulate recruitment of coat proteins on the Golgi complex, both of which are targets of BFA. GBF1 localizes at the *cis*-Golgi complex where it regulates COPI recruitment. In contrast, BIG1 and BIG2 localize at the TGN and facilitate clathrin membrane recruitment. How these Arf-GEFs regulate different coats in spite of their well-characterized promiscuity towards class I and II Arfs remains unknown. Here, we provide evidence supporting for the first time the notion that Arf3 is activated uniquely by BIGs at the TGN. Imaging experiments first established that Arf3 appears separate from the *cis*-Golgi markers GBF1 and p115 while colocalizing to a large extent with BIG1 and TGN46. Simultaneous knockdown of both BIGs redistributed Arf3-GFP from Golgi membranes while overexpression of BIG1, but not GBF1, protected Arf3-GFP Golgi localization from BFA-induced redistribution. In a parallel experiment short treatment with BFA of BFY1 cells redistributed AP1/Arf3 while COPI/Arf1 membrane recruitment remained largely unaffected. Shifting temperature to 20°C for 2 hours, a method known to block cargo in *trans*-Golgi compartments, had a dramatic impact on Arf3 distribution. Redistribution of Arf3 from Golgi membranes upon shift to 20°C was not immediate but occurred gradually over 10 minutes. This redistribution was specific for Arf3 since Arf1-GFP, BIG1, TGN46 and AP-1 remained unaffected. Arf1 and Arf3 differ in sequence only in two short regions at the N- and C-termini. We constructed a series of Arf1/Arf3 chimeras and observed that Arf1 chimeras containing the N-terminal region of Arf3 redistributed as WT Arf3 upon shift to 20°C. Conversely, Arf3 chimeras containing the N-terminal region of Arf1 remained unaffected. Further analysis of point mutants identified two residues critical for this property. Using the same Arf1/3 chimeras we were able to demonstrate that the C-terminus directs Arf3's specific localization. Mutagenesis analysis of the variant amino acids from the C-terminus of Arf3 pointed towards A174 and K180 being important in directing Arf3 towards the TGN. Arf3 knockdown had no impact on any of the markers tested or on VSVG trafficking to PM. We conclude that Arf3 is likely activated specifically by BIGs

at the TGN. At the same time, the amino acids at position 9 and 13 in the N-terminus of Arf3 and Arf1 are important in dictating temperature sensitivity while residues A174 and K180 from the C-terminus of Arf3 are important for its specific Golgi localization.

4.2 Results

4.2.1 Arf3 localizes specifically to the *trans*-compartments of the Golgi complex.

The first observation that sparked our interest towards investigating in more detail the specific localization and role of Arf3 was live cell imaging data obtained by Dr. Justin Chun in NRK cells. His data indicate that GBF1-GFP and Arf3-mCherry localize to distinct Golgi compartments (Chun et al., 2008). In order to confirm this unexpected observation we examined the relative distribution of Arf3 and several *cis*- and *trans*-Golgi markers within the Golgi complex. Most of those experiments took advantage of tagged forms of Arf3 expressed at low to moderate levels since none of the available antibodies selectively detect endogenous Arf3 in fixed cells. Some experiments used a pan-specific Arf antibody to detect overexpressed untagged Arf3.

Double labeling experiments in NRK cells confirmed that Arf3 localizes preferentially to a compartment containing *trans*-Golgi markers that is clearly separate from the *cis*-Golgi (Figures 4.1A and 4.2A). Quantifying the extent of overlap with various markers revealed that membrane-bound Arf3 colocalizes with the *trans*-Golgi markers BIG1 (~ 80%) and GalT-GFP (~ 84%) whereas it overlaps to a much smaller extent with the *cis*-Golgi markers GBF1 (~ 37%) and p115 (~ 30%) (Figures 4.1B and 4.2B). Similar results were obtained in HeLa cells (Figures 4.3 and 4.4). Importantly, Arf3 tagged with either GFP or the smaller HA epitope localized like untagged Arf3 to *trans*-compartments labelled with GalT-GFP (Figure 4.2). All these observations suggest that Arf3 localizes at the *trans*-side of the Golgi complex and that epitope-tagging does not interfere with this process.

4.2.2 BIGs are critical for Arf3 recruitment to the *trans*-side of the Golgi complex.

The specific localization for Arf3 described above (Figures 4.1, 4.2, 4.3 and 4.4) and the fact that the only Arf-GEFs enriched at the *trans*-side of the Golgi complex are BIG1 and BIG2 (Zhao et al., 2002) prompted us towards the next logical question: could there be a functional link between BIGs and Arf3? We

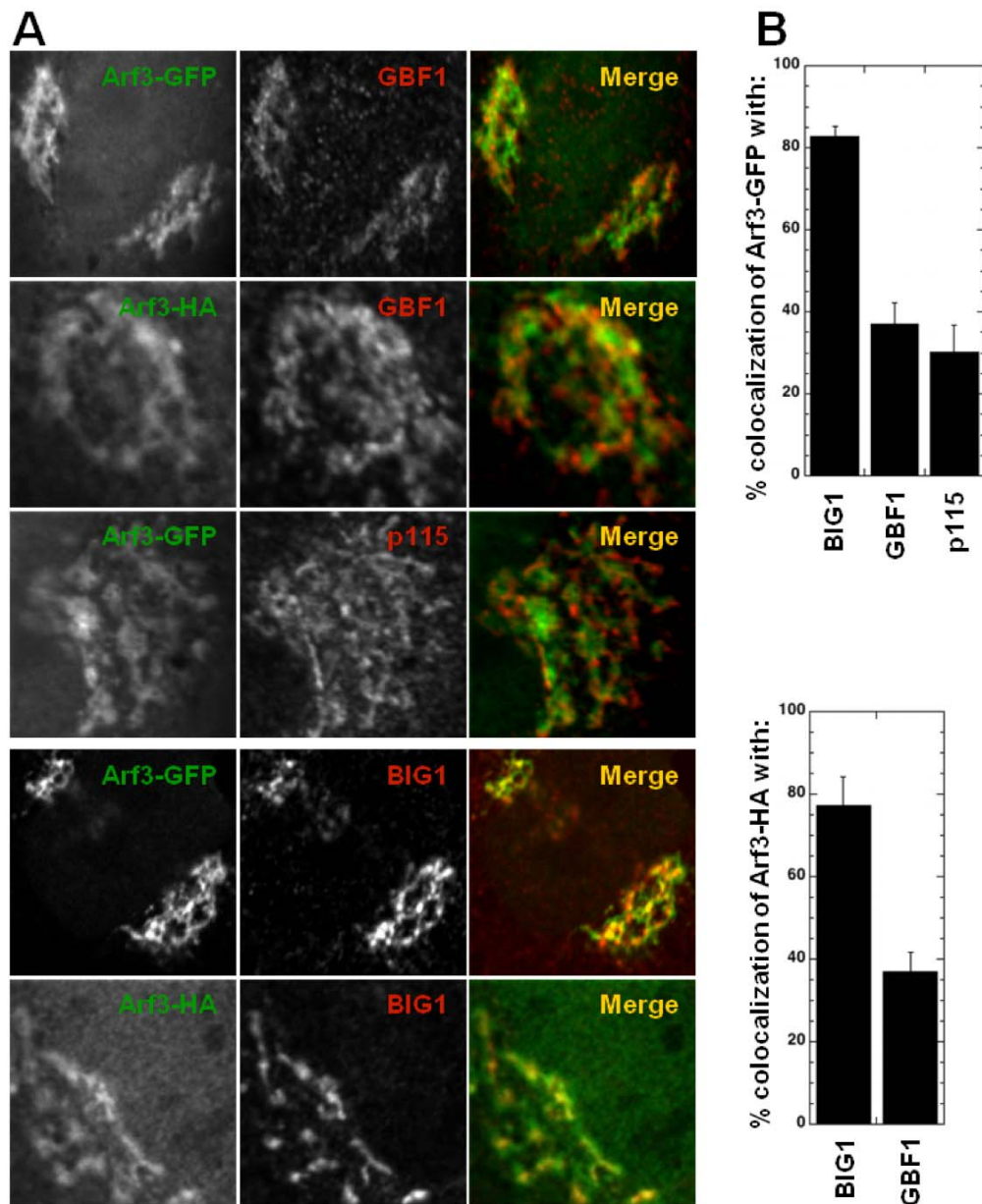


Figure 4.1. Arf3 localizes in a tag independent manner to a compartment distinct from the *cis*-Golgi.

A. NRK cells were transfected for 24 h with plasmids encoding Arf3-GFP or Arf3-HA as indicated. Fixed cells were stained for the specified markers and images were acquired using a confocal microscope. Representative images selected from at least 2 separate experiments are shown. **B.** Quantitative analysis of signal overlap between Arf3 and the specified markers was performed as described in section 2.9.6. Error bars correspond to the mean \pm SD ($n \geq 16$ cells from 2 separate experiments).

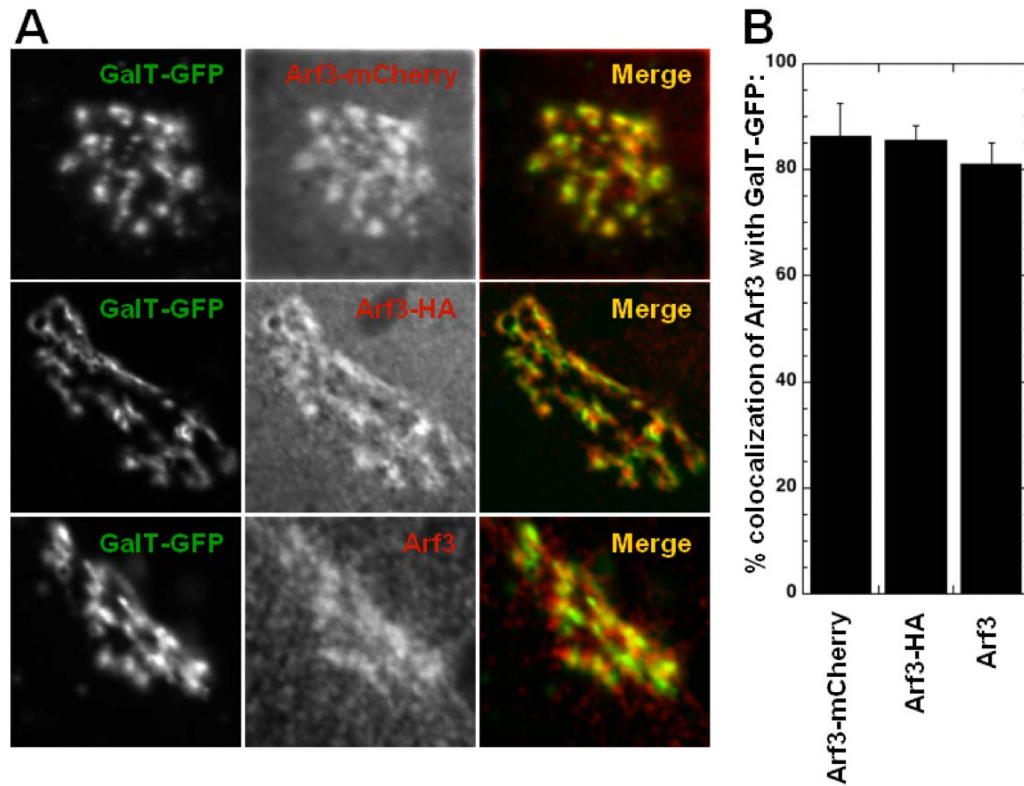


Figure 4.2. Arf3 localizes in a tag independent manner to the *trans*-side of the Golgi complex.

A. NRK cells were transfected for 24 h with plasmids encoding Arf3-mCherry, Arf3-HA, untagged Arf3 and GalT-GFP as indicated. Fixed cells were stained for the specified markers and images were acquired using a confocal microscope. Untagged Arf3 was stained using a pan specific Arf antibody (clone 1D9). Representative images selected from at least 2 separate experiments are shown. **B.** Quantitative analysis of signal overlap between Arf3 and GalT-GFP was performed as described in section 2.9.6. Error bars correspond to the mean \pm SD ($n \geq 16$ cells from 2 separate experiments).

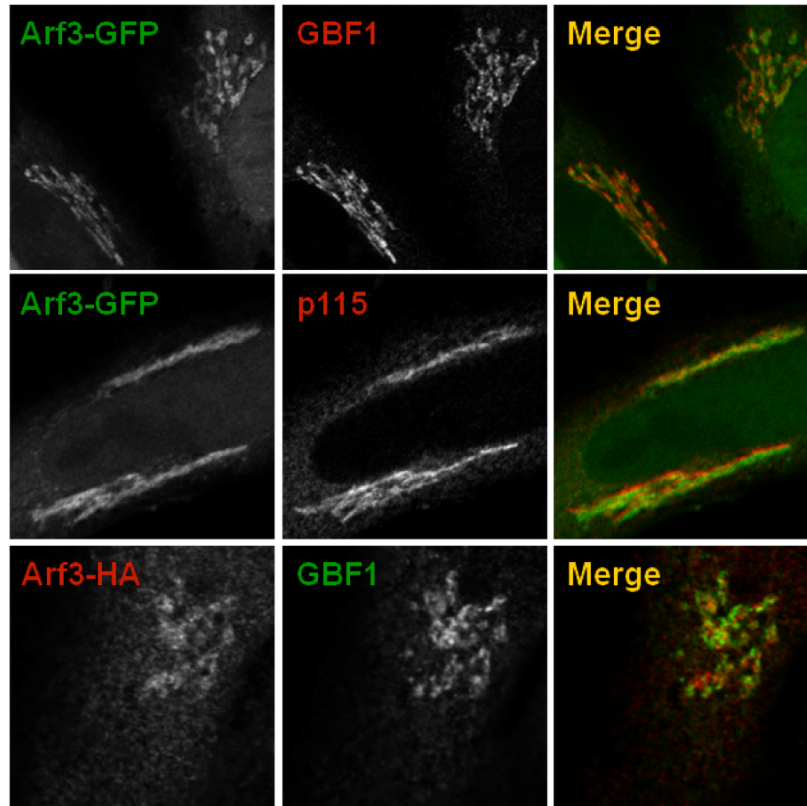


Figure 4.3. Arf3 localizes to a compartment clearly distinct from the *cis*-Golgi in HeLa cells.

HeLa cells were transfected for 24 h with plasmids encoding Arf3-GFP or Arf3-HA as indicated. Fixed cells were stained for the specified markers and images were acquired using a confocal microscope. Representative images selected from at least 2 separate experiments are shown. Red and green signal show distinct but sometimes complementary pattern.

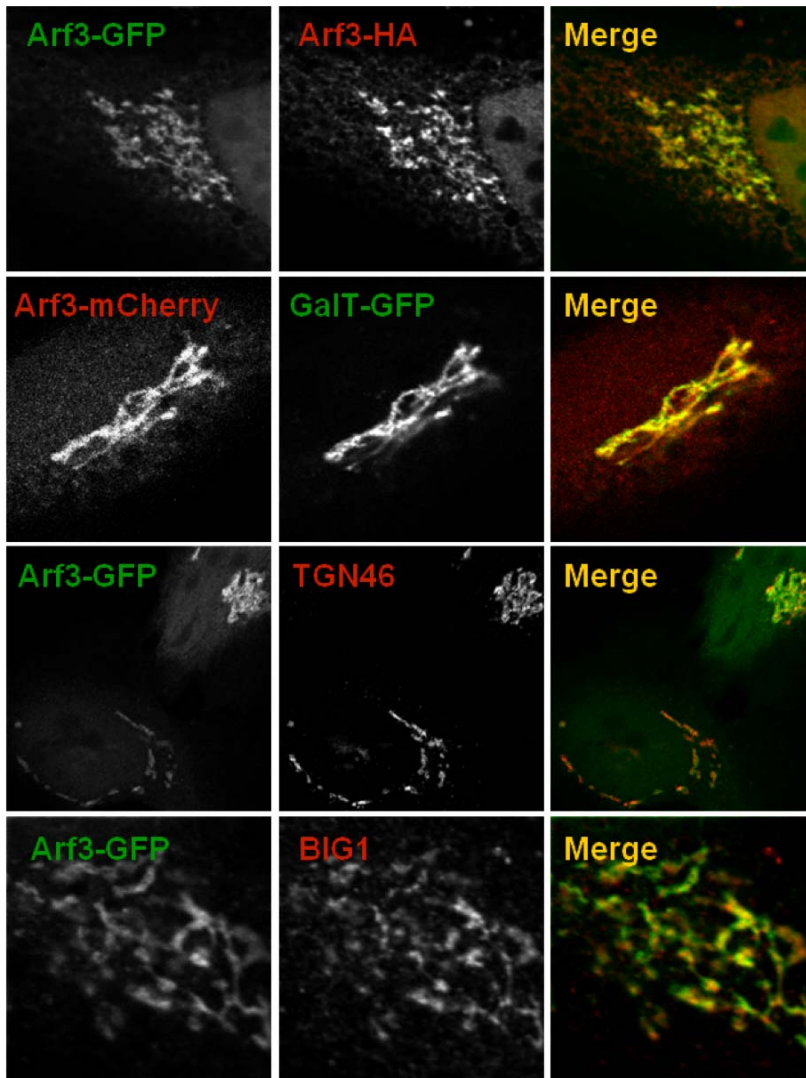


Figure 4.4. Arf3 also localizes to the *trans*-side of the Golgi complex in HeLa cells, regardless of the tag.

HeLa cells were transfected with plasmids encoding Arf3-GFP, Arf3-mCherry, Arf3-HA and/or GalT-GFP as indicated. Fixed cells were stained for the specified markers and images were acquired using a confocal microscope. Representative images selected from at least 2 separate experiments are shown. Although red and green signal vary in intensity, patterns are similar and signal largely overlap.

tested this hypothesis by a series of three complementary experiments. We first examined if overexpression of BIG1 prevented dispersal of Arf3-GFP after short BFA treatment. Overexpression of the Arf-GEF should protect the membrane recruitment of its effectors from the effect of BFA in a similar fashion as GBF1 or BIG1 overexpression protected COP1 or AP-1, respectively (Figure 3.1 A and B). As predicted, Arf3-GFP fully dispersed in control cells shortly after BFA addition, but remained Golgi-localized in cells overexpressing even moderate levels of BIG1 (Figure 4.5A, top panels). In contrast, overexpression of GBF1 even to very high levels did not prevent BFA-induced redistribution of Arf3-GFP (Figure 4.5A, bottom panels). Quantitative analysis of cells overexpressing either BIG1 or GBF1 confirmed that Arf3-GFP still localized to juxtannuclear membranes in $94 \pm 2\%$ of BIG1 overexpressing cells but in only $4 \pm 1.3\%$ of GBF1 overexpressing cells (Figure 4.5B).

To determine if BIGs were required for Arf3 activation and recruitment to *trans*-Golgi compartments we performed complementary knockdown experiments. We previously established that knockdown of BIGs disperses the TGN but does not affect the GBF1/COP1 system and maintenance of a polarized Golgi stack (Manolea et al., 2008). Since Arf1 localizes preferentially towards the *cis*-Golgi (Honda et al., 2005), it should depend primarily on GBF1, not BIGs for its recruitment. We therefore predicted the *cis*- and *trans*-localized Arf1 and Arf3 would be differentially affected by loss of BIGs. To test this possibility, we co-transfected HeLa cells with plasmids encoding Arf1-GFP and Arf3-Cherry and examined the impact of BIGs knockdown on their distribution. As predicted, knockdown of BIGs, measured by dispersal of juxtannuclear AP-1, caused redistribution of Arf3 but not Arf1 (Figure 4.6A). Quantitative analysis showed Arf3 associated with the Golgi complex in only $4 \pm 3.6\%$ of cells with AP-1 redistributed while Arf1 was still membrane recruited in $98 \pm 2.6\%$ of BIGs knockdown cells (Figure 4.6B).

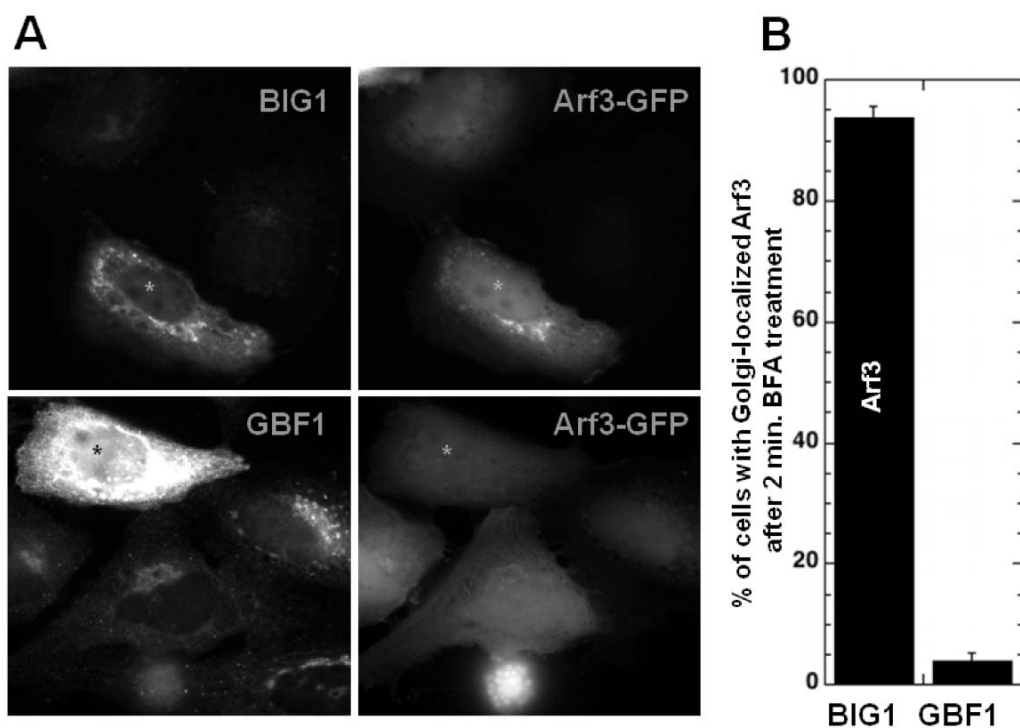


Figure 4.5. Overexpression of BIG1, but not GBF1, protects Arf3 from BFA-induced redistribution.

A. HeLa cells were co-transfected with plasmids encoding Arf3-GFP and either BIG1 or GBF1. After 24 hours, cells were treated with 5 μ g/ml BFA for 2 min and then fixed and stained for BIG1 or GBF1. Representative epifluorescence images are shown. Small asterisks label the nucleus of transfected cells. **B.** Quantitative analysis of cells overexpressing BIG1/GBF1 showing the percentage of cells with Arf3 localized to the Golgi complex after BFA treatment was performed as described in section 2.9.4. Error bars correspond to the mean \pm SD ($n \geq 30$ cells from at least 4 separate experiments as in **A**).

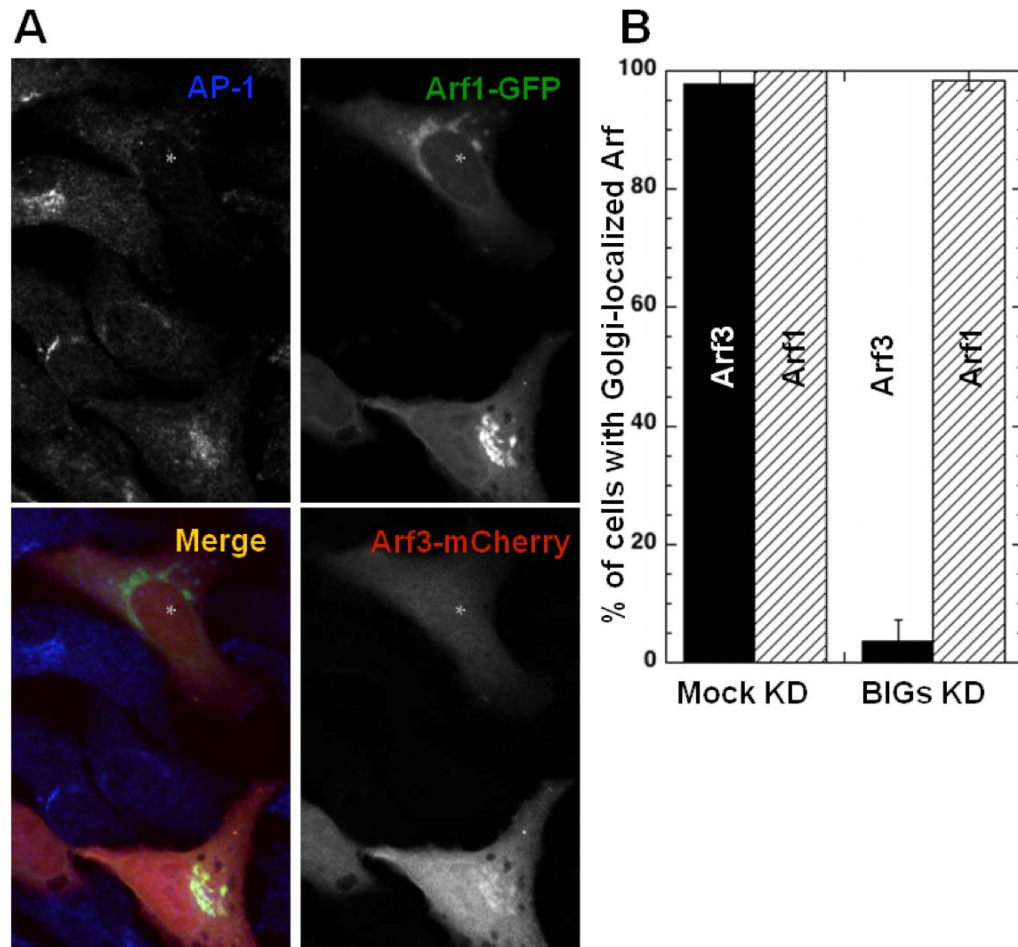


Figure 4.6. BIGs knockdown redistributes Arf3 but not Arf1 from Golgi membranes.

HeLa cells were transfected with either irrelevant RNA (Mock KD) or a pool of siRNA duplexes targeting BIG1 and BIG2 (BIGs KD) for 72 hours. 48 hours before fixation, cells were co-transfected with Arf1-GFP and Arf3-mCherry. **A.** Fixed cells were stained for AP-1 and images were acquired using a confocal microscope. Small asterisks label the nucleus in a cell with efficient BIGs KD. **B.** Quantitative analysis of cells with Mock KD or BIGs KD showing the percentage of cells with Arf3 or Arf1 localized to the Golgi complex was performed as described in section 2.9.5. Error bars correspond to the mean \pm SD ($n \geq 30$ cells from at least 4 separate experiments as in B).

4.2.3 Arf3 distribution remains sensitive to BFA in CHO mutant cells with BFA resistant GBF1/COPI system.

The unexpected dependence of Arf3 membrane recruitment on BIGs prompted us to test the functional link between the BIGs and Arf3 using one additional approach. This time we took advantage of a CHO-derived mutant cell line, BFY1 that acquired a Golgi-specific resistance to BFA so that markers of the TGN and endosomes, but not of the Golgi stack, dispersed upon BFA treatment. Current evidence suggests that BFY-1 cells acquired a BFA resistant GBF1/COPI system but retained a BIGs/clathrin system sensitive to BFA. This gave us the opportunity to test if Arf3 remained sensitive to short treatment with BFA in the BFY1 cell line, suggesting that Arf3 functions with BIGs at the TGN.

We first verified the predicted BFA resistance and sensitivity of the GBF1/COP1 and BIGs/clathrin systems, respectively. As expected, whereas all tested markers were sensitive to BFA in the parental CHO cell line (Figures 4.7 and 4.8, top panels), the GBF1/COP1 system in BFY1 cells acquired resistance to short BFA treatment (Figure 4.7, bottom panels) while BIGs represented here by AP-1 remained sensitive (Figure 4.8, bottom panels). More importantly, Arf1 and Arf3 displayed the predicted differential sensitivity to BFA in BFY1 cells (Figures 4.7 and 4.8, bottom panels). We are confident about these results since COPI and Arf1 remained membrane associated in the same BFY1 cells that show redistributed Arf3 or AP-1, respectively.

To confirm our results, we directly compared the behaviour of the two Arfs in BFY1 cells co-transfected with plasmids encoding Arf3-mCherry and Arf1-GFP. As expected, recruitment of Arf3-mCherry appeared sensitive to a short BFA treatment while Arf1-GFP retained most of its juxtannuclear localization (Figure 4.9) and was thus minimally sensitive to BFA. All these observations taken together reinforce the functional link we describe between the TGN localized Arf3 and the BIGs.

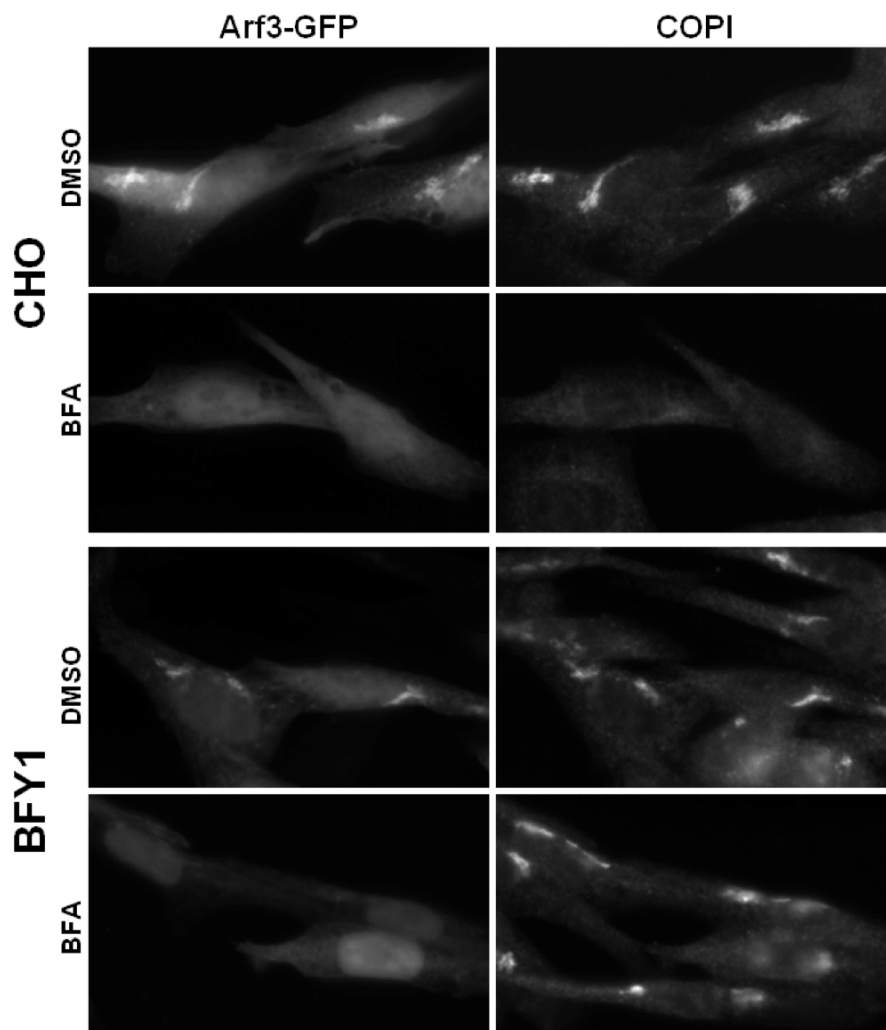


Figure 4.7. Membrane recruitment of Arf3 remains BFA sensitive in BFY1 cells.

CHO and BFY1 cells were transfected with a plasmid encoding Arf3-GFP. After 24 hours, cells were treated with 5 μ g/ml BFA for 2 min and then fixed and stained for COPI. Representative epifluorescence images are shown selected from at least 2 separate experiments are shown. As expected, COPI remains membrane associated even after treatment with BFA.

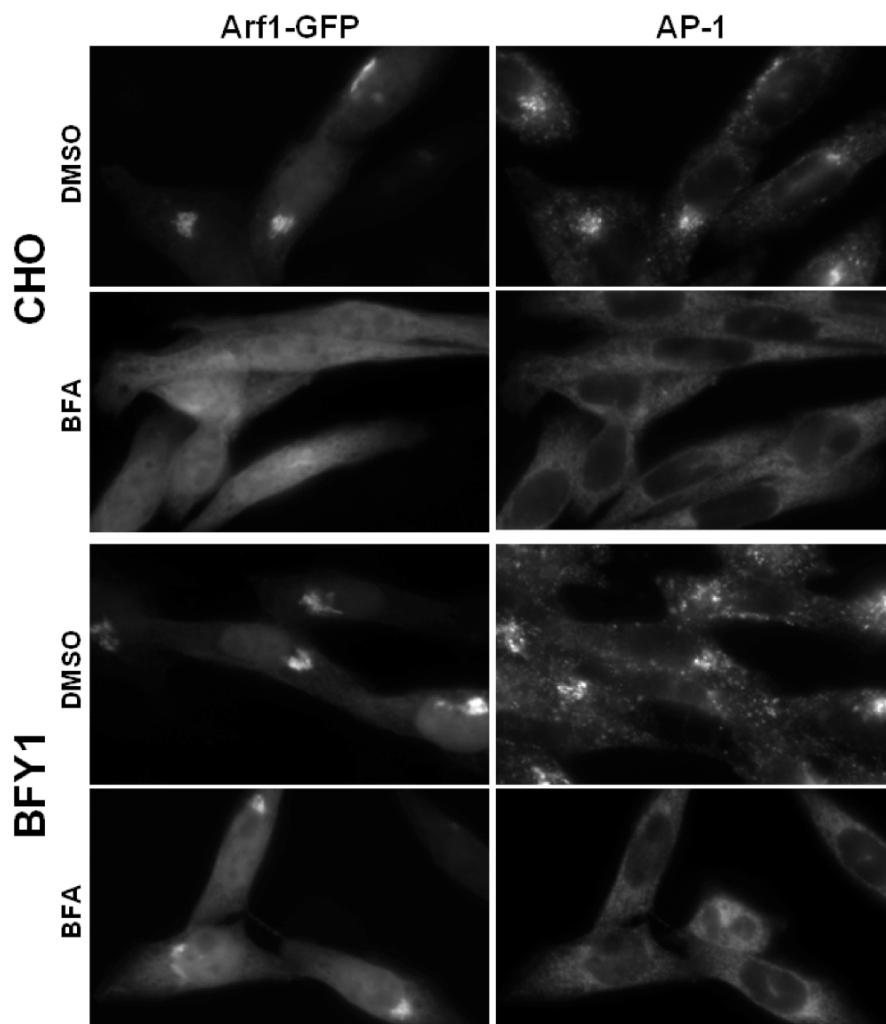


Figure 4.8. Arf1 remains membrane associated after short BFA treatment while AP-1 redistributes in BFY1 cells.

CHO and BFY1 cells were transfected with a plasmid encoding Arf1-GFP. After 24 hours, cells were treated with 5 μ g/ml BFA for 2 min and then fixed and stained for AP-1. Representative epifluorescence images selected from at least 2 separate experiments are shown.

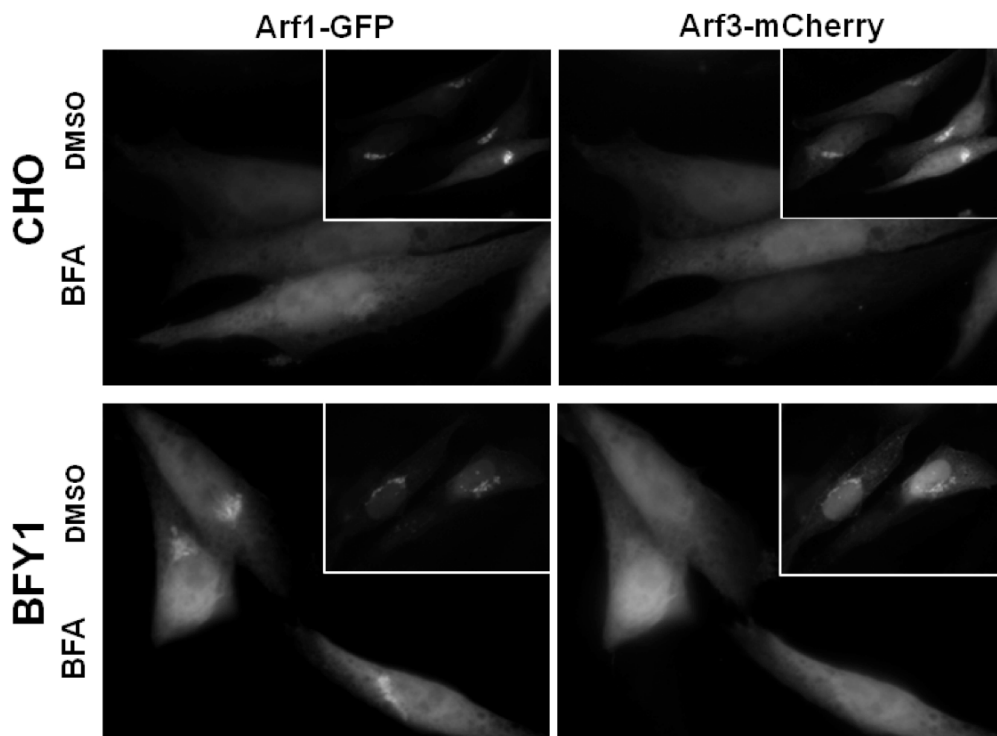


Figure 4.9. Arf3 redistributes in BFY1 cells after short BFA treatment while Arf1 remains membrane associated.

CHO and BFY1 cells were cotransfected with plasmids encoding Arf1-GFP and Arf3-mCherry. After 24 hours, cells were treated with 5 μ g/ml BFA for 2 min and then fixed. Representative epifluorescence images selected from at least 2 separate experiments are shown.

4.2.4 Temperature shift to and from 20°C slowly redistributes Arf3 between Golgi membranes and cytosol.

It was previously demonstrated that shifting temperature to 20°C blocks cargo protein progression at *trans*-Golgi compartments and likely impacts TGN sorting functions (Griffiths et al., 1989; Matlin and Simons, 1983; Saraste et al., 1986). The observations that Arf3 localizes to *trans*-Golgi compartments (Figures 4.1, 4.2, 4.3 and 4.4) and that its membrane recruitment requires TGN-localized BIGs (Figures 4.5, 4.6 and 4.9), prompted us to test if shifting temperature to 20°C would affect Arf3. Indeed, lowering the temperature had a major impact on Arf3 membrane recruitment (Figure 4.10A, top panels). However, redistribution of Arf3 from Golgi membranes upon shift to 20°C was not immediate, but proceeded with a $t_{1/2}$ of approximately 10 minutes (Figure 4.10B, left graph). When the temperature was shifted back to 37°C from 20°C, Arf3 re-associated with Golgi membranes but recruitment was also delayed with a $t_{1/2}$ of approximately 7.5 minutes (Figure 4.10A, bottom panels and Figure 4.10B, right graph). This delay in Arf3 redistribution between Golgi membranes and cytosol upon temperature shift suggests enzymatic or lipid membrane remodelling processes being key regulators in Arf3 membrane recruitment. The reduction in Arf3 recruitment at 20°C did not result from trivial explanations such as loss of BIGs or disappearance of the TGN since the distribution of Arf1, TGN46, BIG1 or AP-1 remained unaffected (Figure 4.11).

One lipid component that could be affected by the temperature shift is the TGN localized PtdIns(4)P. In order to accurately monitor the levels of PtdIns(4)P we took advantage of a chimera containing YFP and two copies of the PH domain of PI(4)P adaptor protein (FAPP) 2 (FAPP-PH-YFP) (Godi et al., 2004; Levine and Munro, 2002). Unfortunately, the signal for FAPP-PH-YFP in the large majority of cells analyzed after the temperature shift had very similar intensity and pattern with the one observed in the cells fixed at 37°C (Figure 4.11). The experiment suggests that the PtdIns(4) levels are not affected significantly by the temperature change.

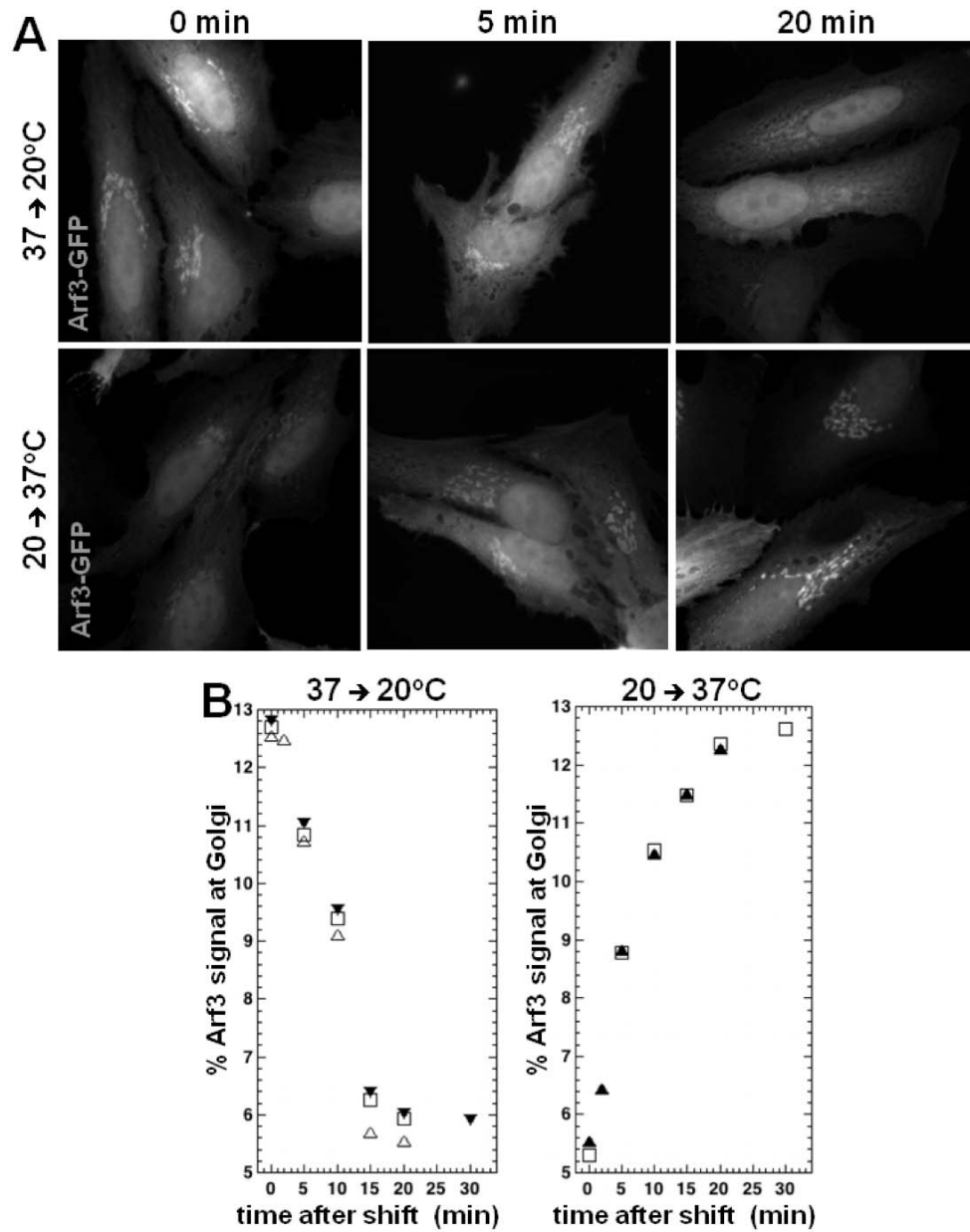
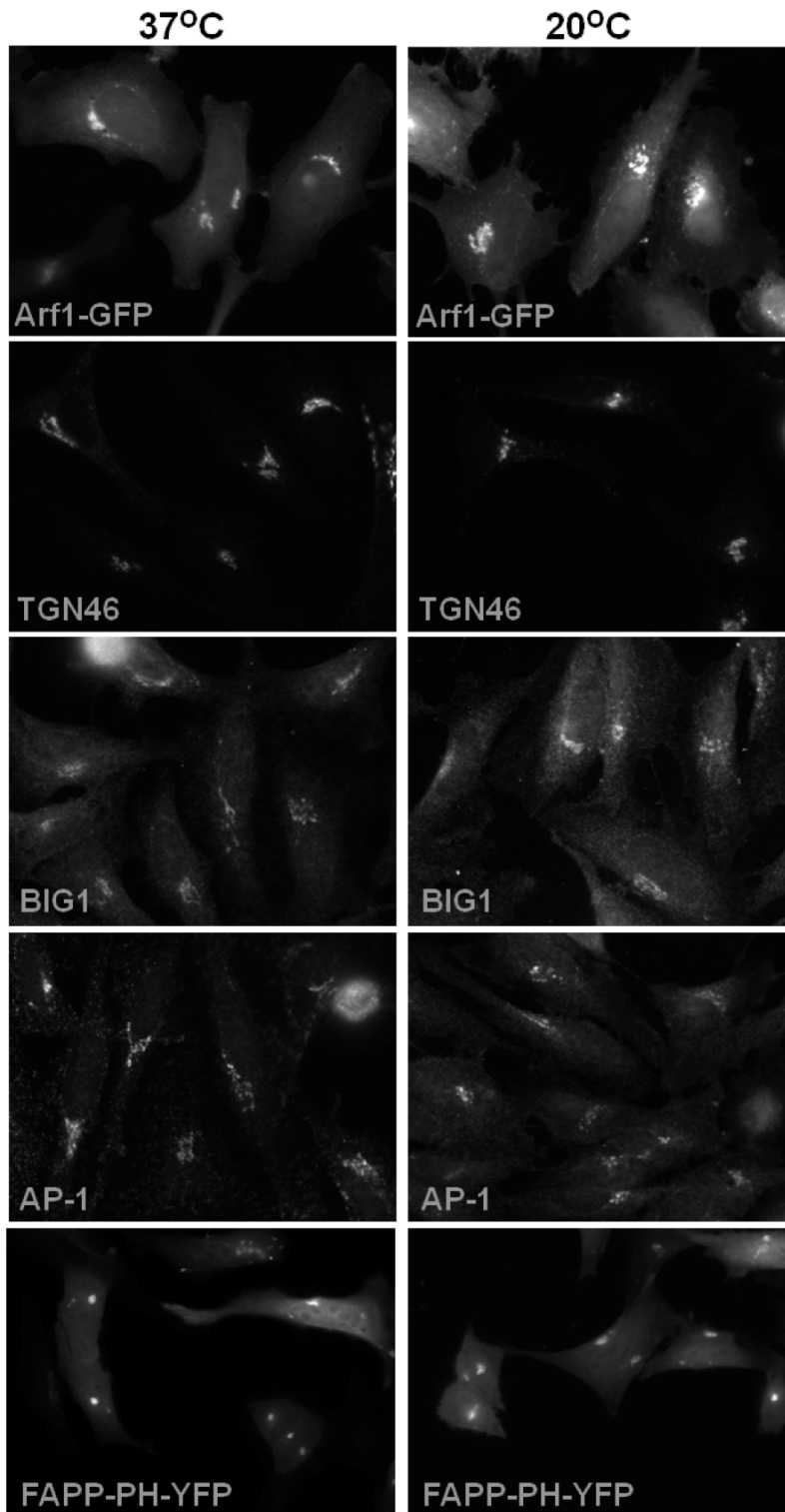


Figure 4.10. Arf3 redistributes slowly between Golgi membranes and cytosol upon temperature shift to either 20°C or 37°C.

A. HeLa cells were transfected with a plasmid encoding Arf3-GFP for 24 hours. Cells were then shifted from 37°C to 20°C (top panels), or kept at 20°C for 1 hour and then shifted to 37°C (bottom panels). Cells were fixed at the indicated time following shift. Representative epifluorescence images are shown. **B.** Quantitative analysis of Arf3 signal at the Golgi complex expressed as percent of total cell signal for temperature shift experiments performed as in **A.** ($n \geq 20$ cells/time point from at least 2 separate experiments).

Figure 4.11. Temperature shift to 20°C has no impact on Golgi membrane recruitment of Arf1-GFP, TGN46, BIG1, AP-1 or FAPP-PH-YFP.

HeLa cells were transfected with a plasmid encoding for Arf1-GFP or FAPP-PH-YFP or transfection reagent only for 24 hours. Cells were either fixed directly from 37°C (left panels) or shifted from 37°C to 20°C for either 30 minutes (FAPP-PH-YFP) or 2 hours (remaining right panels) and then fixed. Cells were stained for the specified markers and images were acquired using identical settings for the 37°C and the 20°C samples. Representative epifluorescence images selected from at least 2 separate experiments are shown.



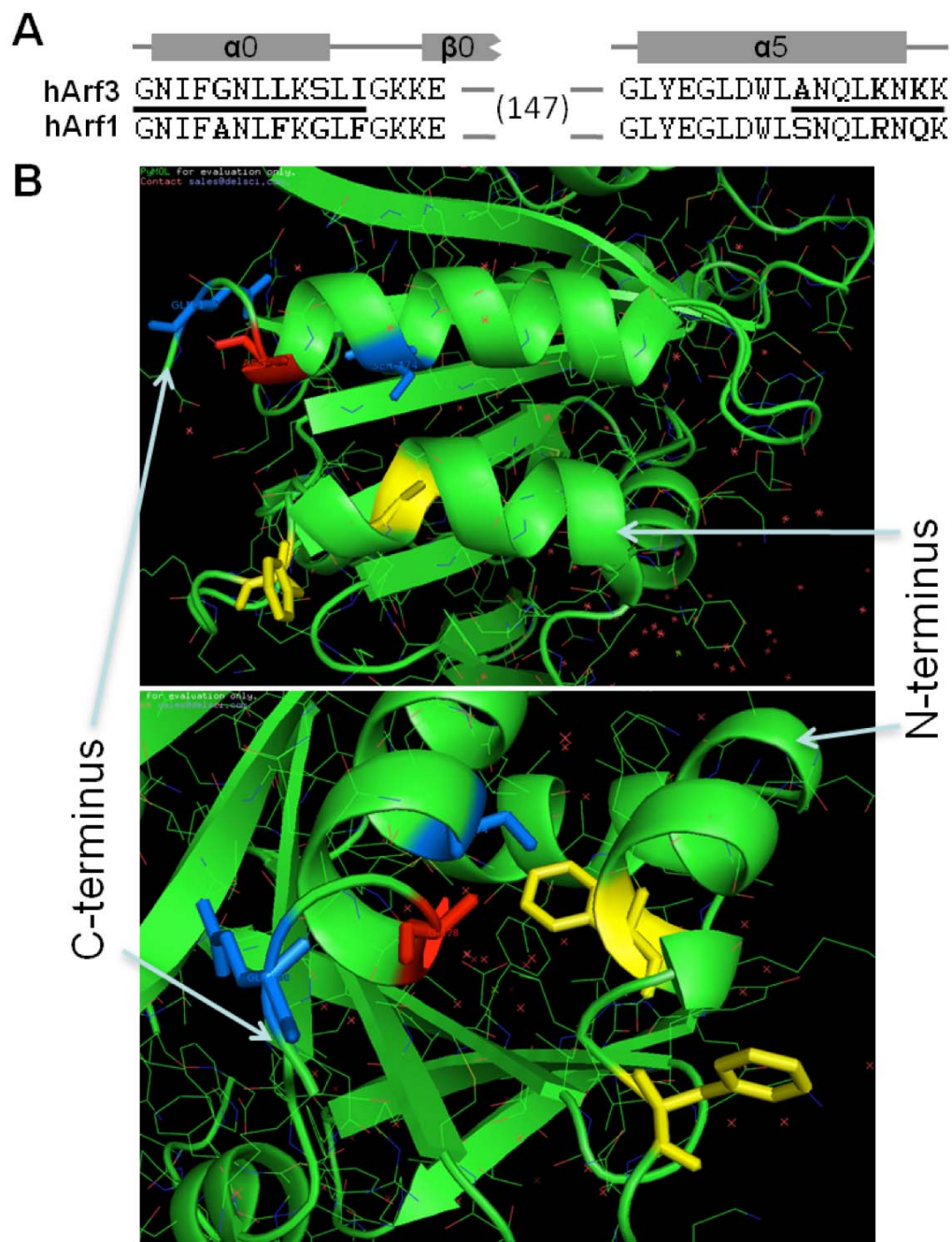


Figure 4.12. Arf3 and Arf1 differ only at their N- and C-termini

A. Sequence alignment of the N- and C-terminal regions of hArf3 and hArf1, showing the corresponding secondary structure. Lines indicate the swapped regions. Variant residues shown in bold. **B.** Snapshots of 2 different views of the N-terminal and C-terminal helices of full length Arf1-GDP (Amor et al, 1994) were visualized using PyMOL. Residues that are different between Arf3 and Arf1 are displayed in color.

4.2.5 Temperature sensitivity for membrane recruitment of Arf3 and Arf1 is encrypted within their N-terminal helices.

The sequences of human Arf1 and Arf3 differ in only two short regions at the N- and C-termini (Figure 4.12A). To identify which region is important for temperature sensitivity we generated Arf3/Arf1 chimeras in which the variant regions were swapped (regions marked by a line in Figure 4.12A). Analysis of these chimeras revealed that Arf1 constructs containing the N-terminal region of Arf3 (black bar) redistributed as WT Arf3 upon shift to 20°C (Figure 4.13). Conversely, Arf3 chimeras containing the N-terminal region of Arf1 (hatched bar) remained unaffected by the temperature change, like WT Arf1 (Figure 4.13). These results indicated that temperature sensitivity lies in the sequence of the N-terminal helix.

Two unique aromatic residues in Arf1 have been implicated in membrane association (Antonny et al., 1997; Losonczi et al., 2000) and were selected for further analysis. We swapped the two F residues from Arf1 (F9 and F13) with the corresponding residues from Arf3 (L9 and I13) resulting in two chimeras, Arf3FF (L9F, I13F) and Arf1LI (F9L, F13I). The results from experiments using these chimeras clearly demonstrate that Arf3FF-GFP mutant behaves as WT Arf1 since it recruits well to membranes and is not affected by the 20°C temperature shift (Figure 4.14). On the other hand, the Arf1LI-GFP mutant behaves as WT Arf3, recruiting less efficiently to membranes and showing significant decrease in membrane association at 20°C (Figure 4.14). We conclude that residues L9 and I13 are crucial in directing the temperature sensitivity of Arf3, while an F at positions 9 and 13 will render an Arf resistant to temperature variation.

4.2.6 The C-terminal helix dictates localization of Arf3 to *trans*-Golgi compartments

Arf3 and Arf1 not only seem to have different temperature behaviors as we have seen in the previous section (Figure 4.13) but they also differ in localization within the Golgi complex. Arf3 concentrates towards the *trans*-side of the Golgi complex as we previously demonstrated (Figures 4.1, 4.2, 4.3 and 4.4) while Arf1 seems to be recruited preferentially towards the *cis*-side (Honda et al., 2005). The

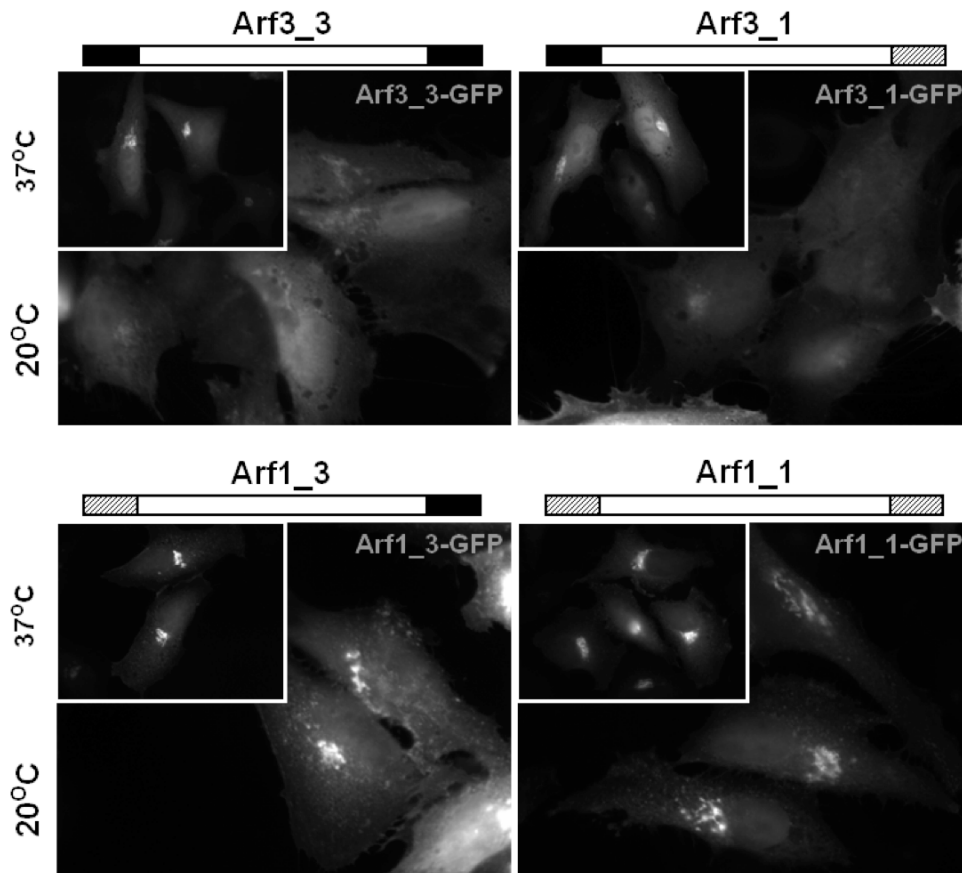


Figure 4.13. The N-terminal helix determines the temperature sensitivity of Arf3.

HeLa cells were transfected with the indicated Arf3/Arf1 chimeras tagged with GFP. After 24 hours, cells were either kept 37°C or shifted to 20°C for 30 minutes and then fixed. Representative epifluorescence images selected from at least 2 separate experiments are shown. A schematic representation of transfected chimera is shown above each panel.

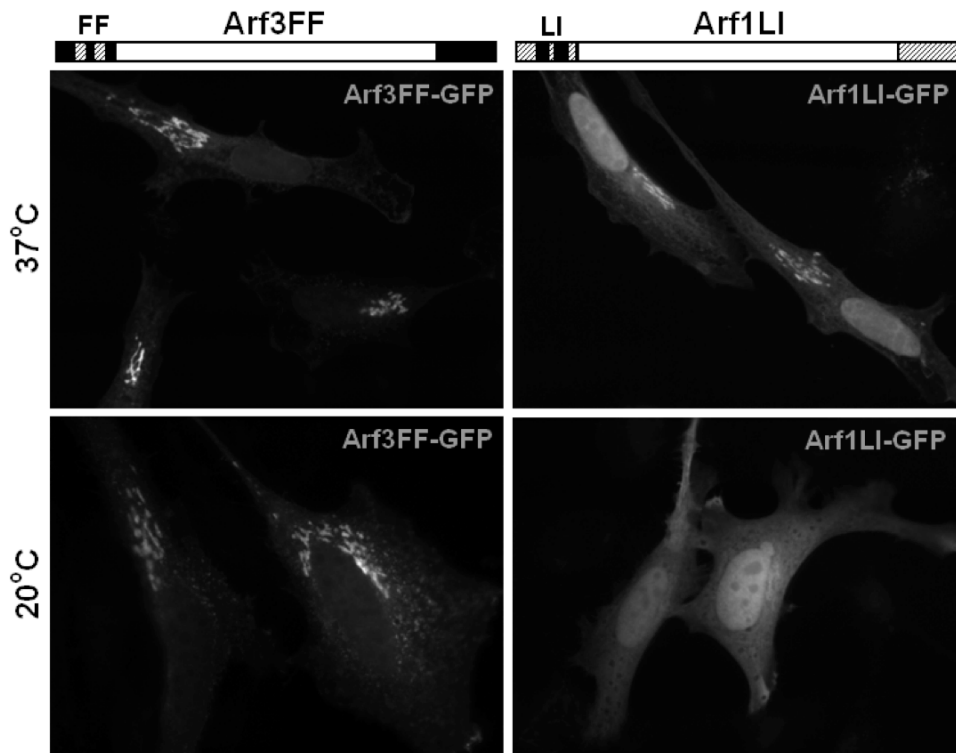


Figure 4.14. Two residues in the N-terminal helix dictate the temperature sensitivity for membrane recruitment of Arf3 and Arf1.

HeLa cells were transfected with either Arf3FF-GFP or Arf1LI-GFP constructs as indicated. After 24 hours, cells were either kept at 37°C or shifted to 20°C for 30 minutes and then fixed. Representative epifluorescence images are shown selected from at least 2 separate experiments. Schematic representation of each construct shown above each set of panels.

availability of Arf3/Arf1 chimeras allowed us to determine which region might be important for directing the specific localization of Arf3. We initially suspected that the same N-terminal region important for membrane binding and temperature sensitivity might also be important for directing the specific localization of Arf3. To our surprise, the nature of the C-terminal rather than of the N-terminal helix in Arf3 appeared to dictate concentration of the chimeras on *trans*-Golgi compartments (Figure 4.15A). Quantitative analysis of signal overlap between the Arf3/Arf1 swap chimeras and GBF1, p115 and BIG1 confirmed accumulation of Arf3_1-GFP and Arf1_3-GFP towards the *cis*- and *trans*-side of the Golgi complex, respectively (Figure 4.15B). These results point towards the C-terminus as being critical in targeting specifically Arf3 to the *trans*-side of the Golgi complex.

For further analysis we constructed single mutants at the C-terminus in which Arf1 residues were substituted one by one into Arf3. HeLa cells transfected with these constructs were then examined for a change from an Arf3-like *trans*-Golgi complex localization to a more Arf1-like distribution on the *cis*-side of the Golgi stack. Analysis of HeLa cells expressing either Arf3A174S-GFP or Arf3K180Q-GFP revealed localization patterns similar to the *cis*-Golgi marker p115 and different from the *trans*-Golgi marker TGN46 (Figure 4.16A). Quantifying the extent of colocalization revealed that membrane-bound Arf3A174S-GFP and Arf3K180Q-GFP indeed colocalizes with the *cis*-Golgi marker p115 (~ 70% and 65%, respectively) and overlap to a much smaller extent with the *trans*-Golgi marker TGN46 (~ 40% and 35%, respectively) (Figure 4.16B). These preliminary results suggest that both residues A174 and K180 are important in directing Arf3 specific localization.

4.2.7 Arf3 knockdown does not disperse the TGN and does not block VSVG traffic at the Golgi complex.

Most secretory proteins traffic from the ER through the Golgi complex towards the PM. This is the route employed by the glycoprotein of vesicular stomatitis virus, VSVG, that was used in Chapter 3 to assess the impact of GBF1 knockdown and BIGs knockdown on protein traffic (see Figures 3.8, 3.9, 3.13-

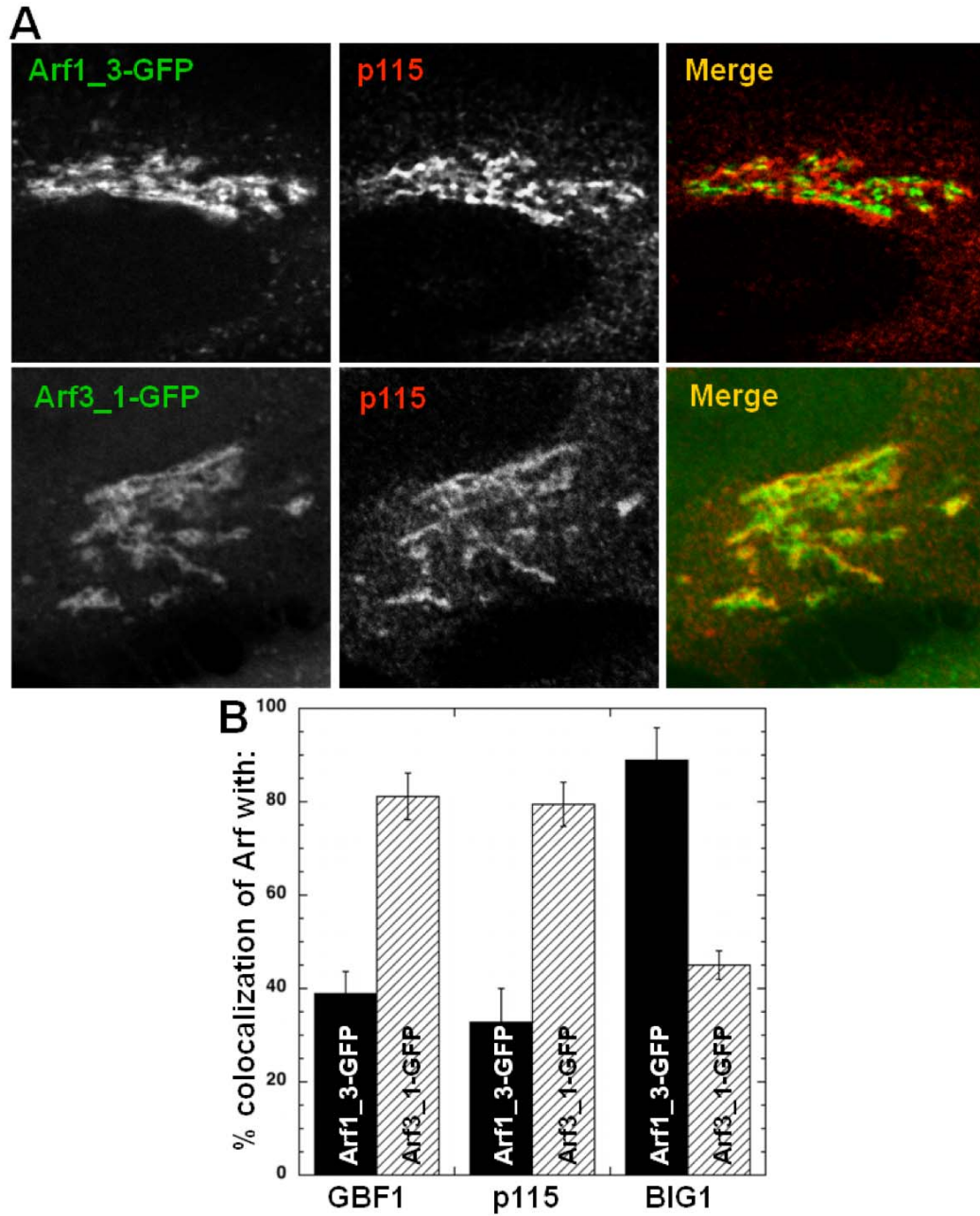


Figure 4.15. The C-terminal helix of Arf3 is required for concentration on the TGN.

A. HeLa cells were transfected with the indicated Arf3/Arf1 chimeras tagged with GFP. After 24 hours, cells were fixed and stained for p115. Images were acquired using a confocal microscope.

B. Quantitative analysis of experiments similar to **A** showing signal overlap between the Arf3/Arf1 swap constructs and the specified markers. Error bars correspond to the mean \pm SD ($n \geq 7$ cells from 2 separate experiments).

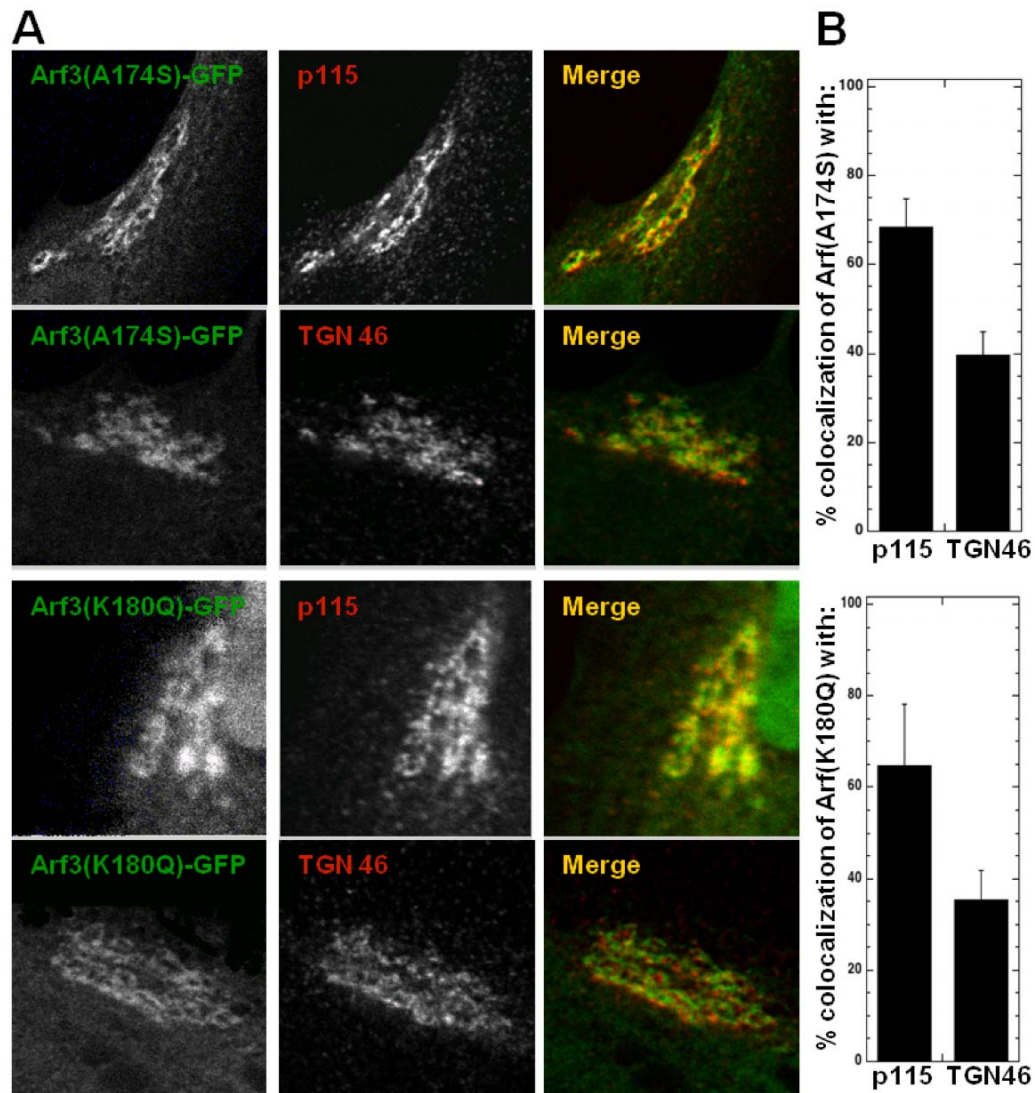


Figure 4.16. Two residues in the C-terminal helix are critical for the specific localization pattern of Arf3.

A. HeLa cells were transfected with the indicated Arf3A174S-GFP or Arf3K180Q-GFP chimeras. After 24 hours, cells were fixed and stained for p115 or TGN46. Images were acquired using a confocal microscope. **B.** Quantitative analysis of experiments similar to **A** showing signal overlap between the Arf3/Arf1 swap single mutants and the specified markers. Error bars correspond to the mean \pm SD ($n \geq 10$ cells from 2 separate experiments).

3.15). As mentioned earlier, traffic through this pathway is sensitive to shifts in temperature with two well-characterized blocks at 15 °C and 20°C. For example, EM studies revealed that a shift to 20°C blocks VSVG at the TGN (Griffiths et al., 1989). The observations that Arf3 localizes specifically to the *trans*-side of the Golgi complex and that Arf3 shows a dramatic decrease in membrane recruitment after the downshift to 20°C (Figure 4.10) suggested a potential connection between Arf3 and the temperature-dependent blockage of VSVG at the Golgi complex.

To test this hypothesis, we analyzed cells treated with a pool of two validated siRNAs that effectively block exogenous Arf3-GFP expression from co-transfected plasmids (Figure 4.17). This was the only way to assess for the effectiveness of the Arf3 knockdown since the commercially available antibodies against Arf3 that we tested failed to give an immunoblots signal for either endogenous or overexpressed Arf3 (Figure 4.18). In order to maximize the knockdown effectiveness we doubled the siRNA amounts that were used and waited for an additional two days (three days in total). We first confirmed that an effective 20°C block could be observed using epifluorescence. Upon shift to the permissive temperature, a thermo-sensitive form of VSVG reaches the PM in control cells in less than 90 minutes (Figure 4.19A left panels and Figure 4.19B). A shift to 20°C effectively prevented VSVG appearance at the PM and caused its arrest at the Golgi complex (Figure 4.19A middle panels) in the vast majority of cells examined (Figure 4.19B). To our surprise, VSVG was not blocked at the Golgi complex but reached the PM in all the cells transfected with Arf3 siRNAs (Figure 4.19 A and C). Parallel experiments established that treatment with Arf3 siRNAs had no impact on the TGN as judged by staining for TGN46 and BIG1 or the clathrin adaptors AP-1 and GGA3 (Figure 4.20). These observations are consistent with previously published data suggesting that knockdown of Arf3 by itself did not significantly impact TGN architecture, clathrin adaptors recruitment or VSVG trafficking (Volpicelli-Daley et al., 2005).

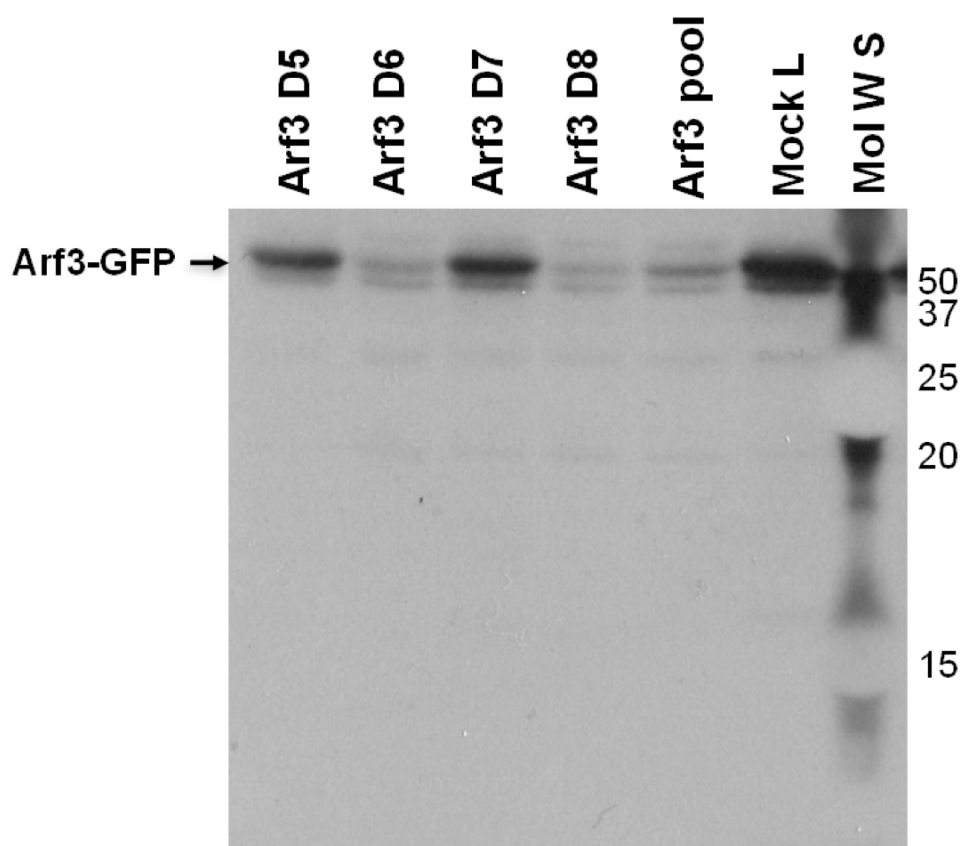


Figure 4.17. Arf3-targeted siRNAs, either individually or a pool, efficiently prevent Arf3-GFP expression.

HeLa cells were cotransfected with the indicated siRNAs targeting Arf3 and 1 μ g of plasmid encoding for Arf3-GFP for 24 h as described in Chapter 2. Detergent lysates were prepared and equal amounts of total protein were separated on a 15% SDS-PAGE gel. Following transfer to a nitrocellulose membrane, blots were probed with an anti-GFP antibody. Blots shown are representative of 3 separate experiments. Note the absence of cleavage products of the Arf3-GFP chimera. Gels were calibrated with Molecular Weight Standards (Mol W S) whose mobility is indicated on the right.

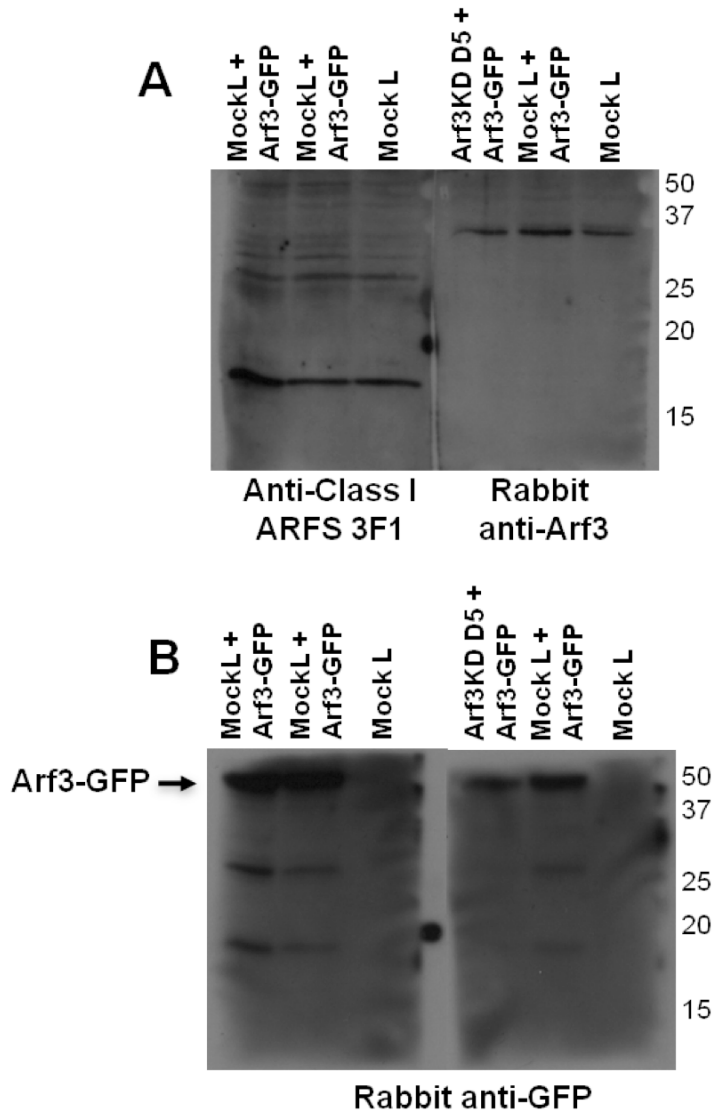


Figure 4.18. Two commercial antibodies against Arf3 do not yield any immunoblot signal for either endogenous or overexpressed Arf3.

HeLa cells were transfected with siRNAs targeting Arf3 (Duplex 5) or Luciferase (MockL) and with 1 μ g of plasmid encoding for Arf3-GFP (+Arf3-GFP) for 24 h as described in Chapter 2. Detergents lysates were prepared and equal amounts of total protein were separated on a 15% SDS-PAGE gel. Following transfer to a nitrocellulose membrane, blots were probed either with the specified commercial anti-Arf3 antibodies (**A**) or with an anti-GFP antibody (**B**). Arf3-GFP mobility shown while endogenous Arf3 should be just above the 20 kDa. Blots shown are representative of 3 separate experiments. The mobility of each molecular weight standard is shown on the right side for top panels and in-between for bottom panels.

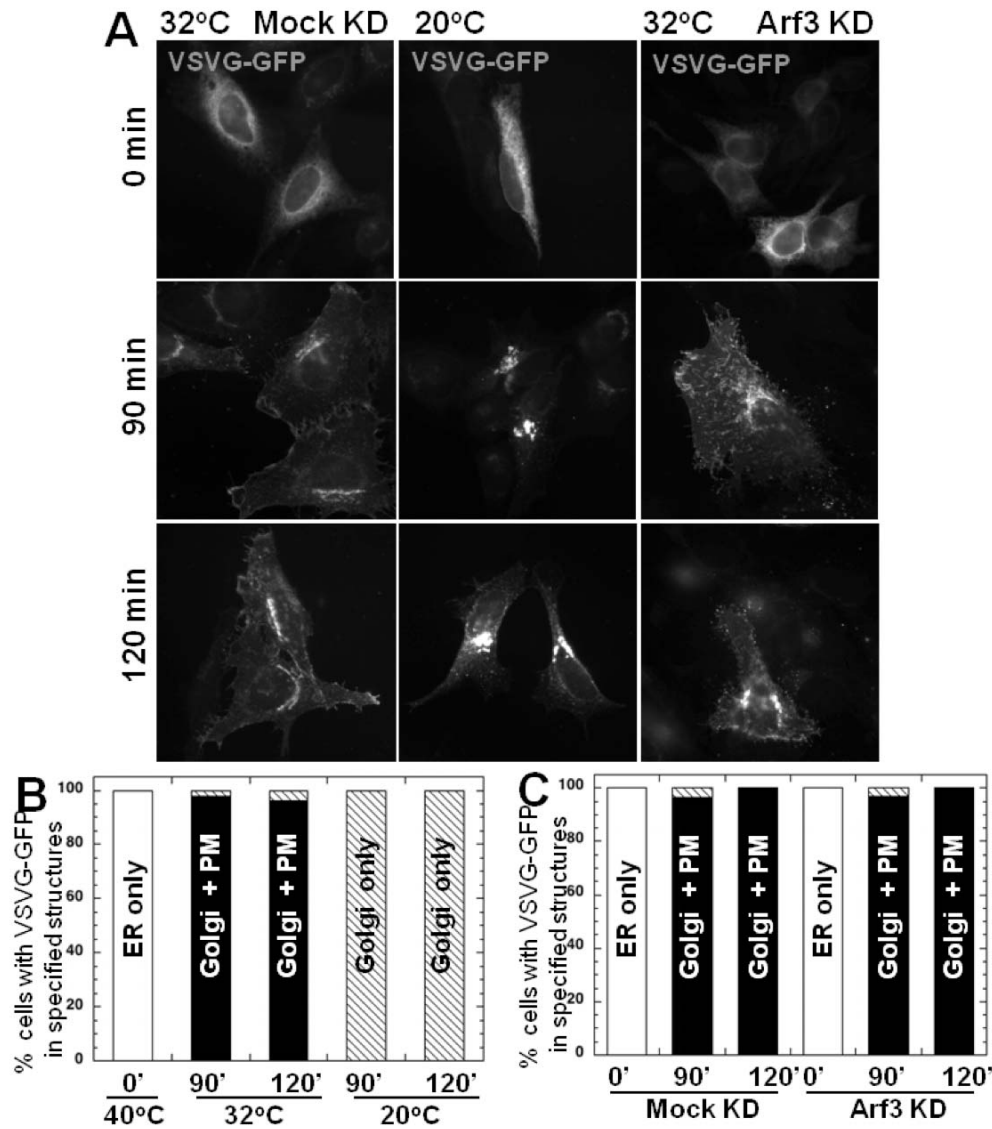


Figure 4.19. Shift to 20°C, but not Arf3 knockdown, blocks VSVG traffic at the Golgi complex.

A. HeLa cells were transfected at $t=0$ with either irrelevant siRNA (Mock KD, left panels), no RNA (middle panels) or a pool of two validated Arf3 siRNA duplexes (Arf3 KD, right panels). Fifty hours post-transfection, cells were transfected again with a plasmid encoding VSVGts045-GFP. Temperature was shifted initially to 40°C for 4 hours and then to either 32°C or 20°C for the length of time specified. Representative epifluorescence images are shown. **B.** Quantitative analysis showing percent of cells with VSVG in specified structures following release at the two different temperatures and time points. **C.** Quantitative analysis showing percentage of cells with VSVG in specified structures following release at the indicated time points in either Mock or Arf3 KD cells. **B and C.** ER only, Golgi only and Golgi + PM distribution presented as white, hatched and black columns respectively.

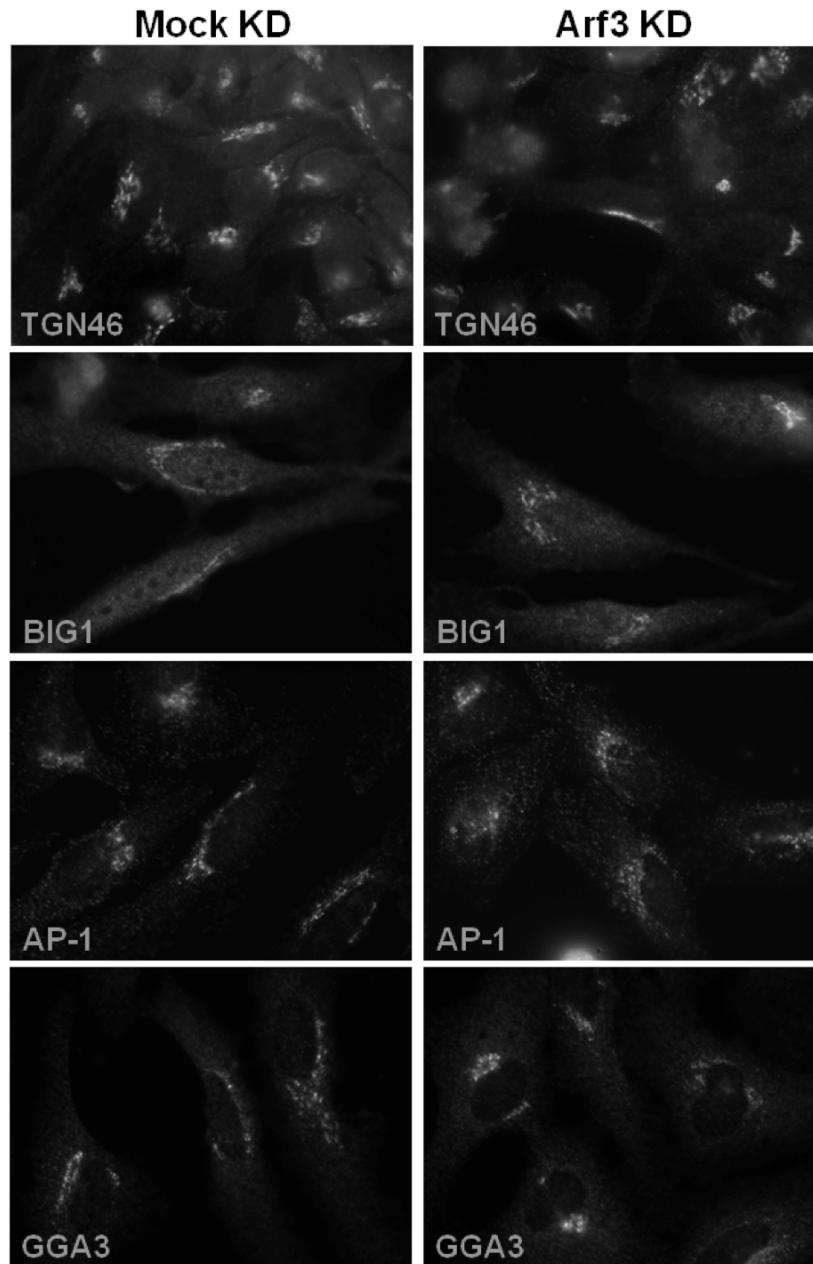


Figure 4.20. Arf3 knockdown has no effect on either TGN structure or membrane recruitment of clathrin adaptors AP1 and GGA3.

HeLa cells were transfected with either irrelevant siRNA (Mock KD, left panels) or a pool of two validated Arf3 siRNA duplexes (Arf3 KD, right panels) as described in Chapter 2. 72 hours post transfection cells were fixed and stained for the specified markers. Representative epifluorescence images selected from at least 2 separate experiments are shown.

4.3 Discussion

Following up on a serendipitous observation, we established that Arf3 localizes preferentially to the *trans*-side of the Golgi complex, where it overlaps significantly with the *trans*-markers BIG1 and GalT-GFP and shows good separation from the *cis*-markers p115 and GBF1. The C-terminus of Arf3 appears critical for targeting Arf3 to *trans*-compartments within the Golgi complex. A more detailed mutagenesis analysis revealed the importance of the amino acids A174 and K180 for directing Arf3 to the *trans*-side of the Golgi complex. Three complementary approaches established a functional link between Arf3 and the only Arf-GEFs localized at the TGN, BIG1 and BIG2. These included overexpression and knockdown of the specific Arf-GEFs, as well as brief BFA treatment of BFA-resistant BFY1 cell line. Our studies also uncovered a unique temperature sensitivity for Arf3 membrane recruitment upon shift to 20°C. This redistribution between the Golgi membranes and cytosol occurred slowly, with a half time of approximately 10 minutes. Analysis of swap chimeras and point mutants identified two residues at positions 9 and 13 of the N-terminal helix that appear to determine temperature sensitivity of Arf3 or Arf1. Lastly, whereas temperature shift to 20°C clearly blocked VSVG trafficking at the Golgi complex, Arf3 knockdown did not affect either VSVG trafficking to the PM or the localization of several markers of the Golgi stack or TGN.

4.3.1 Arf3 is uniquely recruited to the TGN

In a series of experiments using confocal microscopy we confirmed a previous observation by Dr. Justin Chun in our laboratory, namely that Arf3 localizes separately from the *cis*-Golgi marker GBF1. We also extended and strengthened this observation by localizing Arf3 more specifically to the *trans*-side of the Golgi complex. This conclusion is based on a large number of complementary observations that involved multiple tagged forms in several cell lines co-stained for a wide variety of markers.

The lack of specific antibodies that will selectively recognize endogenous Arf3 forced us to use some other means to examine the intracellular localization

of Arf3. We made use of either epitope-tagged Arf3 chimeras or stained for overexpressed untagged Arf3 using a pan specific Arf antibody (clone 1D9) that recognises Arf1, 3, 5 and to a lesser extent Arf4. In order to address concerns that arise from the use of tags, we varied the size of the tag by using either the large GFP or a smaller epitope like HA (Figures 4.1, 4.2, 4.3 and 4.4.). Importantly, we also confirmed that tagged Arf3 chimeras yielded the same localisation pattern as overexpressed untagged Arf3 (Figure 4.2). To add another level of confidence to our unexpected results we performed all the experiments in both NRK cells and HeLa cells and used multiple markers for both the *cis*- and the *trans*-side of the Golgi complex. Quantification was performed with NRK cells because this cell line displays better separation of *cis*- and *trans*-Golgi complex markers than HeLa cells, in our hands. Previous studies established that GBF1 and p115 localize towards the *cis*-side of the Golgi complex while BIG1 and GalT are localized towards the *trans*-side (Schaub et al., 2006; Zhao et al., 2002). The degree of separation of Arf3 with GBF1 and p115, as well as the degree of colocalization with GalT-GFP and BIG1 strongly suggests that Arf3 localizes at the TGN and most probably also at the *trans*-Golgi cisternae.

As in any experiments involving overexpression, we had to take into account the level of expression for each of the chimera tested. To avoid interference with normal function and proper localization of both endogenous and exogenously expressed proteins, we selected for analysis transfected cells with levels of overexpression as low as possible. We were able to get a sense for the level of overexpression of each construct by observing the ratio between the Golgi localisation and the cytoplasmic localisation. In other words, the cells with low to medium levels of expression from the monolayer were the cells with a clear Golgi complex localization and little cytoplasmic staining and these cells were favoured for subsequent analysis. On the other hand, cells with high cytoplasmic staining, sometime to the level of obstructing the Golgi complex signal, were considered to have high levels of overexpression and were not included in our analysis.

It may be important to note that the Arf3-GFP construct reproducibly yielded lower signal and much better ratio for Golgi complex versus cytoplasm

compared with the Arf3-HA construct. This likely does not result from high background signal due to nonspecific binding of the anti-HA antibody. We think that Arf3-HA indeed expressed to higher levels than Arf3-GFP since preliminary results suggest that Arf3 overexpression over a certain level interferes with GBF1 membrane recruitment and this was observed more often with Arf3-HA than with Arf3-GFP. This very intriguing observation will be discussed in more detail in the last section of the chapter. To conclude, we were very careful in our overexpression experiments to analyse cells with low to intermediate level of expression and avoid high levels of overexpression.

4.3.2 Arf3 is most likely activated by BIGs at the TGN

A series of three complementary experiments firmly established a functional link between the BIGs and Arf3 first suggested by their very similar localization patterns. First, the overexpression of BIG1 but not GBF1 protected Arf3 localization to the Golgi complex from a short BFA treatment (Figure 4.5). This result agrees with data presented in chapter 3 that demonstrated selective effects of GBF1 or BIG1 overexpression on early and late compartments (Figure 3.1). We have no explanation for the apparent contradiction with a previous report that overexpression of GBF1 can protect Arf1, 3, 4 and 5 from BFA-induced redistribution (Kawamoto et al., 2002). Secondly, knockdown of BIGs redistributed Arf3 from the membranes but had no significant impact on Arf1 Golgi localization (Figure 4.6). Lastly, a brief BFA treatment of BFY1 cells, a cell line with a BFA-resistant GBF1 system but BFA-sensitive BIGs system, redistributed Arf3 from the Golgi membranes while Arf1 was only marginally affected (Figure 4.9).

Each of the approaches summarized in the previous paragraph has strengths and weaknesses that differ from one experiment to another and therefore make the experiments complement each other. For example, even though overexpression or knockdown of BIGs might have some other unanticipated effects, the probability that these “off target” effects would be the same and account for the effect on Arf3 should be minimal. On the other hand, the BFY1 experiment, even though we do not know the exact mechanism that makes the

GBF1 compartment selectively resistant to BFA, provides independent confirmation of our results. Altogether, the three experiments combine to strengthen our conclusion.

4.3.3 The unexpected localization of Arf3 to the *trans*-compartments of the Golgi complex is mediated by the C-terminus

To tease out the region in Arf3 important for its specific localization we constructed swap chimeras between Arf1 and Arf3. This approach was greatly facilitated by the fact that Arf1 and Arf3 are 96% identical in sequence and that variations are limited to the N-terminus (4 amino acids) and the C-terminus (3 amino acids) (Figure 4.12A). Quantitative analysis of the colocalization of chimeras with either GBF1, p115 or BIG1 clearly suggested that Arf3_1-GFP localized towards the *cis*-side of the Golgi complex, while Arf1_3-GFP localized like Arf3 towards the *trans*-side (Figure 4.15). Analysis of single point mutants revealed that mutation of either A174 or K180 into the corresponding Arf1 residues caused the construct to lose the *trans*-localization specific to Arf3 and accumulate instead on the *cis*-side of the Golgi stack (Figure 4.16). These results point towards the C-terminal fragment and, more precisely, residues S174 and Q180 as being involved in directing Arf3 to the *trans*-side of the Golgi complex.

We initially expected that the same N-terminal region important for temperature sensitivity and for insertion into the lipid membrane (Losonczi et al., 2000) would be also the one important in directing the specific localization for Arf3. The presence of the N-terminus at the membrane provides obvious opportunities to either make contact with a specific lipid environment or to interact with a specific protein. This would provide a targeting mechanism to direct Arf3 to a specific location within the Golgi complex. However, the quantification analysis demonstrated unambiguously that the region important in Arf3 specific localization is not the N-terminus but rather the C-terminus (Figure 4.15B).

The mechanism through which residues A174 or K180 target Arf3 to *trans*-Golgi compartments remains unknown. The mechanism could be either direct, the amino acids being part of a targeting sequence that binds a putative

receptor, or could be indirect, through changes in the tertiary structure of the protein important for binding a putative receptor or lipid domain. As it can be seen from the crystal structure of Arf1 (Figure 4.12B), those residues lie on the surface and are very close to the loop between the N-terminus and the rest of the protein core. Since the N-terminus makes close contact with the lipid membrane (Losonczi et al., 2000), therefore the two residues should be available for interaction with a putative receptor. This prediction is based on the assumption that Arf1 and Arf3 being almost identical in sequence should also be very similar in structure. This is likely the case since structures for Arf4 and Arf5 have been reported and found nearly identical to that of Arf1 in that region.

4.3.4 The unusual temperature sensitivity of Arf3 is dictated by two specific amino acids present in the N-terminal helix

Arf3 has not only a particular localization pattern, but seems to have also unique temperature sensitivity. We observed that shifting cells from 37°C to 20°C had a major impact on Arf3 membrane recruitment while Arf1 remained unaffected. Importantly, this effect was fully reversible as Arf3 returned to Golgi membranes with similar kinetics following a shift from 20°C to 37°C. Using the Arf3/Arf1 chimeras we were able to demonstrate that the temperature sensitivity determinant lies within the N-terminus of Arf3 and Arf1. A more detailed analysis using mutagenesis identified hydrophobic amino acids 9 and 13 as being important in directing temperature sensitivity.

Of the four residues different between the Arf3 and Arf1 N-termini, several lines of evidence made us focus initially on hydrophobic residues at positions 9 and 13. First, the myristoylated N-terminal helix has been implicated in Arf-membrane association and hydrophobic residues in Arf1 appear to interact directly with the membrane (Antonny et al., 1997). Second, the long aliphatic L and I residues at positions 9 and 13 appear unique to Arf3 since F residues are found in the single ancestral Arfs present in organisms like *Giardia lamblia* and *Dictyostelium discoideum*, as well as in Arf1, 2, 4 and 5 in nearly all other species examined (Figure 4.21). Lastly, L and/or I residues are present at those positions in all Arf3 sequences examined (Figure 4.21). This observation suggests that the

Figure 4.21. Sequence alignment of human, bovine and other non mammalian Arfs.

Sequence alignment of the amino and carboxy termini of Arfs encoded in several representative genomes of the supergroups **Excavata**, (*Giardia lamblia* and *Trypanosoma brucei*); **Chromalveolata** (*Tetrahymena thermophila* and *Toxoplasma gondii*); **Archaeplastida** (*Physcomitrella patens* and *Chlamydomonas reinhardtii*); **Amoebozoa** (*Dictyostelium discoideum*) and **Opisthokonta** (*Saccharomyces cerevisiae*, *Drosophila melanogaster* and *Caenorabhditis elegans* and *Homo sapiens*).

¶ Several genomes encode a single ancestral Arf. The two ScArfs are more related to each other than to any other Arfs.

* Those are the only Class I Arfs expressed in those organisms.

	1	2	3	4	5	6	7	8	9	0	1	2	3	4	5	6	7	8	9	
Class I	HsAr f 3	M	G	N	I	F	G	N	L	L	K	S	L	I	G	K	K	E	M	R
	DrAr f 3	M	G	N	I	F	G	N	L	L	K	S	L	I	G	K	K	E	M	R
	SsAr f 3	M	G	N	I	F	G	N	L	L	K	S	L	L	G	K	K	E	M	R
	XlAr f 3	M	G	N	I	F	G	N	L	L	K	S	L	L	G	K	K	E	M	R
	BtAr f 2	M	G	N	V	F	E	K	L	F	K	S	L	F	G	K	K	E	M	R
	SsAr f 2	M	G	N	M	F	G	S	L	F	K	G	L	F	G	K	K	E	M	R
	DrAr f 2	M	G	N	M	F	A	G	L	F	K	N	L	F	G	K	K	E	M	R
	HsAr f 1	M	G	N	I	F	A	N	L	F	K	G	L	F	G	K	K	E	M	R
	DrAr f 1	M	G	N	V	F	A	N	L	F	K	G	L	F	G	K	K	E	M	R
	SsAr f 1	M	G	N	M	F	A	G	L	F	K	N	L	F	G	K	K	E	M	R
	XlAr f 1	M	G	N	I	F	A	N	L	F	K	G	L	F	G	K	K	E	M	R
	¶ScAr f 1	M	G	L	F	A	S	K	L	F	S	N	L	F	G	N	K	E	M	R
	¶ScAr f 2	M	G	L	Y	A	S	K	L	F	S	N	L	F	G	N	K	E	M	R
	*DmAr f I	M	G	N	V	F	A	N	L	F	K	G	L	F	G	K	K	E	M	R
	*CeAr f I	M	G	N	V	F	G	S	L	F	K	G	L	F	G	K	R	E	M	R
	*CrAr f	M	G	L	R	F	T	K	A	L	S	R	L	F	G	K	K	E	M	R
Single Arf	GlAr f	M	G	Q	G	A	S	K	I	F	G	K	L	F	S	K	K	E	V	R
	TtAr f	M	G	I	Q	L	S	K	L	F	D	K	I	F	N	K	V	E	M	R
	TgAr f	M	G	L	S	V	S	R	L	W	S	R	L	F	G	K	R	E	M	R
	PpAr	M	G	L	T	F	T	K	L	F	T	R	L	F	S	K	Q	E	M	R
	DdAr f	M	G	L	A	F	G	K	L	F	S	R	F	F	G	K	K	D	M	R

temperature sensitivity of Arf3 is conserved throughout all species and might be an important feature of Arf3 function. Also, the presence of F9 and F13 in nearly all the other Arfs that localize at the Golgi complex suggests that their membrane recruitment might be temperature insensitive as observed with Arf1. Still, we cannot conclude that L and I are important for temperature sensitivity since we do not know yet whether it is the loss of F or gain of L and I that alters the temperature sensitivity of the Arf. A change of the amino acids to A might help clarify the temperature sensitivity/insensitivity mechanism. At the same time, we did not confirmed yet that the variant amino acids at positions 6 and 11 do not affect the above described features of Arf3/Arf1. Future mutagenesis analysis will be needed to settle this issue.

4.3.5 Redistribution of Arf3 following temperature shift is a relatively slow process.

. The mechanism underlying the distinct temperature sensitivity of Arf3 or Arf1 remains a mystery. When cells were shifted from 37°C to 20°C, the proportion of Arf3 present at the Golgi membranes decreased dramatically while Arf1 remained unaffected. This effect was fully reversible as Arf3 returned to Golgi membranes with similar kinetics following a shift from 20°C to 37°C. Importantly, the redistribution of Arf3 from the Golgi membranes was not an immediate one, but occurred with a considerable delay, having a half time of approximately 10 minutes. Also reassociation to Golgi membranes upon shift from 20°C to 37°C occurred with a similar delay, having a half time of approximately 7.5 minutes. We hypothesize that the recovery was slightly faster because all the cellular events happen faster at 37°C compared with the events occurring at 20°C. The delay in the redistribution to and from the Golgi complex and cytosol suggests a rearrangement of the membrane composition, most probably lipids, or post-translational changes in a putative membrane receptor. The temperature sensitivity does not seem to be a property of an Arf localized only to the TGN, since the Arf3_1-GFP construct redistributed from the *cis*-Golgi membranes upon shift to 20°C (Figures 4.13 and 4.15). This observation suggests that the temperature sensitivity is mainly an intrinsic property of the Arf and depends to a

lesser degree on the nature of the lipid membrane or the receptor. However, we cannot exclude the possibility that the temperature shift drastically alters lipid composition and the *cis-trans*-organization that would induce a loss in Golgi complex polarization with eventual redistribution of Arf3-like proteins, a possibility worth testing in the near future.

We tested if Golgi-associated PtdIns(4)*P* levels, sensed by FAPP-PH-YFP (Godi et al., 2004), would be affected by lowering the temperature to 20°C. The localization of FAPP-PH-YFP at the Golgi complex did not seem to be affected by the temperature change suggesting that PtdIns(4)*P* levels are not affected (Figure 4.11). Still, this experiment was done in fixed cells and a subtle change in PtdIns(4)*P* levels could have been missed. Live cell imaging experiments, even though technically challenging, might provide more accurate kinetics data that might reveal a small change in PtdIns(4) levels that could still be significant and affect Arf3 membrane localization.

4.3.6 Arf3 function still remains a mystery

Even though we have some clues, the function of Arf3 still eludes us. One classical way to gain insight into any protein function is to knockdown its expression. Previously, Volpicelli-Daley and colleagues (Volpicelli-Daley et al., 2005) investigated the effect of Arf3 knockdown without finding any effect on any of the markers tested. We hypothesised that these authors did not observe effects because they were using shRNAs expressed from a plasmid, a method that might not be very effective in knocking down the levels of Arf3 sufficiently enough to see an effect. Since a knockdown obtained with transfected siRNAs is supposed to be more robust than using shRNAs, we reattempted Arf3 knockdown experiments hoping this time for a more efficient knockdown and quantifiable effects. Unfortunately, when we attempted to investigate how efficient the Arf3 knockdown was, neither of the two anti-Arf3 antibodies tested were successful in recognizing the endogenous protein by immunoblotting (Figure 4.19). To overcome this problem we elected to examine the impact of single and pooled siRNAs on expression of Arf3-GFP. This approach identified two of the four siRNAs tested as the most effective in preventing expression of Arf3-GFP (Figure

4.18). A pool of those two oligos was used for subsequent studies. Unfortunately, even when using high quantities of siRNAs and long time points, we were unable to observe an effect on either clathrin adaptors or other TGN markers tested (Figure 4.20). I recognize that this conclusion is true only if we obtained an effective knockdown of endogenous Arf3. Future experiments should confirm the efficiency of Arf3 knockdown and then should test for additional markers or processes that might be regulated by Arf3 function, such as Mannose 6 Phosphate Receptor distribution and cathepsin D trafficking.

We also tested an intriguing link between Arf3 function and VSVG trafficking out of the TGN. This link was suggested by the apparently coincident loss of Arf3 membrane recruitment and blockage of VSVG in the TGN upon shift to 20°C. We first confirmed that a 20°C block could be readily observed using immuno-fluorescence. When we tested the impact of Arf3 knockdown on VSVG trafficking to the PM, quantification analysis clearly showed no difference between the mock-treated cells and the siRNAs treated cells (Figure 4.19). This result may not be so surprising since Arf3 seems to be functionally related to BIGs and we previously demonstrated that knockdown of BIGs has no impact on VSVG trafficking towards the PM (Figure 3.13 and 3.14). It may be important to note that even if the lack of VSVG sorting at the TGN does not result from loss of Arf3 function, the two effects may share a common mechanism. Indeed, the 20°C temperature shift may slowly alter the TGN to cause both loss of Arf3 recruitment and VSVG trafficking.

Finding proteins whose membrane recruitment or localization is affected by shifting temperature to 20°C in a fashion similar to Arf3 provides an alternate avenue to identify candidates that work in conjunction with Arf3. Unfortunately, the localization of all the markers tested did not appear to be affected by the temperature change. In the future we could perform experiments testing not only for additional markers, but also for a change in activity of proteins that might be affected by the 20°C block. In case we obtain some positive results, we do realise that some of these markers or processes might not be directly related to Arf3, as observed for the VSVG (Figure 4.19).

Arf3 might have a surprising additional function besides the most probable one of regulating recruitment of clathrin adaptors at the TGN. As alluded to earlier in the thesis, overexpression of Arf3 at high levels caused consistent reduction of GBF1 recruitment to Golgi membranes. Furthermore, the level of expression of Arf3 correlated directly with the intensity of the down regulation. We hypothesise that the presence of Arf3 at the *trans*-side of the Golgi complex serves as a negative regulator for GBF1 membrane recruitment, making it possible to maintain two different structural entities within the same Golgi complex: the Golgi stack with GBF1/COPI system being major regulators at this location and the TGN with BIGs/clathrin being governors at this quasi independent side of the Golgi complex. A more detailed discussion about why and how Arf3 might prevent GBF1 membrane recruitment is presented in Chapter 5. Future experiments will be needed in order to bring light on these Arf3 functions at the *trans*-Golgi complex.

CHAPTER FIVE:

GENERAL DISCUSSION AND FUTURE PERSPECTIVES

5.1 Synopsis

The work presented in this thesis explored new avenues to characterize the roles of GBF1, BIGs and Arf3 at the Golgi complex. Initially, complementary overexpression and RNA-based knockdown approaches established that GBF1 regulates COPI recruitment on *cis*-Golgi compartments, while BIGs appear specialized for clathrin adaptor proteins on the *trans*-side of the Golgi complex. Overexpressed GBF1 protected COPI from BFA-induced redistribution while its knockdown prevented Golgi complex assembly. In contrast, overexpressed BIG1 protected clathrin adaptor proteins but not COPI from BFA-induced redistribution, while BIGs knockdown caused redistribution of several TGN markers and had no impact on GBF1, COPI and several other Golgi stack markers. Surprisingly, knockdown of GBF1 and/or COPI did not prevent export of VSVGtsO45 from the ER, but caused its accumulation into peripheral vesiculo-tubular clusters. Even more surprisingly, BIGs knockdown prevented neither traffic of VSVGtsO45 to the plasma membrane nor assembly of a polarized Golgi stack. Our observations indicate that COPII is the only coat required for sorting and export from the ER exit sites, while GBF1 but not BIGs, is required for COPI recruitment, Golgi sub-compartmentalization and cargo progression to the cell surface. BIGs appear specialized for clathrin adaptor recruitment and for assembly and maintenance of the TGN. Furthermore, other observations suggested for the first time the notion that Arf3 is activated uniquely by BIGs at the *trans*-side of the Golgi complex. Initially, imaging experiments established that Arf3 appears separate from *cis*-Golgi markers while colocalizing to a large extent with *trans*-Golgi compartments. Subsequently, a series of three separate experiments involving overexpression, knockdown and the mutant cell line BFY1 established a functional link between Arf3 and BIGs. On the other hand, shifting temperature to 20°C redistributed Arf3 from Golgi membranes. This redistribution was specific for Arf3 since Arf1-GFP, TGN46, BIG1 and AP-1 remained unaffected. Arf1 and Arf3 differ in sequence only in two short regions at the N- and C-termini. Taking advantage of Arf1/Arf3 chimeras we observed that the N-terminal region of Arf3 and Arf1 seems to be directing the temperature

sensitivity of the proteins while the C-terminus seems to be important in directing the specific localization of Arf3. Further analysis of point mutants identified two residues in either the N-terminus of Arf3/1 and the C-terminus of Arf3 which are critical for each of the properties above mentioned. Unfortunately, Arf3 knockdown had no impact on any of the markers tested or on VSVG trafficking to PM. We conclude that Arf3 is specifically activated by BIGs at the *trans*-side of the Golgi complex. Figure 5.1 presents in a diagram form the main findings and conclusions. The data and the ideas presented in this thesis have uncovered many potential directions for future research. The discussion that follows emphasizes the significance of our findings and proposes potential directions that may be pursued to extend the work presented.

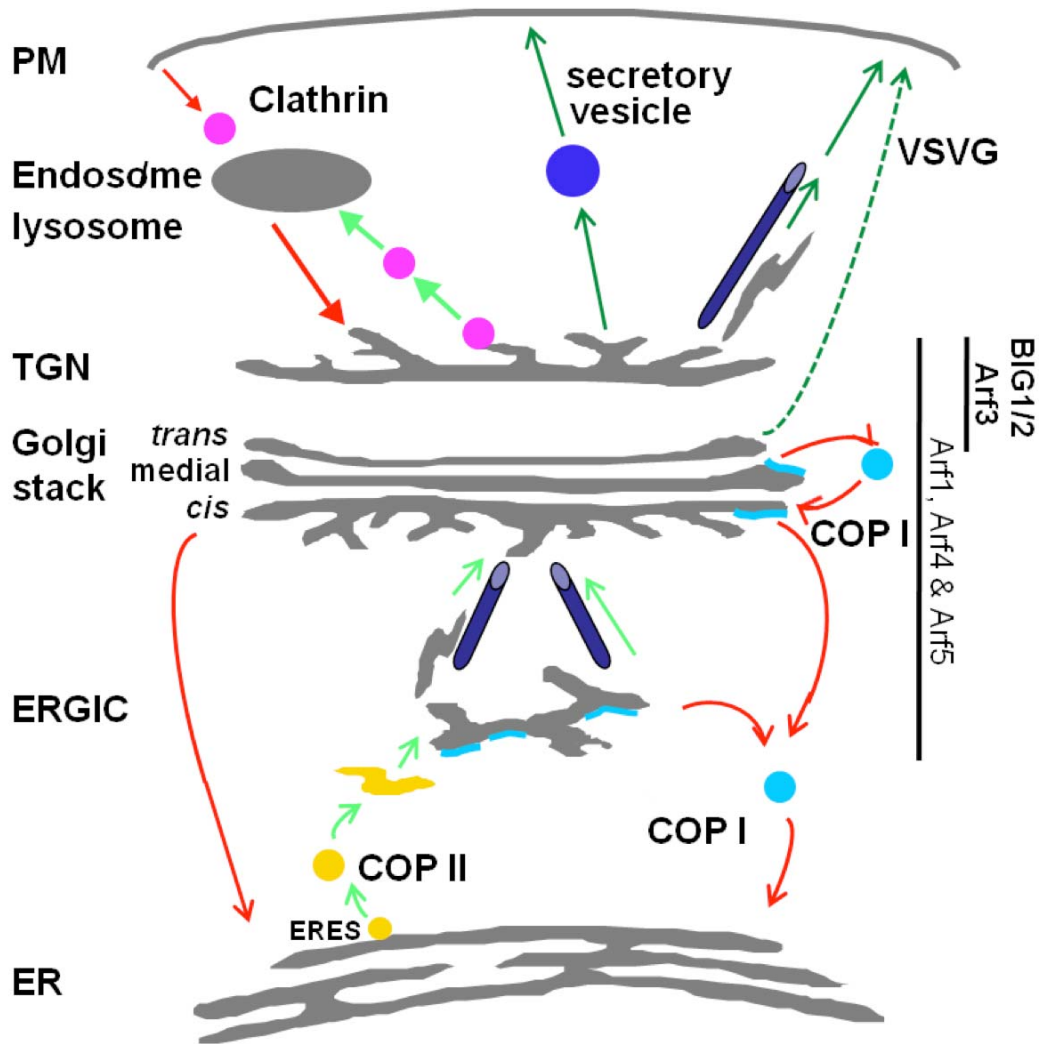


Figure 5.1. Diagram representing major findings and conclusions depicted on to the secretory pathway.

- Traffic out of ERES depends only on COPII and is independent of GBF1/COPI machinery.
- GBF1/COPI machinery alone is sufficient to drive the maturation process responsible for Golgi complex organization.
- TGN is represented separate from the Golgi stack to suggest the separate identities of the two compartments of the Golgi complex.
- Sorting to PM could be BIGs dependent (light green arrows) and BIGs independent (dark green arrows).
- Sorting and trafficking of VSVG to the PM is independent of BIGs and can occur with similar kinetics from both TGN (continuous dark green arrows) and *trans*-cisterna (discontinuous arrow).
- Arf3 localizes specifically to TGN where is activated uniquely by BIGs.

5.2 Mechanism of sorting from the Golgi complex to PM.

One of our most unexpected results was that knockdown of BIGs had no detectable effect on VSVG export to the PM. This finding was later confirmed by Ishizaki and colleagues (Ishizaki et al., 2008). This result came as a surprise for two reasons: because BIGs are the only Arf-GEFs known to be present at the TGN to regulate sorting of cargo and exit from the Golgi complex (Zhao et al., 2002), and because the BIGs homologue, Sec7, is essential for secretion in yeast (Achstetter et al., 1988). Our finding seems to contradict the dogma of that time, but, after a more careful evaluation of the literature we were able to find experimental data that agrees with our findings and can contribute to a new understanding of the sorting process from the Golgi complex to the PM. Initial data came from experiments using BFA. In cells treated with the fungal metabolite, only a portion of the VSVG cargo was redistributed to the ER with a significant amount remaining in the Golgi region. Export from the Golgi region to the PM continued even in the presence of BFA, suggesting that export mechanisms remain active in the absence of BIGs activity (Chege and Pfeffer, 1990). Our observations are also in line with previous demonstration that the clathrin coat assembles only on the last cisterna leaving earlier cisternae to produce Golgi to PM carriers (Ladinsky et al., 1999; Mogelsvang et al., 2004). More recently the laboratory of Lippincott-Schwartz proposed a new model for trafficking and sorting at the Golgi complex, the rapid-partitioning model. This model is based on sorting of lipids into different domains at each level of the Golgi and association of proteins with their preferred lipid environment (Patterson et al., 2008). This brings us back to our data about the VSVG export to the PM which seems to be independent of BIGs suggesting that the sorting and exiting mechanism of VSVG at the Golgi could be a lipid based one. This mechanism most probably occurs at the TGN, but in the absence of BIGs and a TGN structure, the lipid sorting mechanism occurs with similar efficiency at the *trans*-side of the Golgi stack.

5.3 Identifying Arf3 receptors localized to the TGN

The restricted localization pattern of Arf3 towards the *trans*-side of the Golgi complex, suggestive of a specific putative membrane receptor at this location, came as a complete surprise for a number of reasons. Initially, multiple Arf3 effectors were identified, including Arfaptin 1, Arfaptin 2 (Kanoh et al., 1997), mitotic kinesin-like protein 1 (MKLP1) (Boman et al., 1999) and phospholipase D (PLD) (Cockcroft et al., 1994), but subsequent work established that none of these discriminated between Arf1 and Arf3. Furthermore, *in vitro* and *in vivo* studies established that Golgi-localized GEFs could activate equally Arf1 and Arf3 (Islam et al., 2007; Kawamoto et al., 2002; Shin et al., 2004). Lastly, Donaldson and colleagues identified a centrally located MXXE motif, present in all Class I Arfs, that targets Arf1 to its receptor membrin on *cis*-Golgi membranes and should target Arf3 similarly to the same location (Honda et al., 2005).

A few more recent observations in the literature suggest that Arf1 and Arf3 may perform different functions at different locations after all, suggesting different putative membrane receptors. An initial study of the biochemical properties of Arf1 and Arf3 suggested that the two Arfs might have different functions at the Golgi complex (Taylor *et al.*, 1992). Furthermore, in an attempt to identify specific function for each of the Arfs using an shRNA-based approach, Volpicelli-Daley *et al.*, discovered that double knockdown of Arf1+Arf4 and Arf3+Arf4 caused dramatically different effects (Volpicelli-Daley et al., 2005). More recently, Chun *et al.*, reported that Arf3, unlike Arf1 or class II Arfs, did not localize to ERGIC structures or Golgi compartments containing GBF1 (Chun et al., 2008). All these data together strengthen our observation that Arf3 localizes and most probably functions in a distinct compartment than Arf1, suggesting recruitment by different membrane receptors or by different membrane targeting mechanisms.

The exact mechanism by which the C-terminus of Arf3, and more precisely the amino acids Ala 174 and Lys 180, direct Arf3 to the *trans*-side of the Golgi complex remains to be uncovered. The C-terminal helix of Arf3 could be important in targeting Arf3 to its specific location within the Golgi complex by

participating in two different targeting mechanisms. First, the C-terminal helix of Arf3 might be a specific signal sequence that would, by itself, direct the Arf3 to *trans*-Golgi compartments. Alternatively, a more complicated targeting mechanism, might involve a combination of the C-terminus together with other structural components of Arf3 such as the N-terminus, in a tri-dimensional recognition patch in which the C-terminal helix is a crucial component. If the C-terminal helix of Arf3 acts as a targeting sequence on its own, then it should be targeted to the Golgi complex and more specifically to *trans*-compartments. One way to test if the C-terminus of Arf3 acts as a targeting sequence directing Arf3 to its specific localization would be to assemble additional constructs in which the C-terminal helix of Arf3, or Arf1 as a control, would be attached to GFP. It could be that the interaction between the C-terminal helix and the putative *trans*-localized receptor for Arf3 might be a weak one and that the membrane interaction of the full length Arf3 might be immediately stabilized by subsequent interactions with either the BIGs, clathrin adaptors or an Arf-GAP. One alternative to enhance the putative faint Golgi signal would be to use an anti-GFP antibody followed by a fluorescent secondary antibody. In case there is still no clear Golgi localization with the Arf3C-terminus-GFP construct and the anti-GFP antibody staining, additional chimeras could be constructed to increase the chance of detecting this weak interaction. A chimera composed of three copies of the Arf3 C-terminus in frame with GFP (Arf3CtermX3-GFP) could be constructed. One alternative might be to tag the C-terminal helix with a dimeric protein such as GST, or dimeric fluorescent protein. If any one of these Arf3 C-terminus constructs would localize to the Golgi complex, and more precisely to the *trans*-Golgi compartments, this could be interpreted that the C-terminal helix acts as a targeting signal that directs Arf3 to its specific localization within the Golgi complex. This targeting signal could override the MXXE targeting motif present in Arf1 and Arf3 that would normally localize both proteins to the membrane-rich membranes of the *cis*-Golgi complex.

Another way to confirm the specific localization of Arf3 would be to identify the putative membrane receptor that recruits Arf3 specifically to the

trans-side of the Golgi complex. Chimeras tagged with the Arf3 C-terminal helix that localize at the Golgi complex could be further used in pull-down experiments, most probably with the use of bi-functional cross-linkers. One other option to identify the putative receptor for Arf3 would be a candidate approach testing all known *trans*-Golgi localized SNAREs for their potential involvement in Arf3 membrane recruitment. Briefly, the localization pattern of Arf3 would be compared with TGN-localized SNAREs to give an initial hint about the potential receptor. Afterwards, the relationship would be confirmed by *in vitro* binding experiments, or by monitoring Arf3 distribution following either knockdown of the candidate or combination of its overexpression and short BFA-treatment.

5.4 Examining the function of Arf3 at the *trans*-side of the Golgi complex

Elucidating Arf3 function might prove more challenging than we initially thought. The large majority of the literature to date, most probably because of the vast similarity between the sequences, localization patterns and effectors of Arf1 and Arf3, suggests Arf3 functions in a redundant fashion with Arf1 (Islam et al., 2007; Kawamoto et al., 2002; Shin et al., 2004; Togawa et al., 1999). This might be the reason why Arf1 is the most studied of the two while little attention was given to Arf3. We established, for the first time, that Arf3 actually localizes more towards the *trans*-side of the Golgi complex (Figures 4.1, 4.2, 4.3 and 4.4) in contrast with Arf1 which localizes more towards the *cis*-side (Honda et al., 2005). Because the TGN is considered to be the main sorting centre for proteins and lipids (De Matteis and Luini, 2008), our discovery suggests that Arf3 may regulate the sorting of cargo on its way out of the Golgi complex. Investigating in more detail the localization for Arf3 using EM might give us a better sense of its function. Localization of Arf3 within the TGN to regions marked by the clathrin coat would suggest a different function than if Arf3 localized to TGN regions lacking the clathrin coat or to the most *trans*-cisterna of the Golgi stack. This would be a strong indication that Arf3 functions in clathrin-dependent or clathrin-independent sorting. Alternatively, concentration of Arf3 towards the rims of the cisternae would suggest a different function than an Arf3 evenly localized throughout the

cisternae. Also, a good colocalization with BIG1 and BIG2 and a good separation from GBF1 might be a good argument towards a new and exciting function that we are going to discuss towards the end of this subchapter.

Arf3 mutants are another option to get insight into the function of the protein. Dominant-inactive mutants like Arf3 T31N and Arf3 N126I as well as dominant-active mutants like Arf3 Q71L were constructed and used in the past to elucidate the function of Arf3. By overexpressing the N126I and T31N mutants, most probably at too high levels, Volpicelli-Dalley *et al.*, concluded that Arf3, together with Arf1 and Arf4, participate in COPI membrane recruitment and Golgi complex maintenance (Volpicelli-Daley *et al.*, 2005). Shin *et al.*, by means of the T31N mutant found that Arf3, in a parallel fashion with Arf1, exaggerates the BIG2(E738K)-induced tubulation of endosomal membranes, supporting the idea that BIG2 has an exchange activity toward Arf1 and Arf3 *in vivo* (Shin *et al.*, 2004). Further studies showed Arf3 to regulate the localization of clathrin adaptor AP-4 to the TGN, even though it seems to do it to a lesser extent than Arf1 (Boehm *et al.*, 2001). Future experiments using the Arf3 T31N and Q71L mutants could investigate the potential new role of Arf3 at the *trans*-side of the Golgi complex. Additional experiments might also investigate if the T31N or Q71L would have an impact on TGN architecture, clathrin membrane recruitment, sorting to and from endosomes. Further tests would examine if there is an impact on phosphoinositide metabolism and in particular on PI4P production, considering the facts that is the most abundant PIP present at the TGN and might have an important role in regulating lipid based sorting (D'Angelo *et al.*, 2008). Complementary experiments should test if Arf3 Q71L expression would protect clathrin adaptors membrane recruitment, or any other process that is BFA sensitive and might be regulated by Arf3, from short BFA treatment.

Over the years, additional functions have been suggested for Arf3. Furthermore, Arf3 might have a totally surprising and crucial function in maintaining the polarity between the two major regulatory systems that work at the Golgi complex, the GBF1/COP1 system at the Golgi stack and BIGs/clathrin system at the TGN. We serendipitously observed that Arf3 overexpression,

especially at high levels, was consistently accompanied by significant reduction in membrane recruitment of GBF1 (Figure 5.2). Furthermore, the extent of reduction in GBF1 signal correlated with the level of expression of Arf3. We therefore hypothesise that the presence of Arf3 on the *trans*-side of the Golgi complex provides a negative regulatory effect for GBF1 membrane recruitment. This would provide an efficient mechanism to maintain the functional polarization of two different entities within the same Golgi complex: the Golgi stack with GBF1/COPI system being major regulator at this location while the TGN having the BIGs/clathrin controlling the opposite side of the Golgi complex. Multiple observations in the literature, as presented in the Introduction in 1.3.1, support the notion that within the same Golgi complex there are actually two separate entities that function in close proximity. In order to be able to regulate the transition to and the maintenance of the TGN compartment, despite the massive flow of proteins and membranes from the Golgi stack, a very efficient regulatory mechanism must be in place. The Arf3 negative regulatory effect on GBF1 membrane recruitment as well as a positive effect on BIGs activity might provide the necessary mechanism (Figure 5.3). The localization pattern for Arf3 that we describe in chapter 4 would certainly fit with this proposed mechanism. We plan to further test our hypothesis using Arf3 knockdown, Arf3 mutants and *in vitro* testing experiments. If our hypothesis is right, then Arf3 knockdown or the Arf3T31N dominant negative mutant should allow GBF1 to localize also to the *trans*-compartment of the Golgi complex. At the same time, the dominant-active mutant Arf3Q71L, expressed at high enough levels to saturate the TGN binding sites and bleed into the *cis*-side of the Golgi complex, should be much more efficient in getting GBF1 off the membranes than the WT Arf3 is.

5.5 The mechanism of temperature (in)sensitivity of Arf3 and Arf1

One intriguing property of Arf3 membrane association was its unusual temperature sensitivity. Redistribution between Golgi membranes and cytosol occurred slowly with a half time of 10 minutes for the redistribution to cytosol at 20°C and about 7.5 minutes for recruitment back to the Golgi complex at 37°C.

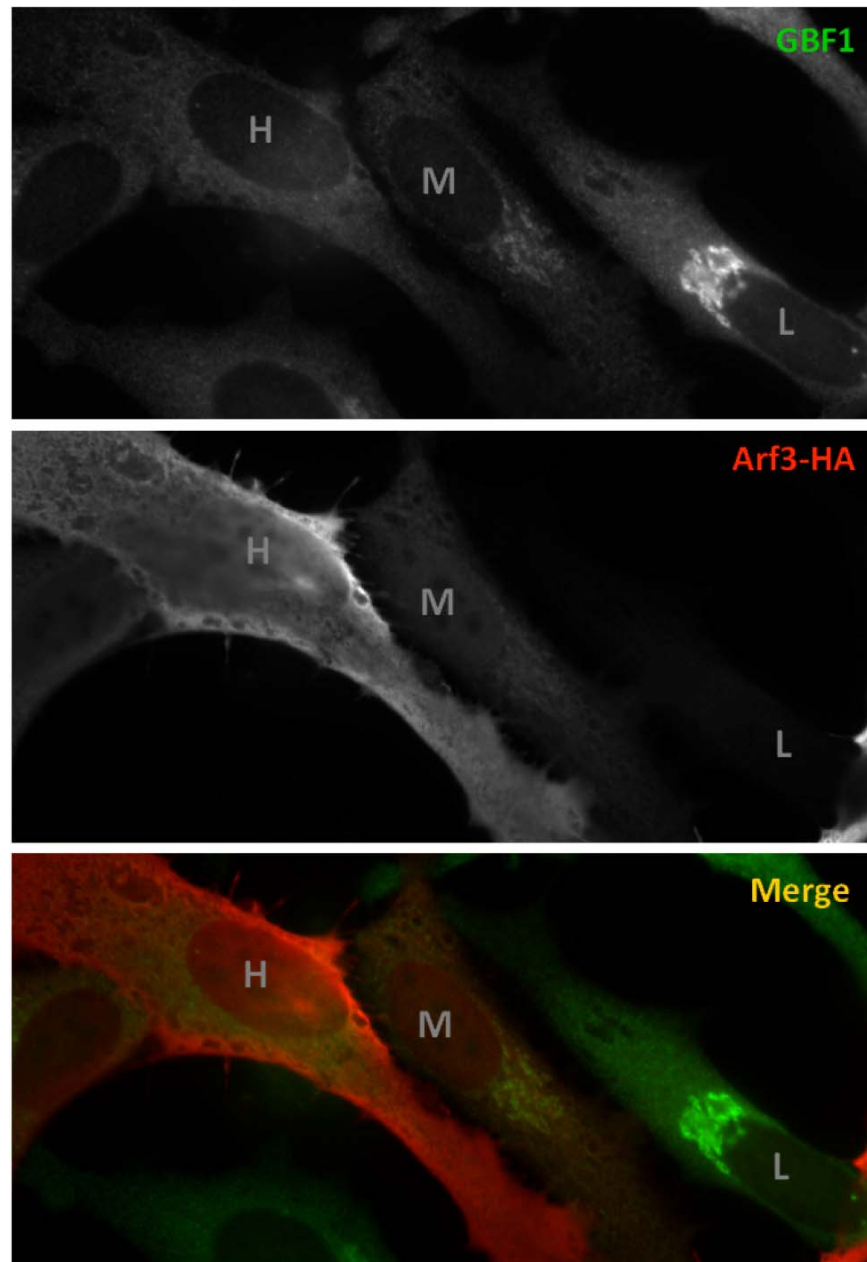


Figure 5.2. Arf3-HA overexpression at high levels displaces endogenous GBF1 from the Golgi membranes.

HeLa cells were transfected with a plasmid encoding for Arf3-HA for 24 h. Cells were then fixed and stained for GBF1 and HA as indicated. Representative epifluorescence images are shown. **L**, **M** and **H** over the nuclei of the transfected cells represent **Low**, **Medium** and **High** levels of expression for the Arf3-HA construct.

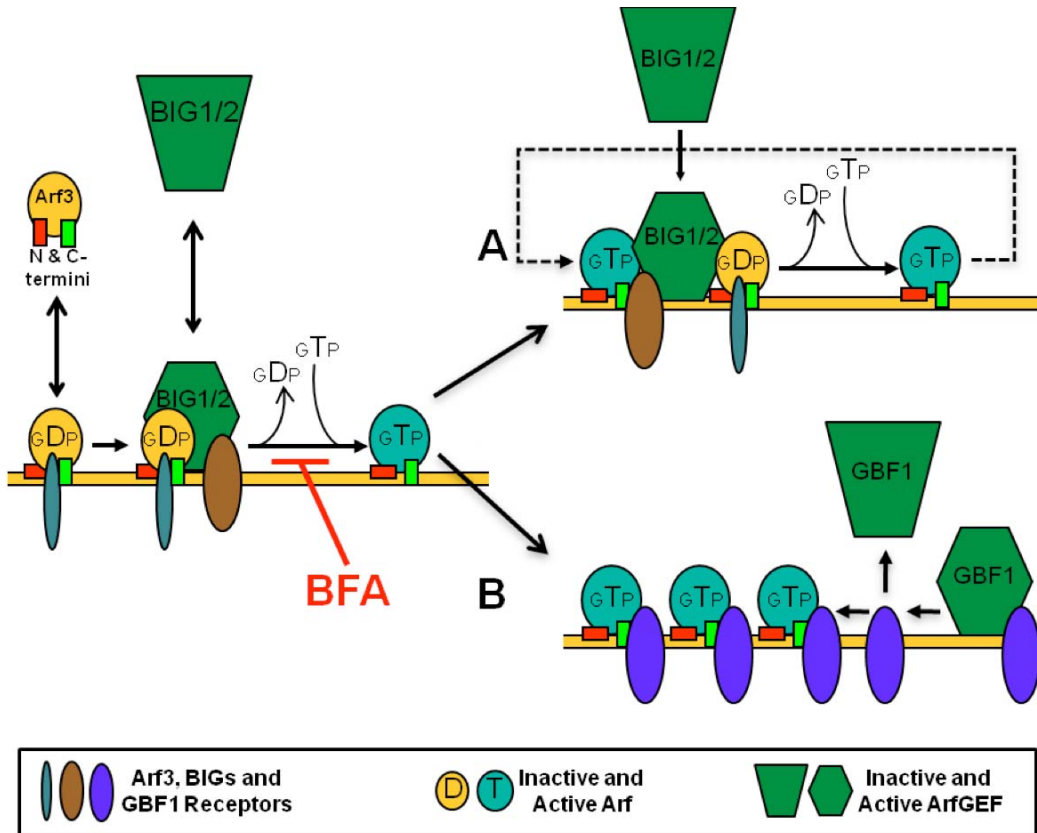


Figure 5.3. Arf3 could function in up-regulating BIGs and down-regulating GBF1 membrane recruitment.

Soluble Arf3-GDP and BIGs are recruited to the membrane through association with organelle-specific receptors. While the myristoylated N-terminus of Arf3 (red) binds the lipid bilayer the C-terminus of Arf3 (light green) is important in binding the specific membrane receptor. At the membrane, BIGs promote release of GDP and binding of GTP, a reaction blocked by the drug BFA. Active Arf3-GTP locked on the membrane can either promote BIGs activity by promoting or stabilizing BIGs membrane recruitment (A) or inhibit GBF1 membrane recruitment by sequestering its receptor (B).

Elucidation of the mechanism responsible for the distinct temperature sensitivity of Arf3 or Arf1 might yield valuable insight on Arf3 function. One possibility might be that lowering the temperature would increase the strength of the hydrophobic bonds present between the N-terminus and the hydrophobic groove where the N-terminus usually rests when Arf3 is in the cytosol. This mechanism would prevent or slow down the movement of the N-terminus out of the hydrophobic groove at the lower temperature, conformational change necessary for Arf3 to bind the membranes and then to be activated. However, this mechanism predicts an immediate repercussion on Arf3 membrane recruitment after the temperature shift and therefore does not fit with the delayed redistribution observed in our experiments. Actually, the delay in the redistribution to and from the Golgi complex and cytosol suggest most probably a change in lipid composition of the Golgi complex or a post-translational modification on a putative receptor. One other possibility that we can consider might be post-translational changes in a putative membrane receptor. A test of this possibility will first require identification of this putative receptor.

As a speculation, it would be very tempting to convert the temperature “insensitive” Arfs to “sensitive” ones by mutating amino acids F9 and F13 to L9 and I13 and see what would be the effect of shifting temperature to 20°C on a series of markers and processes. This would have to be done in cells that were co-transfected with siRNAs targeting the endogenous Arf and the mutants would have to be engineered to be RNAi resistant. The advantage of this method would be that we would be able to see immediate effects of the “temperature knockdown” and prevent unexpected adaptive processes that could happen over several days in a classic knockdown experiment.

5.6 Concluding remarks

Since the identification of the first Arf (Enomoto and Gill, 1980; Kahn and Gilman, 1984) and the first Arf-GEF (Chardin et al., 1996), much progress has been made in characterizing their biochemical and molecular properties. As described in this thesis, we helped to better understand the functions of GBF1,

BIGs and Arf3 at the Golgi complex. While our work confirmed in an elegant way the sole requirement for COPII during export out of ERES, the role of GBF1 in COPI membrane recruitment and Golgi complex formation and maintenance, the similar role of BIGs in clathrin membrane recruitment and TGN formation and maintenance, we also had some surprising discoveries. We were intrigued by the fact that BIGs knockdown had no impact on the kinetics of VSVG trafficking to the cell surface or on the polarization of the Golgi stack. We were also intrigued by the particular localization pattern of Arf3 as well as by its unique temperature sensitivity. However, our work is just the beginning for our understanding of Arf3 function at the *trans*-side of the Golgi complex and some important questions remain unanswered. For example, what is the exact mechanism that specifies a particular location on the Golgi membranes where a specific Arf, like Arf3, or Arf-GEF is going to be recruited? If there is a specific membrane receptor for each Arf or Arf-GEF? and if so, what are their identities? What role play and how important are lipids in trafficking and sorting within and out of the Golgi complex? And last but not least, what is the function of Arf3 at the *trans*-side of the Golgi complex? Is Arf3 regulating lipid remodelling and lipid sorting at TGN? Is Arf3 the “magic” switch that turns the Golgi stack membranes into TGN membranes? Answers to these questions will ultimately lead to a better understanding of Arfs and ArfGEFs function at the Golgi complex as well as to a more global understanding of the nature and function of the Golgi complex.

CHAPTER SIX:

REFERENCES

- Achstetter, T., A. Franzusoff, C. Field, and R. Schekman. 1988. SEC7 encodes an unusual, high molecular weight protein required for membrane traffic from the yeast Golgi apparatus. *J. Biol. Chem.* 263:11711-11717.
- Allan, V.J., and T.E. Kreis. 1986. A microtubule-binding protein associated with membranes of the Golgi apparatus. *J Cell Biol.* 2229-39.
- Altan-Bonnet, N., R. Sougrat, and J. Lippincott-Schwartz. 2004. Molecular basis for Golgi maintenance and biogenesis. *Curr Opin Cell Biol.* 16:364-72.
- Alvarez, C., R. Garcia-Mata, E. Brandon, and E. Sztul. 2003. COPI Recruitment Is Modulated by a Rab1b-dependent Mechanism. *Mol Biol Cell.* 14:2116-27.
- Antonny, B., S. Beraud-Dufour, P. Chardin, and M. Chabre. 1997. N-terminal hydrophobic residues of the G-protein ADP-ribosylation factor-1 insert into membrane phospholipids upon GDP to GTP exchange. *Biochemistry.* 36:4675-84.
- Antonny, B., D. Madden, S. Hamamoto, L. Orci, and R. Schekman. 2001. Dynamics of the COPII coat with GTP and stable analogues. *Nat Cell Biol.* 3:531-7.
- Aoe, T., E. Cukierman, A. Lee, D. Cassel, P.J. Peters, and V.W. Hsu. 1997. The KDEL receptor, ERD2, regulates intracellular traffic by recruiting a GTPase-activating protein for ARF1. *Embo J.* 16:7305-16.
- Aoe, T., I. Huber, C. Vasudevan, S.C. Watkins, G. Romero, D. Cassel, and V.W. Hsu. 1999. The KDEL receptor regulates a GTPase-activating protein for ADP-ribosylation factor 1 by interacting with its non-catalytic domain. *Journal of Biological Chemistry.* 274:20545-9.
- Appenzeller, C., H. Andersson, F. Kappeler, and H.P. Hauri. 1999. The lectin ERGIC-53 is a cargo transport receptor for glycoproteins. *Nat Cell Biol.* 1:330-4.
- Aridor, M., J. Weissman, S. Bannykh, C. Nuoffer, and W.E. Balch. 1998. Cargo selection by the COPII budding machinery during export from the ER. *J Cell Biol.* 141:61-70.
- Balch, W.E., R.A. Kahn, and R. Schwaninger. 1992. ADP-ribosylation factor is required for vesicular trafficking between the endoplasmic reticulum and the cis-Golgi compartment. *J. Biol. Chem.* 267:13053-13061.
- Baloyannis, S.J., V. Costa, and D. Michmizos. 2004. Mitochondrial alterations Alzheimer's disease. *American Journal of Alzheimer's Disease and Other Dementias.* 19:89-93.
- Bannykh, S.I., and W.E. Balch. 1997. Membrane dynamics at the endoplasmic reticulum-Golgi interface. *J Cell Biol.* 138:1-4.
- Bannykh, S.I., T. Rowe, and W.E. Balch. 1996. The organization of endoplasmic reticulum export complexes. *J Cell Biol.* 135:19-35.
- Bard, F., and V. Malhotra. 2006. The formation of TGN-to-plasma-membrane transport carriers. *Annu Rev Cell Dev Biol.* 22:439-55.
- Barlowe, C. 1995. COPII: a membrane coat that forms endoplasmic reticulum-derived vesicles. *Febs Lett.* 369:93-6.
- Barlowe, C. 2000. Traffic COPs of the early secretory pathway. *Traffic.* 1:371-7.
- Barlowe, C. 2003. Signals for COPII-dependent export from the ER: what's the ticket out? *Trends Cell Biol.* 13:295-300.

- Barzilay, E., N. Ben-Califa, K. Hirschberg, and D. Neumann. 2005. Uncoupling of brefeldin a-mediated coatomer protein complex-I dissociation from Golgi redistribution. *Traffic*. 6:794-802.
- Becker, B., B. Bolinger, and M. Melkonian. 1995. Anterograde transport of algal scales through the Golgi complex is not mediated by vesicles. *Trends Cell Biol.* 5:305-7.
- Belov, G.A., N. Altan-Bonnet, G. Kovtunovych, C.L. Jackson, J. Lippincott-Schwartz, and E. Ehrenfeld. 2007. Hijacking components of the cellular secretory pathway for replication of poliovirus RNA. *J Virol.* 81:558-67.
- Ben-Tekaya, H., K. Miura, R. Pepperkok, and H.P. Hauri. 2005. Live imaging of bidirectional traffic from the ERGIC. *J Cell Sci.* 118:357-67.
- Beraud-Dufour, S., S. Paris, M. Chabre, and B. Antonny. 1999. Dual interaction of ADP ribosylation factor 1 with Sec7 domain and with lipid membranes during catalysis of guanine nucleotide exchange. *J Biol Chem.* 274:37629-36.
- Beraud-Dufour, S., S. Robineau, P. Chardin, S. Paris, M. Chabre, J. Cherfils, and B. Antonny. 1998. A glutamic finger in the guanine nucleotide exchange factor ARNO displaces Mg²⁺ and the beta-phosphate to destabilize GDP on ARF1. *Embo J.* 17:3651-9.
- Berger, S. 1998. Physical and biochemical characterization of ADP-ribosylation factors. In Dept of Chemistry and Biochemistry. University of Colorado, Boulder.
- Bergmann, J.E. 1989. Using temperature-sensitive mutants of VSV to study membrane protein biogenesis. *Methods Cell Biol.* 32:85-110.
- Bethune, J., M. Kol, J. Hoffmann, I. Reckmann, B. Brugger, and F. Wieland. 2006. Coatomer, the Coat Protein of COPI Transport Vesicles, Discriminates Endoplasmic Reticulum Residents from p24 Proteins. *Mol. Cell. Biol.* 26:8011-8021.
- Béthune, J., F. Wieland, and J. Moelleken. 2006. COPI-mediated Transport. *Journal of Membrane Biology.* 211:65-79.
- Bigay, J., J.F. Casella, G. Drin, B. Mesmin, and B. Antonny. 2005. ArfGAP1 responds to membrane curvature through the folding of a lipid packing sensor motif. *Embo J.*
- Bigay, J., P. Gounon, S. Robineau, and B. Antonny. 2003. Lipid packing sensed by ArfGAP1 couples COPI coat disassembly to membrane bilayer curvature. *Nature.* 426:563-6.
- Boehm, M., R.C. Aguilar, and J.S. Bonifacino. 2001. Functional and physical interactions of the adaptor protein complex AP- 4 with ADP-ribosylation factors (ARFs). *Embo J.* 20:6265-76.
- Boman, A.L., and R.A. Kahn. 1995. Arf proteins: the membrane traffic police? *Trends Biochem Sci.* 20:147-50.
- Boman, A.L., J. Kuai, X. Zhu, J. Chen, R. Kuriyama, and R.A. Kahn. 1999. Arf proteins bind to mitotic kinesin-like protein 1 (MKLP1) in a GTP-dependent fashion. *Cell Motility & the Cytoskeleton.* 44:119-32.
- Boman, A.L., P.D. Salo, M.J. Hauglund, N.L. Strand, S.J. Rensink, and O. Zhdankina. 2002. ADP-ribosylation factor (ARF) interaction is not sufficient for yeast GGA protein function or localization. *Mol Biol Cell.* 13:3078-95.

- Boman, A.L., T.C. Taylor, P. Melancon, and K.L. Wilson. 1992. A role for ADP-ribosylation factor in nuclear vesicle dynamics. *Nature*. 358:512-4.
- Bonfanti, L., A.A. Mironov, Jr., J.A. Martinez-Menarguez, O. Martella, A. Fusella, M. Baldassarre, R. Buccione, H.J. Geuze, A.A. Mironov, and A. Luini. 1998. Procollagen traverses the Golgi stack without leaving the lumen of cisternae: evidence for cisternal maturation. *Cell*. 95:993-1003.
- Bonifacino, J.S. 2004. The GGA proteins: adaptors on the move. *Nat Rev Mol Cell Biol*. 5:23-32.
- Bonifacino, J.S., and B.S. Glick. 2004. The mechanisms of vesicle budding and fusion. *Cell*. 116:153-66.
- Bonifacino, J.S., and C.L. Jackson. 2003. Endosome-specific localization and function of the ARF activator GNOM. *Cell*. 112:141-2.
- Bonifacino, J.S., and J. Lippincott-Schwartz. 2003. Coat proteins: shaping membrane transport. *Nat Rev Mol Cell Biol*. 4:409-14.
- Bonifacino, J.S., and R. Rojas. 2006. Retrograde transport from endosomes to the trans-Golgi network. *Nat Rev Mol Cell Biol*. 7:568-79.
- Bonifacino, J.S., and L.M. Traub. 2003. Signals for sorting of transmembrane proteins to endosomes and lysosomes. *Annu Rev Biochem*. 72:395-447.
- Borgonovo, B., J. Ouwendijk, and M. Solimena. 2006. Biogenesis of secretory granules. *Current Opinion in Cell Biology*. 18:365-370.
- Borsig, L., T. Imbach, M. Hochli, and E.G. Berger. 1999. alpha1,3Fucosyltransferase VI is expressed in HepG2 cells and codistributed with beta1,4galactosyltransferase I in the golgi apparatus and monensin-induced swollen vesicles. *Glycobiology*. 9:1273-80.
- Boyadjiev, S.A., J.C. Fromme, J. Ben, S.S. Chong, C. Nauta, D.J. Hur, G. Zhang, S. Hamamoto, R. Schekman, M. Ravazzola, L. Orci, and W. Eyaid. 2006. Cranio-lenticulo-sutural dysplasia is caused by a SEC23A mutation leading to abnormal endoplasmic-reticulum-to-Golgi trafficking. *Nat Genet*. 38:1192-7.
- Bremser, M., W. Nickel, M. Schweikert, M. Ravazzola, M. Amherdt, C.A. Hughes, T.H. Sollner, J.E. Rothman, and F.T. Wieland. 1999. Coupling of coat assembly and vesicle budding to packaging of putative cargo receptors. *Cell*. 96:495-506.
- Bui, Q., M.-P. Golinelli-Cohen, and C. Jackson. 2009. Large Arf1 guanine nucleotide exchange factors: evolution, domain structure, and roles in membrane trafficking and human disease. *Molecular Genetics and Genomics*.
- Cavenagh, M.M., J.A. Whitney, K. Carroll, C. Zhang, A.L. Boman, A.G. Rosenwald, I. Mellman, and R.A. Kahn. 1996. Intracellular distribution of Arf proteins in mammalian cells. Arf6 is uniquely localized to the plasma membrane. *J Biol Chem*. 271:21767-74.
- Chardin, P., S. Paris, B. Antony, S. Robineau, S. Beraud-Dufour, C.L. Jackson, and M. Chabre. 1996. A human exchange factor for ARF contains Sec7- and pleckstrin-homology domains. *Nature*. 384:481-4.
- Chavrier, P., and B. Goud. 1999. The role of ARF and Rab GTPases in membrane transport. *Curr Opin Cell Biol*. 11:466-75.

- Chege, N.W., and S.R. Pfeffer. 1990. Compartmentation of the Golgi complex: brefeldin-A distinguishes trans-Golgi cisternae from the trans-Golgi network. *J Cell Biol.* 111:893-9.
- Cherfils, J., and P. Chardin. 1999. GEFs: structural basis for their activation of small GTP-binding proteins. *Trends Biochem Sci.* 24:306-11.
- Cherfils, J., J. Menetrey, M. Mathieu, G. Le Bras, S. Robineau, S. Beraud-Dufour, B. Antonny, and P. Chardin. 1998. Structure of the Sec7 domain of the Arf exchange factor ARNO. *Nature.* 392:101-5.
- Chun, J., Z. Shapovalova, S.Y. Dejgaard, J.F. Presley, and P. Melancon. 2008. Characterization of Class I and II ADP-Ribosylation Factors (Arfs) in Live Cells: GDP-bound Class II Arfs Associate with the ER-Golgi Intermediate Compartment Independently of GBF1. *Mol Biol Cell.* 19:3488-500.
- Citterio, C., H.D. Jones, G. Pacheco-Rodriguez, A. Islam, J. Moss, and M. Vaughan. 2006. Effect of protein kinase A on accumulation of brefeldin A-inhibited guanine nucleotide-exchange protein 1 (BIG1) in HepG2 cell nuclei. *Proc Natl Acad Sci U S A.* 103:2683-8.
- Claude, A., B.P. Zhao, C.E. Kuziemy, S. Dahan, S.J. Berger, J.P. Yan, A.D. Arnold, E.M. Sullivan, and P. Melancon. 1999. GBF1: A novel Golgi-associated BFA-resistant guanine nucleotide exchange factor that displays specificity for ADP-ribosylation factor 5. *J Cell Biol.* 146:71-84.
- Cockcroft, S., G.M. Thomas, A. Fensome, B. Geny, E. Cunningham, I. Gout, I. Hiles, N.F. Totty, O. Truong, and J.J. Hsuan. 1994. Phospholipase D: a downstream effector of ARF in granulocytes. Vol. 263. 523-526.
- Cohen, L.A., A. Honda, P. Varnai, F.D. Brown, T. Balla, and J.G. Donaldson. 2007. Active Arf6 recruits ARNO/cytohesin GEFs to the PM by binding their PH domains. *Mol Biol Cell.* 18:2244-53.
- Connerly, P.L., M. Esaki, E.A. Montegna, D.E. Strongin, S. Levi, J. Soderholm, and B.S. Glick. 2005. Sec16 is a determinant of transitional ER organization. *Curr Biol.* 15:1439-47.
- Cosson, P., and F. Letourneur. 1994. Coatamer interaction with di-lysine endoplasmic reticulum retention motifs. *Science.* 263:1629-31.
- Cox, R., R.J. Mason-Gamer, C.L. Jackson, and N. Segev. 2004. Phylogenetic analysis of Sec7-domain-containing Arf nucleotide exchangers. *Mol Biol Cell.* 15:1487-505.
- Cukierman, E., I. Huber, M. Rotman, and D. Cassel. 1995. The ARF1 GTPase-activating protein: zinc finger motif and Golgi complex localization. *Science.* 270:1999-2002.
- D'Angelo, G., M. Vicinanza, A. Di Campli, and M.A. De Matteis. 2008. The multiple roles of PtdIns(4)P - not just the precursor of PtdIns(4,5)P2. *J Cell Sci.* 121:1955-1963.
- D'Souza-Schorey, C., and P. Chavrier. 2006. ARF proteins: roles in membrane traffic and beyond. *Nat Rev Mol Cell Biol.* 7:347-58.
- D'Souza-Schorey, C., G. Li, M.I. Colombo, and P.D. Stahl. 1995. A regulatory role for ARF6 in receptor-mediated endocytosis. *Science.* 267:1175-8.

- Dascher, C., and W.E. Balch. 1994. Dominant inhibitory mutants of ARF1 block endoplasmic reticulum to Golgi transport and trigger disassembly of the Golgi apparatus. *J Biol Chem.* 269:1437-48.
- De Matteis, M.A., A. Di Campli, and G. D'Angelo. 2007. Lipid-transfer proteins in membrane trafficking at the Golgi complex. *Biochim Biophys Acta.* 1771:761-8.
- De Matteis, M.A., and A. Godi. 2004a. PI-loting membrane traffic. *Nat Cell Biol.* 6:487-92.
- De Matteis, M.A., and A. Godi. 2004b. Protein-lipid interactions in membrane trafficking at the Golgi complex. *Biochim Biophys Acta.* 1666:264-74.
- De Matteis, M.A., and A. Luini. 2008. Exiting the Golgi complex. *Nat Rev Mol Cell Biol.* 9:273-284.
- Deitz, S.B., A. Rambourg, F. Kepes, and A. Franzusoff. 2000. Sec7p directs the transitions required for yeast Golgi biogenesis. *Traffic.* 1:172-83.
- Delphine, D., G. Christoph, K. Annett, S. Emma, L. Hakon, B. Andre Le, and J. Ralf. 2007. Apical Sorting by Galectin-3-Dependent Glycoprotein Clustering. *Traffic.* 8:379-388.
- Derby, M.C., C. van Vliet, D. Brown, M.R. Luke, L. Lu, W. Hong, J.L. Stow, and P.A. Gleeson. 2004. Mammalian GRIP domain proteins differ in their membrane binding properties and are recruited to distinct domains of the TGN. *J Cell Sci.* 117:5865-74.
- Deretic, D., A.H. Williams, N. Ransom, V. Morel, P.A. Hargrave, and A. Arendt. 2005. Rhodopsin C terminus, the site of mutations causing retinal disease, regulates trafficking by binding to ADP-ribosylation factor 4 (ARF4). *Proc Natl Acad Sci U S A.* 102:3301-6.
- Dominguez, M., K. Dejgaard, J. Fullekrug, S. Dahan, A. Fazel, J.P. Paccard, D.Y. Thomas, J.J. Bergeron, and T. Nilsson. 1998. gp25L/emp24/p24 protein family members of the cis-Golgi network bind both COP I and II coatomer. *J Cell Biol.* 140:751-65.
- Donaldson, J.G. 2000. Filling in the GAPs in the ADP-ribosylation factor story. *Proc Natl Acad Sci U S A.* 97:3792-4.
- Donaldson, J.G. 2003. Multiple roles for Arf6: sorting, structuring, and signaling at the plasma membrane. *J Biol Chem.* 278:41573-6.
- Donaldson, J.G., D. Cassel, R.A. Kahn, and R.D. Klausner. 1992a. ADP-ribosylation factor, a small GTP-binding protein, is required for binding of the coatomer protein beta-COP to Golgi membranes. *Proc Natl Acad Sci U S A.* 89:6408-12.
- Donaldson, J.G., D. Finazzi, and R.D. Klausner. 1992b. Brefeldin A inhibits Golgi membrane-catalysed exchange of guanine nucleotide onto ARF protein. *Nature.* 360:350-2.
- Donaldson, J.G., and A. Honda. 2005. Localization and function of Arf family GTPases. *Biochem Soc Trans.* 33:639-42.
- Donaldson, J.G., and C.L. Jackson. 2000. Regulators and effectors of the ARF GTPases. *Curr Opin Cell Biol.* 12:475-82.

- Donaldson, J.G., R.A. Kahn, J. Lippincott-Schwartz, and R.D. Klausner. 1991. Binding of ARF and beta-COP to Golgi membranes: possible regulation by a trimeric G protein. *Science*. 254:1197-9.
- Donaldson, J.G., J. Lippincott-Schwartz, G.S. Bloom, T.E. Kreis, and R.D. Klausner. 1990. Dissociation of a 110-kD peripheral membrane protein from the Golgi apparatus is an early event in brefeldin A action. *J Cell Biol*. 111:2295-306.
- Donohoe, B.S., B.-H. Kang, and L.A. Staehelin. 2007. Identification and characterization of COPIa- and COPIb-type vesicle classes associated with plant and algal Golgi. *Proceedings of the National Academy of Sciences*. 104:163-168.
- Doray, B., P. Ghosh, J. Griffith, H.J. Geuze, and S. Kornfeld. 2002. Cooperation of GGAs and AP-1 in packaging MPRs at the trans-Golgi network. *Science*. 297:1700-3.
- Drin, G., J.F. Casella, R. Gautier, T. Boehmer, T.U. Schwartz, and B. Antonny. 2007. A general amphipathic alpha-helical motif for sensing membrane curvature. *Nat Struct Mol Biol*. 14:138-46.
- Duden, R. 2003. ER-to-Golgi transport: COP I and COP II function (Review). *Mol Membr Biol*. 20:197-207.
- Elbashir, S.M., J. Harborth, K. Weber, and T. Tuschl. 2002. Analysis of gene function in somatic mammalian cells using small interfering RNAs. *Methods*. 26:199-213.
- Elsner, M., H. Hashimoto, J.C. Simpson, D. Cassel, T. Nilsson, and M. Weiss. 2003. Spatiotemporal dynamics of the COPI vesicle machinery. *EMBO Rep*. 4:1000-4.
- Enomoto, K., and D.M. Gill. 1980. Cholera toxin activation of adenylate cyclase. Roles of nucleoside triphosphates and a macromolecular factor in the ADP ribosylation of the GTP-dependent regulatory component. *J. Biol. Chem*. 255:1252-1258.
- Esmon, B., P. Novick, and R. Schekman. 1981. Compartmentalized assembly of oligosaccharides on exported glycoproteins in yeast. *Cell*. 25:451-60.
- Espenshade, P., R.E. Gimeno, E. Holzmacher, P. Teung, and C.A. Kaiser. 1995. Yeast SEC16 gene encodes a multidomain vesicle coat protein that interacts with Sec23p. *J Cell Biol*. 131:311-24.
- Eugster, A., G. Frigerio, M. Dale, and R. Duden. 2004. The alpha- and beta'-COP WD40 domains mediate cargo-selective interactions with distinct di-lysine motifs. *Mol Biol Cell*. 15:1011-23.
- Farquhar, M.G., and G.E. Palade. 1981. The Golgi apparatus (complex)-(1954-1981)-from artifact to center stage. *J Cell Biol*. 91:77s-103s.
- Farquhar, M.G., and G.E. Palade. 1998. The Golgi apparatus: 100 years of progress and controversy. *Trends Cell Biol*. 8:2-10.
- Fischer, K.D., J.B. Helms, L. Zhao, and F.T. Wieland. 2000. Site-specific photocrosslinking to probe interactions of Arf1 with proteins involved in budding of COPI vesicles. *Methods*. 20:455-64.

- Franco, M., P. Chardin, M. Chabre, and S. Paris. 1995. Myristoylation of ADP-ribosylation factor 1 facilitates nucleotide exchange at physiological Mg^{2+} levels. *J. Biol. Chem.* 270:1337-41.
- Franco, M., P. Chardin, M. Chabre, and S. Paris. 1996. Myristoylation-facilitated binding of the G protein ARF1GDP to membrane phospholipids is required for its activation by a soluble nucleotide exchange factor. *J Biol Chem.* 271:1573-8.
- Franzusoff, A., K. Redding, J. Crosby, R.S. Fuller, and R. Schekman. 1991. Localization of components involved in protein transport and processing through the yeast Golgi apparatus. *J Cell Biol.* 112:27-37.
- Franzusoff, A., and R. Schekman. 1989. Functional compartments of the yeast Golgi apparatus are defined by the *sec7* mutation. *Embo J.* 8:2695-702.
- Frigerio, G., N. Grimsey, M. Dale, I. Majoul, and R. Duden. 2007. Two human ARFGAPs associated with COP-I-coated vesicles. *Traffic.* 8:1644-55.
- Fromme, J.C., L. Orci, and R. Schekman. 2008. Coordination of COPII vesicle trafficking by Sec23. 18:330-336.
- Fromme, J.C., and R. Schekman. 2005. COPII-coated vesicles: flexible enough for large cargo? *Curr Opin Cell Biol.* 17:345-52.
- Fujita, Y., E. Ohama, M. Takatama, S. Al-Sarraj, and K. Okamoto. 2006. Fragmentation of Golgi apparatus of nigral neurons with α -synuclein-positive inclusions in patients with Parkinson's disease. *Acta Neuropathologica.* 112:261-265.
- Futai, E., S. Hamamoto, L. Orci, and R. Schekman. 2004. GTP/GDP exchange by Sec12p enables COPII vesicle bud formation on synthetic liposomes. *Embo J.* 23:4146-55.
- Garcia-Mata, R., and E. Sztul. 2003. The membrane-tethering protein p115 interacts with GBF1, an ARF guanine-nucleotide-exchange factor. *EMBO Rep.* 4:320-5.
- Garcia-Mata, R., T. Szul, C. Alvarez, and E. Sztul. 2003. ADP-ribosylation factor/COPI-dependent events at the endoplasmic reticulum-Golgi interface are regulated by the guanine nucleotide exchange factor GBF1. *Mol Biol Cell.* 14:2250-61.
- Geldner, N., N. Anders, H. Wolters, J. Keicher, W. Kornberger, P. Muller, A. Delbarre, T. Ueda, A. Nakano, and G. Jurgens. 2003. The Arabidopsis GNOM ARF-GEF mediates endosomal recycling, auxin transport, and auxin-dependent plant growth. *Cell.* 112:219-30.
- Ghosh, P., J. Griffith, H.J. Geuze, and S. Kornfeld. 2003. Mammalian GGAs act together to sort mannose 6-phosphate receptors. *J Cell Biol.* 163:755-66.
- Ghosh, P., and S. Kornfeld. 2004. The GGA proteins: key players in protein sorting at the trans-Golgi network. *Eur J Cell Biol.* 83:257-62.
- Gilchrist, A., C.E. Au, J. Hiding, A.W. Bell, J. Fernandez-Rodriguez, S. Lesimple, H. Nagaya, L. Roy, S.J.C. Gosline, M. Hallett, J. Paiement, Robert E. Kearney, T. Nilsson, and J.J.M. Bergeron. 2006. Quantitative Proteomics Analysis of the Secretory Pathway. 127:1265-1281.

- Gimeno, R.E., P. Espenshade, and C.A. Kaiser. 1996. COPII coat subunit interactions: Sec24p and Sec23p bind to adjacent regions of Sec16p. *Mol Biol Cell*. 7:1815-23.
- Gleeson, P.A., J.G. Lock, M.R. Luke, and J.L. Stow. 2004. Domains of the TGN: coats, tethers and G proteins. *Traffic*. 5:315-26.
- Glick, B.S., and A. Nakano. 2009. Membrane Traffic within the Golgi Stack. *Annual Review of Cell and Developmental Biology*. 25.
- Godi, A., A. Di Campi, A. Konstantakopoulos, G. Di Tullio, D.R. Alessi, G.S. Kular, T. Daniele, P. Marra, J.M. Lucocq, and M.A. De Matteis. 2004. FAPPs control Golgi-to-cell-surface membrane traffic by binding to ARF and PtdIns(4)P. *Nat Cell Biol*. 6:393-404.
- Goldberg, J. 1998. Structural basis for activation of ARF GTPase: mechanisms of guanine nucleotide exchange and GTP-myristoyl switching. *Cell*. 95:237-48.
- Gommel, D.U., A.R. Memon, A. Heiss, F. Lottspeich, J. Pfannstiel, J. Lechner, C. Reinhard, J.B. Helms, W. Nickel, and F.T. Wieland. 2001. Recruitment to Golgi membranes of ADP-ribosylation factor 1 is mediated by the cytoplasmic domain of p23. *Embo J*. 20:6751-60.
- Griffiths, G., S.D. Fuller, R. Back, M. Hollinshead, S. Pfeiffer, and K. Simons. 1989. The dynamic nature of the Golgi complex. *J Cell Biol*. 108:277-97.
- Griffiths, G., R. Pepperkok, J.K. Locker, and T.E. Kreis. 1995. Immunocytochemical localization of beta-COP to the ER-Golgi boundary and the TGN. *J Cell Sci*. 108:2839-56.
- Griffiths, G., and K. Simons. 1986. The trans Golgi network: sorting at the exit site of the Golgi complex. *Science*. 234:438-443.
- Guo, Q., E. Vasile, and M. Krieger. 1994. Disruptions in Golgi structure and membrane traffic in a conditional lethal mammalian cell mutant are corrected by epsilon-COP. *J Cell Biol*. 125:1213-24.
- Hampl, V., L. Hug, J.W. Leigh, J.B. Dacks, B.F. Lang, A.G.B. Simpson, and A.J. Roger. 2009. Phylogenomic analyses support the monophyly of Excavata and resolve relationships among eukaryotic "supergroups". *Proceedings of the National Academy of Sciences*. 106:3859-3864.
- Hannan, L.A., M.P. Lisanti, E. Rodriguez-Boulant, and M. Edidin. 1993. Correctly sorted molecules of a GPI-anchored protein are clustered and immobile when they arrive at the apical surface of MDCK cells. *J. Cell Biol*. 120:353-358.
- Hara-Kuge, S., O. Kuge, L. Orci, M. Amherdt, M. Ravazzola, F.T. Wieland, and J.E. Rothman. 1994. En bloc incorporation of coatamer subunits during the assembly of COP-coated vesicles. *J Cell Biol*. 124:883-92.
- Harborth, J., S.M. Elbashir, K. Bechert, T. Tuschl, and K. Weber. 2001. Identification of essential genes in cultured mammalian cells using small interfering RNAs. *J Cell Sci*. 114:4557-4565.
- Harlow, E., and D. Lane. 1988. *Antibodies, A laboratory Manual*. Cold Spring Harbor Laboratory, Cold Spring Harbor. 726 pp.
- Hauri, H.P., and A. Schweizer. 1992. The endoplasmic reticulum-Golgi intermediate compartment. *Curr Opin Cell Biol*. 4:600-8.
- Helms, J.B., D.J. Palmer, and J.E. Rothman. 1993. Two distinct regulations of ARF bound to Golgi membranes. *J. Cell Biol*.:751-760.

- Helms, J.B., and J.E. Rothman. 1992. Inhibition by brefeldin A of a Golgi membrane enzyme that catalyses exchange of guanine nucleotide bound to ARF. *Nature*. 360:352-4.
- Hinners, I., and S.A. Tooze. 2003. Changing directions: clathrin-mediated transport between the Golgi and endosomes. *J Cell Sci*. 116:763-71.
- Honda, A., O.S. Al-Awar, J.C. Hay, and J.G. Donaldson. 2005. Targeting of Arf-1 to the early Golgi by membrin, an ER-Golgi SNARE. *J Cell Biol*. 168:1039-51.
- Honda, A., M. Nogami, T. Yokozeki, M. Yamazaki, H. Nakamura, H. Watanabe, K. Kawamoto, K. Nakayama, A.J. Morris, M.A. Frohman, and Y. Kanaho. 1999. Phosphatidylinositol 4-phosphate 5-kinase alpha is a downstream effector of the small G protein ARF6 in membrane ruffle formation. *Cell*. 99:521-32.
- Hosaka, M., K. Toda, H. Takatsu, S. Torii, K. Murakami, and K. Nakayama. 1996. Structure and intracellular localization of mouse ADP-ribosylation factors type 1 to type 6 (ARF1-ARF6). *J Biochem*. 120:813-9.
- Huynh, D.P., H.-T. Yang, H. Vakharia, D. Nguyen, and S.M. Pulst. 2003. Expansion of the polyQ repeat in ataxin-2 alters its Golgi localization, disrupts the Golgi complex and causes cell death. *Hum. Mol. Genet*. 12:1485-1496.
- Inoue, H., and P.A. Randazzo. 2007. Arf GAPs and Their Interacting Proteins. *Traffic*.
- Ishizaki, R., H.W. Shin, H. Mitsuhashi, and K. Nakayama. 2008. Redundant Roles of BIG2 and BIG1, Guanine-Nucleotide Exchange Factors for ADP-Ribosylation Factors in Membrane Traffic between the trans-Golgi Network and Endosomes. *Mol Biol Cell*. 19:2650-60.
- Islam, A., X. Shen, T. Hiroi, J. Moss, M. Vaughan, and S.J. Levine. 2007. The brefeldin A-inhibited guanine nucleotide-exchange protein, BIG2, regulates the constitutive release of TNFR1 exosome-like vesicles. *J Biol Chem*. 282:9591-9.
- Jackson, C.L., and J.E. Casanova. 2000. Turning on ARF: the Sec7 family of guanine-nucleotide-exchange factors. *Trends Cell Biol*. 10:60-7.
- Jie, L., T. Grace, F. Rebecca, H. Jonathon, W. Christopher, and S. Volney. 2006. Overlapping expression of ARFGEF2 and Filamin A in the neuroependymal lining of the lateral ventricles: Insights into the cause of periventricular heterotopia. *The Journal of Comparative Neurology*. 494:476-484.
- John, G.L., A.H. Luke, H. Fiona, A.G. Paul, and L.S. Jennifer. 2005. E-Cadherin Transport from the trans-Golgi Network in Tubulovesicular Carriers is Selectively Regulated by Golgin-97. *Traffic*. 6:1142-1156.
- Kahn, R.A., and A.G. Gilman. 1984. Purification of a protein cofactor required for ADP-ribosylation of the stimulatory regulatory component of adenylate cyclase by cholera toxin. *J. Biol. Chem*. 259:6228-6234.
- Kakinuma, T., H. Ichikawa, Y. Tsukada, T. Nakamura, and B.-H. Toh. 2004. Interaction between p230 and MACF1 is associated with transport of a glycosyl phosphatidyl inositol-anchored protein from the Golgi to the cell periphery. *Experimental Cell Research*. 298:388-398.

- Kanoh, H., B.T. Williger, and J.H. Exton. 1997. Arfaptin 1, a putative cytosolic target protein of ADP-ribosylation factor, is recruited to Golgi membranes. *J Biol Chem.* 272:5421-9.
- Karecla, P.I., and T.E. Kreis. 1992. Interaction of membranes of the Golgi complex with microtubules in vitro. *European Journal of Cell Biology.* 57:139-146.
- Kawamoto, K., Y. Yoshida, H. Tamaki, S. Torii, C. Shinotsuka, S. Yamashina, and K. Nakayama. 2002. GBF1, a Guanine Nucleotide Exchange Factor for ADP-Ribosylation Factors, is Localized to the cis-Golgi and Involved in Membrane Association of the COPI Coat. *Traffic.* 3:483-95.
- Kepes, F., A. Rambourg, and B. Satiat-Jeunemaitre. 2005. Morphodynamics of the secretory pathway. *Int Rev Cytol.* 242:55-120.
- Klausner, R.D., J.G. Donaldson, and S.J. Lippincott. 1992. Brefeldin A: insights into the control of membrane traffic and organelle structure. *J Cell Biol.* 116:1071-80.
- Kliouchnikov, L., J. Bigay, B. Mesmin, A. Parnis, M. Rawet, N. Goldfeder, B. Antonny, and D. Cassel. 2009. Discrete Determinants in ArfGAP2/3 Conferring Golgi Localization and Regulation by the COPI Coat. *Mol. Biol. Cell.* 20:859-869.
- Kreis, T.E., and H.F. Lodish. 1986. Oligomerization is essential for transport of vesicular stomatitis viral glycoprotein to the cell surface. *Cell.* 46:929-37.
- Kuehn, M.J., J.M. Herrmann, and R. Schekman. 1998. COPII-cargo interactions direct protein sorting into ER-derived transport vesicles. *Nature.* 391:187-90.
- Kuroda, F., J. Moss, and M. Vaughan. 2007. Regulation of brefeldin A-inhibited guanine nucleotide-exchange protein 1 (BIG1) and BIG2 activity via PKA and protein phosphatase 1gamma. *Proc Natl Acad Sci U S A.* 104:3201-6.
- Ladinsky, M.S., J.R. Kremer, P.S. Furcinitti, R.J. McIntosh, and K.E. Howell. 1994. HVEM tomography of the *trans*-Golgi network: structural insights and identification of a lace-like vesicle coat. *J. Cell Biol.* 127:29-38.
- Ladinsky, M.S., D.N. Mastronarde, J.R. McIntosh, K.E. Howell, and L.A. Staehelin. 1999. Golgi structure in three dimensions: functional insights from the normal rat kidney cell. *J Cell Biol.* 144:1135-49.
- Ladinsky, M.S., C.C. Wu, S. McIntosh, J.R. McIntosh, and K.E. Howell. 2002. Structure of the Golgi and Distribution of Reporter Molecules at 20 degrees C Reveals the Complexity of the Exit Compartments. *Mol Biol Cell.* 13:2810-25.
- Lanoix, J., J. Ouwendijk, C.C. Lin, A. Stark, H.D. Love, J. Ostermann, and T. Nilsson. 1999. GTP hydrolysis by arf-1 mediates sorting and concentration of Golgi resident enzymes into functional COP I vesicles. *Embo J.* 18:4935-48.
- Lee, M.C., E.A. Miller, J. Goldberg, L. Orci, and R. Schekman. 2004. Bi-directional protein transport between the ER and Golgi. *Annu Rev Cell Dev Biol.* 20:87-123.
- Lee, S.Y., J.S. Yang, W. Hong, R.T. Premont, and V.W. Hsu. 2005. ARFGAP1 plays a central role in coupling COPI cargo sorting with vesicle formation. *J Cell Biol.* 168:281-90.

- Lenhard, J.M., R.A. Kahn, and P.D. Stahl. 1992. Evidence for ADP-ribosylation factor (ARF) as a regulator of in vitro endosome-endosome fusion. *J Biol Chem.* 267:13047-52.
- Letourneur, F., E.C. Gaynor, S. Hennecke, C. Demolliere, R. Duden, S.D. Emr, H. Riezman, and P. Cosson. 1994. Coatamer is essential for retrieval of dilysine-tagged proteins to the endoplasmic reticulum. *Cell.* 79:1199-1207.
- Levine, T.P., and S. Munro. 2002. Targeting of Golgi-specific pleckstrin homology domains involves both PtdIns 4-kinase-dependent and -independent components. *Curr Biol.* 12:695-704.
- Li, H., R. Adamik, G. Pacheco-Rodriguez, J. Moss, and M. Vaughan. 2003. Protein kinase A-anchoring (AKAP) domains in brefeldin A-inhibited guanine nucleotide-exchange protein 2 (BIG2). *Proc Natl Acad Sci U S A.* 100:1627-32.
- Li, J., P.J. Peters, M. Bai, J. Dai, E. Bos, T. Kirchhausen, K.V. Kandror, and V.W. Hsu. 2007. An ACAP1-containing clathrin coat complex for endocytic recycling. *J Cell Biol.* 178:453-64.
- Li, Y., W.G. Kelly, J.M.J. Logsdon, A.M. Schurko, B.D. Harfe, K.L. Hill-Harfe, and R.A. Kahn. 2004. Functional genomic analysis of the ADP-ribosylation factor family of GTPases: phylogeny among diverse eukaryotes and function in *C. elegans*. *FASEB J.* 18:1834-1850.
- Liang, J.O., and S. Kornfeld. 1997. Comparative activity of ADP-ribosylation factor family members in the early steps of coated vesicle formation on rat liver Golgi membranes [published erratum appears in *J Biol Chem* 1998 Jan 23;273(4):2488]. *J Biol Chem.* 272:4141-8.
- Liang, J.O., T.C. Sung, A.J. Morris, M.A. Frohman, and S. Kornfeld. 1997. Different domains of mammalian ADP-ribosylation factor 1 mediate interaction with selected target proteins. *J Biol Chem.* 272:33001-8.
- Lin, P., F. Li, Y.W. Zhang, H. Huang, G. Tong, M.G. Farquhar, and H. Xu. 2007. Calnuc binds to Alzheimer's β -amyloid precursor protein and affects its biogenesis. *Journal of Neurochemistry.* 100:1505-1514.
- Lippincott-Schwartz, J., N.B. Cole, and J.G. Donaldson. 1998. Building a secretory apparatus: role of ARF1/COPI in Golgi biogenesis and maintenance. *Histochem Cell Biol.* 109:449-62.
- Lippincott, S.J., J.G. Donaldson, A. Schweizer, E.G. Berger, H.P. Hauri, L.C. Yuan, and R.D. Klausner. 1990. Microtubule-dependent retrograde transport of proteins into the ER in the presence of brefeldin A suggests an ER recycling pathway. *Cell.* 60:821-36.
- Lippincott, S.J., L. Yuan, C. Tipper, M. Amherdt, L. Orci, and R.D. Klausner. 1991. Brefeldin A's effects on endosomes, lysosomes, and the TGN suggest a general mechanism for regulating organelle structure and membrane traffic. *Cell.* 67:601-16.
- Lippincott, S.J., L.C. Yuan, J.S. Bonifacino, and R.D. Klausner. 1989. Rapid redistribution of Golgi proteins into the ER in cells treated with brefeldin A: evidence for membrane cycling from Golgi to ER. *Cell.* 56:801-13.
- Losev, E., C.A. Reinke, J. Jellen, D.E. Strongin, B.J. Bevis, and B.S. Glick. 2006. Golgi maturation visualized in living yeast. *Nature.* 441:1002-6.

- Losonczi, J.A., F. Tian, and J.H. Prestegard. 2000. Nuclear Magnetic Resonance Studies of the N-Terminal Fragment of Adenosine Diphosphate Ribosylation Factor 1 in Micelles and Bicelles: Influence of N-Myristoylation. *J Biol Chem*. Vol. 275. 3804-3816.
- Luini, A., A. Ragnini-Wilson, R.S. Polishchuck, and M.A. De Matteis. 2005. Large pleiomorphic traffic intermediates in the secretory pathway. *Curr Opin Cell Biol*. 17:353-61.
- Majoul, I., K. Sohn, F.T. Wieland, R. Pepperkok, M. Pizza, J. Hillemann, and H.D. Soling. 1998. KDEL receptor (Erd2p)-mediated retrograde transport of the cholera toxin A subunit from the Golgi involves COPI, p23, and the COOH terminus of Erd2p. *J Cell Biol*. 143:601-12.
- Majoul, I., M. Straub, S.W. Hell, R. Duden, and H.D. Soling. 2001. KDEL-cargo regulates interactions between proteins involved in COPI vesicle traffic: measurements in living cells using FRET. *Dev Cell*. 1:139-53.
- Mancias, J.D., and J. Goldberg. 2005. Exiting the endoplasmic reticulum. *Traffic*. 6:278-85.
- Manolea, F., A. Claude, J. Chun, J. Rosas, and P. Melançon. 2008. Distinct Functions for Arf Guanine Nucleotide Exchange Factors at the Golgi Complex: GBF1 and BIGs Are Required for Assembly and Maintenance of the Golgi Stack and trans-Golgi Network, Respectively. *Mol Biol Cell*. 19:523-35.
- Mansour, S.J., J. Skaug, X.H. Zhao, J. Giordano, S.W. Scherer, and P. Melançon. 1999. p200 ARF-GEP1: a Golgi-localized guanine nucleotide exchange protein whose Sec7 domain is targeted by the drug brefeldin A. *Proc Natl Acad Sci U S A*. 96:7968-73.
- Martinez-Menarguez, J.A., H.J. Geuze, J.W. Slot, and J. Klumperman. 1999. Vesicular tubular clusters between the ER and Golgi mediate concentration of soluble secretory proteins by exclusion from COPI-coated vesicles. *Cell*. 98:81-90.
- Martinez-Menarguez, J.A., R. Prekeris, V.M. Oorschot, R. Scheller, J.W. Slot, H.J. Geuze, and J. Klumperman. 2001. Peri-Golgi vesicles contain retrograde but not anterograde proteins consistent with the cisternal progression model of intra-Golgi transport. *J Cell Biol*. 155:1213-24.
- Matlin, K.S., and K. Simons. 1983. Reduced temperature prevents transfer of a membrane glycoprotein to the cell surface but does not prevent terminal glycosylation. *Cell*. 34:233-43.
- Matsuura-Tokita, K., M. Takeuchi, A. Ichihara, K. Mikuriya, and A. Nakano. 2006. Live imaging of yeast Golgi cisternal maturation. *Nature*. 441:1007-10.
- Melancon, P., B.S. Glick, V. Malhotra, P.J. Weidman, T. Serafini, M.L. Gleason, L. Orci, and J.E. Rothman. 1987. Involvement of GTP-binding "G" proteins in transport through the Golgi stack. *Cell*. 51:1053-62.
- Mesmin, B., G. Drin, S. Levi, M. Rawet, D. Cassel, J. Bigay, and B. Antony. 2007. Two lipid-packing sensor motifs contribute to the sensitivity of ArfGAP1 to membrane curvature. *Biochemistry*. 46:1779-90.
- Miller, E.A., T.H. Beilharz, P.N. Malkus, M.C. Lee, S. Hamamoto, L. Orci, and R. Schekman. 2003. Multiple cargo binding sites on the COPII subunit Sec24p

- ensure capture of diverse membrane proteins into transport vesicles. *Cell*. 114:497-509.
- Mironov, A.A., G.V. Beznoussenko, P. Nicoziani, O. Martella, A. Trucco, H.S. Kweon, D. Di Giandomenico, R.S. Polishchuk, A. Fusella, P. Lupetti, E.G. Berger, W.J. Geerts, A.J. Koster, K.N. Burger, and A. Luini. 2001. Small cargo proteins and large aggregates can traverse the Golgi by a common mechanism without leaving the lumen of cisternae. *J Cell Biol*. 155:1225-38.
- Misumi, Y., Y. Misumi, K. Miki, A. Takatsuki, G. Tamura, and Y. Ikehara. 1986. Novel blockade by brefeldin A of intracellular transport of secretory proteins in cultured rat hepatocytes. *J Biol Chem*. 261:11398-403.
- Miura, K., K.M. Jacques, S. Stauffer, A. Kubosaki, K. Zhu, D.S. Hirsch, J. Resau, Y. Zheng, and P.A. Randazzo. 2002. ARAP1: a point of convergence for Arf and Rho signaling. *Mol Cell*. 9:109-19.
- Mogelsvang, S., N. Gomez-Ospina, J. Soderholm, B.S. Glick, and L.A. Staehelin. 2003. Tomographic evidence for continuous turnover of Golgi cisternae in *Pichia pastoris*. *Mol Biol Cell*. 14:2277-91.
- Mogelsvang, S., B.J. Marsh, M.S. Ladinsky, and K.E. Howell. 2004. Predicting function from structure: 3D structure studies of the mammalian Golgi complex. *Traffic*. 5:338-45.
- Monetta, P., I. Slavin, N. Romero, and C. Alvarez. 2007. Rab1b interacts with GBF1 and modulates both ARF1 dynamics and COPI association. *Mol Biol Cell*. 18:2400-10.
- Morin-Ganet, M.N., A. Rambourg, S.B. Deitz, A. Franzusoff, and F. Kepes. 2000. Morphogenesis and dynamics of the yeast Golgi apparatus. *Traffic*. 1:56-68.
- Morinaga, N., R. Adamik, J. Moss, and M. Vaughan. 1999. Brefeldin A inhibited activity of the sec7 domain of p200, a mammalian guanine nucleotide-exchange protein for ADP-ribosylation factors. *J Biol Chem*. 274:17417-23.
- Morinaga, N., S.C. Tsai, J. Moss, and M. Vaughan. 1996. Isolation of a brefeldin A-inhibited guanine nucleotide-exchange protein for ADP ribosylation factor (ARF) 1 and ARF3 that contains a Sec7-like domain. *Proc Natl Acad Sci U S A*. 93:12856-60.
- Mossessova, E., R.A. Corpina, and J. Goldberg. 2003. Crystal structure of ARF1*Sec7 complexed with Brefeldin A and its implications for the guanine nucleotide exchange mechanism. *Mol Cell*. 12:1403-11.
- Mossessova, E., J.M. Gulbis, and J. Goldberg. 1998. Structure of the guanine nucleotide exchange factor Sec7 domain of human arno and analysis of the interaction with ARF GTPase. *Cell*. 92:415-23.
- Mouratou, B., V. Biou, A. Joubert, J. Cohen, D.J. Shields, N. Geldner, G. Jurgens, P. Melançon, and J. Cherfils. 2005. The domain architecture of large guanine nucleotide exchange factors for the small GTP-binding protein Arf. *BMC Genomics*. 6:20.
- Mourelatos, Z., N.K. Gonatas, A. Stieber, M.E. Gurney, and M.C. Dal Canto. 1996. The Golgi apparatus of spinal cord motor neurons in transgenic mice expressing mutant Cu,Zn superoxide dismutase becomes fragmented in early, preclinical stages of the disease. *Proceedings of the National Academy of Sciences of the United States of America*. 93:5472-5477.

- Moyer, B.D., B.B. Allan, and W.E. Balch. 2001. Rab1 interaction with a GM130 effector complex regulates COPII vesicle cis-Golgi tethering. *Traffic*. 2:268-76.
- Muniz, M., C. Nuoffer, H.P. Hauri, and H. Riezman. 2000. The Emp24 complex recruits a specific cargo molecule into endoplasmic reticulum-derived vesicles. *Journal of Cell Biology*. 148:925-30.
- Myers, K.R., and J.E. Casanova. 2008. Regulation of actin cytoskeleton dynamics by Arf-family GTPases. *Trends Cell Biol*. 18:184-92.
- Nelson, D.S., C. Alvarez, Y.S. Gao, R. Garcia-Mata, E. Fialkowski, and E. Sztul. 1998. The membrane transport factor TAP/p115 cycles between the Golgi and earlier secretory compartments and contains distinct domains required for its localization and function. *J Cell Biol*. 143:319-31.
- Ni, X., M. Canuel, and C.R. Morales. 2006. The sorting and trafficking of lysosomal proteins. *Histol Histopathol*. 21:899-913.
- Nickel, W., J. Malsam, K. Gorgas, M. Ravazzola, N. Jenne, J.B. Helms, and F.T. Wieland. 1998. Uptake by COPI-coated vesicles of both anterograde and retrograde cargo is inhibited by GTPgammaS in vitro. *J Cell Sci*. 111:3081-90.
- Nickel, W., and F.T. Wieland. 1998. Biosynthetic protein transport through the early secretory pathway. *Histochem Cell Biol*. 109:477-86.
- Nie, Z., D.S. Hirsch, and P.A. Randazzo. 2003. Arf and its many interactors. *Curr Opin Cell Biol*. 15:396-404.
- Nie, Z., and P.A. Randazzo. 2006. Arf GAPs and membrane traffic. *J Cell Sci*. 119:1203-11.
- Nishimura, N., S. Bannykh, S. Slabough, J. Matteson, Y. Altschuler, K. Hahn, and W.E. Balch. 1999. A di-acidic (DXE) code directs concentration of cargo during export from the endoplasmic reticulum. *J Biol Chem*. 274:15937-46.
- Niu, T.K., A.C. Pfeifer, J. Lippincott-Schwartz, and C.L. Jackson. 2005. Dynamics of GBF1, a Brefeldin A-sensitive Arf1 exchange factor at the Golgi. *Mol Biol Cell*. 16:1213-22.
- Novick, P., C. Field, and R. Schekman. 1980. Identification of 23 complementation groups required for post-translational events in the yeast secretory pathway. *Cell*. 21:205-15.
- Ombretta, F., and D. Jürgen. 2008. Intermediate Organelles of the Plant Secretory Pathway: Identity and Function. *Traffic*. 9:1599-1612.
- Ooi, C.E., E.C. Dell'Angelica, and J.S. Bonifacino. 1998. ADP-Ribosylation factor 1 (ARF1) regulates recruitment of the AP-3 adaptor complex to membranes. *J Cell Biol*. 142:391-402.
- Opat, A.S., C. van Vliet, and P.A. Gleeson. 2001. Trafficking and localisation of resident Golgi glycosylation enzymes. *Biochimie*. 83:763-773.
- Oprins, A., R. Duden, T.E. Kreis, H.J. Geuze, and J.W. Slot. 1993. Beta-COP localizes mainly to the cis-Golgi side in exocrine pancreas. *J Cell Biol*. 121:49-59.
- Orci, L., B.S. Glick, and J.E. Rothman. 1986. A new type of coated vesicular carrier that appears not to contain clathrin: its possible role in protein transport within the Golgi stack. *Cell*. 46:171-84.

- Orci, L., M. Ravazzola, M. Amherdt, A. Perrelet, S.K. Powell, D.L. Quinn, and H.P. Moore. 1987. The trans-most cisternae of the Golgi complex: a compartment for sorting of secretory and plasma membrane proteins. *Cell*. 51:1039-51.
- Orci, L., M. Ravazzola, A. Volchuk, T. Engel, M. Gmachl, M. Amherdt, A. Perrelet, T.H. Sollner, and J.E. Rothman. 2000. Anterograde flow of cargo across the golgi stack potentially mediated via bidirectional "percolating" COPI vesicles. *Proc Natl Acad Sci U S A*. 97:10400-5.
- Orci, L., M. Tagaya, M. Amherdt, A. Perrelet, J.G. Donaldson, S.J. Lippincott, R.D. Klausner, and J.E. Rothman. 1991. Brefeldin A, a drug that blocks secretion, prevents the assembly of non-clathrin-coated buds on Golgi cisternae. *Cell*. 64:1183-95.
- Ostermann, J., L. Orci, K. Tani, M. Amherdt, M. Ravazzola, Z. Elazar, and J.E. Rothman. 1993. Stepwise assembly of functionally active transport vesicles. *Cell*. 75:1015-25.
- Palade, G. 1975. Intracellular aspects of the process of protein synthesis. *Science*. 189:347-58.
- Pasqualato, S., L. Renault, and J. Cherfils. 2002. Arf, Arl, Arp and Sar proteins: a family of GTP-binding proteins with a structural device for 'front-back' communication. *EMBO Rep*. 3:1035-41.
- Patterson, G.H., K. Hirschberg, R.S. Polishchuk, D. Gerlich, R.D. Phair, and J. Lippincott-Schwartz. 2008. Transport through the Golgi Apparatus by Rapid Partitioning within a Two-Phase Membrane System. 133:1055-1067.
- Pelham, H.R. 2001. Traffic through the Golgi apparatus. *J Cell Biol*. 155:1099-101.
- Pelham, H.R., and J.E. Rothman. 2000. The debate about transport in the Golgi--two sides of the same coin? *Cell*. 102:713-9.
- Pepperkok, R., J. Scheel, H. Horstmann, H.P. Hauri, G. Griffiths, and T.E. Kreis. 1993. Beta-COP is essential for biosynthetic membrane transport from the endoplasmic reticulum to the Golgi complex in vivo. *Cell*. 74:71-82.
- Pepperkok, R., J.A. Whitney, M. Gomez, and T.E. Kreis. 2000. COPI vesicles accumulating in the presence of a GTP restricted arf1 mutant are depleted of anterograde and retrograde cargo. *J Cell Sci*. 113:135-44.
- Peter, F., H. Plutner, H. Zhu, T.E. Kreis, and W.E. Balch. 1993. Beta-COP is essential for transport of protein from the endoplasmic reticulum to the Golgi in vitro. *J Cell Biol*. 122:1155-67.
- Peters, P.J., V.W. Hsu, C.E. Ooi, D. Finazzi, S.B. Teal, V. Oorschot, J.G. Donaldson, and R.D. Klausner. 1995. Overexpression of wild-type and mutant ARF1 and ARF6: distinct perturbations of nonoverlapping membrane compartments. *J Cell Biol*. 128:1003-17.
- Peyroche, A., R. Courbeyrette, A. Rambourg, and C.L. Jackson. 2001. The ARF exchange factors Gea1p and Gea2p regulate Golgi structure and function in yeast. *J Cell Sci*. 114:2241-53.
- Peyroche, A., S. Paris, and C.L. Jackson. 1996. Nucleotide exchange on ARF mediated by yeast Gea1 protein. *Nature*. 384:479-81.

- Piper, R.C., and J.P. Luzio. 2007. Ubiquitin-dependent sorting of integral membrane proteins for degradation in lysosomes. *Current Opinion in Cell Biology*. 19:459-465.
- Polishchuk, R.S., and A.A. Mironov. 2004. Structural aspects of Golgi function. *Cell Mol Life Sci*. 61:146-58.
- Poon, P.P., D. Cassel, A. Spang, M. Rotman, E. Pick, R.A. Singer, and G.C. Johnston. 1999. Retrograde transport from the yeast Golgi is mediated by two ARF GAP proteins with overlapping function. *Embo J*. 18:555-64.
- Presley, J.F., N.B. Cole, T.A. Schroer, K. Hirschberg, K.J. Zaal, and J. Lippincott-Schwartz. 1997a. ER-to-Golgi transport visualized in living cells. *Nature*. 389:81-5.
- Presley, J.F., N.B. Cole, T.A. Schroer, K. Hirschberg, K.J. Zaal, and J. Lippincott-Schwartz. 1997b. ER-to-Golgi transport visualized in living cells [see comments]. *Nature*. 389:81-5.
- Puertollano, R., R.C. Aguilar, I. Gorshkova, R.J. Crouch, and J.S. Bonifacino. 2001a. Sorting of mannose 6-phosphate receptors mediated by the GGAs. *Science*. 292:1712-6.
- Puertollano, R., P.A. Randazzo, J.F. Presley, L.M. Hartnell, and J.S. Bonifacino. 2001b. The GGAs promote ARF-dependent recruitment of clathrin to the TGN. *Cell*. 105:93-102.
- Puri, S., C. Bachert, C.J. Fimmel, and A.D. Linstedt. 2002. Cycling of early Golgi proteins via the cell surface and endosomes upon luminal pH disruption. *Traffic*. 3:641-53.
- Puthenveedu, M.A., and A.D. Linstedt. 2005. Subcompartmentalizing the Golgi apparatus. *Curr Opin Cell Biol*. 17:369-75.
- Rabouille, C., and J. Klumperman. 2005. Opinion: The maturing role of COPI vesicles in intra-Golgi transport. *Nat Rev Mol Cell Biol*. 6:812-7.
- Rambourg, A., and Y. Clermont. 1990. Three-dimensional electron microscopy: structure of the Golgi apparatus. *Eur J Cell Biol*. 51:189-200.
- Rambourg, A., Y. Clermont, and F. Kepes. 1993. Modulation of the Golgi apparatus in *Saccharomyces cerevisiae* sec7 mutants as seen by three-dimensional electron microscopy. *Anat Rec*. 237:441-52.
- Rambourg, A., C.L. Jackson, and Y. Clermont. 2001. Three dimensional configuration of the secretory pathway and segregation of secretion granules in the yeast *Saccharomyces cerevisiae*. *J Cell Sci*. 114:2231-9.
- Randazzo, P.A., and D.S. Hirsch. 2004. Arf GAPs: multifunctional proteins that regulate membrane traffic and actin remodelling. *Cell Signal*. 16:401-13.
- Rein, U., U. Andag, R. Duden, H.D. Schmitt, and A. Spang. 2002. ARF-GAP-mediated interaction between the ER-Golgi v-SNAREs and the COPI coat. *J Cell Biol*. 157:395-404.
- Renault, L., P. Christova, B. Guibert, S. Pasqualato, and J. Cherfils. 2002. Mechanism of domain closure of Sec7 domains and role in BFA sensitivity. *Biochemistry*. 41:3605-12.
- Renault, L., B. Guibert, and J. Cherfils. 2003. Structural snapshots of the mechanism and inhibition of a guanine nucleotide exchange factor. *Nature*. 426:525-30.

- Robinson, M.S. 2004. Adaptable adaptors for coated vesicles. *Trends Cell Biol.* 14:167-74.
- Robinson, M.S., and T.E. Kreis. 1992. Recruitment of coat proteins onto Golgi membranes in intact and permeabilized cells: effects of brefeldin A and G protein activators. *Cell.* 69:129-38.
- Rodriguez-Boulan, E., G. Kreitzer, and A. Musch. 2005. Organization of vesicular trafficking in epithelia. *Nat Rev Mol Cell Biol.* 6:233-47.
- Rodriguez-Boulan, E., and A. Musch. 2005. Protein sorting in the Golgi complex: shifting paradigms. *Biochim Biophys Acta.* 1744:455-64.
- Rothman, J.E. 1994. Mechanisms of intracellular protein transport. *Nature.* 372:55-63.
- Rothman, J.E., and L. Orci. 1992. Molecular dissection of the secretory pathway. *Nature.* 355:409-15.
- Rothman, J.E., and F.T. Wieland. 1996. Protein sorting by transport vesicles. *Science.* 272:227-34.
- Saeki, N., H. Tokuo, and M. Ikebe. 2005. BIG1 is a binding partner of myosin IXb and regulates its Rho-GTPase activating protein activity. *J Biol Chem.* 280:10128-34.
- Saenz, J.B., W.J. Sun, J.W. Chang, J. Li, B. Bursulaya, N.S. Gray, and D.B. Haslam. 2009. Golgicide A reveals essential roles for GBF1 in Golgi assembly and function. *Nat Chem Biol.*
- Sakurai, A., K. Okamoto, Y. Fujita, Y. Nakazato, K. Wakabayashi, H. Takahashi, and N.K. Gonatas. 2000. Fragmentation of the Golgi apparatus of the ballooned neurons in patients with corticobasal degeneration and Creutzfeldt-Jakob disease. *Acta Neuropathologica.* 100:270-274.
- Sakurai, A., K. Okamoto, M. Yaguchi, Y. Fujita, Y. Mizuno, Y. Nakazato, and N. Gonatas. 2002. Pathology of the inferior olivary nucleus in patients with multiple system atrophy. *Acta Neuropathologica.* 103:550-554.
- Sandvig, K., and B. van Deurs. 2002. Membrane traffic exploited by protein toxins. *Annu Rev Cell Dev Biol.* 18:1-24.
- Saraste, J., and E. Kuismanen. 1992. Pathways of protein sorting and membrane traffic between the rough endoplasmic reticulum and the Golgi complex. *Semin Cell Biol.* 3:343-55.
- Saraste, J., G.E. Palade, and M.G. Farquhar. 1986. Temperature-sensitive steps in the transport of secretory proteins through the Golgi complex in exocrine pancreatic cells. *Proc Natl Acad Sci U S A.* 83:6425-9.
- Sata, M., J.G. Donaldson, J. Moss, and M. Vaughan. 1998. Brefeldin A-inhibited guanine nucleotide-exchange activity of Sec7 domain from yeast Sec7 with yeast and mammalian ADP ribosylation factors. *Proc Natl Acad Sci U S A.* 95:4204-8.
- Sato, K., and A. Nakano. 2004. Reconstitution of coat protein complex II (COPII) vesicle formation from cargo-reconstituted proteoliposomes reveals the potential role of GTP hydrolysis by Sar1p in protein sorting. *J Biol Chem.* 279:1330-5.
- Sato, K., and A. Nakano. 2007. Mechanisms of COPII vesicle formation and protein sorting. *FEBS Lett.*

- Scales, S.J., R. Pepperkok, and T.E. Kreis. 1997. Visualization of ER-to-Golgi transport in living cells reveals a sequential mode of action for COPII and COPI. *Cell*. 90:1137-48.
- Schaub, B.E., B. Berger, E.G. Berger, and J. Rohrer. 2006. Transition of galactosyltransferase 1 from trans-Golgi cisterna to the trans-Golgi network is signal mediated. *Mol Biol Cell*. 17:5153-62.
- Scheiffele, P., P. Verkade, A.M. Fra, H. Virta, K. Simons, and E. Ikonen. 1998. Caveolin-1 and -2 in the Exocytic Pathway of MDCK Cells. *J. Cell Biol.* 140:795-806.
- Scott, P.M., P.S. Bilodeau, O. Zhdankina, S.C. Winistorfer, M.J. Hauglund, M.M. Allaman, W.R. Kearney, A.D. Robertson, A.L. Boman, and R.C. Piper. 2004. GGA proteins bind ubiquitin to facilitate sorting at the trans-Golgi network. *Nat Cell Biol*. 6:252-259.
- Seelig, H.P., P. Schranz, H. Schroter, C. Wiemann, and M. Renz. 1994. Macrogolgin--a new 376 kD Golgi complex outer membrane protein as target of antibodies in patients with rheumatic diseases and HIV infections. *J Autoimmun.* 7:67-91.
- Seemann, J., E. Jokitalo, M. Pypaert, and G. Warren. 2000. Matrix proteins can generate the higher order architecture of the Golgi apparatus. *Nature*. 407:1022-6.
- Shaywitz, D.A., P.J. Espenshade, R.E. Gimeno, and C.A. Kaiser. 1997. COPII subunit interactions in the assembly of the vesicle coat. *J Biol Chem*. 272:25413-6.
- Sheen, V.L., V.S. Ganesh, M. Topcu, G. Sebire, A. Bodell, R.S. Hill, P.E. Grant, Y.Y. Shugart, J. Imitola, S.J. Khoury, R. Guerrini, and C.A. Walsh. 2004. Mutations in ARFGEF2 implicate vesicle trafficking in neural progenitor proliferation and migration in the human cerebral cortex. *Nat Genet*. 36:69-76.
- Shen, X., M.S. Hong, J. Moss, and M. Vaughan. 2007. BIG1, a brefeldin A-inhibited guanine nucleotide-exchange protein, is required for correct glycosylation and function of integrin beta1. *Proc Natl Acad Sci U S A*. 104:1230-5.
- Shen, X., K.F. Xu, Q. Fan, G. Pacheco-Rodriguez, J. Moss, and M. Vaughan. 2006. Association of brefeldin A-inhibited guanine nucleotide-exchange protein 2 (BIG2) with recycling endosomes during transferrin uptake. *Proc Natl Acad Sci U S A*. 103:2635-40.
- Shin, H.W., N. Morinaga, M. Noda, and K. Nakayama. 2004. BIG2, a guanine nucleotide exchange factor for ADP-ribosylation factors: its localization to recycling endosomes and implication in the endosome integrity. *Mol Biol Cell*. 15:5283-94.
- Shin, H.W., and K. Nakayama. 2004. Guanine nucleotide-exchange factors for arf GTPases: their diverse functions in membrane traffic. *J Biochem (Tokyo)*. 136:761-7.
- Shinotsuka, C., S. Waguri, M. Wakasugi, Y. Uchiyama, and K. Nakayama. 2002a. Dominant-negative mutant of BIG2, an ARF-guanine nucleotide exchange factor, specifically affects membrane trafficking from the trans-Golgi network

- through inhibiting membrane association of AP-1 and GGA coat proteins. *Biochem Biophys Res Commun.* 294:254-60.
- Shinotsuka, C., Y. Yoshida, K. Kawamoto, H. Takatsu, and K. Nakayama. 2002b. Overexpression of an ADP-ribosylation factor-guanine nucleotide exchange factor, BIG2, uncouples brefeldin A-induced adaptor protein-1 coat dissociation and membrane tubulation. *J Biol Chem.* 277:9468-73.
- Short, B., A. Haas, and F.A. Barr. 2005. Golgins and GTPases, giving identity and structure to the Golgi apparatus. *Biochim Biophys Acta.* 1744:383-95.
- Spang, A., K. Matsuoka, S. Hamamoto, R. Schekman, and L. Orci. 1998. Coatamer, Arf1p, and nucleotide are required to bud coat protein complex I-coated vesicles from large synthetic liposomes. *Proc Natl Acad Sci U S A.* 95:11199-204.
- Springer, S., A. Spang, and R. Schekman. 1999. A primer on vesicle budding. *Cell.* 97:145-8.
- Stearns, T., M.C. Willingham, D. Botstein, and R.A. Kahn. 1990. ADP-ribosylation factor is functionally and physically associated with the Golgi complex. *Proc Natl Acad Sci U S A.* 87:1238-42.
- Stéphane, L., and J.M. Peter. 2007. The Arf GEF GBF1 Is Required for GGA Recruitment to Golgi Membranes. *Traffic.* 8:1440-1451.
- Stephens, D.J., and R. Pepperkok. 2002. Imaging of procollagen transport reveals COPI-dependent cargo sorting during ER-to-Golgi transport in mammalian cells. *J Cell Sci.* 115:1149-60.
- Stieber, A., Y. Chen, S. Wei, Z. Mourelatos, J. Gonatas, K. Okamoto, and N.K. Gonatas. 1998. The fragmented neuronal Golgi apparatus in amyotrophic lateral sclerosis includes the trans-Golgi-network: functional implications. *Acta Neuropathologica.* 95:245-253.
- Stieber, A., Z. Mourelatos, and N.K. Gonatas. 1996. In Alzheimer's disease the Golgi apparatus of a population of neurons without neurofibrillary tangles is fragmented and atrophic. *American Journal of Pathology.* 148:415-426.
- Storrie, B., R. Pepperkok, and T. Nilsson. 2000. Breaking the COPI monopoly on Golgi recycling. *Trends in Cell Biology.* 10:385-91.
- Supek, F., D.T. Madden, S. Hamamoto, L. Orci, and R. Schekman. 2002. Sec16p potentiates the action of COPII proteins to bud transport vesicles. *J Cell Biol.* 158:1029-38.
- Szul, T., R. Garcia-Mata, E. Brandon, S. Shestopal, C. Alvarez, and E. Sztul. 2005. Dissection of membrane dynamics of the ARF-guanine nucleotide exchange factor GBF1. *Traffic.* 6:374-85.
- Szul, T., R. Grabski, S. Lyons, Y. Morohashi, S. Shestopal, M. Lowe, and E. Sztul. 2007. Dissecting the role of the ARF guanine nucleotide exchange factor GBF1 in Golgi biogenesis and protein trafficking. *J Cell Sci.* 120:3929-40.
- Takamine, K., K. Okamoto, Y. Fujita, A. Sakurai, M. Takatama, and N.K. Gonatas. 2000. The involvement of the neuronal Golgi apparatus and trans-Golgi network in the human olivary hypertrophy. *Journal of the Neurological Sciences.* 182:45-50.

- Takatsu, H., K. Yoshino, K. Toda, and K. Nakayama. 2002. GGA proteins associate with Golgi membranes through interaction between their GGAH domains and ADP-ribosylation factors. *Biochem J.* 365:369-78.
- Tang, B.L., Y. Wang, Y.S. Ong, and W. Hong. 2005. COPII and exit from the endoplasmic reticulum. *Biochim Biophys Acta.* 1744:293-303.
- Tang, B.L., T. Zhang, D.Y. Low, E.T. Wong, H. Horstmann, and W. Hong. 2000. Mammalian homologues of yeast sec31p. An ubiquitously expressed form is localized to endoplasmic reticulum (ER) exit sites and is essential for ER-Golgi transport. *J Biol Chem.* 275:13597-604.
- Tanigawa, G., L. Orci, M. Amherdt, M. Ravazzola, J.B. Helms, and J.E. Rothman. 1993. Hydrolysis of bound GTP by ARF protein triggers uncoating of Golgi-derived COP-coated vesicles. *J. Cell Biol.* 123:1365-1371.
- Taylor, T.C., R.A. Kahn, and P. Melançon. 1992. Two distinct members of the ADP-ribosylation factor family of GTP-binding proteins regulate cell-free intra-Golgi transport. *Cell.* 70:69-79.
- Taylor, T.C., M. Kanstein, P. Weidman, and P. Melançon. 1994. Cytosolic ARFs are required for vesicle formation but not for cell-free intra-Golgi transport: evidence for coated vesicle-independent transport. *Mol Biol Cell.* 5:237-52.
- Thorne-Tjomslund, G., M. Dumontier, and J.C. Jamieson. 1998. 3D topography of noncompact zone Golgi tubules in rat spermatids: a computer-assisted serial section reconstruction study. *Anat Rec.* 250:381-96.
- Togawa, A., N. Morinaga, M. Ogasawara, J. Moss, and M. Vaughan. 1999. Purification and cloning of a brefeldin A-inhibited guanine nucleotide-exchange protein for ADP-ribosylation factors. *J Biol Chem.* 274:12308-15.
- Torii, S., T. Banno, T. Watanabe, Y. Ikehara, K. Murakami, and K. Nakayama. 1995. Cytotoxicity of brefeldin A correlates with its inhibitory effect on membrane binding of COP coat proteins. *J Biol Chem.* 270:11574-80.
- Trucco, A., R.S. Polishchuk, O. Martella, A. Di Pentima, A. Fusella, D. Di Giandomenico, E. San Pietro, G.V. Beznoussenko, E.V. Polishchuk, M. Baldassarre, R. Buccione, W.J. Geerts, A.J. Koster, K.N. Burger, A.A. Mironov, and A. Luini. 2004. Secretory traffic triggers the formation of tubular continuities across Golgi sub-compartments. *Nat Cell Biol.* 6:1071-81.
- Tsai, S.C., R. Adamik, R.S. Haun, J. Moss, and M. Vaughan. 1992. Differential interaction of ADP-ribosylation factors 1, 3, and 5 with rat brain Golgi membranes. *Proc Natl Acad Sci U S A.* 89:9272-6.
- Uemura, T., T. Ueda, R.L. Ohniwa, A. Nakano, K. Takeyasu, and M.H. Sato. 2004. Systematic analysis of SNARE molecules in Arabidopsis: dissection of the post-Golgi network in plant cells. *Cell Struct Funct.* 29:49-65.
- Velloso, L.M., K. Svensson, G. Schneider, R.F. Pettersson, and Y. Lindqvist. 2002. Crystal structure of the carbohydrate recognition domain of p58/ERGIC-53, a protein involved in glycoprotein export from the endoplasmic reticulum. *J Biol Chem.* 277:15979-84.
- Volpicelli-Daley, L.A., Y. Li, C.J. Zhang, and R.A. Kahn. 2005. Isoform-selective Effects of the Depletion of Arfs1-5 on Membrane Traffic. *Mol Biol Cell.*

- Wang, C.W., S. Hamamoto, L. Orci, and R. Schekman. 2006. Exomer: A coat complex for transport of select membrane proteins from the trans-Golgi network to the plasma membrane in yeast. *J Cell Biol.* 174:973-83.
- Wang, J., H.-Q. Sun, E. Macia, T. Kirchhausen, H. Watson, J.S. Bonifacino, and H.L. Yin. 2007. PI4P Promotes the Recruitment of the GGA Adaptor Proteins to the Trans-Golgi Network and Regulates Their Recognition of the Ubiquitin Sorting Signal. *Mol. Biol. Cell.* 18:2646-2655.
- Wang, Y.J., J. Wang, H.Q. Sun, M. Martinez, Y.X. Sun, E. Macia, T. Kirchhausen, J.P. Albanesi, M.G. Roth, and H.L. Yin. 2003. Phosphatidylinositol 4 phosphate regulates targeting of clathrin adaptor AP-1 complexes to the Golgi. *Cell.* 114:299-310.
- Ward, T.H., R.S. Polishchuk, S. Caplan, K. Hirschberg, and J. Lippincott-Schwartz. 2001. Maintenance of Golgi structure and function depends on the integrity of ER export. *J Cell Biol.* 155:557-70.
- Waters, M.G., D.O. Clary, and J.E. Rothman. 1992. A novel 115-kD peripheral membrane protein is required for intercisternal transport in the Golgi stack. *J Cell Biol.* 118:1015-26.
- Waters, M.G., T. Serafini, and J.E. Rothman. 1991. 'Coatomer': a cytosolic protein complex containing subunits of non-clathrin-coated Golgi transport vesicles. *Nature.* 349:248-51.
- Weide, T., M. Bayer, M. Koster, J.P. Siebrasse, R. Peters, and A. Barnekow. 2001. The Golgi matrix protein GM130: a specific interacting partner of the small GTPase rab1b. *EMBO Rep.* 2:336-41.
- Weigert, R., M.G. Silletta, S. Spano, G. Turacchio, C. Cericola, A. Colanzi, S. Senatore, R. Mancini, E.V. Polishchuk, M. Salmona, F. Facchiano, K.N. Burger, A. Mironov, A. Luini, and D. Corda. 1999. CtBP/BARS induces fission of Golgi membranes by acylating lysophosphatidic acid. *Nature.* 402:429-33.
- Weimer, C., R. Beck, P. Eckert, I. Reckmann, J. Moelleken, B. Brugger, and F. Wieland. 2008. Differential roles of ArfGAP1, ArfGAP2, and ArfGAP3 in COPI trafficking. *J. Cell Biol.* 183:725-735.
- Wendeler, M.W., J.P. Paccaud, and H.P. Hauri. 2007. Role of Sec24 isoforms in selective export of membrane proteins from the endoplasmic reticulum. *EMBO Rep.* 8:258-64.
- Wessels, E., D. Duijsings, K.H. Lanke, S.H. van Dooren, C.L. Jackson, W.J. Melchers, and F.J. van Kuppeveld. 2006a. Effects of picornavirus 3A Proteins on Protein Transport and GBF1-dependent COP-I recruitment. *J Virol.* 80:11852-60.
- Wessels, E., D. Duijsings, T.K. Niu, S. Neumann, V.M. Oorschot, F. de Lange, K.H. Lanke, J. Klumperman, A. Henke, C.L. Jackson, W.J. Melchers, and F.J. van Kuppeveld. 2006b. A viral protein that blocks Arf1-mediated COP-I assembly by inhibiting the guanine nucleotide exchange factor GBF1. *Dev Cell.* 11:191-201.
- Wood, S.A., J.E. Park, and W.J. Brown. 1991. Brefeldin A causes a microtubule-mediated fusion of the trans-Golgi network and early endosomes. *Cell.* 67:591-600.

- Xu, D., and J.C. Hay. 2004. Reconstitution of COPII vesicle fusion to generate a pre-Golgi intermediate compartment. *J Cell Biol.* 167:997-1003.
- Xu, K.F., X. Shen, H. Li, G. Pacheco-Rodriguez, J. Moss, and M. Vaughan. 2005. Interaction of BIG2, a brefeldin A-inhibited guanine nucleotide-exchange protein, with exocyst protein Exo70. *Proc Natl Acad Sci U S A.* 102:2784-9.
- Yamaji, R., R. Adamik, K. Takeda, A. Togawa, G. Pacheco-Rodriguez, V.J. Ferrans, J. Moss, and M. Vaughan. 2000. Identification and localization of two brefeldin A-inhibited guanine nucleotide-exchange proteins for ADP-ribosylation factors in a macromolecular complex. *Proc Natl Acad Sci U S A.* 97:2567-72.
- Yan, J.P., M.E. Colon, L.A. Beebe, and P. Melancon. 1994. Isolation and characterization of mutant CHO cell lines with compartment-specific resistance to brefeldin A. *J. Cell. Biol.* 126:65-75.
- Yang, J.S., S.Y. Lee, M. Gao, S. Bourgoïn, P.A. Randazzo, R.T. Premont, and V.W. Hsu. 2002. ARFGAP1 promotes the formation of COPI vesicles, suggesting function as a component of the coat. *J Cell Biol.* 159:69-78.
- Yang, J.S., S.Y. Lee, S. Spano, H. Gad, L. Zhang, Z. Nie, M. Bonazzi, D. Corda, A. Luini, and V.W. Hsu. 2005. A role for BARS at the fission step of COPI vesicle formation from Golgi membrane. *Embo J.* 24:4133-43.
- Ye, B., Y. Zhang, W. Song, S.H. Younger, L.Y. Jan, and Y.N. Jan. 2007. Growing Dendrites and Axons Differ in Their Reliance on the Secretory Pathway. 130:717-729.
- Yeaman, C., A.H.L. Gall, A.N. Baldwin, L. Monlauzeur, A.L. Bivic, and E. Rodriguez-Boulan. 1997. The O-glycosylated Stalk Domain Is Required for Apical Sorting of Neurotrophin Receptors in Polarized MDCK Cells. *J. Cell Biol.* 139:929-940.
- Zeghouf, M., B. Guibert, J.C. Zeeh, and J. Cherfils. 2005. Arf, Sec7 and Brefeldin A: a model towards the therapeutic inhibition of guanine nucleotide-exchange factors. *Biochem Soc Trans.* 33:1265-8.
- Zeuschner, D., W.J. Geerts, E. van Donselaar, B.M. Humbel, J.W. Slot, A.J. Koster, and J. Klumperman. 2006. Immuno-electron tomography of ER exit sites reveals the existence of free COPII-coated transport carriers. *Nat Cell Biol.* 8:377-83.
- Zhao, L., J.B. Helms, B. Brugger, C. Harter, B. Martoglio, R. Graf, J. Brunner, and F.T. Wieland. 1997. Direct and GTP-dependent interaction of ADP ribosylation factor 1 with coatamer subunit beta. *Proc Natl Acad Sci U S A.* 94:4418-23.
- Zhao, X., A. Claude, J. Chun, D.J. Shields, J.F. Presley, and P. Melançon. 2006. GBF1, a cis-Golgi and VTCs-localized ARF-GEF, is implicated in ER-to-Golgi protein traffic. *J Cell Sci.* 119:3743-53.
- Zhao, X., T.K. Lasell, and P. Melançon. 2002. Localization of large ADP-ribosylation factor-guanine nucleotide exchange factors to different Golgi compartments: evidence for distinct functions in protein traffic. *Mol Biol Cell.* 13:119-33.

Zhu, Y., B. Doray, A. Poussu, V.P. Lehto, and S. Kornfeld. 2001. Binding of GGA2 to the lysosomal enzyme sorting motif of the mannose 6- phosphate receptor. *Science*. 292:1716-8.